Pertanika Journal of

SCIENCE & TECHNOLOGY

JST

VOL. 31 (S1) 2023

A Special Issue Devoted to
Toward Successful Implementation of Circular Economy

Guest Editor
Mohd Sapuan Salit

PERTANIKA
JOURNALS

A scientific journal published by Universiti Putra Malaysia Press

Pertanika Journal of Science & Technology
Pertanika Journal of Science & Technology

Pertanika Journal of Science & Technology

About the Journal

Overview

Pertanika Journal of Science & Technology (JST) is the official journal of Universiti Putra Malaysia published by UPM Press. It is an open-access online scientific journal which is free of charge. It publishes the scientific outputs. It neither accepts nor commissions third party content.

Recognized internationally as the leading peer-reviewed interdisciplinary journal devoted to the publication of original papers, it serves as a forum for practical approaches to improving quality in issues pertaining to science and engineering and its related fields.

JST is currently published 6 issues a year, periodically in January, March, April, July, August, and October. It is considered for publication of original articles according to its scope. The journal publishes in **English** and it is open to authors around the world regardless of the nationality.

The Journal is available world-wide.

Aims and scope

Pertanika Journal of Science and Technology aims to provide a forum for high quality research related to science and engineering research. Areas relevant to the scope of the journal include: bioinformatics, bioscience, biotechnology and bio-molecular sciences, chemistry, computer science, ecology, engineering, engineering design, environmental control and management, mathematics and statistics, medicine and health sciences, nanotechnology, physics, safety and emergency management, and related fields of study.

History

Pertanika was founded in 1978. A decision was made in 1992 to streamline *Pertanika* into three journals as Pertanika Journal of Tropical Agricultural Science, Pertanika Journal of Science & Technology, and Pertanika Journal of Social Sciences & Humanities to meet the need for specialised journals in areas of study aligned with the interdisciplinary strengths of the university.

After almost 28 years, as an interdisciplinary Journal of Science & Technology, the journal now focuses on research in science and engineering and its related fields.

Goal of *Pertanika*

Our goal is to bring the highest quality research to the widest possible audience.

Quality

We aim for excellence, sustained by a responsible and professional approach to journal publishing. Submissions are guaranteed to receive a decision within 14 weeks. The elapsed time from submission to publication for the articles averages 5-6 months.

Abstracting and indexing of *Pertanika*

The journal is indexed in SCOPUS (Elsevier), Clarivate-Emerging Sources Citation Index [ESCI (Web of Science)], BIOSIS, National Agricultural Science (NAL), Google Scholar, MyCite and ISC.

Future vision

We are continuously improving access to our journal archives, content, and research services. We have the drive to realise exciting new horizons that will benefit not only the academic community, but society itself.

Citing journal articles

The abbreviation for Pertanika Journal of Science & Technology is *Pertanika J. Sci. Technol.*

Publication policy

Pertanika policy prohibits an author from submitting the same manuscript for concurrent consideration by two or more publications. It prohibits as well publication of any manuscript that has already been published either in whole or substantial part elsewhere. It also does not permit publication of manuscript that has been published in full in Proceedings.

Code of Ethics

The *Pertanika* Journals and Universiti Putra Malaysia takes seriously the responsibility of all of its journal publications to reflect the highest in publication ethics. Thus all journals and journal editors are expected to abide by the Journal's codes of ethics. Refer to *Pertanika*'s **Code of Ethics** for full details, or visit the Journal's web link at http://www.pertanika.upm.edu.my/code_of_ethics.php

International Standard Serial Number (ISSN)

An ISSN is an 8-digit code used to identify periodicals such as journals of all kinds and on all media–print and electronic. All *Pertanika* journals have ISSN as well as an e-ISSN.

Pertanika Journal of Science & Technology: ISSN 0128-7680 (*Print*); ISSN 2231-8526 (*Online*).

Lag time

A decision on acceptance or rejection of a manuscript is reached in 3 to 4 months (average 14 weeks). The elapsed time from submission to publication for the articles averages 5-6 months.

Authorship

Authors are not permitted to add or remove any names from the authorship provided at the time of initial submission without the consent of the Journal's Chief Executive Editor.

Manuscript preparation

Refer to *Pertanika*'s **Instructions to Authors** through the official website.

Editorial process

Authors are notified with an acknowledgement containing a *Manuscript ID* on receipt of a manuscript, and upon the editorial decision regarding publication.

Pertanika follows a **double-blind peer-review** process. Manuscripts deemed suitable for publication are usually sent to reviewers. Authors are encouraged to suggest names of at least three potential reviewers at the time of submission of their manuscript to *Pertanika*, but the editors will make the final choice. The editors are not, however, bound by these suggestions.

Notification of the editorial decision is usually provided within ten to fourteen weeks from the receipt of manuscript. Publication of solicited manuscripts is not guaranteed. In most cases, manuscripts are accepted conditionally, pending an author's revision of the material.

The Journal's peer-review

In the peer-review process, three referees independently evaluate the scientific quality of the submitted manuscripts.

Peer reviewers are experts chosen by journal editors to provide written assessment of the **strengths** and **weaknesses** of written research, with the aim of improving the reporting of research and identifying the most appropriate and highest quality material for the journal.

Pertanika Journal of Science & Technology
Pertanika Journal of Science & Technology

Pertanika Journal of Science & Technology
Pertanika Journal of Science & Technology

Operating and review process

What happens to a manuscript once it is submitted to *Pertanika*? Typically, there are seven steps to the editorial review process:

1. The Journal's Chief Executive Editor (CEE) and the Editorial Board Members (EBMs) examine the paper to determine whether it is appropriate for the journal and should be reviewed. If not appropriate, the manuscript is rejected outright and the author is informed.

2. The CEE sends the article-identifying information having been removed, to 2 or 3 reviewers who are specialists in the subject matter represented by the article. The CEE requests them to complete the review within 3 weeks.

   Comments to authors are about the appropriateness and adequacy of the theoretical or conceptual framework, literature review, method, results and discussion, and conclusions. Reviewers often include suggestions for strengthening of the manuscript. Comments to the editor are in the nature of the significance of the work and its potential contribution to the research field.

3. The Editor-in-Chief (EiC) examines the review reports and decides whether to accept or reject the manuscript, invites the author(s) to revise and resubmit the manuscript, or seek additional review reports. Final acceptance or rejection rests with the CEE and EiC, who reserve the right to refuse any material for publication. In rare instances, the manuscript is accepted with almost no revision. Almost without exception, reviewers' comments (to the author) are forwarded to the author. If a revision is indicated, the editor provides guidelines to the authors for attending to the reviewers' suggestions and perhaps additional advice about revising the manuscript.

4. The authors decide whether and how to address the reviewers' comments and criticisms and the editor's concerns. The authors return a revised version of the paper to the CEE along with specific information describing how they have answered' the concerns of the reviewers and the editor, usually in a tabular form. The author(s) may also submit a rebuttal if there is a need especially when the authors disagree with certain comments provided by reviewer(s).

5. The CEE sends the revised paper out for re-review. Typically, at least 1 of the original reviewers will be asked to examine the article.

6. When the reviewers have completed their work, the EiC examines their comments and decides whether the paper is ready to be published, needs another round of revisions, or should be rejected. If the decision is to accept, the CEE is notified.

7. The CEE reserves the final right to accept or reject any material for publication, if the processing of a particular manuscript is deemed not to be in compliance with the S.O.P. of *Pertanika*. An acceptance letter is sent to all authors.

   The editorial office ensures that the manuscript adheres to the correct style (in-text citations, the reference list, and tables are typical areas of concern, clarity, and grammar). The authors are asked to respond to any minor queries by the editorial office. Following these corrections, page proofs are mailed to the corresponding authors for their final approval. At this point, **only essential changes are accepted**. Finally, the manuscript appears in the pages of the journal and is posted online.

Pertanika Journal of

SCIENCE & TECNOLOGY

A Special Issue Devoted to

Toward Successful Implementation of Circular Economy

VOL. 31 (S1) 2023

(Special Issue)

Guest Editor

Mohd Sapuan Salit

PERTANIKA JOURNALS

A scientific journal published by Universiti Putra Malaysia Press

PJST

Pertanika Journal of Science & Technology

AN INTERNATIONAL PEER-REVIEWED JOURNAL

EDITORIAL OFFICE

JOURNAL DIVISION
Putra Science Park
1st Floor, IDEA Tower II
UPM-MTDC Technology Centre
Universiti Putra Malaysia
43400 Serdang, Selangor Malaysia.

Gen Enquiry
Tel. No: +603 9769 1622 | 1616
E-mail:
executive_editor.pertanika@upm.edu.my
URL: www.journals-jd.upm.edu.my

PUBLISHER

UPM Press
Universiti Putra Malaysia
43400 UPM, Serdang, Selangor, Malaysia.
Tel: +603 9769 8851
E-mail: penerbit@putra.upm.edu.my
URL: http://penerbit.upm.edu.my

ABSTRACTING AND INDEXING OF PERTANIKA JOURNALS

The journal is indexed in SCOPUS (Elsevier), Clarivate-Emerging Sources Citation Index (ESCI), BIOSIS, National Agricultural Science (NAL), Google Scholar, MyCite, ISC. In addition, Pertanika JSSH is recipient of "CREAM" Award conferred by Ministry of Higher Education (MoHE), Malaysia.

Pertanika Journal of Science & Technology
Vol. 31 (S1) 2023

Contents

Preface

Natural fibre composites are emerging materials that recently attracted the attention of academics, policymakers and industrial practitioners due to their advantages. Lightweight, renewability, low cost, and comparable specific strength and stiffness properties to traditional glass fibre composites are among the important attributes of these materials. As such, they are widely used in industries such as automotive, office furniture, energy, building materials and food packaging. In this special issue of the Pertanika Journal of Science and Technology, experts from different international and national institutions have published nine research and review papers on natural fibre composites. The theme is “Towards Successful Implementation of Circular Economy.” Natural fibres covered in this special issue include coconut coir, kenaf, durian skin, sugar palm, *Wrightia tinctoria* and *Cebia pentandra* fibres. The contributors used multi-integrated optimization solvers, resin coating treatment, and IoT for their research. Different properties of natural fibre composites are described, including mechanical, environmental, thermal, flammability, and morphological properties.

Guest Editor
Mohd Sapuan Salit *(Prof. Ir. Dr.)*

Pertanika J. Sci. & Technol. 31 (S1): 1 - 19 (2023)

PERTANIKA JOURNALS

SCIENCE & TECHNOLOGY

Journal homepage: http://www.pertanika.upm.edu.my/

Optimizing the Mechanical Performance of Green Composite Materials Using Muti-integrated Optimization Solvers

Mahmoud Mohammad Rababah* and Faris Mohammed AL-Oqla

Department of Mechanical Engineering, Faculty of Engineering, The Hashemite University, P. O. Box 330127, Zarqa 13133, Jordan

ABSTRACT

Natural fiber composites are potential alternatives for synthetic materials due to environmental issues. The overall performance of the fiber composites depends on the reinforcement conditions. Thus, this work aimed to optimize the reinforcement conditions of the natural fiber composites to improve their mechanical performance via applying an integrated scheme of Genetic Algorithm (GA), Particle Swarm Optimization (PSO), and differential evolution (DE) methods considering various reinforcement conditions including fiber length, fiber loading, and treatment time for optimal characteristics of the composite mechanical performance. The B-Spline approximation function was adopted to predict the experimental performance of green composites. The B-Spline approximation function demonstrated incomparable accuracy compared to linear or quadratic regressions. The function is then optimized using an integrated optimization method. Results have demonstrated that optimal reinforcement conditions for the maximized desired mechanical performance of the composite were achieved with high accuracy. The robustness of the proposed approach was approved using various surface plots of the considered input-output parameter relations. Pareto front or the non-dominated solutions of the desired output mechanical properties were also obtained to demonstrate the interaction between the desired properties to facilitate finding the optimal reinforcement conditions of the composite materials.

ARTICLE INFO

Article history:
Received: 06 March 2023
Accepted: 24 July 2023
Published: 27 October 2023

DOI: https://doi.org/10.47836/pjst.31.S1.01

E-mail addresses:
m_rababah@hu.edu.jo (Mahmoud Mohammad Rababah)
Fmaloqla@hu.edu.jo (Faris Mohammed AL- Oqla)
*Corresponding author

Keywords: B-Spline, composite materials, epoxy, mechanical properties, natural fibers, optimization

ISSN: 0128-7680
e-ISSN: 2231-8526

INTRODUCTION

The undesirable impact of single-use plastics on the environment is currently an issue across the globe. The petroleum-based plastic packaging materials are continuously building up in landfills and leaching into the environment (AL-Oqla et al., 2021; Ariawan et al., 2022; Ismail et al., 2022; Wegmann et al., 2022). Handling plastic waste is important to the environment, and converting these wastes to biodegradable plastics can support reducing the environmental impact. The use of eco-friendly materials has been increasing with time as a result of global environmental awareness (Abral et al., 2019; Agarwal & Mthembu, 2022; Al-Jarrah & Al-Oqla, 2022; Al-Oqla et al., 2022; Vijay et al., 2021). Therefore, developing recyclable and environmentally sustainable materials has become an attractive and important field of research. Natural fibers have been utilized to replace petroleum-based synthetic fibers steadily.

The mechanical, thermal, electrical, and structural properties of natural fibers and biodegradable polymers are, somehow, different from synthetic fibers and petroleum-based plastics (Al-Oqla & Thakur, 2021; Al-Oqla & Hayajneh, 2022; Du et al., 2022; Fares et al., 2022; Ilyas et al., 2020). Composites are made of reinforcements set in a matrix. The reinforcement is usually the strong constituent used as the load-carrying material comparable to the matrix. Composites' acceptance has been boosted by their resistance to corrosion, low maintenance, ease of creating durable objects in one piece, and design flexibility. It has an influence on the maritime industry in developing strong items at lower costs (Al-Oqla et al., 2023; Al-Oqla & Sapuan, 2018, 2020; Aridi et al., 2016; Taraborrelli et al., 2019; Vijay et al., 2019).

Because of the beneficial properties, the abundance, and the low cost of natural fibers, they are considered a new generation of reinforcements for polymer matrices. The properties of the natural fibers are inconsistent based on several factors, including the age, type, climate, and place on the tree. Their mechanical performance is usually lower than other desired materials, but their specific properties are potential due to their relatively low density. Thus, arrangements with polymer matrices have been proposed (Al-Oqla, 2021b, 2023; Al-Oqla & Hayajneh, 2020; Balıkoğlu et al., 2020; Rojas et al., 2019). Natural-based composites are considered green bio-composites composed of natural fibers. The natural fibers added value to the bio-composites with a wide range of physical, mechanical, and biological properties. Production of bio-composites can be performed by various manufacturing techniques such as hand lay-up, compression molding extrusion, injection molding, sheet molding, resin transfer molding, filament winding, and pultrusion (Fairuz et al., 2014; Khan et al., 2018; Rababah et al., 2022). Several factors can affect the overall mechanical performance of green natural fiber composite materials, including the natural fiber type, the chemical treatment, the fiber/matrix compatibility, and the interface quality. The natural fiber’s hydrophilicity and polymer matrix hydrophobicity

affect the interfacial bonding between both materials in the bio-composites. To enhance such bonding, chemical and physical treatments are essential to the fiber surface (Al-Oqla, 2021a; Al-Oqla et al., 2022; Borsoi et al., 2020; Hayajneh et al., 2022; Nurazzi et al., 2021). Therefore, proper reinforcement conditions such as different fiber lengths, fiber types, and treatment conditions have to be optimized with various available methodologies, including optimization techniques, artificial intelligence, and others, in order to enhance the overall performance of composites (Al-Oqla, 2022; Al-Oqla & Al-Jarrah, 2021; BaniHani et al., 2022; Belaadi et al., 2020; Feito et al., 2019; Nawafleh & Al-Oqla, 2022a, 2022b).

Several studies were conducted to optimize the different parameters affecting the performance of natural fiber composites. Razak et al. (2012) were concerned with optimizing the PANI amount, the acid concentration, and the molar ratio in polyaniline-coated kenaf fiber composites. They aimed to obtain an optimal response for the unit break and the electrical conductivity characteristics (Razak et al., 2012). Another study by Toupe et al. (2015) was conducted to optimize four different mechanical parameters (tensile stress at yield, flexural modulus, tensile modulus, and impact strength) of flax fiber/postconsumer recycled plastic composite (Toupe et al., 2015). The input parameters considered were all extrusion-injection process parameters. Yusof et al. (2016) applied the Taguchi method to find the best fiber-matrix combinations and their weight ratio for optimal tensile strength (Yusof et al., 2016). Some other researchers used different methods for optimizing the natural fiber composites (Al-Shrida et al., 2023; Chaudhuri et al., 2013; Fares et al., 2019; Yaghoobi & Fereidoon, 2019).

Accordingly, this work aims to enhance the mechanical performance of green composite materials by optimizing the reinforcement environment of the natural fiber composites, considering various reinforcement conditions, including the fiber length, fiber loading, and treatment time, for optimal characteristics of the composite mechanical performance. It was performed utilizing B-Spline approximation functions to predict the experimental performance of the green composites and then optimizing these functions using an integrated solver of Genetic Algorithm (GA), Particle Swarm Optimization (PSO), and differential evolution (DE) methods to end up with the optimal reinforcement condition for the maximized desired mechanical performance of the composite to enhance their implementations in various industrial applications.

METHODOLOGY

The approach developed here is composed of two stages. In the first stage, the experimental data are used to build prediction models for the tensile strength and the elongation to break percent in B-spline fitting functions. These B-spline functions' accuracy is statistically compared to the experimental values using the root mean square errors. Once the approximation functions are validated, the optimization is conducted in the second stage of this approach.

An integrated approach is developed to obtain the optimal conditions of fiber length, fiber percent, and treatment time for optimal characteristics for the tensile strength and the elongation percent of the composite to enhance achieving the optimal reinforcement conditions of the natural fiber-reinforced composite materials to maximize their desired mechanical performance. Here, a B-Spline approximation function is developed as a fitting function for the experimental data for each property (Tensile strength and elongation). To elaborate more, based on the desired orders in the input variables' domains, a B-Spline function based on the least squares approximation of the experimental data is established for both the tensile strength and elongation. Both B-Spline functions produce exact values similar to the experimental data with root-mean-square errors of less than $1x10^{-14}$.

Linear and quadratic regression functions are also derived as fitting functions for both properties to demonstrate the superiority of the B-Spline approximations over the regression approximations where large errors were found. The B-spline approximation functions are then optimized using an integrated solver composed of a Genetic Algorithm (GA), a Particle Swarm Optimization (PSO), and a differential evolution (DE). These solvers are operated simultaneously by sharing and interchanging the same population after each iteration. It will reduce the dependency of the solvers' accuracy on the tuning parameters involved and decrease the possibility of premature convergence to local solutions. The literature has more details on this optimization method (Rababah, 2011).

The optimization process covered all possible cases by optimizing the input conditions of fiber length, fiber percent, and treatment time for (1) maximizing the tensile strength, (2) maximizing the elongation percent, (3) minimizing the elongation percent, and (4) studying the combination of the tensile strength with the elongation percent where two cases are involved. Experimental data for the mechanical tensile properties of short and randomly oriented Borassus flabellifer fiber/ Epoxy composite materials with different fiber lengths, fiber loadings, alkali treatment times, and their corresponding tensile strength and elongation at break were adopted from literature (Balakrishna et al., 2013; Verma et al., 2015) and considered for the optimization. They are arranged and tabulated for convenience in Table 1.

Table 1
Mechanical properties of the fiber/epoxy composite for different fiber lengths, fiber percent, and heat treatment time

Fiber length (mm)	Percent of fiber	Alkali treatment time (h)	Tensile strength (MPa)	Elongation (%)
3	20	2	13.741	2.51
3	30	2	15.796	6.66
3	40	2	16.857	4.78

Table 1 *(Continue)*

Fiber length (mm)	Percent of fiber	Alkali treatment time (h)	Tensile strength (MPa)	Elongation (%)
3	20	4	14.866	10.47
3	30	4	16.451	3.57
3	40	4	17.187	6.09
3	20	6	17.416	2.42
3	30	6	18.178	5.32
3	40	6	19.742	4.27
5	20	2	20.612	4.06
5	30	2	19.165	12.17
5	40	2	20.499	15.89
5	20	4	20.853	5.35
5	30	4	19.980	3.27
5	40	4	21.158	6.42
5	20	6	20.585	9.56
5	30	6	21.602	13.79
5	40	6	22.296	8.6
7	20	2	19.116	2.5
7	30	2	21.604	4.65
7	40	2	21.899	1.84
7	20	4	21.733	17.37
7	30	4	22.471	19.40
7	40	4	23.174	11.45
7	20	6	22.766	3.70
7	30	6	23.008	3.24
7	40	6	27.283	10.23

RESULTS AND DISCUSSION

For comparison purposes, several regression models are developed and compared with the B-Spline approximation functions and the experimental data listed above.

Regression Approximation

The data provided in Table 1 are approximated to linear and quadratic regression functions for both properties (Tensile strength and elongation percent). The linear regression function is in the form:

$$R_1(x_1, x_2, x_3) = a_0 + a_1x_1 + a_2x_2 + a_3x_3 \quad (1)$$

where x_1, x_2, and x_3 are the fiber percent, the treatment time, and the fiber length, respectively. For tensile strength (TS), the linear regression function is expressed as:

$$TS_1(x_1, x_2, x_3) = 6.9767 + 0.10226x_1 + 0.65519x_2 + 1.4672x_3 \quad (2)$$

The comparison between the tensile strength obtained from the regression function with the experimental values is described in Figure 1 with a root-mean-square error of 0.9885 MPa.

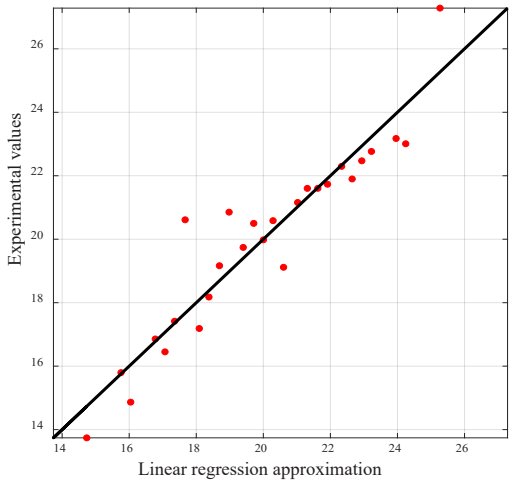

Figure 1. Linear regression vs. Experimental values of the tensile strength

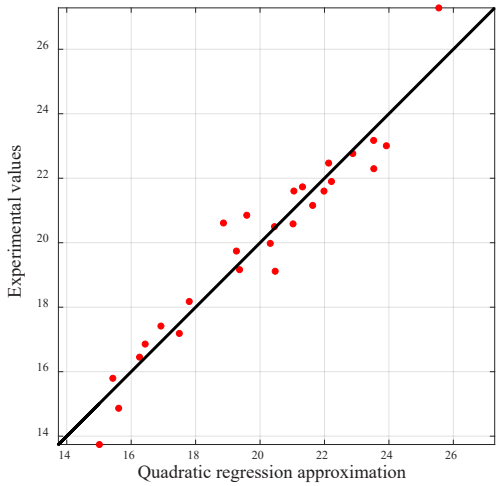

Figure 2. Quadratic regression vs. Experimental values of the tensile strength

Quadratic regression is also conducted for the tensile strength. The function is in the form:

$$R_2(x_1, x_2, x_3) = a_0 + a_1x_1 + a_2x_2 + a_3x_3 + a_4x_1x_2 + a_5x_1x_3 + a_6x_2x_3 + a_7x_1^2 + a_8x_2^2 + a_9x_3^2 \quad (3)$$

The regression function is expressed as

$$TS_2(x_1, x_2, x_3) = 6.9557 - 0.14001x_1 - 0.55986x_2 + 4.0275x_3 + 0.011533x_1x_2 - 0.004075x_1x_3 + 0.031167x_2x_3 + 0.0029294x_1^2 + 0.089153x_2^2 - 0.28072x_3^2 \quad (4)$$

The comparison between the tensile strength obtained from the quadratic regression function with the experimental values is described in Figure 2 with a root-mean-square error of 0.7849 MPa.

Their functions were represented as surfaces at constant values of the fiber length, as shown in Figures 3 and 4 for the linear and the quadratic approximations, respectively, to have better insight into the linear and the quadratic regression approximations and their accuracy compared to the experimental values.

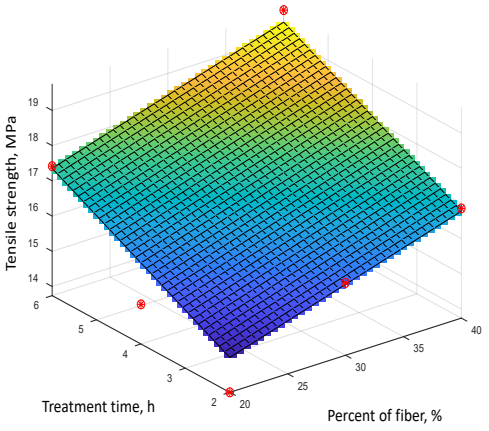

(a)

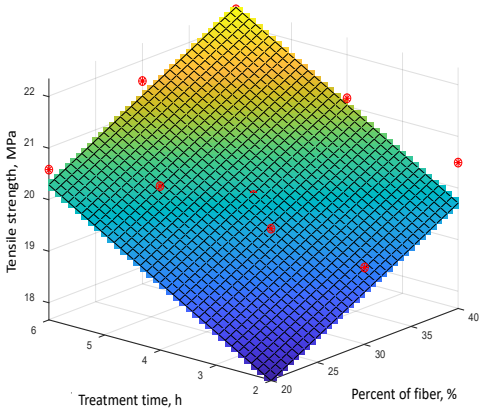

(b)

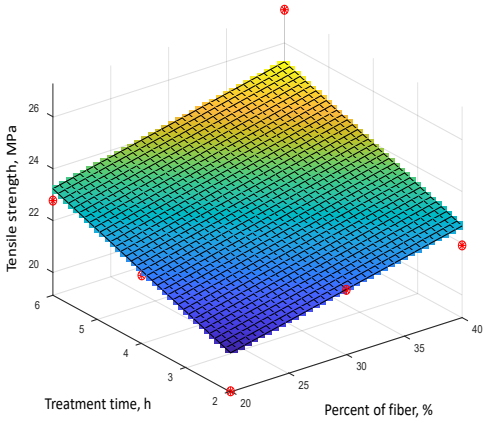

(c)

Figure 3. The linear regression approximation and the experimental data points for the tensile strength at fiber lengths of (a) 3 mm, (b) 5 mm, and (c) 7 mm

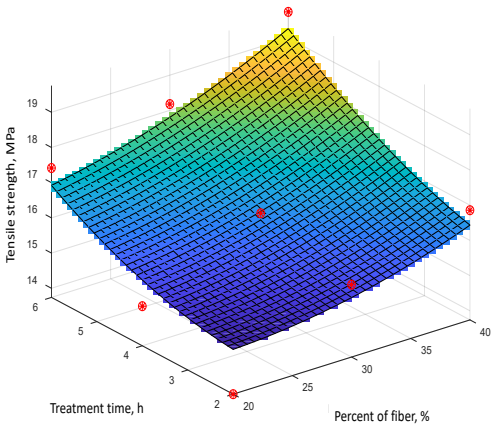

(a)

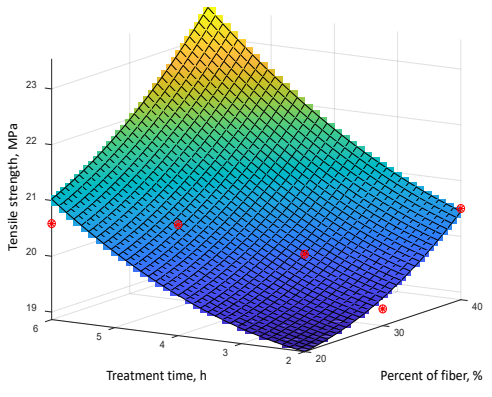

(b)

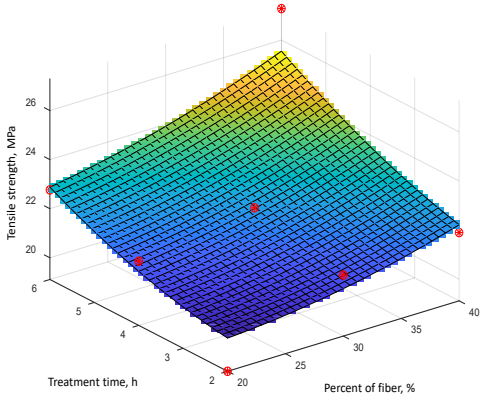

(c)

Figure 4. The quadratic regression approximation and the experimental data points for the tensile strength at fiber lengths of (a) 3 mm, (b) 5 mm, and (c) 7 mm

Similarly, the linear and the quadratic regression functions are generated for the elongation at break percent; the approximation functions revealed root mean square errors of 4.6287 and 4.2514 percent for the linear and the quadratic functions, respectively. Their values are plotted with the experimental values (Figures 5 and 6).

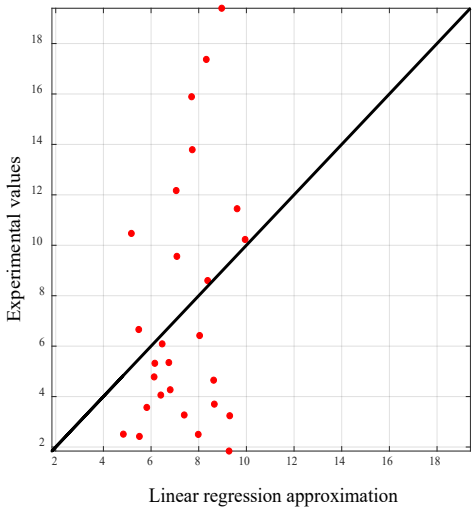

Figure 5. Linear regression vs. experimental values of the elongation percent

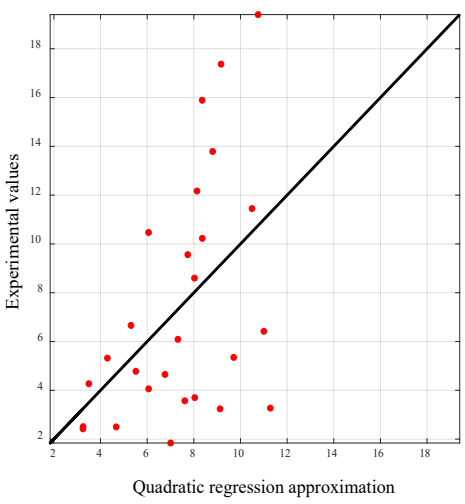

Figure 6. Quadratic regression vs. Experimental values of the elongation percent

To better understand the regression approximations and their accuracy compared to the elongation percent's experimental values, their functions were also represented as surfaces at constant values of the fiber length (Figures 7 and 8) for the linear and the quadratic approximations, respectively.

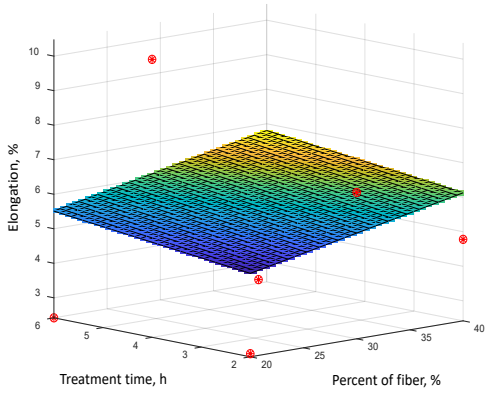

(a)

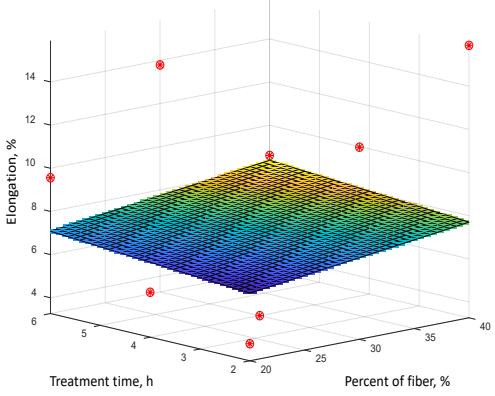

(b)

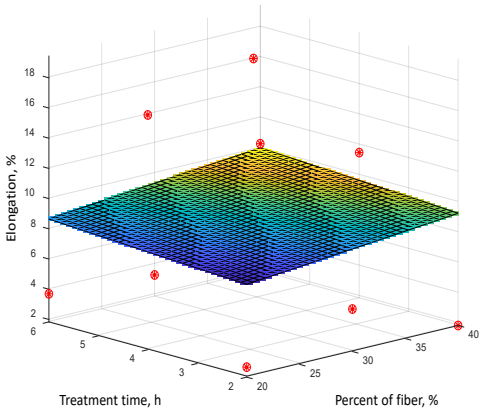

(c)

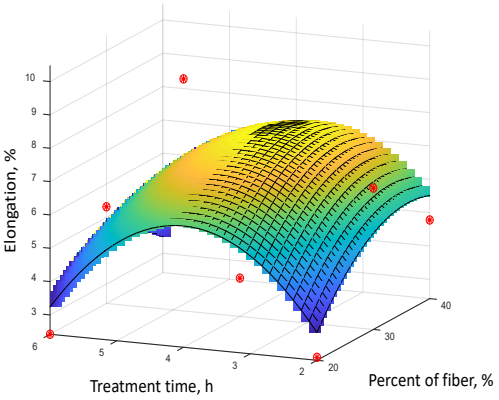

(a)

Figure 7. The linear regression approximation and the experimental data points for the elongation percent at fiber lengths of (a) 3 mm, (b) 5 mm, and (c) 7 mm

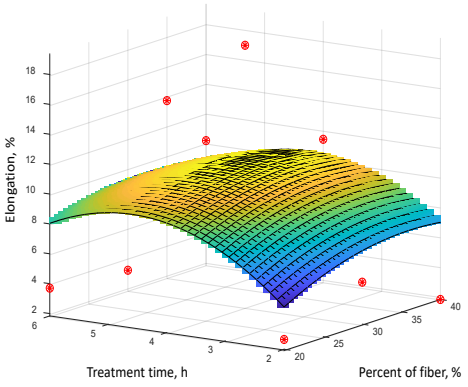

(b)

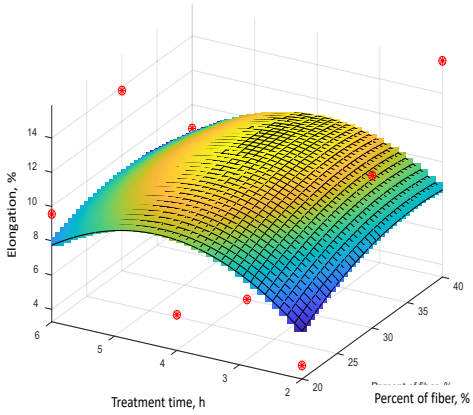

(c)

Figure 8. The quadratic regression approximation and the experimental data points for the elongation percent at fiber lengths of (a) 3 mm, (b) 5 mm, and (c) 7 mm

B-Spline Approximation

Considering the experimental data, two B-spline approximation functions are developed: $\mathbf{S_1}$ for the Tensile strength and $\mathbf{S_2}$ for the elongation percent. The B-Spline functions are in the form:

$$S(u,v,w) = \sum_{i=0}^{l}\sum_{j=0}^{m}\sum_{k=0}^{n} \mathbf{P}_{ijk} N_{i,r_1}(u) N_{j,r_2}(v) N_{k,r_3}(w) \qquad 0 \le \mathrm{u,v,w} \le 1 \tag{5}$$

where in general

$$N_{i,r} = (u - u_i)\frac{N_{i,r-1}(u)}{u_{i+r-1} - u_i} + (u_{i+r} - u)\frac{N_{i+1,r-1}(u)}{u_{i+r} - u_{i+1}} \tag{6}$$

where

$$N_{i,1} = \begin{cases} 1 & u_i \le u \le u_{i+1} \\ 0 & otherwise \end{cases} \tag{7}$$

and the knot vector is defined as

$$\mathbf{KV} = u_i = \begin{cases} 0 & i < r \\ i - r + 1 & r \le i \le n \\ n - r + 2 & i > n \end{cases} \tag{8}$$

For the experimental data listed above, the B-Spline function is produced by considering $l = m = n = 2$, and the base function order $r_1 = r_2 = r_2 = 3$. $\mathbf{P}_{ijk}$ are the control points of the B-Spline function that provide the best approximation for the data points.

A visual representation of the B-Spline approximation function is impossible since three input parameters affect the output. However, the B-Spline approximation function can be represented as a surface at a particular value of one input parameter (the fiber length). Figure 9 represents the B-Spline approximation function of the tensile strength as 3 surfaces at fiber lengths 3 mm, 5 mm, and 7 mm. The experimental data in Table 1 are also represented in the figure as 3D points to show the fitting function's accuracy and smoothness.

On the other hand, Figure 10 represents the B-Spline approximation function of the Elongation percent as 3 surfaces at fiber lengths 3 mm, 5 mm, and 7 mm. The experimental data are also represented in the figure to emphasize the smoothness and the accuracy of the fitting function.

However, before proceeding further with the optimization and to reduce the effect of the variances in both the inputs' spans and the outputs' spans on the accuracy of the B-spline functions or the sensitivity of the optimization method, the data provided in Table 1 is normalized and provided in Table 2 for convenience.

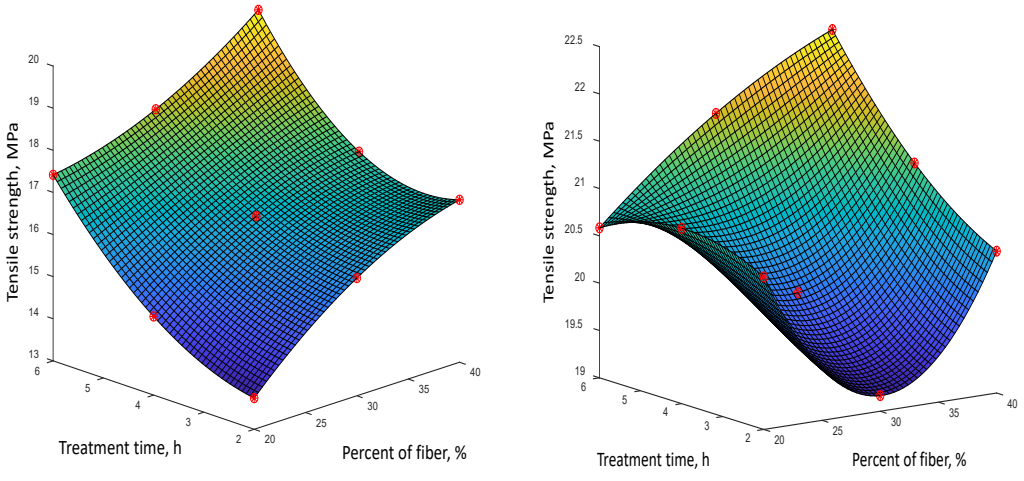

(a) (b)

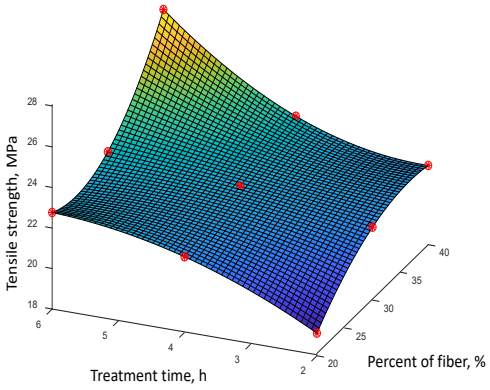

(c)

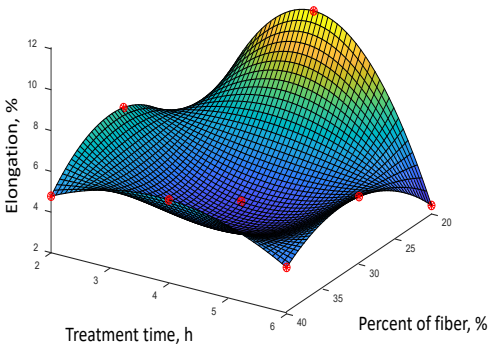

(a)

Figure 9. The B-Spline approximation and the experimental data points for the tensile strength at fiber lengths of (a) 3 mm, (b) 5 mm, and (c) 7 mm

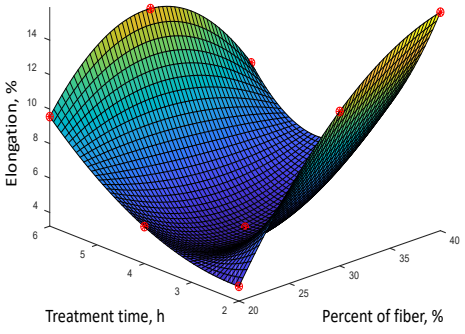

(b)

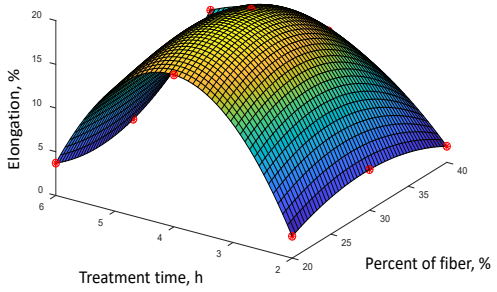

(c)

Figure 10. The B-Spline approximation and the experimental data points for the elongation percent at fiber lengths of (a) 3 mm, (b) 5 mm, and (c) 7 mm

Table 2
Normalized values for the mechanical properties of the composite

Normalized values for fiber length	Normalized values for percent of fiber	Normalized values for treatment time	Normalized values for tensile strength	Normalized values for elongation percent
0	0	0	0	0.0382
0	0.5	0	0.1518	0.2745
0	1	0	0.2301	0.1674
0	0	0.5	0.0831	0.4915
0	0.5	0.5	0.2001	0.0985
0	1	0.5	0.2545	0.2420

Table 2 *(Continue)*

Normalized values for fiber length	Normalized values for percent of fiber	Normalized values for treatment time	Normalized values for tensile strength	Normalized values for elongation percent
0	0	1	0.2714	0.0330
0	0.5	1	0.3276	0.1982
0	1	1	0.4431	0.1384
0.5	0	0	0.5074	0.1264
0.5	0.5	0	0.4005	0.5883
0.5	1	0	0.4990	0.8001
0.5	0	0.5	0.5252	0.1999
0.5	0.5	0.5	0.4607	0.0814
0.5	1	0.5	0.5477	0.2608
0.5	0	1	0.5054	0.4396
0.5	0.5	1	0.5805	0.6805
0.5	1	1	0.6317	0.3850
1	0	0	0.3969	0.0376
1	0.5	0	0.5806	0.1600
1	1	0	0.6024	0
1	0	0.5	0.5902	0.8844
1	0.5	0.5	0.6447	1.0000
1	1	0.5	0.6966	0.5473
1	0	1	0.6664	0.1059
1	0.5	1	0.6843	0.0797
1	1	1	1.0000	0.4778

B-Spline Function Optimization

After showing the accuracy of the B-Spline approximation functions compared with the experimental data and normalizing these data, a global optimization method is required to predict the optimal conditions of the fiber length, fiber percent, and treatment time for optimal mechanical properties. An integrated global optimization method was utilized here (Churchwell et al., 2020; Sbayti et al., 2020). This method employs integration of the existing global optimization techniques such as Particle Swarm Optimization (PSO), Genetic Algorithm (GA), and Differential Evolution (DE) to run simultaneously by sharing and interchanging the same population at each iteration. It would increase the robustness of

the optimization method by decreasing the possibility of premature convergence to some local solutions and by decreasing the dependency of the solvers' accuracy on the tuning parameters involved (Churchwell et al., 2020; Rababah, 2011).

The optimization is performed on the B-spline approximation functions developed to find the optimal conditions for optimal characteristics of (1) the tensile strength, (2) the elongation percent, and (3) the best combinations of both the tensile strength and the elongation percent. The lower and upper bounds of the inputs (fiber length, fiber percent, and treatment time) are set to 20% of the normalized values, that is [-0.2 1.2]. The optimization is provided as follows:

Tensile Strength Optimization. A population size of 500 is used. The optimization method required 4 main iterations with total function counts of 38173. The optimization method revealed that the best tensile strength could be obtained at the upper bounds for the fiber length, fiber percent, and treatment time at values of 7.8 mm, 44%, and 6.8 h, respectively. The tensile strength predicted at these conditions is 41.995 MPa.

This result indicates that the tensile strength increases with the fiber length, fiber percent, and treatment time. However, it is well known that this fact is not limitless. In other words, increasing these parameters above a specific threshold will reverse the process due to fiber agglomeration and decrease the fiber-matrix contacts. Thus, obtaining more experimental data beyond the upper bound will strengthen the accuracy of determining the optimal solution.

Elongation Percent Optimization. A population size of 500 is also used. The optimization method is conducted twice to obtain the optimal conditions for the global minimum and the global maximum of the elongation percent, as either can be important depending on the targeted application. The global maximum of the elongation percent is obtained after 4 main iterations with a total function count of 28328. The optimal conditions are a fiber length of 7.8 mm, a fiber percent of 26.77%, and a treatment time of 3.903 h. The maximum elongation is predicted as 31.507%. Conversely, minimizing the elongation percent is preferred for some applications. The minimization uses the same approximation function and reveals the best elongation characteristics near zero (0.0051%). It is obtained by setting the fiber length to 4.4314 mm, the treatment time to 2.0493 h, and the fiber percent to 16.1621%.

The optimal fiber length predicted is in the upper bound of 7.8 mm for maximizing the elongation to break percent. Care should be taken before generalizing this conclusion, as discussed previously.

Tensile Strength-elongation Percent Optimization. The tensile strength and elongation are important, with different weights depending on the applications. The combination of

both characteristics is investigated, and the Pareto-fronts are generated. It is conducted by considering two cases for the optimal characteristics depending on the required applications: first, maximizing both the tensile strength and the elongation, and second, maximizing the tensile strength and minimizing the elongation percent.

For case I, where the goal is to maximize both the tensile strength and the elongation percent, a Pareto-front is obtained considering the optimal conditions of the fiber length, fiber percent, and treatment time in the range of the original data provided. In other words, the fiber length in the range [3 –7 mm], the fiber percent in the range [20 – 40%], and the treatment time in the range [2 – 6 h]. The Pareto front is shown in Figure 11. According to the Pareto-front, it is obvious that there is no dominant solution that can be adopted, and the selection will be dependent on the weight and importance of the two characteristics.

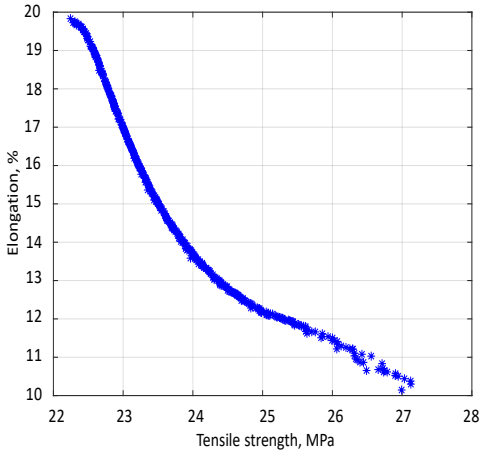

Figure 11. Pareto-Front for the optimal tensile strength and elongation percent, case I

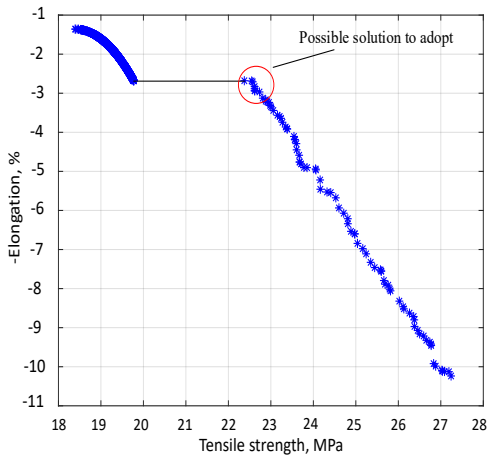

Figure 12. Pareto-Front for the optimal tensile strength and elongation percent, case II

For case II, the goal is to maximize the tensile strength and minimize the elongation percent. It is conducted and revealed in the Pareto front provided in Figure 12, where the elongation is multiplied by the negative sign for more convenience. A possible solution to be adopted is the region highlighted by the red circle with a tensile strength of 22.5481 MPa and an elongation percent of 2.6857%. This solution is obtained for a fiber length of 6.9992 mm, fiber percent of 27.3230%, and treatment time of 5.9974 h. However, as mentioned above, the final selection will completely depend on the weight and importance of the two characteristics according to the designer's and the consumers' needs.

Before proceeding to the conclusion, it is worth saying that the B-Spline functions can represent the scattered data than the regression models. Their fitting capabilities promote their use as prediction models. These models can be used for prediction or optimization

purposes. However, to ensure accurate and robust results, it is recommended to work on wider ranges for the input parameters and to use larger experimental data.

On the other side, using the B-Spline functions in this way is restricted to parameters of numeric nature. In other words, finding the best fiber type, matrix type, or such categorized-nature parameters is impossible in the introduced approach.

CONCLUSION

Due to the characteristics of the natural fiber composites, where their overall performance depends on the reinforcement conditions, the optimization process for the reinforcement conditions is much desired. It can be concluded that the B-Spline approximation functions better represent the experimental data than the regression models. It was statistically measured in terms of the mean square errors. For tensile strength, the errors were $1x10^{-14}$ MPa, 0.9885 MPa, and 0.7849 MPa for the B-Spline approximation, the linear regression, and the quadratic regression, respectively. Moreover, for the elongation-to-break percent, the errors were 2.4×10^{-12}, 4.63, and 4.25 percent for the B-Spline approximation, the linear regression, and the quadratic regression, respectively. Optimizing the B-Spline functions was conducted using a multi-integrated optimization technique where all possible cases were investigated. The different combinations of the tensile strength and the elongation-to-break percent were also investigated. The optimization revealed that the optimal tensile strength of 41.995 MPa can be obtained for a fiber length of 7.8 mm, fiber percent of 44%, and treatment time of 6.8 h. The optimization also revealed that no dominant individual input solution is available to maximize overall performance. Thus, the non-dominated solutions of the desired output mechanical properties were obtained to demonstrate the interaction between the desired properties via Pareto-front figures that can be adopted for the desired combination depending on the weighted importance of the involved characteristics.

ACKNOWLEDGEMENT

The authors acknowledge the anonymous reviewers for their supporting comments.

REFERENCES

Abral, H., Basri, A., Muhammad, F., Fernando, Y., Hafizulhaq, F., Mahardika, M., Sugiarti, E., Sapuan, S. M., Ilyas, R. A., & Stephane, I. (2019). A simple method for improving the properties of the sago starch films prepared by using ultrasonication treatment. *Food Hydrocolloids*, *93*, 276-283. https://doi.org/10.1016/j.foodhyd.2019.02.012

Agarwal, A., & Mthembu, L. (2022). Structural analysis and weight optimization of automotive chassis by Latin hypercube sampling using metal matrix composites. *Materials Today: Proceedings*, *60*(3), 2132-2140. https://doi.org/10.1016/j.matpr.2022.02.059

Al-Jarrah, R., & Al-Oqla, F. M. (2022). A novel integrated BPNN/SNN artificial neural network for predicting the mechanical performance of green fibers for better composite manufacturing. *Composite Structures*, *289*, 115475. https://doi.org/10.1016/j.compstruct.2022.115475

Al-Oqla, F. M., Alaaeddin, M., & El-Shekeil, Y. (2021). Thermal stability and performance trends of sustainable lignocellulosic olive/low density polyethylene biocomposites for better environmental green materials. *Engineering Solid Mechanics*, *9*(4), 439-448. https://doi.org/10.5267/j.esm.2021.5.002

Al-Oqla, F. M., & Thakur, V. K. (2021). Toward chemically treated low-cost lignocellulosic parsley waste/polypropylene bio-composites for resourceful sustainable bio-products. *International Journal of Environmental Science and Technology*, *19*(7), 668-6690. https://doi.org/10.1007/s13762-021-03601-x

Al-Oqla, F. M. (2021a). Performance trends and deteriorations of lignocellulosic grape fiber/polyethylene biocomposites under harsh environment for enhanced sustainable bio-materials. *Cellulose*, *28*(4), 2203-2213. https://doi.org/10.1007/s10570-020-03649-x

Al-Oqla, F. M. (2021b). Predictions of the mechanical performance of leaf fiber thermoplastic composites by FEA. *International Journal of Applied Mechanics*, *13*(06), 2150066. https://doi.org/10.1142/S1758825121500666

Al-Oqla, F. M. (2022). Manufacturing and delamination factor optimization of cellulosic paper/epoxy composites towards proper design for sustainability. *International Journal on Interactive Design and Manufacturing (IJIDeM)*, 1-9. https://doi.org/10.1007/s12008-022-00980-4

Al-Oqla, F. M. (2023). Biomaterial hierarchy selection framework under uncertainty for more reliable sustainable green products, *75*(7), 2187-2198. https://doi.org/10.1007/s11837-023-05797-4

Al-Oqla, F. M., & Al-Jarrah, R. (2021). A novel adaptive neuro-fuzzy inference system model to predict the intrinsic mechanical properties of various cellulosic fibers for better green composites. *Cellulose*, *28*(13), 8541-8552. https://doi.org/10.1007/s10570-021-04077-1

Al-Oqla, F. M., Alaaeddin, M. H., Hoque, M. E., & Thakur, V. K. (2022). Biopolymers and biomimetic materials in medical and electronic-related applications for environment–health–development nexus: Systematic review. *Journal of Bionic Engineering*, *19*(6), 1562-1577. https://doi.org/10.1007/s42235-022-00240-x

Al-Oqla, F. M., & Hayajneh, M. T. (2020). A hierarchy weighting preferences model to optimise green composite characteristics for better sustainable bio-products. *International Journal of Sustainable Engineering*, *14*(5), 1043-1048. https://doi.org/10.1080/19397038.2020.1822951

Al-Oqla, F. M., & Hayajneh, M. T. (2022). Stress failure interface of cellulosic composite beam for more reliable industrial design. *International Journal on Interactive Design and Manufacturing (IJIDeM)*, *16*(4), 1727-1738. https://doi.org/10.1007/s12008-022-00884-3

Al-Oqla, F. M., Hayajneh, M. T., & Al-Shrida, M. A. M. (2022). Mechanical performance, thermal stability and morphological analysis of date palm fiber reinforced polypropylene composites toward functional bio-products. *Cellulose*, *29*(6), 3293-3309. https://doi.org/10.1007/s10570-022-04498-6

Al-Oqla, F. M., Hayajneh, M. T., & Nawafleh, N. (2023). Advanced synthetic and biobased composite materials in sustainable applications: a comprehensive review. *Emergent Materials*, 1-18. https://doi.org/10.1007/s42247-023-00478-z

Al-Oqla, F. M., & Sapuan, S. (2018). Investigating the inherent characteristic/performance deterioration interactions of natural fibers in bio-composites for better utilization of resources. *Journal of Polymers and the Environment*, *26*(3), 1290-1296. https://doi.org/10.1007/s10924-017-1028-z

Al-Oqla, F. M., & Sapuan, S. (2020). *Advanced processing, properties, and applications of starch and other bio-based polymers.* Elsevier.

Al-Shrida, M. a. M., Hayajneh, M. T., & Al-Oqla, F. M. (2023). Modeling and investigation of the influential reinforcement parameters on the strength of polypropylene lignocellulosic fiber composites using analysis of variances and box-cox transformation technique. *Materials Research*, *26*, e20220386. https://doi.org/10.1590/1980-5373-MR-2022-0386

Ariawan, D., Raharjo, W. P., Diharjo, K., Raharjo, W. W., & Kusharjanta, B. (2022). Influence of tropical climate exposure on the mechanical properties of rHDPE composites reinforced by zalacca midrib fibers. *Evergreen*, *9*(3), 662-672. https://doi.org/10.5109/4842526

Aridi, N., Sapuan, S., Zainudin, E., & Al-Oqla, F. M. (2016). Mechanical and morphological properties of injection-molded rice husk polypropylene composites. *International Journal of Polymer Analysis and Characterization*, *21*(4), 305-313. https://doi.org/10.1080/1023666X.2016.1148316

Balakrishna, A., Rao, D. N., & Rakesh, A. S. (2013). Characterization and modeling of process parameters on tensile strength of short and randomly oriented *Borassus flabellifer* (Asian palmyra) fiber reinforced composite. *Composites Part B: Engineering*, *55*, 479-485. https://doi.org/10.1016/j.compositesb.2013.07.006

Balıkoğlu, F., Demircioğlu, T. K., Yıldız, M., Arslan, N., & Ataş, A. (2020). Mechanical performance of marine sandwich composites subjected to flatwise compression and flexural loading: Effect of resin pins. *Journal of Sandwich Structures & Materials*, *22*(6), 2030-2048. https://doi.org/10.1177/10996362187926

BaniHani, S. M., Al-Oqla, F. M., Hayajneh, M., Mutawe, S., & Almomani, T. (2022). A new approach for dynamic crack propagation modeling based on meshless Galerkin method and visibility based criterion. *Applied Mathematical Modelling*, *107*, 1-19. https://doi.org/10.1016/j.apm.2022.02.010

Belaadi, A., Boumaaza, M., Amroune, S., & Bourchak, M. (2020). Mechanical characterization and optimization of delamination factor in drilling bidirectional jute fibre-reinforced polymer biocomposites. *The International Journal of Advanced Manufacturing Technology*, *111*(7), 2073-2094. https://doi.org/10.1007/s00170-020-06217-6

Borsoi, C., Júnior, M. A. D., Beltrami, L. V. R., Hansen, B., Zattera, A. J., & Catto, A. L. (2020). Effects of alkaline treatment and kinetic analysis of agroindustrial residues from grape stalks and yerba mate fibers. *Journal of Thermal Analysis and Calorimetry*, *139*(5), 3275-3286. https://doi.org/10.1007/s10973-019-08666-y

Chaudhuri, S., Chakraborty, R., & Bhattacharya, P. (2013). Optimization of biodegradation of natural fiber (*Chorchorus capsularis*): HDPE composite using response surface methodology. *Iranian Polymer Journal*, *22*, 865-875. https://doi.org/10.1007/s13726-013-0185-8

Churchwell, J. H., Sowoidnich, K., Chan, O., Goodship, A. E., Parker, A. W., & Matousek, P. (2020). Adaptive band target entropy minimization: Optimization for the decomposition of spatially offset Raman spectra of bone. *Journal of Raman Spectroscopy*, *51*(1), 66-78. https://doi.org/10.1002/jrs.5749

Du, Y., Xu, J., Fang, J., Zhang, Y., Liu, X., Zuo, P., & Zhuang, Q. (2022). Ultralight, highly compressible, thermally stable MXene/aramid nanofiber anisotropic aerogels for electromagnetic interference shielding. *Journal of Materials Chemistry A*, *10*(12), 6690-6700. https://doi.org/10.1039/D1TA11025J

Fairuz, A. M., Sapuan, S. M., Zainudin, E. S., & Jaafar, C. N. A. (2014). Polymer composite manufacturing using a pultrusion process: A review. *American Journal of Applied Sciences*, *11*(10), 1798-1810.

Fares, O., Al-Oqla, F., & Hayajneh, M. (2022). Revealing the intrinsic dielectric properties of mediterranean green fiber composites for sustainable functional products. *Journal of Industrial Textiles*, *51*(5_suppl), 7732S-7754S. https://doi.org/10.1177/15280837221094648

Fares, O., Al-Oqla, F. M., & Hayajneh, M. T. (2019). Dielectric relaxation of mediterranean lignocellulosic fibers for sustainable functional biomaterials. *Materials Chemistry and Physics*, *229*, 174-182. https://doi.org/10.1016/j.matchemphys.2019.02.095

Feito, N., Muñoz-Sánchez, A., Díaz-Álvarez, A., & Miguelez, M. H. (2019). Multi-objective optimization analysis of cutting parameters when drilling composite materials with special geometry drills. *Composite Structures*, *225*, 111187. https://doi.org/10.1016/j.compstruct.2019.111187

Hayajneh, M. T., Mu'ayyad, M., & Al-Oqla, F. M. (2022). Mechanical, thermal, and tribological characterization of bio-polymeric composites: A comprehensive review. *e-Polymers*, *22*(1), 641-663. https://doi.org/10.1515/epoly-2022-0062

Ilyas, R. A., Sapuan, S. M., Atiqah, A., Ibrahim, R., Abral, H., Ishak, M. R., Zainudin, E. S., Nurazzi, N. M., Atikah, M. S. N., Ansari, M. N. M., Asyraf, M. R. M., Supian, A. B. M., & Ya, H. (2020). Sugar palm (*Arenga pinnata* [Wurmb.] Merr) starch films containing sugar palm nanofibrillated cellulose as reinforcement: Water barrier properties. *Polymer Composites*, *41*(2), 459-467. https://doi.org/10.1002/pc.25379

Ismail, A. M., AL-Oqla, F. M., Risby, M. S., & Sapuan, S. M. (2022). On the enhancement of the fatigue fracture performance of polymer matrix composites by reinforcement with carbon nanotubes: A systematic review. *Carbon Letters*, *32*(3), 727-740. https://doi.org/10.1007/s42823-022-00323-z

Khan, T., Hameed Sultan, M. T. B., & Ariffin, A. H. (2018). The challenges of natural fiber in manufacturing, material selection, and technology application: A review. *Journal of Reinforced Plastics and Composites*, *37*(11), 770-779. https://doi.org/10.1177/0731684418756

Nawafleh, N., & AL-Oqla, F. M. (2022a). Artificial neural network for predicting the mechanical performance of additive manufacturing thermoset carbon fiber composite materials. *Journal of the Mechanical Behavior of Materials*, *31*(1), 501-513. https://doi.org/10.1515/jmbm-2022-0054

Nawafleh, N., & AL-Oqla, F. M. (2022b). An innovative fuzzy-inference system for predicting the mechanical behavior of 3D printing thermoset carbon fiber composite materials. *The International Journal of Advanced Manufacturing Technology*, *121*(11), 7273-7286. https://doi.org/10.1007/s00170-022-09822-9

Nurazzi, N., Harussani, M., Aisyah, H., Ilyas, R., Norrrahim, M., Khalina, A., & Abdullah, N. (2021). Treatments of natural fiber as reinforcement in polymer composites—A short review. *Functional Composites and Structures*, *3*(2), 024002. https://doi.org/10.1088/2631-6331/abff36

Rababah, M. (2011). *A practical and optimal approach to CNC programming for five-axis grinding of the end-mill flutes* [Unpublish doctoral thesis]. Concordia University.

Rababah, M. M., AL-Oqla, F. M., & Wasif, M. (2022). Application of analytical hierarchy process for the determination of green polymeric-based composite manufacturing process. *International Journal on Interactive Design and Manufacturing (IJIDeM)*, *16*(3), 943-954. https://doi.org/10.1007/s12008-022-00938-6

Razak, S. I. A., Rahman, W. A. W. A., Sharif, N. F. A., & Yahya, M. Y. (2012). Simultaneous numerical optimization of the mechanical and electrical properties of polyaniline coated kenaf fiber using response surface methodology: nanostructured polyaniline on natural fiber. *Composite Interfaces*, *19*(7), 411-424. https://doi.org/10.1080/15685543.2012.757957

Rojas, C., Cea, M., Iriarte, A., Valdés, G., Navia, R., & Cárdenas-R, J. P. (2019). Thermal insulation materials based on agricultural residual wheat straw and corn husk biomass, for application in sustainable buildings. *Sustainable Materials and Technologies*, *20*, e00102. https://doi.org/10.1016/j.susmat.2019.e00102

Sbayti, M., Bahloul, R., & Belhadjsalah, H. (2020). Efficiency of optimization algorithms on the adjustment of process parameters for geometric accuracy enhancement of denture plate in single point incremental sheet forming. *Neural Computing and Applications*, *32*(13), 8829-8846. https://doi.org/10.1007/s00521-019-04354-y

Taraborrelli, L., Grant, R., Sullivan, M., Choppin, S., Spurr, J., Haake, S., & Allen, T. (2019). Materials have driven the historical development of the tennis racket. *Applied Sciences*, *9*(20), 4352. https://doi.org/10.3390/app9204352

Toupe, J. L., Trokourey, A., & Rodrigue, D. (2015). Simultaneous optimization of the mechanical properties of postconsumer natural fiber/plastic composites: Processing analysis. *Journal of Composite Materials*, *49*(11), 1355-1367. https://doi.org/10.1177/00219983145337

Verma, D., Gope, P., Singh, I., & Jain, S. (2015). Composites from Bagasse fibers, Its characterization and applications. In J. R. Hakeem., M. Jawaid., & O. Y. Alothman (Eds.) *Agricultural biomass based potential materials* (pp. 91-119). Springer.

Vijay, R., Manoharan, S., Vinod, A., Singaravelu, D. L., Sanjay, M., & Siengchin, S. (2019). Characterization of raw and benzoyl chloride treated Impomea pes-caprae fibers and its epoxy composites. *Materials Research Express*, *6*(9), 095307. https://doi.org/10.1088/2053-1591/ab2de2

Vijay, R., Vinod, A., Singaravelu, D. L., Sanjay, M., & Siengchin, S. (2021). Characterization of chemical treated and untreated natural fibers from *Pennisetum orientale* grass-A potential reinforcement for lightweight polymeric applications. *International Journal of Lightweight Materials and Manufacture*, *4*(1), 43-49. https://doi.org/10.1016/j.ijlmm.2020.06.008

Wegmann, S., Rytka, C., Diaz-Rodenas, M., Werlen, V., Schneeberger, C., Ermanni, P., Michaud, V. (2022). A life cycle analysis of novel lightweight composite processes: Reducing the environmental footprint of automotive structures. *Journal of Cleaner Production*, *330*, 129808. https://doi.org/10.1016/j.jclepro.2021.129808

Yaghoobi, H., & Fereidoon, A. (2019). Thermal analysis, statistical predicting, and optimization of the flexural properties of natural fiber biocomposites using Box–Behnken experimental design. *Journal of Natural Fibers*, *16*(7), 987-1005. https://doi.org/10.1080/15440478.2018.1447416

Yusof, F. M., Abd Rahim, M. K. H., Samsudin, A. S., Mohamad Nor, N. H., Ahmad, Z., & Halim, Z. (2016). Optimization of natural fiber composite parameter using Taguchi approach. *Advanced Materials Research*, 1133, 185-188. https://doi.org/10.4028/www.scientific.net/AMR.1133.185

Pertanika J. Sci. & Technol. 31 (S1): 21 - 38 (2023)

PERTANIKA JOURNALS

SCIENCE & TECHNOLOGY

Journal homepage: http://www.pertanika.upm.edu.my/

Environmental Properties of Coconut Fiber/Reinforced Thermoplastic Starch/Beeswax Hybrid Composites

Khuganeshwaran Mogan[1], Ridhwan Jumaidin[1]*, Rushdan Ahmad Ilyas[2,3,4,5] and Zatil Hafila Kamaruddin[6,7]

[1]Fakulti Teknologi dan Kejuruteraan Industri dan Pembuatan, Universiti Teknikal Malaysia Melaka, Hang Tuah Jaya, 76100 Durian Tunggal, Melaka, Malaysia
[2]Faculty of Chemical and Energy Engineering, Universiti Teknologi Malaysia, 81310 UTM, Johor, Malaysia
[3]Centre for Advanced Composite Materials, Universiti Teknologi Malaysia (UTM), Johor Bahru 81310, Malaysia
[4]Institute of Tropical Forest and Forest Products (INTROP), Universiti Putra Malaysia, 43400 UPM Serdang, Selangor, Malaysia
[5]Centre of Excellence for Biomass Utilization, Universiti Malaysia Perlis, 02600, Arau, Perlis, Malaysia
[6]Faculty of Mechanical Engineering, Universiti Teknikal Malaysia Melaka, Hang Tuah Jaya, 76100 Melaka, Malaysia
[7]German-Malaysian Institute, Jalan Ilmiah Taman Universiti, Kajang 43000, Malaysia

ABSTRACT

The creation of degradable biocomposites is anticipated to alleviate the challenges of worldwide environmental contamination and resource exhaustion. The study investigates the effect of coconut fiber on the environmental properties and water affinity behavior of thermoplastic starch/beeswax composite. The biocomposites were fabricated by incorporating the coconut husk fiber range from 10 to 50 wt%. The thermoplastic starch contains cassava starch, glycerol, and beeswax. The modification of the mixture became efficient when the mixing was determined to be stronger when used as a high-pace blender to aid the mixing process. The mixture then underwent a hot compression molding method to form the mixture into the desired sample form. We can conclude from the results that samples with high fiber content absorb less water than those with no fiber content. For moisture absorption, when the fiber content increases, the ability of the fiber to moisture absorption is decreased. The thickness swelling results show that the sample shows less swelling as the fiber percentage increases. For the soil burial test, incorporating 50 wt% coconut fiber decreases the weight reduction for 4 weeks.

ARTICLE INFO

Article history:
Received: 06 March 2023
Accepted: 24 July 2023
Published: 27 October 2023

DOI: https://doi.org/10.47836/pjst.31.S1.02

E-mail addresses:
khuganmoghan98@gmail.com (Khuganeshwaran Mogan)
ridhwan@utem.edu.my (Ridhwan Jumaidin)
ahmadilyas@utm.my (Rushdan Ahmad Ilyas)
zatilhafila@gmail.com (Zatil Hafila Kamaruddin)
*Corresponding author

ISSN: 0128-7680
e-ISSN: 2231-8526

For the water solubility test, the solubility of 50 wt% is the best. Based on the findings, integrating coconut fiber into the modified thermoplastic cassava starch increases the composite properties relative to the non-reinforcement matrix material starch.

Keywords: Biodegradation, coconut fiber, soil burial, thermoplastic starch

INTRODUCTION

Due to the fast development of technology, the environment was exposed to many types of pollution, including microplastic pollution due to synthetic petroleum-based polymer plastics. Thus, engineers and scientists are collaborating to introduce novel biomaterials to reduce environmental harm. Currently, biopolymers reduce pollution, which can be decomposed easily. Recent research focuses on producing a substance composed of starch biopolymers (Abotbina et al., 2022). Starch is one of the best-promised raw materials for biodegradable growth, which can be naturally available carbohydrates from various cultivations (Punia Bangar et al., 2021). Native starch usually exists in a common granule structure with 15–45% crystallinity. Besides that, starch is one of the most important materials used to produce thermoplastic starch with the help of plasticizers as the reinforcement to enhance the mechanical properties, physical properties, and thermal properties of the biopolymer (Diyana et al., 2021; Fuqua et al., 2012; Tarique et al., 2021). The starch can be transformed into thermoplastic, TPS, under high temperature and shear (Yoksan et al., 2022). Thermoplastic starch can produce a naturally reinforced composite using natural fibers (Diyana et al., 2021). The chemical similarities of starch and plant fiber provide strong compatibility when the natural fibers combined with TPS enhance their mechanical properties.

One disadvantage of thermoplastic starch (TPS) for packaging is that it is not as strong as other plastic materials, such as polyethylene, and may break down over time (Ilyas et al., 2018). Additionally, TPS is biodegradable only under certain conditions, such as industrial composting, which may not be readily available. As a result, TPS packaging may not be as durable or sustainable as other plastic packaging options. Many materials can reinforce the composite material (Fuqua et al., 2012). These criteria of the natural fiber encouraged the researchers to develop natural fiber to become natural composites. Due to the low economic development and improving rural areas, natural fiber-reinforced composites have become the prime factor in reducing the world's need for petroleum-based materials (Fuqua et al., 2012).

Adding commercial cellulose fiber or micro-fiber improves the water resistance of the TPS (Ma et al., 2005). Recent studies have shown that the use of natural fiber in the composite will increase the capacity of traditional thermoplastics; it is identified that coconut husk fiber can be used to produce a better and improved quality of reinforced composite with the aid of a plasticizer in the mixture (Mościcki et al., 2012; Thinkohkaew

et al., 2020). In a previous study reported by Jústiz-Smith et al. (2008), the tensile strength values of coconut fibers are comparable to those reported in the literature (Eichhorn et al., 2001), although in the case, the mean value of coconut fiber was smaller than 175 MPa. Previous research suggested that natural fiber, by physical and mechanical characteristics such as tensile strength, is stronger than synthetic fiber. The cellulose content accounts for the high tensile strength of composite materials; thus, materials fabricated from these fibers show good mechanical properties and can be used when the strength is important (Jústiz-Smith et al., 2008). Natural composites are given huge attention for the development of the perceived negative impact of plastics in solid waste disposal (Willett, 2009). Improving bio-natural composite material is supposed to reduce the environmental emissions caused by traditional thermoplastics and introduce better materials that are safer and pollution-free for the users and nature. Several studies were conducted to analyze the potential of natural fiber-reinforced composites. According to a study by Jumaidin et al. (2021), thermoplastic starch was reinforced with banana leaf fiber, significantly enhancing its mechanical properties. Meanwhile, a study conducted by Hazrati et al. (2021) utilized thermoplastic starch and *Dioscorea hispida* fiber to demonstrate that the modification of thermoplastic starch resulted in enhanced material properties. The water solubility of the biocomposite has decreased while its mechanical properties have increased.

Beeswax is wax that occurs naturally and can be obtained from a bee's hive. It is generally known as the most effective hydrophobic organic molecule that may be utilized for reducing water sensitivity. Examining raw beeswax quality is based on its physical color appearance, which indicates its product value. After manipulation, the freshly produced beeswax initially appears light or white but transforms to yellow, dark yellow, and brownish tones. However, the incorporation of beeswax into thermoplastic starch resulted in a reduction of the mechanical properties of the bio-composite due to poor compatibility (Zhang et al., 2018), attributed to the formation of a heterogeneous film and structural discontinuities upon the addition of beeswax. Therefore, the issue of incompatibility must be addressed when combining hydrophilic thermoplastic starch and hydrophobic beeswax. Incorporating natural fiber reinforcement within the thermoplastic starch/beeswax matrix presents a promising solution to address this issue.

Even though studies have reported using thermoplastic starch/beeswax as the matrix in composites, none has reported the utilization of coconut fiber as the reinforcement via the hot compression molding method. Thus, this study aims to investigate the effect of coconut fiber on the environmental properties and water affinity behavior of thermoplastic starch/beeswax composite.

MATERIALS AND METHODS

Materials

The coconut husk was obtained from the coconut farm and soaked in water for 2 weeks. The soaking process helped to extract the fiber as the filler. Then, the coconut husk has isolated the fiber from the rest of the coconut husk. The collected coconut fiber was sun-dried for 1 day to ensure the fiber dried completely. The fiber is then ground to produce a short fiber of approximately 1 cm long with a diameter range of 125 to 300 microns. The fiber is then put in an oven at a temperature of 105°C for 5 hours to eliminate the moisture content of the fiber. Cassava starch obtained was purchased from Antik Sempurna Sdn. Bhd., Shah Alam; *Glycerol* was obtained from QReC (Asia) Sdn. Bhd., Rawang with an AR grade of 99.5% and beeswax was obtained from Aldrich Chemistry.

Sample preparation

Prior to the composite's preparation, thermoplastic cassava starch (TPCS) was mixed with 5% beeswax to reduce the moisture sensitivity of the material. Then, TPCS/Beeswax with coconut fiber was modified by incorporating different amounts of coconut fiber (0, 10, 20, 30, 40, 50 wt.%) into the polymer matrix. The mixture was pressed at 145°C for approximately 1 hour and a cooling process at 30°C for about 15 minutes. The hot pressing was carried out using Go Tech hydraulic testing.

Scanning Electron Microscopy (SEM)

A scanning electron microscope (SEM), Zeiss Evo 18 model, and a 10 kV acceleration voltage were used to analyze tensile fractured surfaces' morphology.

Fourier-Transform Infrared Spectroscopy (FTIR)

The Fourier-Transform Infrared Spectroscopy, FTIR, was used to analyze and detect the presence of the functional groups. The results of this test will be obtained using the JASCO FT/IR-6100 IR spectrometer Japan.

Thickness Swelling

The swelling analysis of the samples was conducted using the enhanced method developed by Jawaid et al. (2011). Five (10 mm × 10 mm × 3 mm) samples were cut and oven dried for 24 h at 105°C ± 2. The samples were immersed in distilled water at room temperature of 23°C ± 1, ranging from 30 minutes to 2 hours. The initial thickness of the sample was recorded as (T_i), and the final thickness of the samples was recorded as (T_f).

$$Thickness\ Swelling\ \%: [\{T_f - T_i\} / T_i]\ X\ 100\%$$

Moisture Content

The moisture content refers to the amount of water present in a sample. The water uptake capacity of each sample was assessed by measuring the weight loss according to the ASTM D 644-94 (1994). Moisture content was evaluated for five samples with measurement (10 mm x 10 mm x 3 mm). The weight of the specimens was registered for the initial weight, W_i, and placed into an oven to undergo the drying process for 24 hours at a temperature of 105°C. The final weight, W_f of the specimen, is recorded immediately after the specimen is removed from the oven to ensure the surrounding moisture will not be absorbed into the specimen while weighing the specimen.

$$Moisture\ Content\ \%: [\{W_f - W_i\} / W_i]\ X\ 100\%$$

Water Absorption

The investigation involved the analysis of water absorption using the ASTM D 570-98 (1998) approach. Five specimens, each measuring (10 × 10 × 3 mm), were subjected to a drying process for 24 hours in an air-circulating oven at a temperature of 105°C ± 2 to remove any residual moisture from the samples. Then, the samples were dipped into the water at room temperature of 23°C ± 1 with a range of time from 30 minutes to 2 hours. The specimens were weighed before, W_i, and after, W_f the immersion to obtain the water absorbed by the samples.

$$Water\ Absorption\ \%: [\{W_f - W_i\} / W_i]\ X\ 100\%$$

Moisture Absorption

Five (5) samples, each with dimensions of 10 x 10 x 3 mm, were prepared. The samples were dried in a vacuum oven at 105°C for 24 hours. After drying, the samples were cooled in a desiccator until they reached constant weight and practical equilibrium. The samples were placed in a relative humidity chamber at 75% and 25°C. The humidity chamber was obtained from GOTECH, GT-7005, China. For the removal of the existing moisture from the samples, the samples were dried in a circulating oven for 24 hours at a temperature of 10°C. The mass of the sample was reported before Mi and after Mf in the humidity chamber phase.

$$Moisture\ Absortion\ \%: [\{M_f - M_i\} / M_i]\ X\ 100\%$$

Density Test

The composite's density measurement was conducted per the ASTM D1895 standard. Five

specimens, each measuring 10 x 10 x 3 mm, were prepared and subjected to drying for 24 hours in an oven maintained at a temperature of 105°C to remove the existing moisture content in the specimen. Then, the densimeter weighed the samples, and the reading was recorded. Later, the specimens were inserted into the water inside the densimeter to identify the specimen's density and volume.

$Density$: $Mass$ / volume

Environmental Testing

Environmental testing is the performance measurement of the material under a specified condition caused by the environment. Two tests were conducted, such as water solubility and soil burial, to analyze the weight loss of the sample after undergoing the testing accordingly.

Water Solubility

The water solubility analysis of the samples was performed using the methodology developed by Zhang et al. (2018) with minor adjustments. Five samples measuring (10 mm x 10 mm x 3 mm) were cut, and the initial weight of the specimens was recorded. Secondly, the specimens were immersed in a container of 30 ml of distilled water and stirred slowly. Once the process was complete, the remaining sample was removed from the container, and the surface water of the sample was cleaned by covering filter paper on the specimen's surface. The samples were dried again for 24 hours at 105°C ± 2 to assess the final weight of the specimens.

$Water\ Solubility$ %: $[\{W_f - W_i\} / W_{i]}\ X\ 100\%$

Soil Burial

The biodegradation test was conducted using the methodology adopted by Jumaidin et al. (2020). The soil mixture was 50% sand and 50% soil obtained. The water content of the soil and the mixture were kept within the range of 30–40% by adding 400 ml of water per day to 1250 g of the mixture. A plastic green mesh was used to cover the sample before burial to ease the removal of the specimen from the soil, which will ensure there is an allowance for the microorganisms and moisture to be in contact with the samples. Firstly, the specimens were weighed to get the initial weight, W_i, before the testing. Secondly, the specimens were covered with soil and stapled together with plastic green mesh before the specimens were buried. Then, the specimens were buried into the polybag with a depth of 10 cm. Fourthly, the specimens were removed from the polybag at specified intervals and

cleaned with distilled water to remove impurities from the sample surface. The specimens were dried for 24 hours in a circulating oven at a temperature of 105°C. The specimens were dried for 24 hours in a circulating oven at a temperature of 105°C and weighed to get the final sample weight, $W_{f.}$

$$Soil\ Burial\ \%: [\{W_f - W_i\} / W_i]\ 100\%$$

RESULT AND DISCUSSION

Scanning Electron Microscopy (SEM)

SEM images of thermoplastic starch reinforced with coconut fiber (0, 10, 20, 30, and 50 wt%) are displayed in Figure 1. In the 0 wt% specimen, the surface of the specimen was observed to be in glossy granular patterns due to the presence of beeswax changes in the composition of the starch. For the specimen with 10 wt% coconut fiber, a crack line can be found on the specimen, acting as phase separation. Thus, the strength between the specimens is weak, and the specimen has no reinforcement. Specimen with 20 wt% fiber, there is no separation between the fiber and the matrix as the fiber mixed homogeneously with the matrixes. Specimen with 30 wt% shows a good adhesion of the matrix and coconut fiber, and specimen with 50 wt% shows the presence of void and fiber breakage as the percentage of fiber increases.

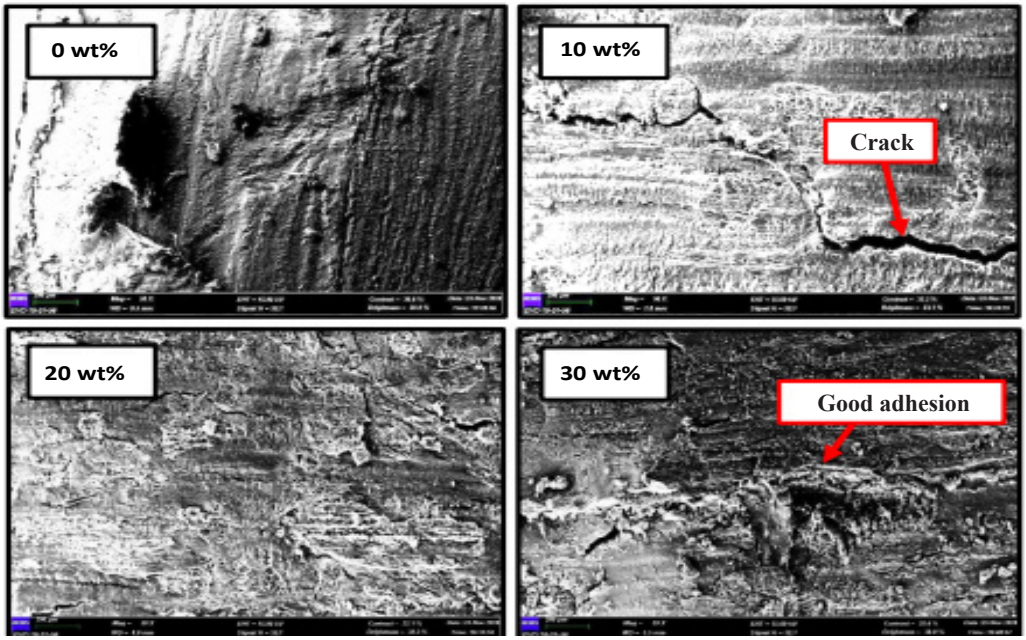

Figure 1. SEM micrograph of TPCS reinforced with coconut fiber

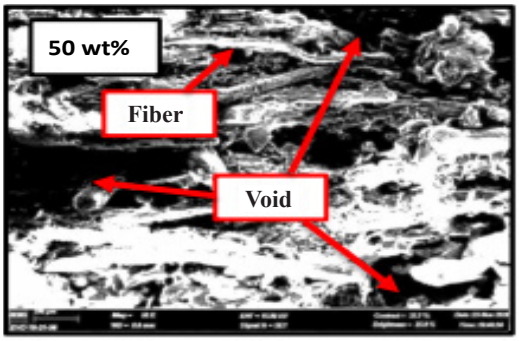

Figure 1. Continue

Fourier-Transform Infrared Spectroscopy (FT-IR)

The pattern of the composites was similar to other fiber composites, even though they had different percentages of fiber. It indicates that combining other materials with starch to form a composite will not be influenced by the starch's chemical composition. The main goal of the FT-IR test was to characterize the chemical bonding of TPCS with cassava starch.

Figure 2 shows the results obtained from the FTIR test on the TPCS and its composite reinforced with coconut fiber. The starch and coconut fiber have contributed to the presence of a hydrogen-bonded hydroxyl group, O-H, which was 3400–3200 cm^{-1}. According to Venkatachalam et al. (2016) findings, the involvement of amylose and amylopectin in jute fiber has been shown to affect the presence of the O-H group in the spectrum. The specimen was also present in the C-H range of aliphatic hydrocarbon groups found in the 2936–2916 cm^{-1} range. The C-H bonding found with 20 to 50 wt% found a decrease from 2919.9 cm^{-1} to 2919.0 cm^{-1}. These findings agree with the study by Alawar et al. (2009), which reported that the presence of the C-H band comes from natural fiber components such as cellulose and hemicellulose. Other than that, the N-H range of hydrocarbon groups was found in

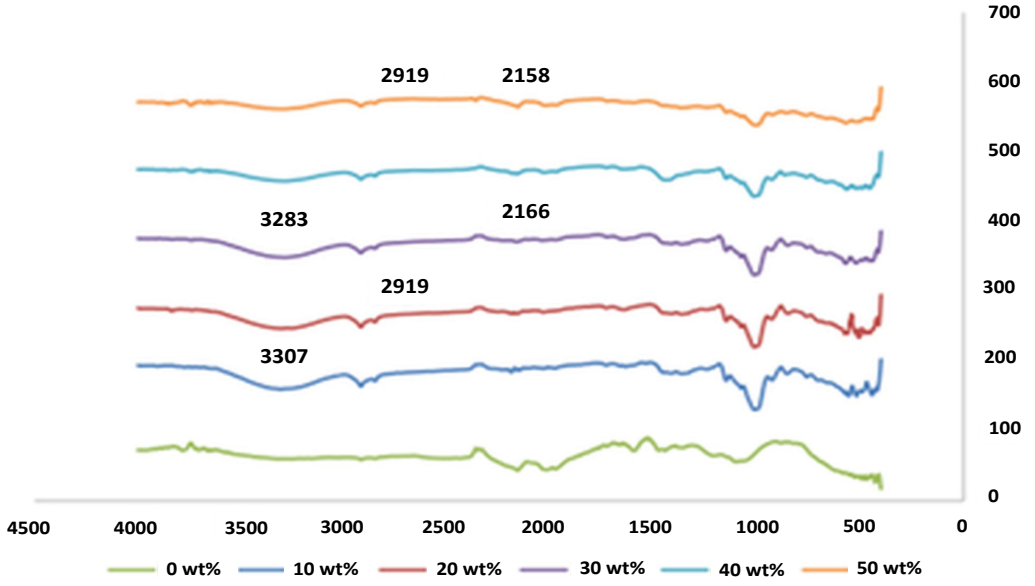

Figure 2. Results obtained from conducting the FTIR test on the TPCS reinforced with coconut fiber

the 2806-2000 cm^{-1} range. The peak found a continuous decrease from specimen 30 wt% to 50 wt% from 2166.6 cm^{-1} to 2158.0 cm^{-1}.

Meanwhile, a small change in the rotation of the O-H bands could be observed as the percentage of fiber loading increases. Specimen with 10 wt% fiber peaks at 3307 cm^{-1}; as the percentage increases, the peak changed to lower the wavenumber as observed with 30 wt% fiber specimens, the peak at 3283.2 cm^{-1}. According to the study conducted by Alawar et al. (2009), the increase of intermolecular hydrogen bonding has been clarified to influence the peak of the spectral band. The results reveal that the TPCS/BW matrix is compatible with the coconut fiber.

Thickness Swelling

Figure 3 shows the thickness swelling for TPCS and its composites. The specimen with a higher fiber proportion was found to swell less. For 30 minutes and 2 hours, the amount of thickness swelling of the specimen with 0 wt% fiber is 21.69% and 39.32%, respectively, and for the specimen with 50 wt% fiber is 6.96% for 30 minutes and 14.17% for 2 hours, respectively. The thickness swelling value for 30 minutes keeps decreasing from 30 wt% to 50 wt% while the swelling value for 2 hours, from 30 to 50 wt%, overall decreasing. This finding concludes that the swelling of the specimen decreases with the rise in the percentage of fiber loading due to the presence of a void in the specimen (Masoodi & Pillai, 2012). A void in the composite influences the specimen's dimensional stability and causes the specimen to start to delaminate because it absorbs water (Masoodi & Pillai, 2012).

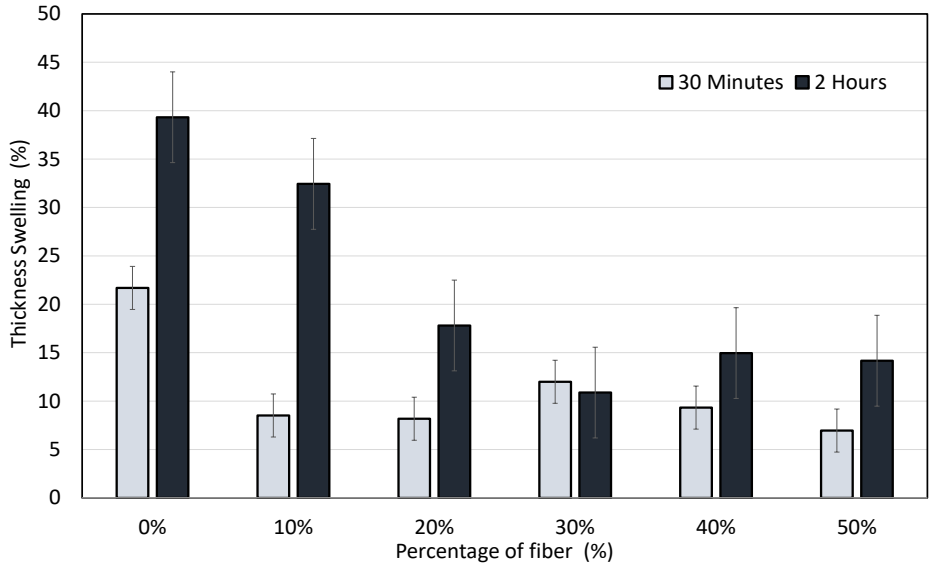

Figure 3. Thickness swelling results from TPCS reinforced with coconut fiber

The observed outcome can be ascribed to fiber in the composites, which exhibits a stiffer configuration than starch, thus imparting greater dimensional stability to the composites (Kamaruddin et al., 2023).

Moisture Content

The moisture content testing is important to conduct in composites' consistency, development, and degradation. Determination of the moisture content is also important for the uniform measurement of the content of other composite materials. The moisture content was tested to determine the amount of moisture in the TPCS matrix specimen and its composite. The moisture content in the composite is influenced by the form of hydrophilic material used, such as glycerol, starch, and fiber (Mubashar et al., 2009).

On the other hand, the moisture content in the composite can impact physical and environmental properties such as water absorption, moisture absorption, water solubility, and biodegradation (Wang et al., 2006). The moisture content analysis indicates that fiber incorporation raises the composite's moisture content due to the hydrophilicity of coconut husk fiber. According to the study conducted by Wang et al. (2006), composites with 40%, 50%, 55%, and 60% fiber loads did not demonstrate the level of which signals the equilibrium moisture absorption.

Figure 4 shows that the specimen with the highest moisture content is 0 wt%, and the lowest moisture content is 40 wt%. The results show that fiber integration reduces the moisture content of the composite, but only for 50 wt% fiber content shows rise, attributed to void. According to the study by Joshi et al. (2004), it was found that the moisture content of TPCS is lower compared to the specimen with natural fiber mixed with TPCS. It proves that the presence of natural fiber increases the moisture content of the composites.

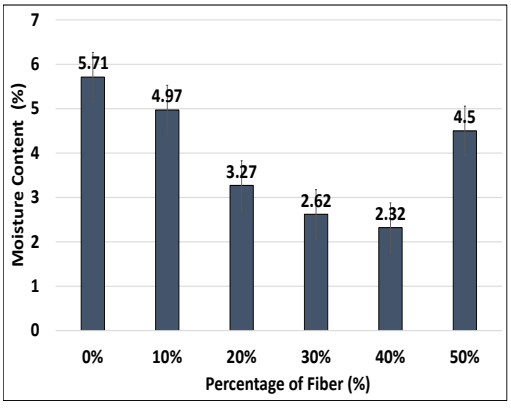

Figure 4. Moisture content results for TPCS reinforced with coconut fiber

Water Absorption

Water absorption of natural composites is a significant concern for their future outdoor applications. Coconut husk fiber water absorption reinforced unsaturated polyester composites following so-called pseudo-Fickian conduct were found (Akil et al., 2009).

Based on testing results, reducing water absorption depended mainly on matrix affinity. Compared to water, the fiber results in a better interface bonding between the

fiber matrix and the bonding created by the higher fiber loading, which prevents water from spreading into the matrix (Akil et al., 2009).

The water absorption ability of the TPCS matrix and its composite when immersed in water for 30 minutes and 2 hours are shown in Figure 5. For most specimens, water absorption results in 40 to 46% absorption when submerged in water for 30 minutes, which shows no substantial difference.

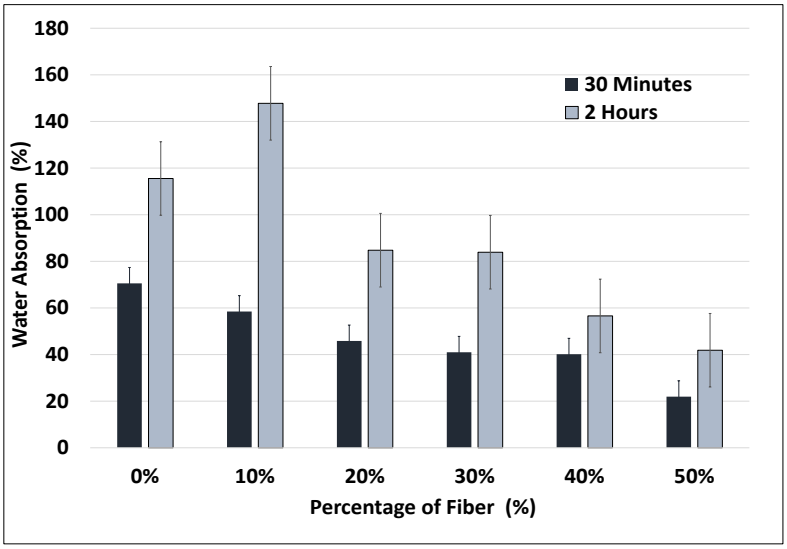

Figure 5. Water absorption result for TPCS reinforced with coconut fiber

As for the specimens submerged in water for 2 hours, it was observed that as fiber content increases, the amount of water absorbed decreases, but only for 10 wt% fiber; there is a rise due to phase separation, as mentioned in SEM micrograph analysis.

The lowest water absorbed in the specimen is fiber, with 50 wt% valued as 41.84% water absorbed. Generally, the 30-minute and 2-hour water absorption graphs show a constant decrease in the amount of water absorbed. Specimen with 30 wt% fiber for 30 minutes absorbed 40.97% of water while absorbed 83.9% of water for 2 hours testing time. According to the study conducted by van Bavel (1996), higher cellulose content in natural fiber can help to increase water absorption.

Moisture Absorption

According to the study conducted by Kim et al. (2016), the rate of absorption of moisture is the rate of transport of water molecules through molecules that can be caused by certain conditions, such as the diffusion coefficient, the state of the atmosphere or equilibrium, and even the dimension of the substance itself. A moisture absorption test is important to be carried out in a composite to identify the rate of moisture absorption by the composite.

This finding is in agreement with the study by Kim et al. (2016), which reported that the absorption of moisture in thermoplastic material is one of the major causes of thermoplastic failure because the presence of moisture absorbed from the environment in the TPS causes the formation of hydrogen intermolecular bonding with the fiber, which weakens the matrix and the fiber interfacial bonding. According to Kim et al. (2016), a weaker matrix and fiber interfacial bonding will cause the rate of water absorption to increase dramatically.

Figure 6 shows the results obtained by conducting a moisture absorption test. Overall results show that the sample completely absorbed the moisture to its potential, suggesting that the sample was extremely hygroscopic. However, the specimen with 0 wt% fiber has the least moisture absorption in terms of fiber loading, and the specimen with 10 wt% has the highest moisture absorption within 5 days. It was found that composite with 20 wt% to 50 wt% fiber has a lower percentage of moisture absorption by 14.17% for 20 wt% fiber, 12.47% for 30 wt% fiber, 10.81% for 40 wt% fiber, and 11.14% for 50 wt% fiber, respectively. The results obtained for 0 wt% are lower than the other fiber loading specimens due to the low interfacial bonding of the specimens' matrix and the presence of the void in the specimen.

This result is correlated with the water absorption test, proving that the interfacial bonding of the specimen's matrix and fiber is better with an increasing percentage of fiber in the specimen. The hydrophilic properties of the fiber cause the moisture absorption of the specimen. This finding agrees with the study by Wang et al. (2006); due to the strong hydrophilic characteristics of bamboo, the increasing amount of bamboo fiber in the TPS and the bamboo composite increase the absorption rate.

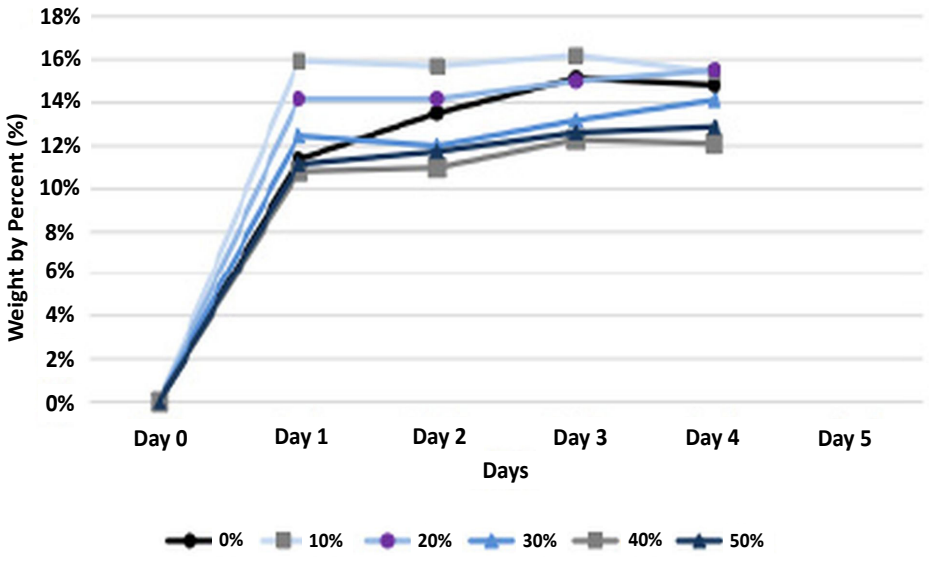

Figure 6. Moisture absorption of TPCS reinforced with coconut fiber

Density Test

According to the study conducted by Kilinç et al. (2017)**,** the strength of the natural composite directly affects the fiber density. Polymer molecular weight, fiber percentage, fiber processing processes, and fiber stretching specifically influence fiber density. Due to the ability of natural fiber to be low cost and low density, the mechanical properties of natural fibers are enhanced with fiber treatment (Bhatnagar et al., 2015).

Figure 7 shows the results obtained from the density test. The results overall increase when the percentage of the fiber increases. The density of the 0 wt% specimen is 1.401. The density of the 10 to 50 wt% was 1.303, 1.250, 1.232, 1.111, and 1.232 kg/m^3, respectively. The densimeter was used to obtain the density of the specimens. The density value of specimens increases as the fiber percentage increases.

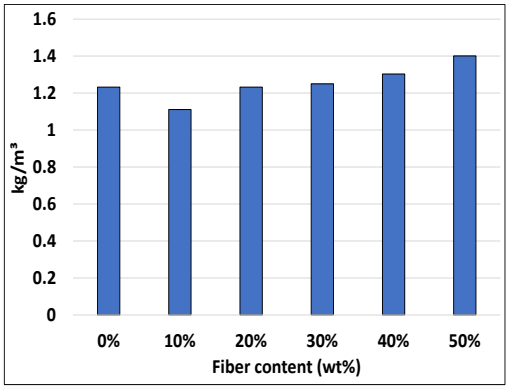

Figure 7. Density of TPCS reinforced with coconut fiber

This result was similar to the moisture content of the coconut fiber composite. This finding agrees with the study of Bhatnagar et al. (2015); the packing reduces due to the presence of long fibers in the composites, interrupting fiber flow and resulting in high void spaces. With the rise in fiber content, the void content in the composite increases. In natural fibers, large concentrations of the hydroxyl group make them polar and hydrophilic. This polar nature in natural fiber-based polymer composites also results in high moisture absorption, leading to fiber swelling and voids in the fiber-matrix interface.

Water Solubility

Another significant quality of using fibers as polymer reinforcement is the tendency of natural fiber to be soluble in water. To effectively soluble in water from natural fibers, it is important to understand the water solubility mechanisms in these materials (Väisänen et al., 2017). From the obtained results, it can be concluded that when the fiber content increases, the water solubility levels are lower.

Figure 8 shows the results of the water solubility of TPCS/BW and its composite. The results show a continuous decrease in the water solubility of the specimen as the fiber percentage increases. The specimen with 0 wt% values water solubility percentage of 46.31%, the specimen with 10 wt% fiber values water solubility percentage of 64%, while 20 to 50 wt% values at 59.38%, 57.95%, 48.22%, and 28.57%, respectively. These

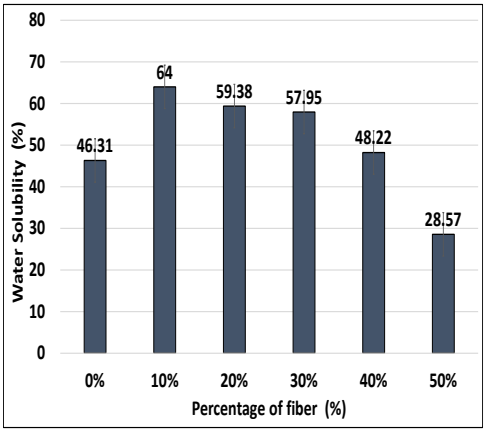

Figure 8. Results of the water solubility of TPCS reinforced with coconut fiber

results are similar to moisture absorption testing. According to the study by Ma et al. (2005), the increasing percentage of fiber in a composite may decrease the solubility of the composite.

This finding is in agreement with the study by Akil et al. (2011), which reported that it is likely that the interfacial bonding of the matrix and fiber is stronger with a higher percentage of fiber, similar to the results obtained from the moisture absorption test. The high fiber usage in the specimen could impair the excluded outcome. Additionally, this observation is consistent with prior research on the development of cornhusk/ sugar palm fiber reinforced corn starch-based hybrids, which indicated that adding sugar palm fiber resulted in reduced sample solubility (Ibrahim et al., 2020).

Soil Burial

"Biodegradation" in the biomedical sector refers to hydrolyzes and oxidations, the main mechanisms of polymer degradation (Mumtaz et al., 2010). Based on Kalka et al. (2014), polymer biodegradation can involve various steps, including polymer degradation by decomposing organisms.

Referring to the results obtained, a mass reduction for the specimens showed a decreasing trend with the increased fiber loading. The soil burial test was similar to the water absorption test result (Mansor et al., 2015). A study by Mumtaz et al. (2010) showed that certain natural fiber composites slow the degradation rate as the fiber percentage increases. This finding agrees with the study by Kalka et al. (2014), which reported that the growth in date palm and flax fiber in the composite reinforced corn starch indicates a decline in the mass reduction percentage. It can be assumed that the higher the fiber content in the samples, the lower the sample's percentage of mass reduction.

Figure 9 shows the results gathered from 4 weeks of soil burial tests. The overall result shows a reduction in the mass of the specimen. For the specimen with 0 wt%, the mass reduction is 45.11%, and the lowest is a specimen with 20 wt% values at 40.33%. In addition, the specimen with fiber content from 30 to 50 wt%, values 50.39%, 50.12%, and 38.85% respectively. This overall result can be obtained compared to the water absorption result. The specimen with 10 wt% fiber mass reduction is higher than the other fiber content specimen due to a void in the specimen.

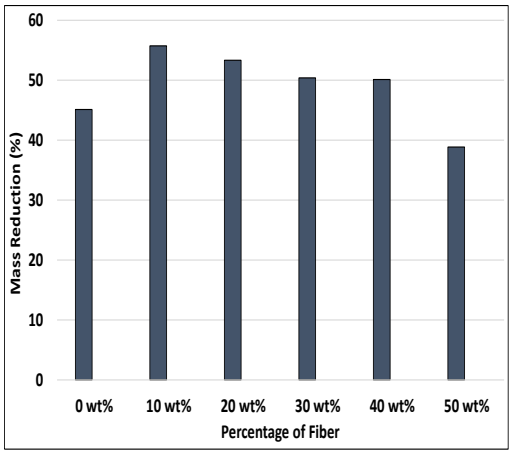

Figure 9. Mass reduction (%) from the soil burial test for TPCS reinforced with coconut fiber

CONCLUSION

Thermoplastic starch reinforced with coconut fiber was successfully prepared through dry mixing and hot-pressing. It was found that incorporating coconut fiber has reduced the water absorption and moisture content of the thermoplastic starch matrix. A decrease in the material's thickness, swelling, and solubility accompanied this finding. Composites with 50 wt% fiber show the least water absorption and swelling percentage. This result can be associated with improving the material's dimensional stability, which is less hydrophilic than the neat thermoplastic starch matrix. Soil burial results show that higher fiber content led to lower degradation activity of the material, where 50% fiber shows the lowest weight reduction. Overall, incorporating coconut fiber has reduced the hydrophilicity characteristic of the material, increasing the potential of this composite as an alternative material for more environmentally friendly bioplastic products.

ACKNOWLEDGMENTS

The author thanks Universiti Teknikal Malaysia Melaka, Malaysia for the financial support from research grant PJP/2021/FTKMP/S01815.

REFERENCES

Abotbina, W., Sapuan, S. M., Sultan, M. T. H., Alkbir, M. F. M., & Ilyas, R. A. (2022). Extraction, characterization, and comparison of properties of cassava bagasse and black seed fibers. *Journal of Natural Fibers*, *19*(16), 14525-14538. https://doi.org/10.1080/15440478.2022.2068103

Akil, H. M., Cheng, L. W., Mohd Ishak, Z. A., Abu Bakar, A., & Abd Rahman, M. A. (2009). Water absorption study on pultruded jute fibre reinforced unsaturated polyester composites. *Composites Science and Technology*, *69*(11-12), 1942-1948 https://doi.org/10.1016/j.compscitech.2009.04.014

Akil, H. M., Omar, M. F., Mazuki, A. A. M., Safiee, S., Ishak, Z. A. M., & Abu Bakar, A. (2011). Kenaf fiber reinforced composites: A review. *Materials and Design*, *32*(8–9), 4107–4121. https://doi.org/10.1016/j.matdes.2011.04.008

Alawar, A., Hamed, A. M., & Al-Kaabi, K. (2009). Characterization of treated date palm tree fiber as composite reinforcement. *Composites Part B: Engineering*, *40*(7), 601-606 https://doi.org/10.1016/j.compositesb.2009.04.018

Bhatnagar, R., Gupta, G., & Yadav, S. (2015). A Review on composition and properties of bagasse fibers. *International Journal of Scientific & Engineering Research*, *6*(5), 143-147.

Diyana, Z. N., Jumaidin, R., Selamat, M. Z., Ghazali, I., Julmohammad, N., Huda, N., & Ilyas, R. A. (2021). Physical properties of thermoplastic starch derived from natural resources and its blends: A review. *Polymers*, *13*(9), 5–20. https://doi.org/10.3390/polym13091396

Eichhorn, S. J., Baillie, C. A., Zafeiropoulos, N., Mwaikambo, L. Y., Ansell, M. P., Dufresne, A., Entwistle, K. M., Herrera-Franco, P. J., Escamilla, G. C., Groom, L., Hughes, M., Hill, C., Rials, T. G., & Wild, P. M. (2001). Current international research into cellulosic fibres and composites. *Journal of Materials Science*, *36*(9), 2107–2131. https://doi.org/10.1023/A:1017512029696

Fuqua, M. A., Huo, S., & Ulven, C. A. (2012). Natural fiber reinforced composites. *Polymer Reviews*, *52*(3–4), 259–320. https://doi.org/10.1080/15583724.2012.705409

Hazrati, K. Z., Sapuan, S. M., Zuhri, M. Y. M., & Jumaidin, R. (2021). Preparation and characterization of starch-based biocomposite films reinforced by *Dioscorea hispida* fibers. *Journal of Materials Research and Technology*, *15*, 1342–1355. https://doi.org/10.1016/j.jmrt.2021.09.003

Ibrahim, M. I. J., Sapuan, S. M., Zainudin, E. S., & Zuhri, M. Y. M. (2020). Preparation and characterization of cornhusk/sugar palm fiber reinforced corn starch-based hybrid composites. *Journal of Materials Research and Technology*, *9*(1), 200–211. https://doi.org/10.1016/j.jmrt.2019.10.045

Ilyas, R. A., Sapuan, S. M., Ishak, M. R., & Zainudin, E. S. (2018). Development and characterization of sugar palm nanocrystalline cellulose reinforced sugar palm starch bionanocomposites. *Carbohydrate Polymers*, *202*, 186–202. https://doi.org/10.1016/j.carbpol.2018.09.002

Jawaid, M., Khalil, A. H. P. S., Khanam, N. P., & Bakar, A. A. (2011). Hybrid composites made from oil palm empty fruit bunches/jute fibres: Water absorption, thickness swelling and density behaviours. *Journal of Polymers and the Environment*, *19*(1), 106–109. https://doi.org/10.1007/s10924-010-0203-2

Joshi, S. V., Drzal, L. T., Mohanty, A. K., & Arora, S. (2004). Are natural fiber composites environmentally superior to glass fiber reinforced composites? *Composites Part A: Applied Science and Manufacturing*, *35*(3), 371–376. https://doi.org/10.1016/j.compositesa.2003.09.016

Jumaidin, R., Ahmad Diah, N., Alamjuri, R. H., Ahmad Rushdan, I., & Yusof, F. A. (2021). Processing and characterisation of banana leaf fibre reinforced thermoplastic cassava starch composites. *Polymers*, *13*(9), 1420. https://doi.org/https://doi.org/10.3390/ polym13091420

Jumaidin, R., Khiruddin, M. A. A., Asyul Sutan Saidi, Z., Salit, M. S., & Ilyas, R. A. (2020). Effect of cogon grass fibre on the thermal, mechanical and biodegradation properties of thermoplastic cassava starch biocomposite. *International Journal of Biological Macromolecules*, *146*, 746–755. https://doi.org/10.1016/j.ijbiomac.2019.11.011

Jústiz-Smith, N. G., Virgo, G. J., & Buchanan, V. E. (2008). Potential of Jamaican banana, coconut coir and bagasse fibres as composite materials. *Materials Characterization*, *59*(9), 1273–1278. https://doi.org/10.1016/j.matchar.2007.10.011

Kalka, S., Huber, T., Steinberg, J., Baronian, K., Müssig, J., & Staiger, M. P. (2014). Biodegradability of all-cellulose composite laminates. *Composites Part A: Applied Science and Manufacturing*, *59*, 37-44. https://doi.org/10.1016/j.compositesa.2013.12.012

Kamaruddin, Z. H., Jumaidin, R., Kamaruddin, Z. H., Asyraf, M. R. M., Razman, M. R., & Khan, T. (2023). Effect of *Cymbopogan citratus* fibre on physical and impact properties of thermoplastic cassava starch/ palm wax composites. *Polymers*, *15*(10), 2364. https://doi.org/10.3390/polym15102364

Kilinç, A. Ç., Durmuşkahya, C., & Seydibeyoğlu, M. Ö. (2017). Natural fibers. In M. O. Seydibeyoğlu, A. K. Mohanty., & M. Misra (Eds.) *Fiber technology for fiber-reinforced composites* (pp. 209-235). Woodhead Publishing. https://doi.org/10.1016/B978-0-08-101871-2.00010-2

Kim, S., Van Zyl, J., Johnson, J., Moghaddam, M., Tsang, L., Colliander, A., Dunbar, S., Jackson, T., Jaruwatanadilok, S., West, R., Berg, A., Caldwell, T., Cosh, M., Lopez-Baeza, E., Thibeault, M., Walker, J., Entekhabi, D., & Yueh, S. (2016, July 10-15). *Surface soil moisture retrieval using L-band SMAP SAR data and its validation*. [Paper presentation]. International Geoscience and Remote Sensing Symposium (IGARSS), Beijing, China. https://doi.org/10.1109/IGARSS.2016.7729028

Ma, X., Yu, J., & Kennedy, J. F. (2005). Studies on the properties of natural fibers-reinforced thermoplastic starch composites. *Carbohydrate Polymers*, *62*(1), 19–24. https://doi.org/10.1016/j.carbpol.2005.07.015

Mansor, M. R., Salit, M. S., Zainudin, E. S., Aziz, N. A., & Ariff, H. (2015). Life cycle assessment of natural fiber polymer composites. In K. R. Hakeem, M. Jawaid., & O. Y. Alothman (Eds.) *Agricultural biomass based potential materials* (pp.121-141). Springer. https://doi.org/10.1007/978-3-319-13847-3_6

Masoodi, R., & Pillai, K. M. (2012). A study on moisture absorption and swelling in bio-based jute-epoxy composites. *Journal of Reinforced Plastics and Composites*, *31*(5), 285–294. https://doi.org/10.0177/0731684411434654

Mościcki, L., Mitrus, M., Wójtowicz, A., Oniszczuk, T., Rejak, A., & Janssen, L. (2012). Application of extrusion-cooking for processing of thermoplastic starch (TPS). *Food Research International*, *47*(2), 291-299. https://doi.org/10.1016/j.foodres.2011.07.017

Mubashar, A., Ashcroft, I. A., Critchlow, G. W., & Crocombe, A. D. (2009). Moisture absorption-desorption effects in adhesive joints. *International Journal of Adhesion and Adhesives*, *29*(8), 751-760. https://doi.org/10.1016/j.ijadhadh.2009.05.001

Mumtaz, T., Khan, M. R., & Hassan, M. A. (2010). Study of environmental biodegradation of LDPE films in soil using optical and scanning electron microscopy. *Micron*, *41*(5), 430-438. https://doi.org/10.1016/j.micron.2010.02.008

Punia Bangar, S., Nehra, M., Siroha, A. K., Petrů, M., Ilyas, R. A., Devi, U., & Devi, P. (2021). Development and characterization of physical modified pearl millet starch-based films. *Foods*, *10*(7), 1609. https://doi.org/10.3390/foods10071609

Tarique, J., Sapuan, S. M., Khalina, A., Sherwani, S. F. K., Yusuf, J., & Ilyas, R. A. (2021). Recent developments in sustainable arrowroot (*Maranta arundinacea* Linn) starch biopolymers, fibres, biopolymer composites and their potential industrial applications: A review. *Journal of Materials Research and Technology*, *13*, 1191–1219. https://doi.org/10.1016/j.jmrt.2021.05.047

Thinkohkaew, K., Rodthongkum, N., & Ummartyotin, S. (2020). Coconut husk (*Cocos nucifera*) cellulose reinforced poly vinyl alcohol-based hydrogel composite with control-release behavior of methylene blue. *Journal of Materials Research and Technology*, *9*(3), 6602-6611. https://doi.org/10.1016/j.jmrt.2020.04.051

Väisänen, T., Das, O., & Tomppo, L. (2017). A review on new bio-based constituents for natural fiber-polymer composites. *Journal of Cleaner Production*, *149*, 582–596. https://doi.org/10.1016/j.jclepro.2017.02.132

van Bavel, C. H. M. (1996). Water relations of plants and soils. *Soil Science*, *161*(4). 257-260. https://doi.org/10.1097/00010694-199604000-00007

Venkatachalam, N., Navaneethakrishnan, P., Rajsekar, R., & Shankar, S. (2016). Effect of pretreatment methods on properties of natural fiber composites: A review. *Polymers and Polymer Composites*, *24*(7), 555-566. https://doi.org/10.1177/096739111602400715

Wang, W., Sain, M., & Cooper, P. A. (2006). Study of moisture absorption in natural fiber plastic composites. *Composites Science and Technology*, *66*(3), 379-386. https://doi.org/10.1016/j.compscitech.2005.07.027

Willett, J. L. (2009). Starch in polymer compositions. In J. BeMiller., & R. Whistler (Eds). *Starch (pp. 715-743)*. Academic Press. https://doi.org/10.1016/B978-0-12-746275-2.00019-7

Yoksan, R., Boontanimitr, A., Klompong, N., & Phothongsurakun, T. (2022). Poly(lactic acid)/thermoplastic cassava starch blends filled with duckweed biomass. *International Journal of Biological Macromolecules*, *203*, 369–378. https://doi.org/10.1016/j.ijbiomac.2022.01.159

Zhang, Y., Simpson, B. K., & Dumont, M. J. (2018). Effect of beeswax and carnauba wax addition on properties of gelatin films: A comparative study. *Food Bioscience*, *26*, 88–95. https://doi.org/10.1016/j.fbio.2018.09.011

Pertanika J. Sci. & Technol. 31 (S1): 39 - 57 (2023)

PERTANIKA JOURNALS

SCIENCE & TECHNOLOGY

Journal homepage: http://www.pertanika.upm.edu.my/

Improved Thermal and Mechanical Properties of Kenaf Fiber/ ABS Polymer Composites via Resin Coating Treatment

Macaulay Mfon Owen[1,2], Emmanuel Okechukwu Achukwu[3], Ahmad Zafir Romli[4,5], Muhammad Hanif Ramlee[6,7], Abdul Halim Abdullah[1], Solehuddin Shuib[1] and Hazizan Md Akil[8]*

[1]Biomechanical and Clinical Engineering (BIOMEC) Research Group, School of Mechanical Engineering, College of Engineering, Universiti Teknologi MARA, UiTM Engineering Campus, 40450 Shah Alam, Selangor, Malaysia

[2]Department of Polymer and Textile Technology, School of Technology, Yaba College of Technology, Yaba, 100001 Lagos, Nigeria

[3]Department of Polymer and Textile Engineering, Faculty of Engineering, Ahmadu Bello University, 810006 Zaria, Nigeria

[4]Centre of Chemical Synthesis and Polymer Composites Research and Technology, Institute of Science IOS, Universiti Teknologi MARA (UiTM), 40450 Shah Alam, Selangor, Malaysia

[5]Faculty of Applied Science, Universiti Teknologi MARA (UiTM), 40450 Shah Alam, Selangor, Malaysia

[6]Bone Biomechanics Laboratory (BBL), Department of Biomedical Engineering and Health Sciences, Faculty of Electrical Engineering, Universiti Teknologi Malaysia, 81310 UTM Johor Bahru, Johor, Malaysia

[7]Bioinspired Devices and Tissue Engineering (BIOINSPIRA) Research Group, Universiti Teknologi Malaysia, 81310 UTM Johor Bahru, Johor, Malaysia

[8]School of Materials and Mineral Resources Engineering, Universiti Sains Malaysia (USM), Engineering Campus, 14300 Nibong Tebal, Penang, Malaysia

ABSTRACT

In developing natural fiber composites (biocomposites), compatibility between natural cellulosic fibers and polymers has always created serious challenges, reducing performance. This study focused on applying a novel approach using epoxy resin as a coating medium to enhance the properties of the fibers and the interface between the hydrophobic polymer and the hydrophilic natural fiber. 10 wt% of uncoated kenaf fibers (KF) and coated kenaf (CKF) fibers were compounded with acrylonitrile butadiene styrene (ABS) thermoplastic polymer in a twin-screw extruder at an optimized temperature of 220°C under the same processing conditions. Fourier transform infrared spectroscopy (FTIR) and scanning electron microscopy (SEM) examined the coated and uncoated fibers' physicochemical compositions and

ARTICLE INFO

Article history:
Received: 06 March 2023
Accepted: 24 July 2023
Published: 27 October 2023

DOI: https://doi.org/10.47836/pjst.31.S1.03

E-mail addresses:
macaulay.owen@uitm.edu.my (Macaulay Mfon Owen)
eoachukwu@abu.edu.ng (Emmanuel Okechukwu Achukwu)
ahmad349@uitm.edu.my (Ahmad Zafir Romli)
m.hanif@utm.my (Muhammad Hanif Ramlee)
halim471@uitm.edu.my (Abdul Halim Abdullah)
solehuddin2455@uitm.edu.my (Solehuddin Shuib)
hazizan@usm.my (Hazizan Md Akil)
*Corresponding author

ISSN: 0128-7680
e-ISSN: 2231-8526

surface properties. The developed composites' thermal, mechanical, and microstructural characteristics were also examined, and the results revealed that the CKF/ABS composites had better interfacial bonding and mechanical characteristics than the uncoated KF/ABS composite. Coating natural fibers with epoxy resin is a novel technique for improving interfaces and developing environmentally friendly composites from natural sources.

Keywords: ABS composites, kenaf fibers, mechanical properties, resin coating, thermal degradation and stability

INTRODUCTION

Natural fibers are environmentally friendly because of their biodegradability and great intrinsic properties, making them suitable with great potential for various industrial applications (Achukwu et al., 2022; Akil et al., 2011; Doumbia et al., 2015; EI-Abbassi et al., 2019; Sapuan et al., 2013; Reddy et al., 2021). They are usually obtained from animals, minerals, or plants and include but are not limited to coir, silk, wool, kenaf, cotton, sisal, hemp, jute, bagasse, flax, and bamboo fibers (Gourier et al., 2017; Uzochukwu et al., 2020; Achukwu, Barnabas, et al., 2015). Thus, more research efforts are being made to replace synthetic fibers with natural fibers to make polymer composites that are environmentally friendly and affordable (Odesanya et al., 2021). Several industries and researchers are turning to lignocellulosic fibers from biomass waste to replace synthetic fibers and reinforced bio-based polymer composites. Due to their biodegradability, low carbon emissions, and accessibility, green composites are becoming more prevalent in the composites industry (Asyraf et al., 2023). Various green composites with good mechanical strength have been produced employing a variety of natural fibers and biodegradable polymer matrices (Asyraf et al., 2022; Ku et al., 2011; Ramesh et al., 2017).

These natural fibers, particularly jute and kenaf fibers from bast origins, are currently being utilized as reinforcement materials in high-temperature engineering thermoplastic composites with applications in the aviation and automotive sectors (Owen, Achukwu, Romli, & Akil, 2023). Natural fiber composites, including kenaf ones, have recently become popular because of their outstanding mechanical qualities. Compared to other natural fibers, kenaf fiber offers many advantages in strength and stiffness (Nurazzi et al., 2021). Due to the significant improvement in mechanical performance, researchers prefer to incorporate kenaf fibers with a polymer matrix (Radzuan et al., 2019). Furthermore, it benefits from reduced harmful fume emissions during production when heated. Therefore, hydrophilic natural fibers are poorly compatible with hydrophobic polymer matrixes. Due to this incompatibility, it is difficult to achieve effective fiber-matrix interface bonding, which results in poor load transfer between the matrices and reinforcing material (Asumani et al., 2012; Norrrahim et al., 2021). This flaw could degrade the composites' mechanical properties and prevent using natural fiber-based composites in load-bearing applications (Achukwu et al., 2023; Feng et al., 2020).

ABS polymer is a high-temperature plastic often processed at around 200–260°C, significantly impacting the finished products' performance. Reports on the thermo-physical characteristics of ABS kenaf composites have been presented in some studies. For instance, a study on the thermo-physical characteristics of kenaf-filled acrylonitrile butadiene styrene (ABS) composites was published by Nikmatin et al. (2017). They looked at the impact of kenaf short fiber and kenaf microparticle size on kenaf-ABS composites. According to their findings, the composite made of kenaf short fiber and ABS has the highest level of crystallinity. However, due to double bonds in the constituent polybutadiene, ABS is occasionally vulnerable to breakdown at high processing temperatures. To overcome this, ABS is frequently combined with various natural polymers that can lessen the impact of the processing temperature (Owen, Achukwu, Arukalam, & Romli, 2022).

When likened to other natural fibers, kenaf fibers have shown superior mechanical properties with applications in non-woven, molded, and extruded products, but the major challenge to their utilization is their incompatibility with hydrophobic polymers and degradation at high processing temperatures. These negatively affect their thermal and mechanical properties. Attempts have been made to address these challenges with varying degrees of success. Reported treatments such as alkalization and silanization have been valuable in solving some of the problems (Achukwu, Dauda, et al., 2015; Achukwu, Ochika et al., 2015; Kabir et al., 2012; Oushabi et al., 2017). Nevertheless, issues regarding degradations at increased processing temperatures have not yet been addressed, particularly with engineering thermoplastics like polybutylene terephthalate (PBT), acrylonitrile butadiene styrene (ABS), and polyethylene terephthalate (PET) (Mohammed et al., 2015; Owen, Achukwu, Akil, et al., 2022). Initial studies on natural fiber-reinforced recycled and virgin polyethylene terephthalate using the resin surface coating treatment revealed remarkable success in enhancing the thermal stabilities and interfacial contact of natural fibers with high-temperature thermoplastics (Owen, Achukwu, Hazizan, et al., 2022; Owen et al., 2018a).

The new surface coating technique was also used to improve the impact properties and thermal stability of leather fiber-filled ABS composites (Owen, Achukwu, Arukalam, Talib, & Romli, 2021; Owen, Achukwu, Arukalam, Muhammad, & Romli, 2021) at 240°C processing temperature. The finding presented the highest impact strength for the coated composite with a value of 0.126 KN/mm^2 at 5 wt% filler loading and more thermal stability than uncoated. It enhanced the processability of natural fibers at high temperatures (improvements in thermal stability), leading to the development of high-strength composites for engineering applications. Owen, Achukwu, Akil, et al. (2022) reported the effect of varying processing temperatures (200, 220, and 240°C) with constant fiber loading, using epoxy resin/hardener and an acetone ratio of 1:5 for coating the kenaf fibers. The tensile and flexural strengths of the epoxy-coated kenaf/ABS composite did not vary much as a

result of the processing temperatures; however, the composites' fatigue behaviors were significantly affected.

The present study presents the improvement in thermal and mechanical properties of resin-coated kenaf fibers in engineering ABS thermoplastic polymer at a single optimized processing temperature of 220°C, using an epoxy/hardener and acetone ratio of 1 (epoxy):4 (acetone) for coating, and the development of cheaper and greener kenaf fiber/ABS composites suitable for high-temperature engineering and load-bearing applications.

EXPERIMENTAL

Materials

Commercial-grade ABS polymer pellets with a density and melt flow index (MFI) of 1.05 g/cm^3 and 8.6 g/10 min, respectively, were provided by Toray Plastics Malaysia Sdn. Bhd., Prai and were employed as the binder. Raw kenaf fibers (KF) shown in Figure 1(b) were provided by the Malaysian Agricultural Research and Development Institute (MARDI), Malaysia. The coating medium (epoxy resin/hardener) and acetone (C_3H_6O) of analytical grade were supplied by Oriental Option Sdn. Bhd., Bayan Lepas, Penang and SYSTERM, Syah Alam, Selangor.

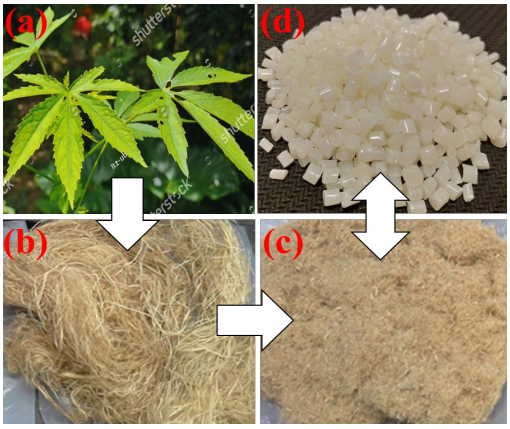

Figure 1. Visual representations of (a) kenaf plant, (b) kenaf fibers, (c) pulverized resin-coated kenaf fiber (5 mm size), and ABS polymer chips

Kenaf Fiber Processing and Resin Surface Coating Treatments

After being dried for 48 hours at 24 ± 1.5°C and 76 ± 1% relative humidity, the provided KF were ground into short fibers (5 mm) (Figure 1c) using the pulverizing apparatus (Fritsch Power Cutting Mill Pulverisette 15, Germany). The fibers were subjected to 6% NaOH for 3 hours to improve ABS compatibility, thermal resistance, and wettability and reduce moisture absorption tendencies of the kenaf fibers. The kenaf fibers were then neutralized with 1% acetic acid before being rinsed with distilled water to maintain a pH of 7. The fibers were dried in an oven for 12 hours at 70°C before being surface coated with epoxy resin made from a 2:1 mixture of epoxy resin and hardener. The resultant mixture was dissolved in acetone at a predetermined optimum ratio of 1 (epoxy):4 (acetone) (Owen et al., 2022c). The coated kenaf fibers were cured for 24 hours at 80°C.

Composites Preparation

At an ideal screw speed and processing temperature of 50 r/min and 220°C, respectively, acrylonitrile butadiene styrene (ABS) was compounded with 10 wt% kenaf fiber and melt-mixed using a twin-screw extruder (model PRISM TSE SYSTEMS 2094, UK). Before being compress-molded into composite sheets for 5 minutes at a continuous compression molding pressure of 65 kg/m^2, the extrudates were ground and dried at 80°C for 3 hours. The times for preheating, hot pressing, and cold pressing (cooled at 25°C) were 2, 3, and 5 minutes, respectively, before the final composite characterization.

Fiber and Composites Characterization

Tensile Testing of Kenaf Fibers. Before the development of the composite, a tensile test was performed on the uncoated kenaf fiber and the kenaf fiber coated with resin. An INSTRON (Shimadzu, Japan) equipped with a suitable load cell type 2511-317 with a maximum load of 10-500 kg was employed to assess the tensile properties (strength and elongation) of the kenaf fibers at a humidity and temperature of 65 ± 2% RH and 20 ± 2°C, respectively. Ten samples were randomly selected from the bale of kenaf fibers according to their maturity, fineness, and length. The linear density in tex was measured, and the fibers were subjected to a tensile strength test using a gauge length of 10 mm following the ASTM D3379 single fiber tensile test standard at a speed of 1 mm/min. Tests were conducted at a standard laboratory atmosphere of 23°C and 50% relative humidity. Ten specimens were tested, and the average value was reported.

Analysis of Kenaf Fibers Using Scanning Electron Microscopy. An SEM micrograph of the fiber surface was taken using a Hitachi Scanning Electron Microscope model (TM 3030 PLUS Japan) at a magnification of 500x and an accelerating voltage of 5–20 kV to investigate the impact of epoxy coating on morphological alterations of kenaf fibers.

Analysis of Kenaf Fibers Using Fourier Transform Infrared Spectroscopy. To look at changes in chemical structures and functional groups, FTIR spectroscopic analysis of both uncoated (KF) and resin-coated kenaf fibers (CKF) was performed using an FTIR spectrometer (Perkin Elmer Spectrum 400, USA). The samples' spectra between 4000 cm^{-1} and 400 cm^{-1} were examined.

Analysis of Kenaf Fibers Using Thermogravimetry. Before inclusion into ABS, thermogravimetric analysis (TGA) was used to evaluate the heat resistance and breakdown temperature of the resin-coated kenaf (CKF) with the uncoated fiber samples. Thermogravimetric analyzer type NETZSCH TG 209 F3 Tarsus Instrument, Germany, was used for this, and test procedures were carried out in line with ASTM D3850 Standards.

In a nitrogen gas environment, the temperature varied from 30 to 600°C at a heating rate of 10°C/min.

Mechanical Testing of the Kenaf Composites. According to ASTM D790 (2017) and ASTM D638-03 (2012), respectively, three-point flexural and tensile tests were performed using a SHIMADZU Autograph Precision Universal Tester (Model AG-X Series, Japan) in a typical laboratory environment of 50% relative humidity and 23°C. Five specimens that were accurately sized and cut out using a band saw were examined for tensile and flexural properties at crosshead speeds of 5 and 2 mm/min, respectively. Additionally, based on ISO 179-1 (2010) standards testing procedures, impact strength was tested using an impact machine of the INSTRON dynatup (model 9250HV USA) design. The strength of composite samples under sudden load applications was tested using this method. Each test employed five replicate specimens, and the findings shown are the average results of tests run on all the composite samples.

Analysis of Kenaf-ABS Composites Using Scanning Electron Microscopy. The microstructural characteristics of kenaf-ABS composites were examined using the SUPRA 40VP Model of the Field Emission Scanning Electron Microscope (ZEISS FE-SEM Germany). To prevent the weak resolution from electrostatic charge and increase the surface conductivity, a thin layer of platinum was sputter coated onto the broken surfaces of the tensile samples using a Quorum Sputter-Coater device (Quorum model Q150RS, UK). The photographs were taken at a 500x resolution with the samples angled at 30° for easier observation.

On an optical microscope (Olympus BX51TRF model, Japan) equipped with an optic camera, the optical pictures of ABS, uncoated kenaf (KF), and coated kenaf fibers (CKF) distributions in the ABS matrix composite system were studied at 10x and 20x magnifications.

RESULTS AND DISCUSSION

FTIR Analysis

The combined FTIR spectra for resin-coated-treated (CKF) and kenaf fiber (KF) are displayed in Figure 2.

The vibration peak intensities of kenaf fibers (KF) were found at 1028–1750 cm^{-1}, which revealed the presence of lignin, cellulose, and hemicelluloses with their broad bands, which was also mentioned by Asim et al. (2016). The CH_2 groups in hemicelluloses and cellulose's C-H stretching vibration are responsible for the absorption peaks at 2910 cm^{-1}. The hydroxyl-OH group can also be found at 3336 cm^{-1} in the kenaf fiber. The spectrum of surface-coated kenaf fiber (CKF) in Figure 2 shows a significant reduction in peak

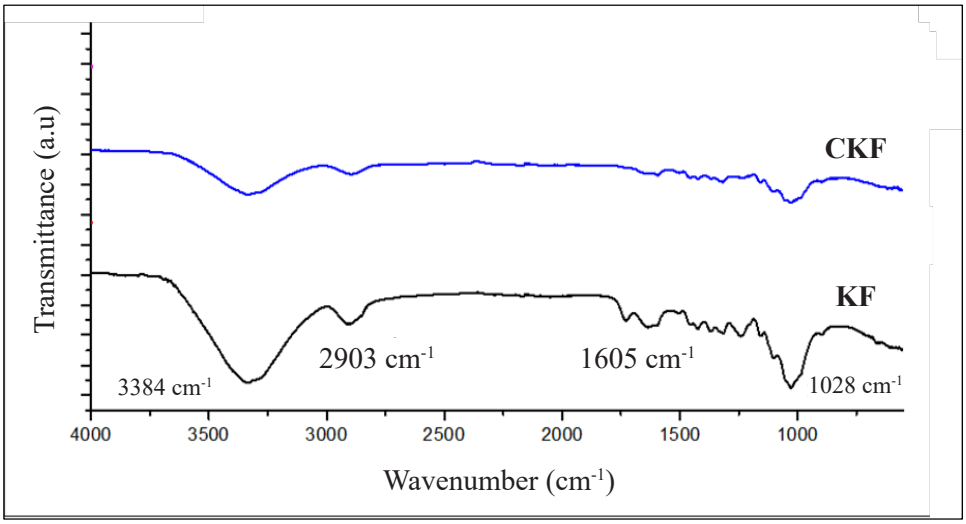

Figure 2. The combined spectra of resin coated kenaf (CKF) and raw kenaf (KF)

intensities, an indication of improved fiber surface concerning kenaf fibers as a result of resin coating treatment. The result means that the surface resin coating treatment has reduced the fiber's hydrophilicity and water intake characteristics without adversely altering the fiber's chemical content. The C=C stretch absorption band of the ester carbonyl group occurred at 1730 cm^{-1}, showing that an ester chain was formed between the hydroxyl group contained in the fiber and the epoxy resin-coated fiber (Razak et al., 2014). The fiber's epoxy resin and cellulosic hydroxyl group interacted well, leading to the missing peaks at 1730 cm^{-1} and 2910 cm^{-1}. Asim et al. (2016) also reported the presence of a vibrational peak between 3336 cm^{-1} and 3400 cm^{-1}, indicating a frequency due to the O-H group.

The aldehyde in lignin and the acetyl ester in hemicelluloses peaked at 1730 cm^{-1}. It was also observed that the spectra of resin-coated kenaf fibers (CKF), which revealed low peak intensity and its effect on lignin and hemicelluloses, are indications of successful coating treatment. Removing lignin, hemicelluloses, and wax effectively broadens the absorption peak at 3336 cm^{-1} relative to the untreated fiber. A large amount of the hydroxyl groups found in the kenaf fiber have been coated by the epoxy resin, which also served as a coupling agent in reducing the moisture absorption characteristics of the kenaf fibers after coating treatment. A similar observation on reduction in the hydroxyl group was reported by Tan et al. (2011) when empty fruit fibers were treated with maleic anhydride, which led to the formation of cross-linked networks.

Tensile Properties of Kenaf Fibers

From the results obtained in Table 1, it was observed that the coating has a significant effect on the tensile properties of kenaf fibers; the breaking load of kenaf fibers increased after coating, and the highest breaking load (29.78 N) was obtained compared to 27.63 N for the raw kenaf fibers at the same gauge length and fiber count.

Table 1

Tensile properties of uncoated and resin-coated kenaf fibers

Sample	Sample Description	Gauge length (mm)	Breaking Force (N)	Tenacity (N/tex)	Elongation (%)	Count (Ne)
Kenaf (KF)	Uncoated kenaf fibers	10	27.63 ± 0.6	71.58 ± 3	7.78 ± 0.2	38.6 ± 0.1
Coted kenaf (CKF)	Resin-coated kenaf fibers	10	29.78 ± 0.3	99.93 ± 5	6.64 ± 0.3	38.6 ± 0.2

Similar behavior can be said for the strength at break (tenacity), which increased to 99.93 N/tex from 71.58 N/tex with decreased elongation at break (7.78 to 6.64%). The decrease in elongation at break can be attributed to the coated surface losing its elasticity due to the encapsulation effect because bast kenaf fibers are long-staple natural fibers that contain numerous element fibers as well as a matrix of lignin and hemicelluloses in each fiber bundle (Asim et al., 2016).

Morphological Analysis of Kenaf Fibers by SEM

The micrographs of resin-coated kenaf fibers (CKF) and kenaf fibers (KF) are shown in Figures 3a and 3b, respectively.

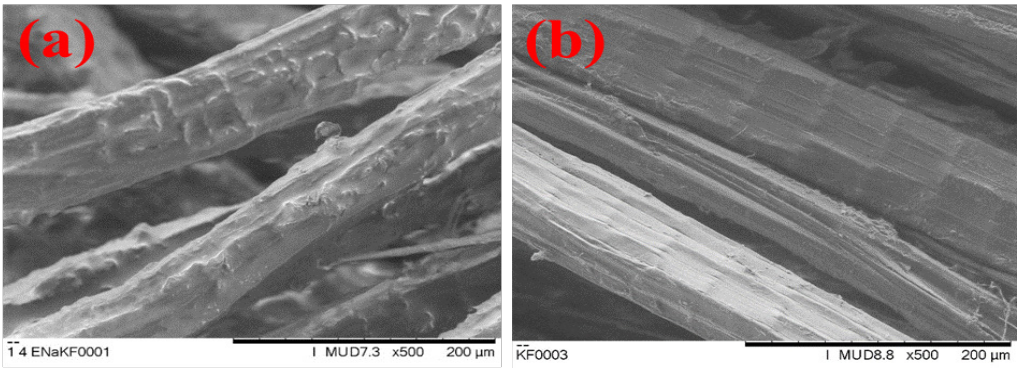

Figure 3. Morphology of (a) resin-coated kenaf fiber (CKF) and (b) kenaf fibers (KF)

It is detected that the resin-treated and coated kenaf fibers, CKF (Figure 3a), revealed some structural changes and a cleaned surface void of impurities as compared to the kenaf fibers due to surface coating treatment, which indicates that the initial fiber surface treatment with NaOH before resin coating treatment removed the surface lignin, hemicelluloses, and pectin substances resulting in rough topography, as also mentioned by Tan et al. (2011). The epoxy-coated kenaf fibers (CKF) also showed smooth surfaces, which confirmed the presence of a coating on the kenaf fibers (Figure 3a). As expected, enhancement in aspect ratio and rough surface topography development is very important in improving the fiber-matrix interface and their adhesion; the mechanical properties will also improve. The epoxy resin has also covered the porous structures on the fibers, providing good mechanical interlocking with the ABS matrix chain, hence developing strong fiber-matrix bonding, as seen in FESEM micrographs. According to Figure 3b's SEM study of raw, untreated kenaf fibers, the surface view of raw kenaf fibers showed the appearance of impurities on the samples, which could account for the weak connection between the fiber and matrix contact. As previously observed, it may cause the composites' poor mechanical properties (Owen, Achukwu et al., 2018).

Thermal Analysis of Resin-coated Kenaf and Uncoated Kenaf Fibers

Figure 4 displays the samples' TGA thermograms, while Table 2 shows the thermal degradation and stability results of uncoated kenaf fibers (KF) and resin-coated kenaf fibers (CKF).

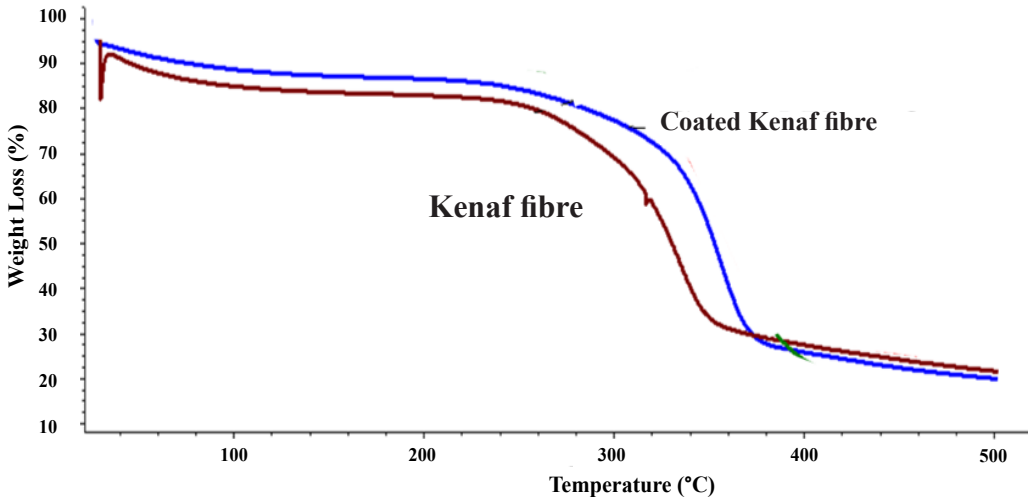

Figure 4. TGA Thermograms of resin-coated kenaf fiber (CKF) and uncoated kenaf fiber (KF)

KF was found to have lower thermal stability, with degradation beginning at around 297.7°C, which is attributed to the breakdown of cellulosic materials like hemicellulose and cellulose and a decomposition temperature of 334.6°C because of the breakdown of noncellulosic components in the fibers (Dehghani et al., 2013). At the same time, CKF's decomposition and beginning of degradation temperatures were stable over 300°C and showed improved thermal stability with peak and onset temperatures of 381.7°C and 331.6°C, respectively, compared to uncoated kenaf fibers (KF), with a minimum mass residual of 10.65%.

When compared to uncoated KF samples, CKF demonstrated a significant improvement in thermal stability. The thermal results are consistent with those from Thitithanasarn et al. (2013), who discovered that the improved contact between the jute fibers and the resins caused the thermoset resin-coated fabrics to break at a greater temperature than the uncoated jute, and it was found that the thermoset resins-coated jute fabric decomposed at a higher temperature than the uncoated jute. The TGA data in Figure 4 show that epoxy coating improved the kenaf fiber's thermal stability without changing the fiber's composition (Dehghani et al., 2013). The onset and peak temperatures of the natural, uncoated kenaf fibers, KF, were 297.7°C and 351.9°C, respectively, with a substantial mass residual value of 18.15%. It suggests CKF is more thermally stable than untreated, kenaf fiber. These outcomes are closely correlated with the composite materials' mechanical characteristics, where the mechanical properties of CKF/ABS composites were superior to the uncoated KF/ABS composites (Figures 5 and 6) at high temperatures (220°C) without fiber degradation. The thermal data obtained have demonstrated that treating the fiber with epoxy resin for a surface resin coating can improve the kenaf fibers' resistance to heat deterioration.

Table 2
Thermal decomposition characteristics thermogravimetric analysis (TGA) of uncoated KF and resin-coated kenaf fiber CKF

Sample codes	Description	Onset degradation temperature (°C)	DTG Peak (°C)	Mass Residual (%)
KF	Kenaf fiber	297.7	351.9	18.15
CKF	Resin coated kenaf	331.6	381.7	10.65

Mechanical Properties

Tensile Properties. The effects of resin coating treatment on the tensile parameters (strength and modulus) of ABS composites filled with kenaf fiber are depicted in Figure 5 for comparison. It can be observed that there are some degrees of improvement in the tensile strength of the coated kenaf/ABS composites compared to the uncoated kenaf-reinforced ABS and KF/ABS composites. The tensile strengths of CKF/ABS composites with epoxy

coating, uncoated KF/ABS, and unfilled ABS were 42.4 MPa, 37.46 MPa, and 39.2 MPa, respectively. The observations are that the strength values of neat ABS dropped slightly upon incorporating the fillers. The tensile strength of CKF/ABS composites was superior as compared to KF/ABS, with about 4.6% improvement, demonstrating a strong interfacial connection between the ABS polymer matrix and the resin-coated kenaf fibers (CKF) as a result of the epoxy coating's impact on increasing tensile strength. Uncoated kenaf KF/ABS composites were discovered to have the lowest modulus (2407.10 MPa), while CKF/ABS composites likewise displayed the highest tensile modulus of 2553.21 MPa.

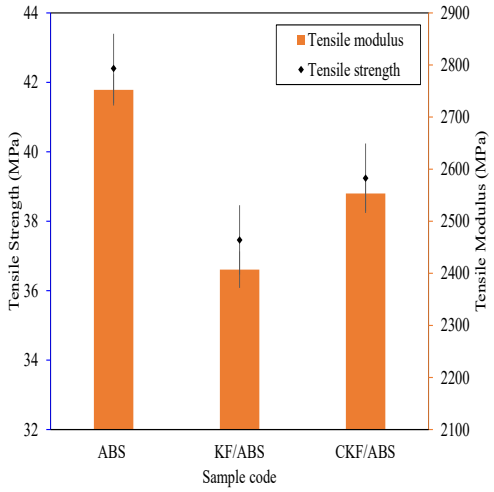

Figure 5. Tensile strength and modulus of resin-coated kenaf fiber (CKF) and uncoated kenaf fiber (KF)

According to the results, resin coating treatment improves the tensile characteristics of ABS composites filled with kenaf fiber, and in comparison to the uncoated composite, epoxy-coated composites produced better tensile characteristics. Due to the jute fabric's higher stiffness following epoxy coating treatment, Thitithanasarn et al. (2012) also noted increased tensile characteristics when applying a similar treatment.

Flexural Properties. Figure 6 shows the flexural strength and modulus of kenaf fiber-filled ABS composites. It can be observed that the coating treatment also improved the resistance to bending for the resultant composites; hence, the flexural strength values of the CKF/ABS composite were 61.09 MPa, which is higher compared to those of the uncoated kenaf (KF/ABS) composite with strength values of 58.21 MPa. The low flexural strength value of the KF/ABS composite could be a result of fiber degradation and low strength caused by poor interfacial adhesion or weak interfaces between raw kenaf and the ABS matrix, which is an incompatibility between the hydrophilic kenaf fibers and the hydrophobic ABS polymer while the KF/ABS composites were typically lower than the CKF/ABS composites, which have an outstanding improvement of 4.7%, and shown the potential that the composite strength could increase with a higher percentage of fiber loading as the modulus of CKF/ABS was higher compared to KF/ABS.

The maximum flexural modulus for the CKF/ABS composites was discovered to be 2400.5 MPa, which is the composites' stiffness and resistance to bending. Due to fiber deterioration, which has been reported to cause poor mechanical characteristics and reduced

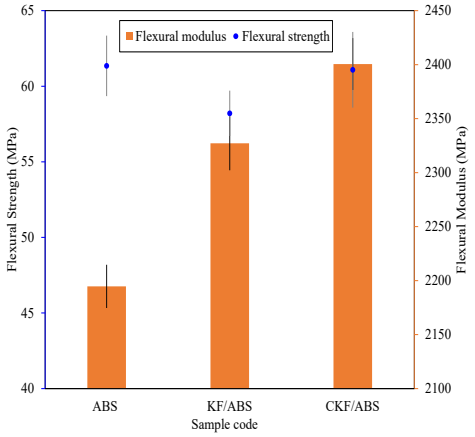

Figure 6. Flexural strength and modulus of resin-coated kenaf fiber (CKF) and uncoated kenaf fiber (KF)

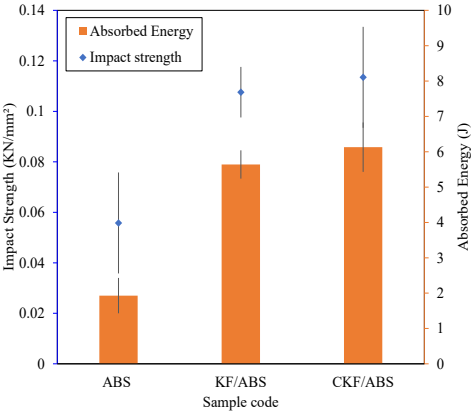

Figure 7. Impact strength and absorbed energy of resin-coated kenaf fiber (CKF) and uncoated kenaf fiber (KF)

cohesive force, untreated composites' inferior flexural capabilities may be caused by fiber breakdown at high temperatures (Pegoretti, 2021).

Impact Properties. Kenaf fiber-filled ABS composites' impact strength and absorbed energy characteristics are shown in Figure 7. The impact strength of the composites is also significantly influenced by the resin coating treatment. The values of all constituent composites were higher than those of unfilled ABS, which demonstrated that adding fillers increased the impact strength. It is a positive contrast to the tensile and flexural property results (Figures 5 and 6), where the strength values of neat ABS dropped slightly upon the incorporation of the kenaf fibers. The impact properties of CKF/ABS were superior (0.1135 KN/mm^2) compared to KF/ABS composites (0.1076 KN/mm^2) due to the epoxy coating treatment effects in improving the impact properties.

Similarly, coated kenaf (CKF/ABS) and uncoated kenaf (KF/ABS) composites had higher impact absorbed energy than clean ABS. With CKF/ABS composites, the highest energy of 6.13 J was discovered, whereas lower energies of 1.93 J and 5.64 J were observed with ABS and uncoated KF/ABS composites, respectively, an indication of the possibility that epoxy resin coatings can act as coupling agents for the kenaf, which delays the fiber thermal degradation and improves the adhesion between the epoxy coated kenaf fiber and the ABS polymer matrix for maximum impact performance. Marzuki et al. (2021) also obtained increased energy absorption, which explained the sufficient fiber-matrix interface in kenaf bast-filled composites because the basic composites of coated kenaf fibers took more energy to make compared to the raw kenaf composites.

Morphological Properties. The pristine ABS, resin-coated kenaf fiber SEM micrographs (CKF), and uncoated raw kenaf fibers (KF) reinforced acrylonitrile butadiene styrene (ABS) composites are shown in Figure 8.

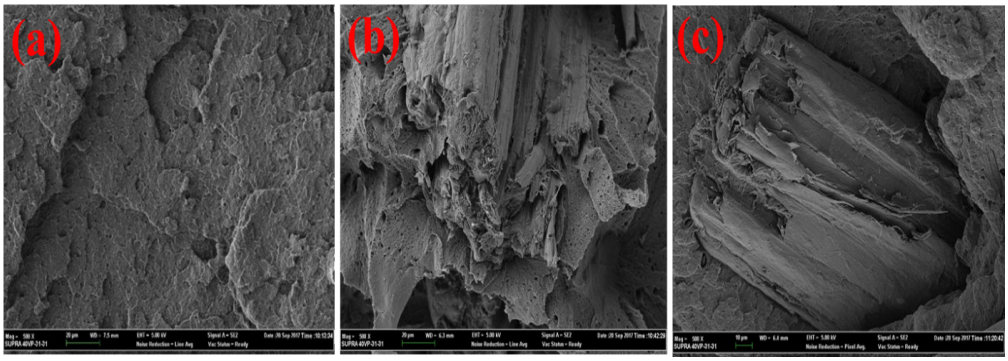

Figure 8. FESEM micrograph of fracture surface morphology of (a) unfilled ABS, (b) CKF/ABS, and (c) KF/ABS composites at 500x magnifications, respectively

Figure 8a in the SEM micrographs of the broken surfaces for the ABS matrix demonstrates that there are no reinforcing fibers in the matrix, but rather is related to the nature of the fractured surfaces for neat ABS. The results of the resin-coated fiber-reinforced composites (CKF/ABS) and raw kenaf (KF/ABS) composites are presented in Figures 8b and 8c, respectively. Figure 8b revealed cracked portions and gaps between the fiber wall and ABS matrix, which signified incompatibility. Azwa and Yousif (2013) attributed the cracks to the debonding at the fiber-matrix interface, which progressed to the surface of the composite. Figures 5 and 6 illustrate how this resulted in the composites' poor mechanical properties and inadequate bonding between the fiber and matrix. The untreated composite system shows evidence of fiber pull-out and cavities.

There is improved bonding between the coated fiber and matrix ABS molecular chain for the coated kenaf (CKF/ABS) composites (Figure 8c). An indication of the surface coating treatment effect may have activated the hydroxyl groups in the treated kenaf fiber, resulting in an effective chemical interlock with the ABS matrix. Strong fiber/matrix interfacial bonding was also seen in CKF/ABS composites, which may be the main reason for the superior mechanical performance compared to untreated composites. At a temperature of 220°C, the CKF/ABS appears to have maintained its integrity without any evidence of fiber degradation in the composite structure. It could be responsible for the superior mechanical strengths recorded for Figure 8b compared to the uncoated kenaf fiber (KF/ABS) composites.

Optical Microscopic Analysis. The optical micrographs of fiber distribution for both ABS, resin-coated kenaf fibers (CKF), and uncoated kenaf fibers (KF) in ABS matrix composite systems are presented in Figures 9a, 9b, and 9c, respectively. In both cases, it is observed that the results showed a good dispersion of fiber in the ABS phase, which can be observed from the diffused boundaries between the matrix and kenaf fibers; they were also discovered to exist as a continuous phase alongside the matrix. It is a sign that the fibers successfully fused during compounding at high pressure and temperature and effectively dispersed during melt mixing. The more successful relations of the epoxy resin with the fibers may be responsible for the superior dispersion and fusion characteristics.

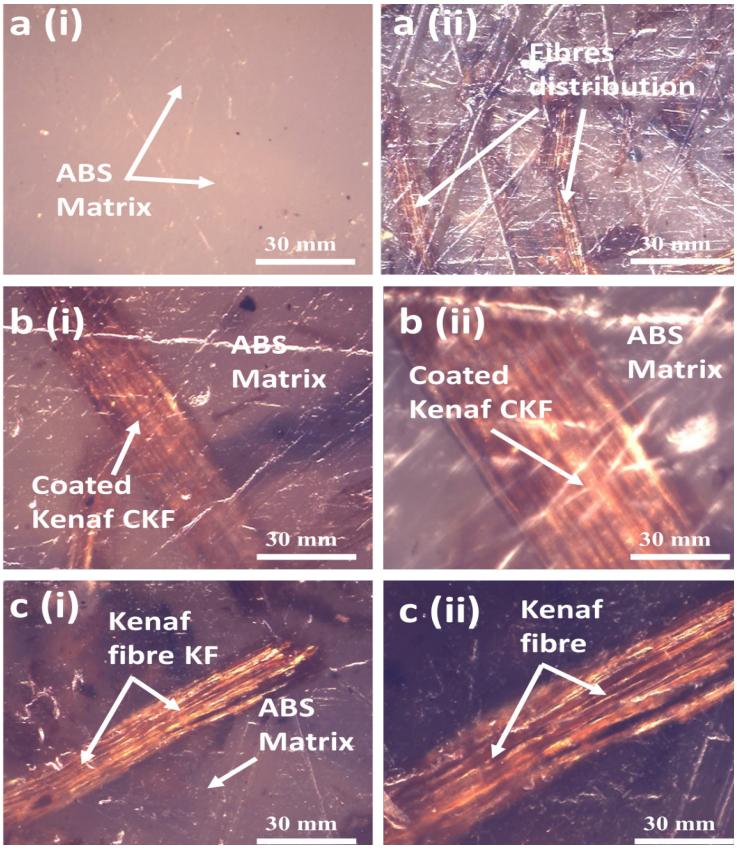

Figure 9. Optical micrograph of ABS composites system showing fiber distribution for a(i) unreinforced ABS, a(ii) reinforced composites, [b(i) & b(ii)] and [c(i) & c(ii)] coated and uncoated kenaf/ABS composites at 10x and 20x magnifications, respectively

The results have revealed a uniform and good dispersion of the fibers during processing, indicating an even distribution of the fibers in the composite system and effective participation in stress transfer (Owen et al., 2018b; Owen et al., 2019).

CONCLUSION

The thermal and mechanical properties of kenaf fiber/ABS polymer composites via resin coating treatment were studied, and it was found that the thermal and mechanical properties of epoxy-coated kenaf fiber-reinforced ABS polymer composites (CKF/ABS) were superior to the uncoated kenaf fiber composites (KF/ABS) when the kenaf fibers were loaded at 10 wt%. FTIR spectra showed how the resin coating has significantly reduced the vibrational peak intensities, which are responsible for the reduced hydrophilicity. The TGA thermograms revealed that coated kenaf fibers were thermally stable with a higher onset degradation temperature of 331.6°C, whereas raw kenaf fibers had lower thermal stability with an onset degradation temperature of 297.7°C. Due to the absence of coated kenaf fiber breakdown, the improved thermal behavior and stability of the resin-coated fiber were further substantiated by the strong interfacial bonding displayed by the FESEM micrographs. This study has addressed kenaf's fiber's poor compatibility and low thermal resistance with polymer matrices. The resultant composite is thus suitable for load-bearing and high-temperature applications.

ACKNOWLEDGEMENTS

The authors gratefully acknowledged the research support from the Biomechanical and Clinical Engineering (BIOMEC) Research Group, School of Mechanical Engineering, College of Engineering, Universiti Teknologi MARA, and the research collaboration with the Centre for Polymer Composites and Technology (PoCresT), Institute of Science IOS, Universiti Teknologi MARA (UiTM), Shah Alam, Malaysia, the Department of Polymer and Textile Engineering, Faculty of Engineering, Ahmadu Bello University, Zaria, Nigeria, and the School of Materials and Mineral Resources Engineering, Universiti Sains Malaysia (USM), Engineering Campus, Nibong Tebal, Penang, Malaysia for the use of their manufacturing and testing facilities.

REFERENCES

Achukwu, E. O., Barnabas, A. M., Mamman, A., & Uzochukwu, M. I. (2015). Fabrication of palm kernel shell epoxy composites and study of their mechanical properties. *Nigerian Journal of Materials Science and Engineering*, *6*(1), 32-38.

Achukwu, E. O., Dauda, B. M., & Ishiaku, U. S. (2015). Mechanical properties of plied cotton fabric-coated unsaturated polyester composites: Effects of alkali treatments. *International Journal of Composite Materials*, *5*(4), 71-78. https://doi.org/10.5923/j.cmaterials.20150504.01

Achukwu, E. O., Ochika, J. O., Adole, A. E. & Owen, M. M. (2015). Tensile properties of alkali treated four-ply cotton woven fabrics for tarpaulin use. *NSUK Journal of Science and Technology*, *5*(2), 69–72.

Achukwu, E. O., Odey J. O., Owen, M. M., Lawal N., Oyilagu G. A., & Adamu A. I. (2022). Physical and mechanical properties of flamboyant (*Delonix regia*) pod-filled polyester composites. *Heliyon*, *8*(1), e08724. https://doi.org/10.1016/j.heliyon.2022.e08724

Achukwu, E. O., Owen, M. M., Danladi, A., Dauda, B. M., Romli, A. Z., Ishiaku, U. S., & Akil, H. M. (2023). Effect of glass fiber loading and reprocessing cycles on the mechanical, thermal, and morphological properties of isotactic polypropylene composites. *Journal of Applied Polymer Science*, *140*(10), e53588. https://doi.org/10.1002/app.53588

Akil, H. M., Omar, M. F., Mazuki, A. A. M., Safiee, S., Ishak, Z. A. M., & Abu Bakar, A. (2011). Kenaf fiber reinforced composites: A review. *Materials & Design*, 32(8-9), 4107–4121. https://doi.org/10.1016/j.matdes.2011.04.008

Asim, M. Jawaid, M., Abdan, K., & Ishak, M. R. (2016). Effect of alkali and silane treatments on mechanical and fibermatrix bond strength of kenaf and pineapple leaf fibers. *Journal of Bionic Engineering*, *13*(30), 426-435. https://doi.org/10.1016/S1672-6529(16)60315-3

ASTM D638-03. (2012). *Standard test method for tensile properties of plastics*. ASTM International. https://www.astm.org/d0638-03.html

ASTM Standard D790. (2017). *Standard test methods for flexural properties of unreinforced and reinforced plastics and electrical insulating materials*. ASTM International. https://www.astm.org/d0790-17.html

Asumani, O. M. L., Reid, R.G., & Paskaramoorthy, R. (2012). The effects of alkali-silane treatment on the tensile and flexural properties of short fibre non-woven kenaf reinforced polypropylene composites. *Composites Part A: Applied Science and Manufacturing*, *43*(9), 1431–1440. https://doi.org/10.1016/j.compositesa.2012.04.007

Asyraf, M. R. M., Syamsir, A., Bathich, H., Itam, Z., Supian, A. B. M., Norhisham, S., Nurazzi, N. M., Khan, T., & Rashid, M. Z. A. (2022). Effect of fibre layering sequences on flexural creep properties of kenaf fibre-reinforced unsaturated polyester composite for structural applications. *Fibers and Polymers*, *23*(11), 3232–3240. https://doi.org/10.1007/s12221-022-4386-7

Asyraf, M. R. M., Syamsir, A., Ishak, M. R., Sapuan, S. M., Nurazzi, N. M., Norrrahim, M. N. F., Ilyas, R. A., Khan, T., & Rashid, M. Z. A. (2023). Mechanical properties of hybrid lignocellulosic fiber-reinforced biopolymer green composites: A review. *Fibers and Polymers*, *24*(2), 337-353. https://doi.org/10.1007/s12221-023-00034-w

Azwa, Z. N. & Yousif, B. F. (2013). Characteristics of kenaf fiber/epoxy composites subjected to thermal degradation. *Polymer Degradation and Stability*, *98*(12), 2752-2759 http://doi.org/10.1016/j.polymdegradstab.2013.10.008

Dehghani, A., Madadi Ardekani, S., Al-Maadeed, M. A., Hassan, A. & Wahit, M. U. (2013). Mechanical and thermal properties of date palm leaf fiber reinforced recycled poly(ethylene terephthalate) composites. *Materials & Design*, *52*, 841-848. http://doi.org/10.1016/j.matdes.2013.06.022

Doumbia, A. S., Castro, M., Jouannet, D., Kervoëlen, A., Falher, T., Cauret, L., & Bourmaud, A. (2015). Flax/polypropylene composites for lightened structures: Multiscale analysis of process and fiber parameters. *Materials Design*, *87*, 331–341. http://doi.org/10.1016/j.matdes.2015.07.139

El Abbassi, F. E, Assarar, M., Ayad, R., Sabhi, H., Buet, S., & Lamdouar, N. (2019). Effect of recycling cycles on the mechanical and damping properties of short alfa fiber reinforced polypropylene composite. *Journal of Renewable Materials*, *7*(3), 253–267. http://doi.org/10.32604/jrm.2019.01759

Feng, N. L., Malingam, S. D., Razali, N., & Subramonian, S. (2020). Alkali and silane treatments towards exemplary mechanical properties of kenaf and pineapple leaf fibre-reinforced composites. *Journal of Bionic Engineering*, *17*, 380–392. https://doi.org/10.1007/s42235-020-0031-6

Gourier, C., Bourmaud, A., Le Duigou, A., & Baley, C. (2017). Influence of PA11 and PP thermoplastic polymers on recycling stability of unidirectional flax fiber reinforced biocomposites. *Polymer Degradation and Stability*, *136*, 1–9. http://doi.org/10.1016/j.polymdegradstab.2016.12.003

ISO 179-1. (2010) *Plastics — Determination of Charpy impact properties — Part 1: Non-instrumented impact test*. International Organization for Standardization. https://www.iso.org/standard/44852.html#:~:text=ISO%20179%2D1%3A2010%20specifies,and%20the%20type%20of%20notch.

Kabir, M. M., Wang, H., Lau, K. T., & Cardona, F. (2012). Chemical treatments on plant-based natural fiber reinforced polymer composites: An overview. *Composites Part B: Engineering*, *43*(7), 2883–2892. https://doi.org/10.1016/j.compositesb.2012.04.053

Ku, H., Wang, H., Pattarachaiyakoop, N., & Trada, M. (2011). A review on the tensile properties of natural fiber reinforced polymer composites. *Composites Part B: Engineering*, *42*(4), 856–873. https://doi.org/10.1016/j.compositesb.2011.01.010

Marzuki, N. H., Wahit, M. U., Arsad, A., Othman, N., & Yusoff, N. I. S. M. (2021). The effect of kenaf loading on the mechanical properties of kenaf-reinforced recycled poly(ethylene terephthalate)/recycled poly(propylene) (rPET/rPP) composite. *Materials Today: Proceedings*, *39*, 959–964. https://doi.org/10.1016/j.matpr.2020.04.333

Mohammed, L., Ansari, M. N. M., Pua, G., Jawaid, M., & Islam, M. S. (2015). A review on natural fiber reinforced polymer composite and its applications. *International Journal of Polymer Science*, 2015, 2015, 243947. https://doi.org/10.1155/2015/243947

Nikmatin, S., Syafiuddin, A., Nugroho, N., Utama, W., & Wismogroho, A. S. (2017). Thermo-physical properties of kenaf-filled acrylonitrile butadiene styrene composites. *MATEC Web of Conferences*, *95*, 03001. https://doi.org/10.1051/matecconf/20179503001

Norrrahim, M. N. F., Kasim, N. A. M., Knight, V. F., Halim, N. A., Shah, N. A. A., Noor, S. A. M., Jamal, S. H., Ong, K. K., Yunus, W. M. Z. W., Farid, M. A. A., Jenol, M. A., & Ahmad, I. R. (2021). Performance evaluation of cellulose nanofiber reinforced polymer composites. *Functional Composites and Structures*, *3*(2), 024001. https://doi.org/10.1088/2631-6331/abeef6.

Nurazzi, N. M., Shazleen, S. S., Aisyah, H. A., Asyraf, M. R. M., Sabaruddin, F. A., Mohidem, N. A., Norrrahim, M. N. F., Kamarudin, S. H., Ilyas, R. A., Ishak, M. R., Abdullah, N., & Nor, N. M. (2021). Effect of silane treatments on mechanical performance of kenaf fibre reinforced polymer composites: A review. *Functional Composites and Structures*, *3*(4), 045003. https://doi.org/10.1088/2631-6331/ac351b

Odesanya, K. O., Ahmad, R., Jawaid, M., Bingol, S., Adebayo, G. O., & Wong, Y. H. (2021). Natural fiber-reinforced composite for ballistic applications: A review. *Journal of Polymers and the Environment*, *29*(12), 3795–3812. https://doi.org/10.1007/s10924-021-02169-4

Oushabi, A., Sair, S., Oudrhiri Hassani, F., Abboud, Y., Tanane, O., & El Bouari, A. (2017). The effect of alkali treatment on mechanical, morphological and thermal properties of date palm fibers (DPFs): Study of the interface of DPF–Polyurethane composite. *South African Journal of Chemical Engineering*, *23*, 116–123. https://doi.org/10.1016/j.sajce.2017.04.005

Owen, M. M. (2019). *Preparation and characterisation of epoxy-coated kenaf fiber-filled recycled and virgin engineering polyethylene terephthalate composites* [Doctoral dissertation, Ahmadu Bello University Zaria]. Ahmadu Bello University Zaria.

Owen, M. M., Achukwu E. O., Ishidi, E. Y., & Romli, A. Z. (2020). Development of thermally improved chrome-tanned waste leather fiber ABS composites. *NSUK Journal of Science and Technology*, *7*(2), 107-112.

Owen, M. M., Achukwu, E. O., & Romli, A. Z. (2018, October 15-18). *Effects of gauge length and chemical modification on the tensile properties of kenaf fibers*. [Paper presentation]. Proceedings of Textile Researchers Association of Nigeria (TRAN 2018), Abuja, Nigeria.

Owen, M. M., Achukwu, E. O., Akil, H. M., Romli, A. Z., Zainol Abidin, M. S., Arukalam, I. O., & Ishiaku, U. S. (2022). Effect of epoxy concentrations on thermo-mechanical properties of kenaf fiber – recycled poly (ethylene terephthalate) composites. *Journal of Industrial Textiles*, *52*, 1–26. https://doi.org/10.1177/15280837221127441

Owen, M. M., Achukwu, E. O., Arukalam, I. O., & Romli, A. Z. (2022). Effect of varying processing temperatures on the mechanical and microstructural properties of kenaf fiber-ABS composites for moderate temperature applications. *Polymers from Renewable Resources*, *13*(3), 154-169. https://doi.org/10.1177/20412479221122676

Owen, M. M., Achukwu, E. O., Arukalam, I. O., Muhammad, M., & Romli, A. Z. (2021). Effect of processing temperatures on the thermal and mechanical properties of leather waste-ABS composites. *Composites and Advanced Materials*, *30*, 1–10. https://doi.org/10.1177/26349833211060056

Owen, M. M., Achukwu, E. O., Arukalam, I. O., Talib, S., & Romli, A. Z. (2021). Improving the thermal stability and impact strength of leather wastes-ABS composites via robust experimental design. *Journal of Materials and Environmental Science*, *12*(5), 673-685.

Owen, M. M., Achukwu, E. O., Hazizan, A. M., Romli, A. Z., & Ishiaku, U. S. (2022). Characterization of recycled and virgin polyethylene terephthalate composites reinforced with modified kenaf fibers for automotive application. *Polymer Composites, 43*(11), 7724–7738. https://doi.org/10.1002/pc.26866

Owen, M. M., Achukwu, E. O., Romli, A. Z., & Akil, H. M. (2023). Recent advances on improving the mechanical and thermal properties of kenaf fibers/engineering thermoplastic composites using novel coating techniques: A review. *Composite Interfaces*, *30*(8), 849-875. https://doi.org/10.1080/09276440.2023.2179238

Owen, M. M., Ishiaku, U. S., Danladi, A., Dauda, B. M., & Romli, A. Z. (2018a). Mechanical properties of epoxy-coated sodium hydroxide and silane treated kenaf/recycled polyethylene terephthalate (RPET)/ composite: Effect of chemical treatment. *National Symposium on Polymeric Materials 2017*, *1985*(1), 030001. https://doi.org/10.1063/1.5047159

Owen, M. M., Ishiaku, U. S., Danladi, A., Dauda, B. M., & Romli, A. Z. (2018b). The effect of surface coating and fiber loading on thermo-mechanical properties of recycled polyethylene terephthalate (RPET)/ epoxy-coated kenaf fibers composites. *AIP Conference Proceedings*, *1985*(1), 030002. https://doi.org/10.1063/1.5047160

Pegoretti, A. (2021). Recycling concepts for short-fiber-reinforced and particle-filled thermoplastic composites: A review. *Advanced Industrial and Engineering Polymer Research*, *4*(2), 93–104. https://doi.org/10.1016/j.aiepr.2021.03.004

Radzuan, N. A. M., Ismail, N. F., Radzi, M. K. F. M., Razak, Z. B., Tharizi, I. B., Sulong, A. B., Haron, C. H. C., & Muhamad, N. (2019). Kenaf composites for automotive components: Enhancement in machinability and moldability. *Polymers*, *11*(10), 1–10. https://doi.org/10.3390/polym11101707

Ramesh, M., Palanikumar, K., & Reddy, K. H. (2017). Plant fibre based bio-composites: Sustainable and renewable green materials. *Renewable and Sustainable Energy Reviews*, *79*, 558–584. https://doi.org/10.1016/j.rser.2017.05.094

Razak, N. I. A., Ibrahim, N. A., Zainuddin, N., Rayung, M., & Saad, W. Z. (2014). The influence of chemical surface modification of kenaf fiber using hydrogen peroxide on the mechanical properties of biodegradable kenaf fiber/poly(lactic acid) composites. *Molecules*, *19*, 2957-2968. https://doi.org/10.3390/molecules19032957

Reddy, P. V., Reddy, R. S., Rao, J. L., Krishnudu, D. M., & Prasad, P. R. (2021). An overview on natural fiber reinforced composites for structural and non-structural applications. *Materials Today: Proceedings*, *45*(7), 6210-6215. https://doi.org/10.1016/j.matpr.2020.10.523

Sapuan, S. M., Pua, F. L., El-Shekeil, Y. A., & AL-Oqla, F. M. (2013). Mechanical properties of soil buried kenaf fiber reinforced thermoplastic polyurethane composites. *Materials & Design*, *50*, 467–470. https://doi.org/10.1016/j.matdes.2013.03.013

Tan, C., Ahmad, I., & Heng M., (2011). Characterization of polyester composites from recycled polyethylene terephthalate reinforced with empty fruit bunch fibers. *Materials & Design*, *32*(8-9), 4493-4501. https://doi.org/10.1016/j.matdes.2011.03.037

Thitithanasarn, S., Yamada, K., Ishiaku, U. S., & Hamada, H. (2013). Jute fabric reinforced engineering thermoplastic sandwich composites. I. The effect of molding time. *Journal of Applied Polymer Science*, *127*(4), 2952–2959. https://doi.org/10.1002/app.37962

Thitithanasarn, S., Yamada, K., Ishiaku, U. S., & Hamada, H. (2012). The effect of curative concentration on thermal and mechanical properties of flexible epoxy coated jute fabric reinforced polyamide 6 composites. *Open Journal of Composite Materials*, *2*(4), 133-138. https://doi.org/10.4236/ojcm.2012.24016

Uzochukwu, M. I., Omobolanle, T. E. Achukwu, E. O., & Akawu, I. (2020). Effect of starch content on the physico-mechanical properties of recycled polypropylene/sweet potato thermoplastic starch blend. *International Journal of Recent Engineering Science*, *7*(2), 38-46.

Pertanika J. Sci. & Technol. 31 (S1): 59 - 85 (2023)

PERTANIKA JOURNALS

SCIENCE & TECHNOLOGY

Journal homepage: http://www.pertanika.upm.edu.my/

Development and Characterisation of Biocomposite Insulator Board from Durian Skin Fibres

Aisyah Humaira Alias[1], Edi Syams Zainudin[1,2]*, Mohd Nurazzi Mohd Norizan[3] and Ahmad Ilyas Rushdan[4]

[1]Advanced Engineering Materials and Composites Research Centre (AEMC), Department of Mechanical and Manufacturing Engineering, Faculty of Engineering, Universiti Putra Malaysia, 43400 Serdang, Selangor, Malaysia
[2]Institute of Tropical Forestry and Forest Products (INTROP), Universiti Putra Malaysia, 43400 Serdang, Selangor, Malaysia
[3]Bioresource Technology Division, School of Industrial Technology, Universiti Sains Malaysia, 11800 Penang, Malaysia
[4]Department of Chemical Engineering, Faculty of Chemical and Energy Engineering, Universiti Teknologi Malaysia, 81310 UTM Johor Bahru, Johor, Malaysia

ABSTRACT

Durian is Malaysia's most popular seasonal fruit, but less than half of the durian fruit is consumed as food. Durian is a type of fruit with a high percentage of waste, which becomes an environmental problem when discarded into the landfill site. Therefore, it is important to utilise durian waste as a potential natural fibre-based composite reinforcement. Durian skin residue is recognised as one of the potential lignocellulosic materials to replace wood in the insulation board industry. The present study aims to develop a low-cost insulation board using durian skin residues as reinforcing materials. Single-layer mats were manually formed, followed by hot pressing using polymeric methane diphenyl diisocyanate (PMDI) resin. The effect of different percentages of PMDI resin (0, 6, 8 and 10%) on the board's physical, mechanical, morphological, and thermal properties was investigated. It was found that 6% PMDI resin is the optimised resin amount to produce PMDI/durian skin fibre composite, and the board with 6% PMDI has the maximum static bending due to enhanced cross-linking by the fibre. In terms of thermal stability and conductivity, the incorporation of 6% of PMDI is considered the best formulation based on the value achieved. The overall results indicated that this study addresses a low-cost innovation for commercial insulation boards as it utilises durian waste and a low dosage of PMDI for implementation in the building and construction industry.

Keywords: Durian waste, insulation board, mechanical properties, physical properties, thermal properties

ARTICLE INFO

Article history:
Received: 06 March 2023
Accepted: 24 July 2023
Published: 27 October 2023

DOI: https://doi.org/10.47836/pjst.31.S1.04

E-mail addresses:
aisyah.humaira@upm.edu.my (Aisyah Humaira Alias)
edisyam@upm.edu.my (Edi Syams Zainudin)
mohd.nurazzi@usm.my (Mohd Nurazzi Mohd Norizan)
ahmadilyas@utm.my (Ahmad Ilyas Rushdan)
*Corresponding author

ISSN: 0128-7680
e-ISSN: 2231-8526

INTRODUCTION

Malaysia has a widely planted durian crop of up to 41%, or over 70,000 hectares (ha) of cultivated land (Zakaria, 2020). With such a large production of durian fruits in Malaysia, it is not inconceivable that this country will be affected by a high production of durian residues covering more than half of the fruit. Durian waste is estimated to be 60–70% of the durian fruit (Manshor et al., 2014). Approximately 40% of durian skin fibre (DSF) may be produced from 1 kg of durian skin residues, or 60–75% of DSF can be obtained from a single fruit. From the waste management perspective, excess durian skin residues can result in massive disposal costs, environmental problems, and odour and visual pollution (Adunphatcharaphon et al., 2020). The alternative approach is to recycle and raise the value of these durian residues into valuable products to lessen the amount of durian that goes to waste (E'Zzati et al., 2018). As a result of this initiative, the declining amount of organic waste disposed of will reduce environmental pollution.

In recent decades, DSF has been explored in many applications, such as a physical adsorbent, multi-mycotoxin binder, protective packaging, potential pharmaceutical applications, and components of building materials (Adunphatcharaphon et al., 2020; Ho & Bhat, 2015; Khedari et al., 2004; Payus et al., 2021; San Ha et al., 2020). For instance, DSF has been identified as a viable agricultural biofiller in the composites sectors due to its excellent physical properties, high crystallinity, biodegradable, renewable source, and low cost (Aimi et al., 2014; Manshor et al., 2014). Developing composite materials using DSF will add value to agricultural waste and minimise pollution by reducing organic waste (Aimi et al., 2014; Manshor et al., 2012). Also, Masrifah et al. (2021) transformed DSF into organic fertiliser for durian crops. The DSF was mixed thoroughly with dolomite before re-mixed with an effective microorganism 4 (EM4). The fermented results from converting durian skin waste into fertiliser can be directly harvested and utilised by farmers.

Due to the current focus on utilising available natural resources, this research focuses on using agricultural waste as reinforcement in composites (Azman et al., 2021). Biocomposites offer numerous benefits, making them an attractive choice in various industries (Sabaruddin et al., 2020). Firstly, they contribute to sustainability by utilising renewable resources such as plant-based fibres and biopolymers, reducing reliance on non-renewable fossil fuel-based materials. This eco-friendly approach helps lower the carbon footprint and promotes a more circular economy. Secondly, biocomposites can reduce weight due to the lightweight nature of natural fibres, leading to enhanced energy efficiency in applications like automotive and aerospace (Ali et al., 2015, 2018; Azammi et al., 2020). Additionally, the incorporation of natural fibres into a biopolymer matrix improves mechanical properties, including tensile strength, stiffness, and impact resistance, making biocomposites suitable for structural applications (Norfarhana et al., 2022; Shaker et al., 2020, 2022). Furthermore, biocomposites based on biopolymers can

be biodegradable, offering advantageous end-of-life options and waste management. The versatility of biocomposites allows for customisation and tailoring of properties to meet specific requirements, providing a wide range of applications. Overall, biocomposites offer sustainable, lightweight, mechanically enhanced, and customisable solutions that contribute to a greener future (Asyraf et al., 2022, Asyraf, Syamsir, et al., 2023 & Asyraf, Nurazzi, et al., 2023). Much research has been conducted on reinforcing natural fibre as filler in polymer to improvise biocomposites' mechanical and physical properties. This research examines composites' characteristics based on polymeric methane diphenyl diisocyanate (PMDI) reinforced with DSF. In this work, PMDI resin was reinforced with DSF in the form of particles to produce a low-cost insulation board. In order to produce a high-quality DSF/PMDI board at a reasonable cost, the physical and mechanical properties of the board with different resin contents (0, 6, 8 and 10%) will be evaluated and discussed in this study. The physical properties of the DS/PMDI board were investigated, where density and dimensional stability tests were used to characterise them. Meanwhile, the mechanical, thermal, and conductivity properties were also carried out. The study's primary objective was to identify the optimal resin content for DSF/PMDI boards with high strength, good dimensional stability, and better thermal properties.

MATERIALS AND METHODS

Materials

Durian skin waste was collected from a fruit stall in Selangor and shredded using a shredder machine, as shown in Figure 1, to produce durian skin particles with a range size of 1 x 2 cm^2. The particles were air-dried for a day and dried in the oven at 70°C until the moisture content (MC) reached 8–10%. The PMDI resin was provided by Evergreen Sdn. Bhd., Shah Alam, Selangor and used in the fabrication process of the boards.

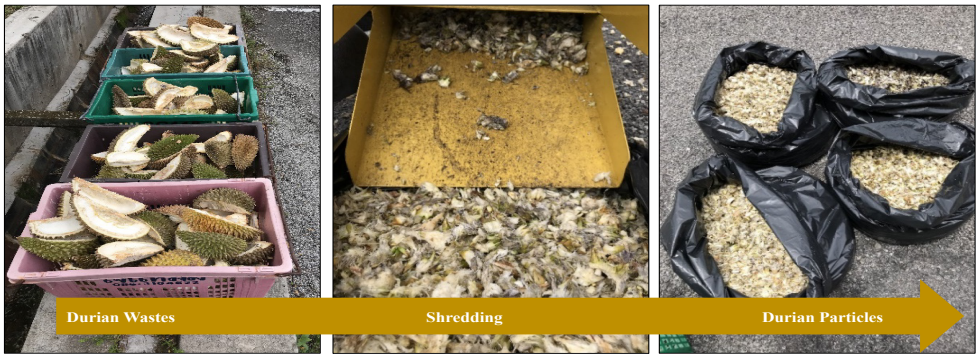

Figure 1. Durian wastes and durian particles

Methods

Fabrication of DSF/PMDI Board. The DSF-reinforced PMDI boards were produced by hot pressing using a manual hand lay-up technique. A specific amount of durian particles was weighed and placed in a rotary drum blender equipped with a pressurised spray nozzle, as shown in Table 1. The PMDI resin was sprayed onto the particles until the entire resin and the particles were blended uniformly. The furnish was collected, placed in a 350 × 350 mm square-shaped mould, and manually formed into a mat. The mats were cold-pressed at room temperature followed by hot-pressed at a pressure of 160 kg/cm² and a temperature of 190°C for 6 min using a computer-controlled press. The targeted density of the board was 0.60 g/cm³. Finally, the single-layer DSF/PMDI boards were conditioned at 23 ± 2°C and RH of 65 ± 5% until their equilibrium MC was obtained. The conditioning ensured that the resin in the board was cured uniformly.

Table 1
The formulations of the DSF-reinforced PMDI boards

Name of Composites	PMDI Resin (%)	PMDI Weight (g)	DSF Weight (g)
DSF/0PMDI	0	0	983.80
DSF/6PMDI	6	51.45	934.60
DSF/8PMDI	8	67.47	919.30
DSF/10PMDI	10	83.98	904.40

Preparation of Test Specimens

The samples were cut into specimens according to the ASTM D1895 (2003) and ASTM D1037 (2020), with 10 mm thickness. Table 2 shows the panel's dimensions for each test and the number of test specimens per board. The samples were then placed in the convection oven at 80°C for 24 h.

Table 2
Dimensions and number of test specimens

Test	Dimensions (mm)	Number of test specimens per board
Water Absorption (WA)	50 × 50	4
Thickness Swelling (TS)	50 × 50	4
Static Bending (SB)	200 × 50	3
Internal Bonding (IB)	50 × 50	4

Characterisation of Board Sample

Density. The DSF/PMDI board's density was determined by measuring each sample's mass and volume. The mass measurement was performed by digital precision balance, and dimensions measurement was performed using a vernier calliper. The density, ρ (g/cm^3), was then calculated according to ASTM D2395 (2022) at room temperature using Equation 1.

$$\rho = \frac{m}{V} \quad (1)$$

where m is the sample mass (g), and V is the sample volume (cm^3).

Dimensional Stability. The test specimens measured the initial weight and thickness using a digital precision balance and vernier calliper before being immersed in distilled water at room temperature according to ASTM D1037 (2020) Method B. The final weight and thickness were measured after 24 h. The percentage of water absorption (WA) was calculated using Equation 2.

$$WA = \frac{W_2 - W_1}{W_1} \times 100 \quad (2)$$

where W_1 is the weight of the sample before immersion (g), and W_2 is the weight of the sample after immersion in distilled water (g).

The percentage of thickness swelling (TS) was calculated using Equation 3.

$$TS = \frac{T_2 - T_1}{T_1} \times 100 \quad (3)$$

where T_1 is the thickness of the sample before immersion (mm), and T_2 is the thickness of the sample after water immersion (mm).

Static Bending. A three-point static bending test was conducted over a span length of 150 mm at 30 mm/min loading speed according to ASTM D1037 (2020) using the Tensile Machine model SHIMADZU AGS-X. The modulus of elasticity (MOE) value was calculated using Equation 4, and the modulus of rupture (MOR) value was calculated using Equation 5.

$$MOE = \frac{PL^3}{4fwt^2} \quad (4)$$

where f is the load-point deflection (mm).

$$MOR = \frac{3PL}{2wt^2} \quad (5)$$

where P is the maximum load at the point of delamination (N), L is the span length (mm), w is the width of the specimen (mm), and t is the thickness of the specimen (mm).

Internal Bonding. The internal bonding (IB) samples were glued to the heated metal blocks having a surface area of 50 × 50 mm with an epoxy resin. Another heated metal block with epoxy glue was placed on the other surface of the IB specimen. The specimens were kept in a conditioning room for 24 h before testing. All specimens were tested at a crosshead speed of 0.7 mm/min according to ASTM D1037 (2020) using an Internal Bonding Machine model LLOYD INSTRUMENT EZ20. The IB strength (N/mm^2) was calculated based on Equation 6.

$$IB = \frac{P'}{bl} \tag{6}$$

where *P'* is the maximum load (N) or force for the test specimen (N), *b* is the width of the test specimen (mm) and *l* = length of the test specimen (mm).

Scanning Electron Microscope (SEM). Scanning electron microscope (SEM) instrument model COMEX EM-30AX was used to observe the IB fracture surfaces of the test specimens to investigate the fracture mechanisms and interface adhesion of the board. The IB test samples were first cut (5 × 10 × 10 mm) at the fracture area before being placed in the SEM. The samples were then coated with gold to prevent the build-up of electron charge and to obtain a clear image of the samples. The magnification settings were set to 100x to investigate the detailed view of the fracture sample.

Thermogravimetric Analysis (TGA)

TGA was carried out using a TA Instruments TGA Q500 analyser in accordance with ASTM E1131 (2020) standards. About 8–10 mg of the composite was used for the TGA analysis. The samples were heated at 10°C per min from 25 to 570°C.

Differential Scanning Calorimetry Analysis (DSC)

The DSC analysis was conducted using a TA Instruments DSC Q1000 analyser according to ASTM D3418 (2021). About 7–9 mg of the composite was used for the DSC study. The glass transition and crystallisation temperatures were measured as functions of temperature in the range of 25–200°C with a heating rate of 10°C/min, and the results were recorded as a function of time.

Dynamic Mechanical Analysis (DMA)

TA instruments in New Castle, DE, USA, made a DMA called a Q800 that was used for the tests according to ASTM E1640 (2018). The specimens were cut at 60 mm (length) by 12 mm (wide) with a thickness of less than 6 mm. They were done at a frequency of 1 Hz

and a height of 30 m. All the specimens were first heated to 25°C in the DMA chamber. Then, dynamic heating scans were done from 25 to 120°C at a heating rate of 3°C/min.

Thermal Conductivity Measurement

Thermal conductivity measurements of each board used in this study were carried out using a NETZSCH HFM436 equipped with a ThermoCube cooling apparatus from Solid State Cooling Systems, USA. The thermal conductivity tests were performed according to the ASTM C518 (2021) standard. Each sample for the dimension of 300 × 300 mm^2 for each insulation board type was tested. The measurements were taken at an average temperature of 22.5°C. The temperature of the upper plate was set at 10°C, and the temperature of the lower plate was set at 35°C. The WinTherm32 software calculated the thermal conductivity, and the data was recovered when the system had reached equilibrium. Prior to conducting the tests, the specimens were conditioned to a moisture content average of 12 ± 3%.

RESULTS AND DISCUSSION

Density

The density of the board is one of the most significant elements of the properties of DSF/PMDI boards, such that by raising this factor, many of the functional aspects of boards are enhanced. The results in Figure 2 showed that the trend in density increased with the PMDI percentage. The density was, however, reduced when the resin content increased to 10%. In this comparison, the DSF/8PMDI board possessed the highest density of 0.581 g/cm^3, while the board without PMDI had the lowest density of 0.375 g/cm^3. The low density in DSF/0PMDI was due to the lack of interaction between DSF particles in the DSF/0PMDI board, as no resin filled the space between them. It eventually reduced the board's compatibility, resulting in a low density. The DSF/8PMDI board might have the highest density because the PMDI resin filled almost entirely the voids or spaces of the DSF particles, making the board less porous, more compact, and stronger. However, as the PMDI was increased to 10%, the density of the board was reduced (0.565 g/cm^3). It might be the consequence of an excessive amount of resin that demands a higher pressing temperature and longer pressing time to penetrate the resin into the voids of the particles (Kusumah et al., 2017).

Dimensional Stability

Water absorption (WA) is the DSF/PMDI board's ability to absorb water, whereas thickness swelling (TS) is the thickness change induced by soaking it in distilled water for 24 h. These tests measure the dimensional stability of the DSF/PMDI board, which impacts how a board product moves and distorts in service and its suitability for varied

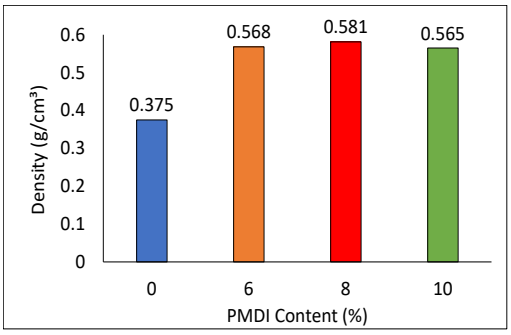

Figure 2. The density of the DSF/PMDI boards at different resin content

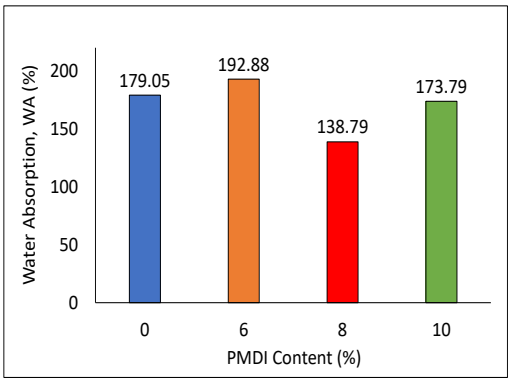

Figure 3. The water absorption of DSF/PMDI boards at different resin content

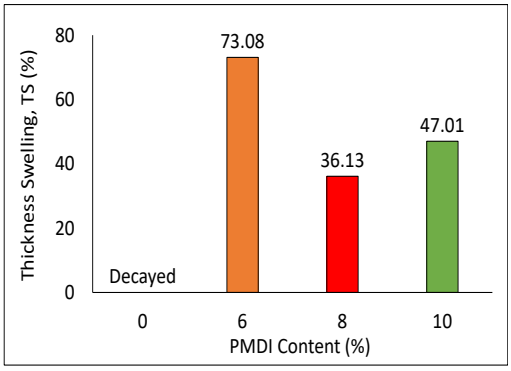

Figure 4. The thickness swelling of DSF/PMDI boards at different resin content

applications (Sargent, 2019). The results obtained in Figure 3 and Figure 4 showed similar trends in TS and WA. The results exhibited that the WA and TS decreased with the increase in resin content. In this comparison, the DSF/8PMDI board had the lowest WA and TS of 138.79% and 36.13%, respectively, whereas the DS/6PMDI board had the highest WA and TS of 192.88% and 73.08%, respectively. Lower WA and TS in the DSF/8PMDI board were found because of good adhesion between the DSF and PMDI. According to Saad and Kamal (2011), excellent chemical components in the resin were effectively cross-linking with the hydroxyl groups of the fibre, thus reducing the board's hygroscopicity.

In addition, due to the high density of the DSF/8PMDI board, the PMDI fills spaces in DSF, thus reducing void formation (Wong et al., 2000). In their study, a high-density board exhibited better flow and cross-linking, resulting in low void formation, less hygroscopic and more moisture resistant. It eventually reduced the water's ability to penetrate the board, resulting in less absorption. The DSF/8PMDI board also had higher PMDI content than the DSF/6PMDI board. A high PMDI content might cause low WA and TS as the PMDI have excellent water-repellence properties. Thus, the optimal PMDI resin was 8% because it had excellent dimensional stability.

Meanwhile, the DSF/6PMDI board had the highest percentage of WA and TS at 192.88% and 73.08%, respectively. Due to the small amount of resin utilised in developing the DSF/6PMDI board, the resin might not be enough to penetrate the particle surfaces

uniformly. It resulted in the greater existence of the void, which provided gaps that promote water absorption. Besides, the DSF/6PMDI board had low density. A study by Saad and Kamal (2011) discovered that a low-density board had a very porous structure that allowed water to penetrate the board and enhanced the WA rate, enabling the board to swell and thus increase the TS. Apart from that, DSF is hydrophilic, and PMDI is hydrophobic; therefore, water molecules penetrated the DSF when the board was wet, influencing fibre-resin interaction (Penjumras et al., 2015). According to a study by Alomayri et al. (2014), this penetration caused the fibre to absorb water and swell, causing micro-cracks that promote water capillarity and transport, allowing cellulose to absorb more water and penetrate the surface (Shaker et al., 2022).

On the other hand, the DSF/10PMDI board had high WA (173.79%) and TS (47.01%) due to the poor penetration and cross-link formation between the PMDI and DSF. According to a study by Liu et al. (2019), pressing at a higher temperature resulted in stronger interfacial adhesion and rapid thermal decomposition of hydrophilic components such as hemicelluloses. Therefore, higher pressing temperatures and time were required to achieve excellent adhesion in all layers of the DSF/10PMDI board (Kusumah et al., 2017). These high values may be related to the fact that no wax or other hydrophobic substance was used during particleboard manufacture. Water-repellent chemicals such as paraffin could be utilised in particleboard production to improve these properties.

Static Bending

The results in Figures 5 and 6 showed that the MOE trend is similar to MOR. In this comparison, the DSF/6PMDI board possessed the highest MOE and MOR at 2487.87 MPa and 8.53 MPa, respectively, while the DSF/0PMDI board had the lowest MOE and MOR of 165.05 MPa and 0.58 MPa, respectively. The low MOE value of the board indicated poor stiffness and rigidity performance, resulting in ductility and flexibility. While the low board's MOR indicated a lower ability to withstand the stresses applied perpendicular to its longitudinal axis. The value of MOE was increased from 165.05 to 2487.87 MPa, and MOR was increased from 0.58 to 8.52 MPa when the PMDI percentage in the DSF/PMDI board increased from 0 to 6%. The addition of PMDI greatly enhanced the MOE and MOR values since cross-linking between the DSF and PMDI improved the board's resistance to stress. This excellent adhesion prevented the DSF from shifting when the samples were subject to loading. It might be attributed to PMDI's effectiveness that coated the DSF particle surfaces and boosted chemical bonding via hydrogen bonds and polyurethane covalent bonds, as Saad and Kamal (2011) mentioned. In their findings, the isocyanate groups of PMDI reacted with water in the DSF particles, creating cross-linked polyureas for better mechanical bonding.

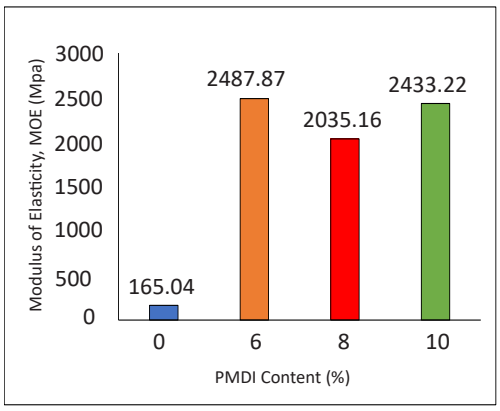

Figure 5. The MOE values of the DSF/PMDI boards at different resin content

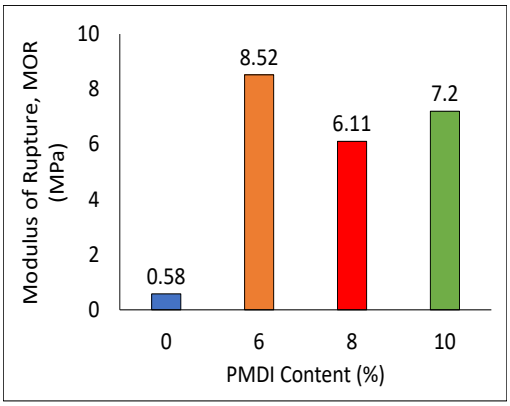

Figure 6. The MOR values of the DSF/PMDI boards at different resin content

However, the MOE and MOR decreased as the PMDI content increased from 6 to 8% to 2035.16 MPa and 6.11 MPa, respectively. Even though a DSF/8PMDI board had a high density and promoted better fibre-resin cross-link, a DSF/6PMDI board might contain more cellulose due to insufficient PMDI resin generated link with the cellulose fibre, as shown in SEM image analysis later. Higher cellulose content increased board stiffness, tensile, and impact strength. Way et al. (2013) reported a similar trend in mechanical properties, stating that additional fibre increased the board's mechanical properties due to fibre modulus being much higher than the PMDI. The study had also been supported by Alamri and Low (2012), in which cellulose fibres increased the fracture toughness of polymer matrices. In their study, increased fibre-rich areas indicated that stress was transferred from the resin to the fibres by absorbing more impact energy during fibre pull-out, breakage, and bridging, improving mechanical properties. The DSF/6PMDI had a higher presence of lignin than the DSF/8PMDI. According to Sahoo et al. (2011), adding lignin reduced the impact strength of composites because it acts as an adhesion promoter. Thus, the DSF/PMDI board with 6% had the optimal PMDI content due to its excellent MOE and MOR, with the highest stiffness and deformation resistance.

MOE and MOR improved when PMDI content was increased from 8 to 10% at 2433.22 MPa and 7.2 MPa, respectively. DSF/8PMDI exhibited poor MOE and MOR that might be due to bonding and fibre breaking, as Nazri et al. (2014) mentioned. Their research observed that the bond breakage was generated by the transmitted load surpassing the bond strength between the fibre-resin surface. Meanwhile, the fibre breakage was caused by the transmitted load surpassing the fibre strength and may have separated the fibres from the resin. However, DSF/10PMDI was lower than DSF/6PMDI, possibly due to the resin-rich region. According to Alamri and Low (2012), resin-rich regions indicated a lack of fibres that carried the transferred load from the resin, resulting in significant localised strains and thus having poor mechanical properties.

Internal Bonding

The results in Figure 7 show that the trend in IB increased with respect to their adhesive percentage. In this comparison, the DSF/10PMDI board possessed the highest IB, 0.612 MPa, while the DSF/0PMDI board had the lowest IB, 0.016 MPa. The increase in IB from 0 to 6% PMDI resulted from adding PMDI resin to the board, which promoted better interfacial bonding between fibres. Additionally, the density of the DSF/6PMDI board was higher than the DS/0PMDI board. High density indicated that the DSF/6PMDI board was less porous and void than the DSF/0PMDI board. The voids caused the inter-fibre bonding to be less effective (Jani & Izran, 2013). In the DSF/6PMDI board, the NCO group in PMDI resin reacted with water and OH groups in the DSF, forming a cross-link of carbon dioxide, amine, and polyurethane. In addition, the hydrogen bond further reacted with polyurethane, forming a rigid polar network and thus enhancing the chemical bonding of the composite. Therefore, it increases the ability to resist the pulling force in the DSF/6PMDI board (Jani & Izran, 2013).

It was noted that the IB of the DSF/6PMDI board was better than those of the DSF/8PMDI board. As mentioned before, although DSF/8PMDI board has a higher density, DSF/6PMDI board contains more lignin, which serves as an extra cross-linking agent by providing phenolic groups for the reaction with PMDI (Ostendorf et al., 2021). In their investigation, the phenolic groups provided by the kraft lignin function as extra cross-linking agents in the reaction with PMDI. Lignin is also a fibre-binding agent (Mossello et al., 2010). Therefore, the DSF/6PMDI board has a higher IB (0.471 MPa) than the DSF/8PMDI board.

The IB of the DSF/PMDI board was found to increase drastically as the resin percentage increased from 8 to 10%, eventually having it as the highest IB among the others (0.612 MPa) because a higher amount of resin promoted better interfacial bonding between fibres in the boards, prolonging the ability to withstand the pulling force generated by the test. A study by Saad and Kamal (2011) discovered that for PF-bonded boards, improvements were observed for IB at resin loadings of 9% and 11%, respectively, compared to 7%. They conclude that higher resin amounts promoted better interfacial adhesion between board particles, boosting the boards' ability to withstand the pulling force. Another factor to support the increase in IB of DSF/10PMDI might be the thick resin that has developed on the surface of the DSF. This thick resin remained on the surface and boosted the IB since PMDI

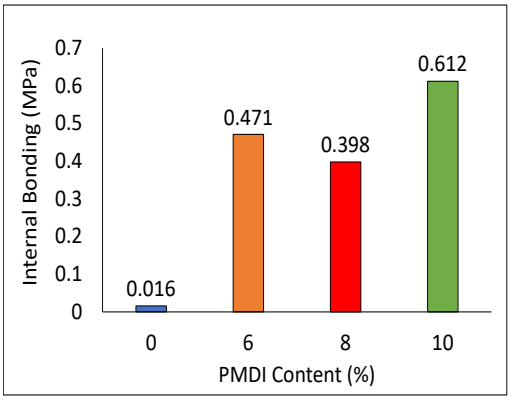

Figure 7. The IB of the DSF/PMDI board at different resin content

is known for its excellent bonding strength. Therefore, the DSF/10PMDI board had the highest IB.

A scanning electron microscope (SEM) was used to determine the fracture of the IB damage in more detail. In this study, the cross-sectional observation of the fracture from the testing was magnified up to 100x to focus on the fibre–matrix interfacial, matrix crack, and void content. Figure 8 shows the SEM micrograph of the DSF/PMDI board.

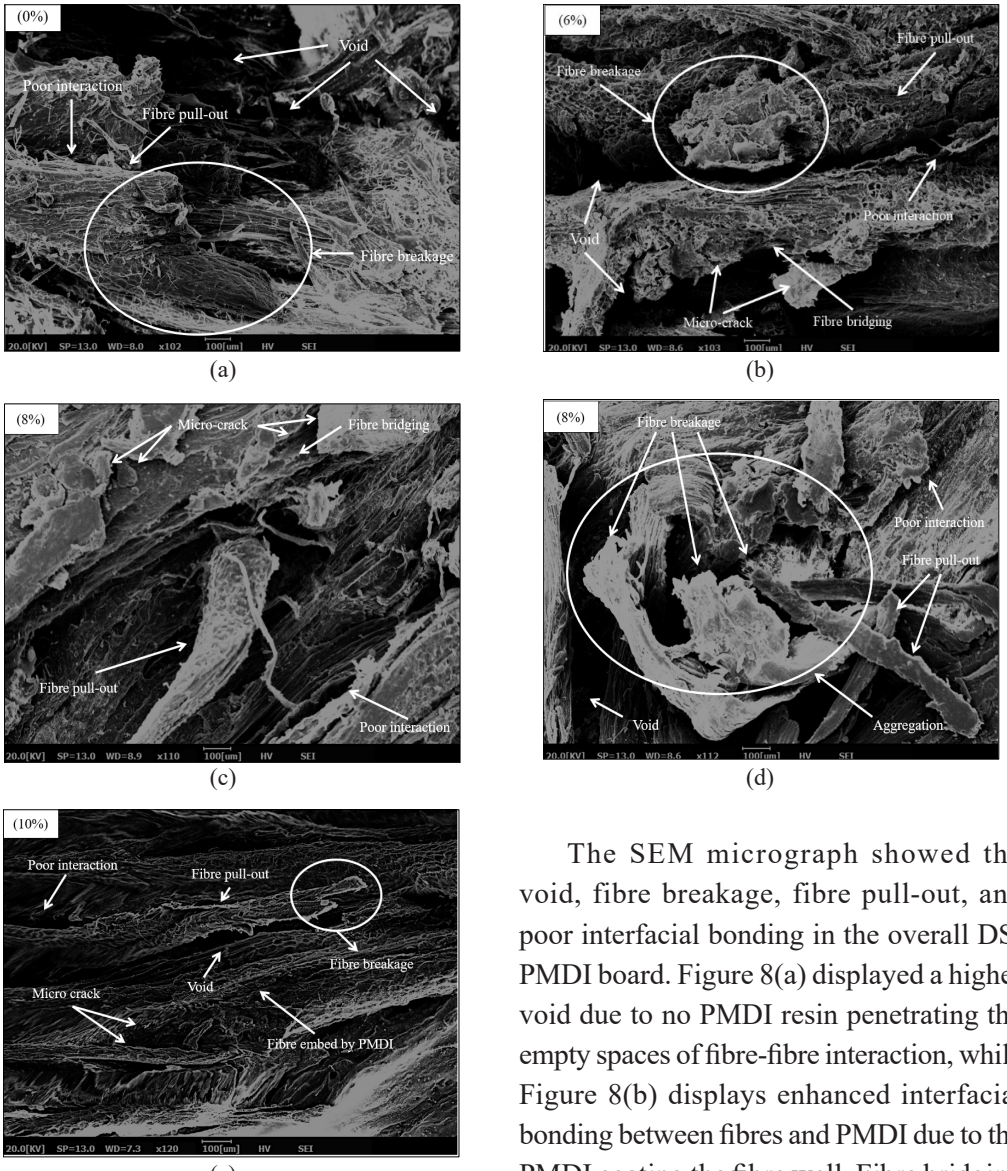

Figure 8. The SEM micrograph images of the DSF/PMDI board at (a) 0, (b) 6, (c–d) 8 and (e) 10% of PMDI

The SEM micrograph showed the void, fibre breakage, fibre pull-out, and poor interfacial bonding in the overall DS/PMDI board. Figure 8(a) displayed a higher void due to no PMDI resin penetrating the empty spaces of fibre-fibre interaction, while Figure 8(b) displays enhanced interfacial bonding between fibres and PMDI due to the PMDI coating the fibre well. Fibre bridging was visible, and the linked fibres between the top and lower layers of the crack plane

inhibited crack development and reduced crack propagation (Yousefi et al., 2016). There was also evidence of fibre breakage and pull-out, indicating that considerable energy was used to break and pull out the fibres, increasing the IB. The PMDI was also can be seen distributed evenly on the DSF surfaces. This adhesion secured the DSF and prevented movement during the IB test (Ibraheem et al., 2011). Their study discovered that kenaf fibres were held by polyurethane better under loading due to good adhesion. Thus, it is evident that the optimal PMDI content was 6% due to excellent morphological behaviour.

Figure 8(c–d) displays a higher number of micro-cracks, uncoated fibre on the fibre-resin surface, and voids, indicating poor adhesion between the DSF and PMDI. An increased number of micro-cracks in the PMDI resulted in fibre delamination. Fibre breakage and pull-out worsened because of the delamination, which separated it from PMDI (Yousefi et al., 2016). A high area of micro-cracks in Figure 8(e) and a high area of uncoated fibre in Figure 8(d) indicated that the DSF/8PMDI board had bad curing. It might be due to a lack of pressing time and temperature during the hot-pressing process, resulting in the DSF and PMDI being left in bulk. It also revealed that the aggregation of the DSF might result from the DSF being pulled out from the PMDI resin. It eventually caused a fibre transition, increased void, and poor interfacial adhesion (Yuan et al., 2019).

Furthermore, Figure 8(e) showed that the high IB measured by DSF/10PMDI may be attributed to the thick PMDI resin staying on the surface, causing PMDI-embedded fibre and low void formation. A low void formation increased the DS/PMDI board's mechanical properties, as Ibraheem et al. (2011) mentioned. According to their research, voids have a negative impact on mechanical properties, behave as defects, and enhance the formation and propagation of cracks.

Thermogravimetric Analysis

Based on all the TGA graphs in Figure 9, it can be said that the trend of the profiles for TGA is almost similar even though they were incorporated with different compositions of PMDI resin. The profiles for all samples show a double weight loss step, which occurred at approximately 43–45°C and 255–262°C. Table 3 shows the summary of the TGA test for the composites. T_{1onset} indicates the first onset degradation temperature, T_{1peak} indicates the first peak degradation temperature, T_{2onset} indicates the second onset degradation temperature, T_{2peak} indicates the first peak degradation temperature, $W_{minorloss}$ indicates the percentage for minor weight loss, and $W_{majorloss}$ indicates the percentage for major weight loss.

Weight loss that happened at approximately 100°C may be related to the elimination of water from the composites, and degradation at the starting temperature may also be related to the breaking of weak ether bonds between lignin units (-O-4 linkage) (Sahoo et al., 2011). Specifically, this showed that the weight loss in composites is related to the heat generated during water vaporisation. It has been broadly observed that the primary

Table 3
Summary of TGA test for the DSF/PMDI boards

Sample	T_{1onset} (°C)	T_{1peak} (°C)	$W_{minorloss}$ (%)	T_{2onset} (°C)	T_{2peak} (°C)	$W_{majorloss}$ (%)	Char Residue at 580°C (%)
DSF/0PMDI	43.98	60.71	8.71	263.28	308.98	58.64	30.52
DSF/6PMDI	43.88	59.79	7.33	255.86	304.45	57.33	31.60
DSF/8PMDI	43.11	58.41	8.58	259.27	305.98	58.68	30.72
DSF/10PMDI	44.38	59.07	7.21	258.25	305.42	58.56	30.80

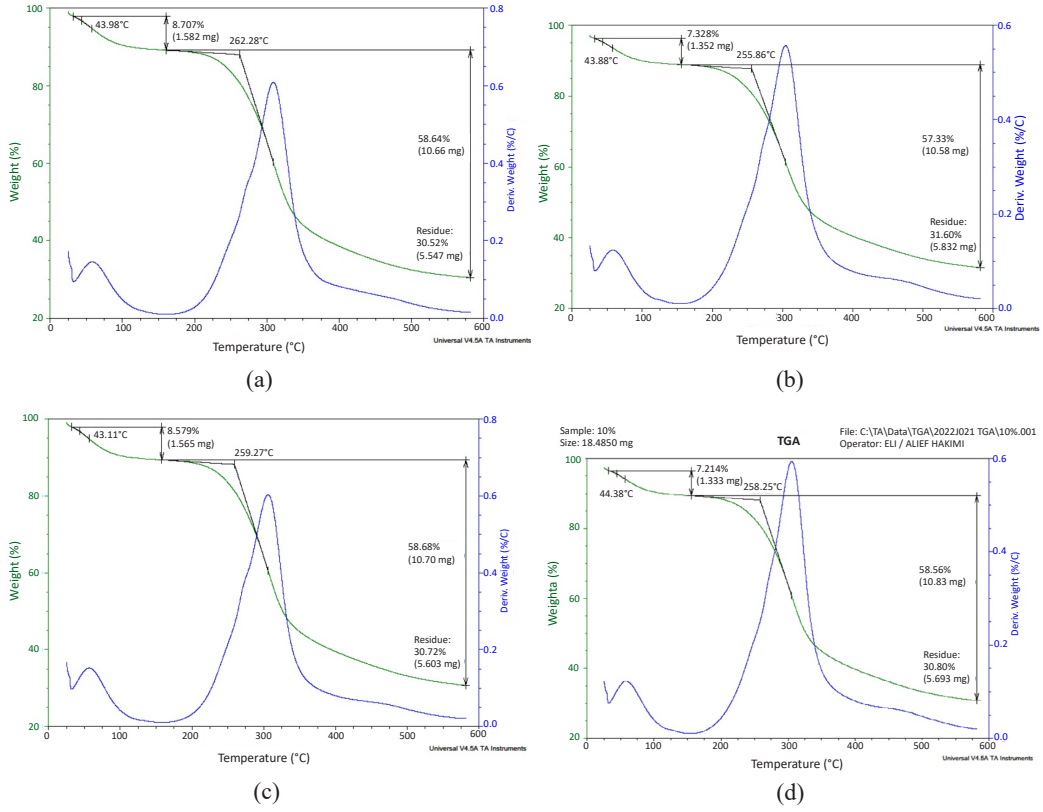

Figure 9. TGA and DTG curves of DSF/PMDI boards for (a) 0, (b) 6, (c) 8 and (d) 10% of PMDI

weight loss describes cellulosic component degradation that occurs largely in amorphous areas to eliminate water molecules at 43-60°C (Ramlee et al., 2021).

The best thermal stability can be expressed as high initial and final temperatures and a high content of char residue (Chee et al., 2019). Based on Table 3, it can be concluded that DSF/6PMDI has the best thermal stability compared to other composites due to the lowest weight loss and highest char residue. When the temperature increased, the final

degradation temperature for DSF/6PMDI was the lowest due to the weak thermal stability of the composite. It may be supported by the fact that the thermal degradation of cellulosic material, consisting of cellulose, hemicellulose, and lignin, is initiated at temperatures around 200 to 400°C (Aimi et al., 2015). Cellulose started decomposing at the highest temperature for second mass loss as it has the highest thermal stability compared to lignin and hemicellulose. This reason is related to cellulose having more crystalline chains than amorphous ones in their structure (Chee et al., 2019). DSF/6PMDI had the highest (31.6%) char residue at 580°C related to highly condensed aromatic structure involvement.

The DTG curves in Figure 9 are crucial as they help determine the maximum temperature for the weight loss step. The secondary weight loss involving thermal degradation of hemicellulose followed by cellulose and lignin was initiated at 250–310ºC (Koay et al., 2018). The percentage of charred residue improved as the lignin percentage of the composite improved. Due to the aromatic components of PMDI, using a PMDI compatibiliser contributed to a modest increase in the percentage of charred residues in the composites (Sahoo et al., 2011). This outcome reflects lignin is flame-resistant ability, further boosted by PMDI addition. The increment in this ability will increase the percentage of char residue. Increasing the char residue will reduce the combustible gases and, at the same time, will save the environment (Shih et al., 2006). These outcomes were similar to the research, which indicated that 6% was the optimum content of PMDI incorporated into kenaf fibre-reinforced thermoplastic polyurethane composites that produced less weight loss and high thermal stability (El-Shekeil et al., 2012).

Differential Scanning Calorimetry Analysis

Differential scanning calorimetry (DSC) is a standard approach for polymer analysis, which strengthens our understanding of the microphase structure when combined with other supporting methods. DSC has been used to identify the materials' phase transition, which could be exothermic or endothermic. For all samples, it was observed that there were similar patterns of profiles, which include double endothermic process and single exothermic. The first indicates the glass transition phase, the second indicates the melting phase for the endothermic process, and the exothermic process shows the cold crystallisation process. Through DSC, the other important thermal properties such as glass transition temperature (T_g), melting temperature (T_m), cold crystallisation temperature (T_c), crystallisation entropy (ΔH_c), and melting entropy (ΔH_m) can be achieved based on Figure 10. Table 4 shows the summary of the DSC test for the boards.

Glass Transition Phase. The T_g in each graph for composites indicates that the energy needed to transition the molecular structure within the composites from a low energy state, such as a solid or glassy state, to a higher energy level, such as a rubbery state, is specified

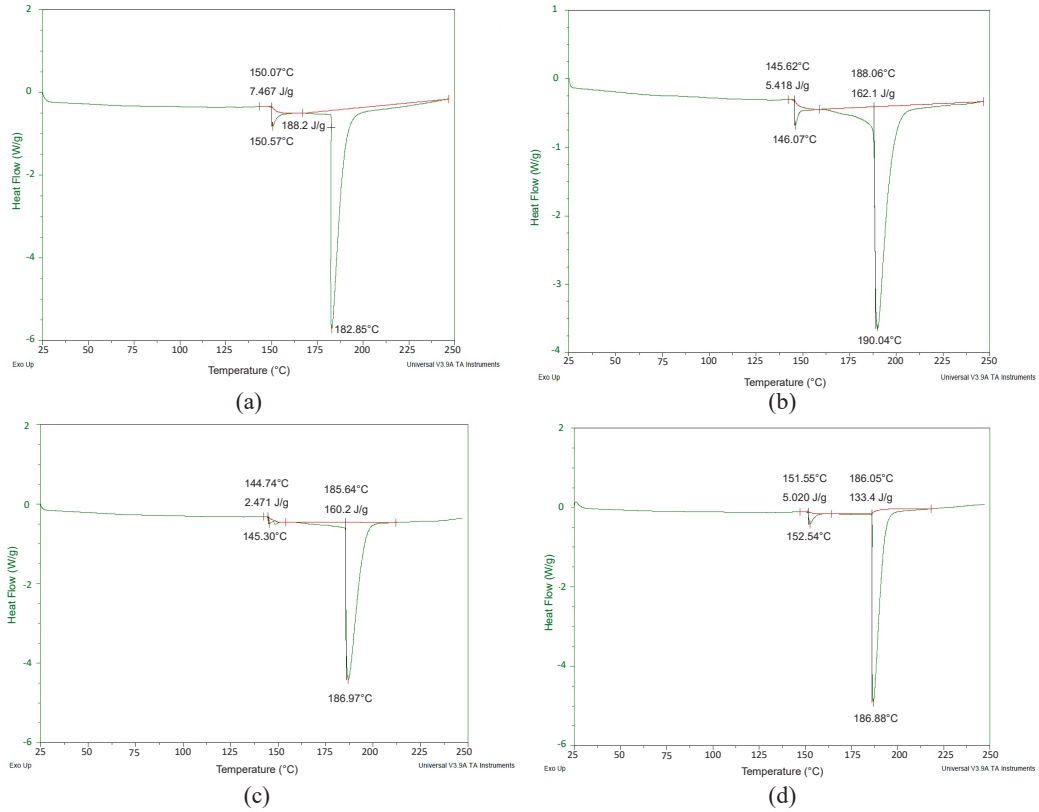

Figure 10. DSC curves of DSF/PMDI boards for (a) 0, (b) 6, (c) 8, and (d) 10% of PMDI.

Table 4
Summary of DSC test findings for the DSF/PMDI boards

Sample	T_g onset (°C)	T_g peak (°C)	T_c peak (°C)	ΔH_c (J/g)	T_m onset (°C)	T_m peak (°C)	ΔH_m (J/g)
DSF/0PMDI	150.07	150.57	163.60	4.603	182.85	182.85	188.2
DSF/6PMDI	145.62	146.07	160.27	1.102	188.06	190.04	162.1
DSF/8PMDI	144.74	145.30	147.20	0.665	185.64	186.97	160.2
DSF/10PMDI	151.55	152.54	165.88	0.643	186.05	186.88	133.4

as the starting point. By comparing the T_g for the composites, DSF/10PMDI has the highest value, which is 152.54°C, followed by DSF/0PMDI (150.57°C), DSF/6PMDI (146.07°C), and DSF/8PMDI (145.30°C). At this phase, polymer chains modify their molecular system to convert from amorphous to crystalline solid by gradually organising their structures (Aisyah et al., 2019). Since the glass transition temperature is higher, a higher temperature is required to change the sample from a glass to a rubbery condition (Azlin et al., 2022).

The glass transition temperature was also modified when the PMDI concentration was raised. A polymer-filler interaction and plasticisation triggered by PMDI addition might be regarded as the potential explanations of the findings reported in this work, although the impact on the thermal properties of natural fibre composites incorporated with PMDI is not very clear (Sahoo et al., 2011).

Cold Crystallisation Phase

Continuous heating of the composites led to the exothermic process known as cold crystallisation, in which the composites change from glassy to an amorphous state (Azlin et al., 2022). It happens between the glass transition and melting phases, which takes place in the 140–170°C range for all the composites. By comparing the T_c for the composites, DSF/10PMDI has the highest value, which is 165.88°C followed by DSF/0PMDI (163.60°C), DSF/6PMDI (160.27°C), and DSF/8PMDI (147.20°C).

Melting Phase. Apart from that, DSF/6PMDI have the highest value, which is 190.04°C, followed by DSF/8PMDI (186.97ºC), DSF/10PMDI (186.88°C), and DSF/0PMDI (182.85°C) after comparing their value of T_m. It can be considered the optimum concentration of PMDI as T_m was increased after DSF had been incorporated with 6% of PMDI content and then decreased with 8 and 10%. This trend also has similarities with the research by El-Shekeil et al. (2012), where they introduced PMDI into kenaf fibre-reinforced thermoplastic polyurethane composites, and the optimum concentration of PMDI was 6%. This alteration in melting temperature signifies an alteration in molecular mobility, such as an alteration in the interfacial adhesion of fibre and polymer. Consequently, the availability of stacking or intermolecular bonding in composites may explain the different content of PMDI, which led to the alteration of the value of T_m.

ΔH_m value is also important as it is associated with the degree of crystallinity of the polymer itself (Manshor et al., 2014). It can be assumed that DSF/0PMDI had the highest degree of crystallinity compared to others as it has the highest value of ΔH_m. The addition of PMDI reduced the crystallinity of composites, and its further decrement was found with the rising concentration of PMDI. Apart from that, there was a large endothermic peak that may be caused by chemical components in natural fibres beginning to degrade at around 200°C (Aisyah et al., 2019). The high peaks for this endothermic indicate that more heat was required to break the polymer chains in composites, and these peaks decreased with increasing concentration of PMDI. In other words, the fibre–matrix interaction modification occurred when the melting temperature changed. As a result, the effect of various percentages of the PMDI additive may be correlated with stacking or intermolecular bonding in composites (El-Shekeil et al., 2012).

Dynamic Mechanical Analysis

Dynamic mechanical analysis (DMA) is a technique that employs a sinusoidal load on a specimen and evaluates the resulting deformation while the sample is exposed to a set temperature program to determine the material's stiffness and damping qualities. The method is especially effective for assessing the influence of moisture on T_g. Table 5 summarises the DMA test OF DSF/PMDI boards. The 0% of the PMDI sample did not undergo this test due to the failure to get below 6 mm of thickness during the sampling process, as the thickness is a crucial requirement for the testing.

Storage Modulus. Figure 11 shows storage modulus curves for all the boards. The storage modulus value decreased with the rising temperature and increasing concentration of PMDI. The decline in storage modulus with temperature may be related to the polymer matrix's enhanced chain mobility at high temperatures, which softens the polymer (Sahoo et al., 2011). During the phase preceding T_g (glassy state), the densely packed molecules caused the composite structure to become extremely stiff and rigid due to the high rigidity of the polymeric chain. In the glass transition phase, it was discovered that the storage modulus fell above T_g, attributable to polymeric chain movement. The movement of polymeric chains influenced both the stiffness and interfacial adhesion. During the third phase (rubbery state), which preceded the glass transition phase, there was no big difference in storage modulus due to increased polymeric chain mobility at elevated temperatures (Jesuarockiam et al., 2019).

DSF/6PMDI achieved the lowest storage modulus values compared to other samples, and the value of storage modulus increased as the concentration of PMDI increased. The decreasing value of the storage modulus represents the decreasing stiffness value for the material (Chee et al., 2019). Storage modulus decreases as temperature increases attributable to chain mobility in the polymer matrix, which leads to the polymer being softer and less rigid and also may happen due to the strengthening of fibres within the composites (Azlin et al., 2022; Sahoo et al., 2011). The amorphous phase may limit chain mobility, reducing the composite's stiffness (Aimi et al., 2015).

Table 5
Summary of DMA test for the DSF/PMDI boards

Sample	T_g Onset—Storage Modulus (°C)	T_g Peak—Loss Modulus (°C)	T_g Peak—Tan Delta (°C)
DSF/6PMDI	82.79	90.48	98.42
DSF/8PMDI	67.89	84.76	100.38
DSF/10PMDI	47.25	67.03	78.79

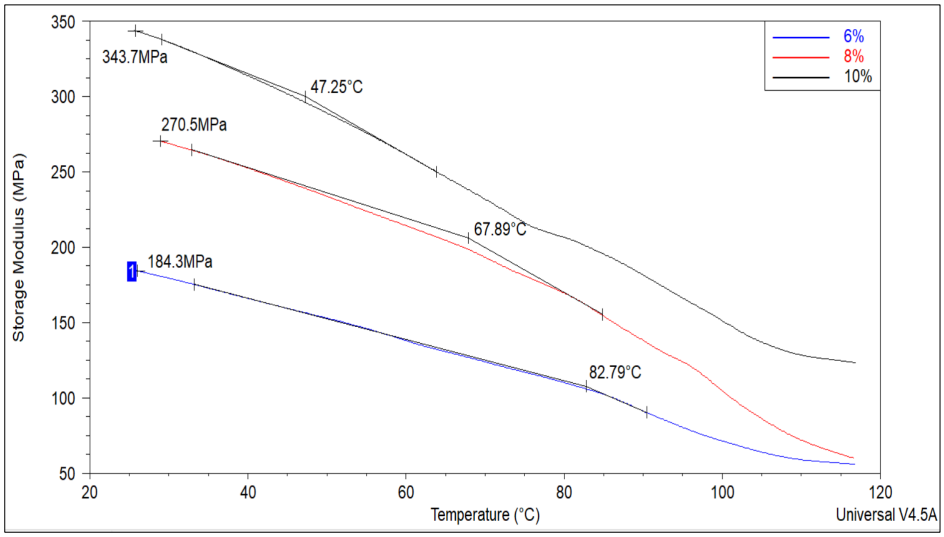

Figure 11. Storage modulus curves for DSF/PMDI boards

Loss Modulus. Figure 12 shows loss modulus curves for all the composites. Based on the figure, DSF/6PMDI has the lowest loss modulus value compared to other composites. The increasing value of loss modulus represents the viscous and damping qualities of the material (Chee et al., 2019). It can be considered that DSF/0PMDI had the lowest loss modulus as it was not strong enough and brittle. The loss modulus measures the material's viscous component to its complex modulus. In the glass transition area, the loss modulus gained a maximum peak, reflecting a large amount of energy loss related to the internal friction and non-elastic deformation in the molecular segmental motion (Chee et al., 2019). The glass transition phase in all composites occurred in a temperature region starting from 60 until 100°C. The T_g started happening when the storage modulus dropped quickly, and the loss modulus reached its maximum value for the loss of mechanical energy. At higher temperatures, the free movement of the polymeric chain caused the loss modulus to fall (Nurazzi et al., 2021).

The value of the T_g can be observed from the graph by observing the peak of the profiles. The T_g value obtained from the peak value of loss modulus stated that DSF/6PMDI had the highest value of 90.48°C, followed by DSP/8PMDI (84.76°C), and then DSF/10PMDI (67.03°C). The T_g obtained from the peak of loss modulus shows that the value decreased with the increasing content of PMDI. The increasing content exceeding 6% decreased the glass transition temperature. The greater the value of T_g, the stronger the interface connection between the fibres and the matrix (Nurazzi et al., 2021).

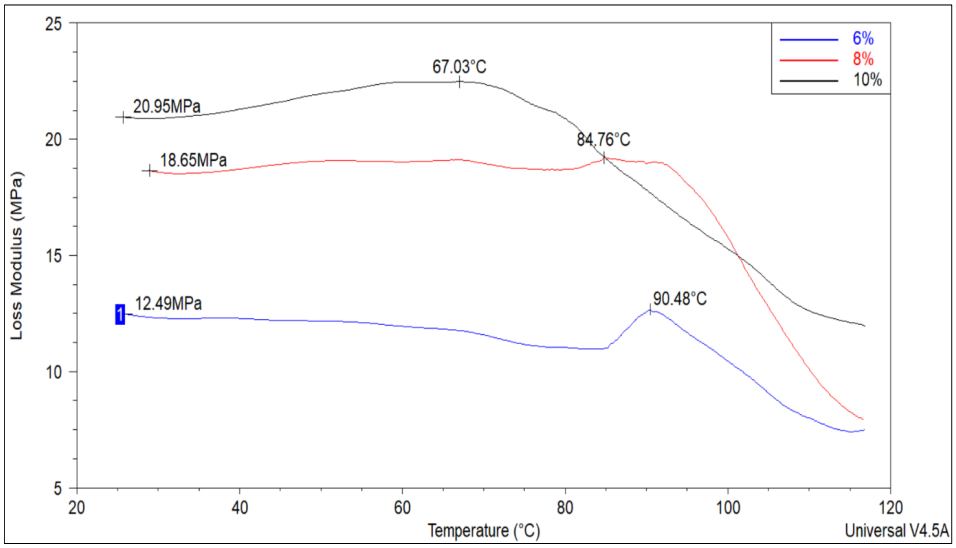

Figure 12. Loss modulus curves for DSF/PMDI boards

Damping Factor (Tan Delta). Figure 13 shows tan delta curves for all the boards. A similar trend can be observed in the graph of the tan delta, which shows an increasing damping factor with increasing temperature for all boards, and this happened due to the chain segments becoming more mobile as the temperature goes up, resulting in a higher value for damping factor (Mohammed et al., 2017). By observing the graph of the tan delta, the highest value was achieved by 8% (100.38°C), followed by 6% (98.42°C) and then 10% (78.79°C) (103.06). The highest value indicates the T_g for the composites. Apart from that, the low damping factor indicates that adhesion related to the filler and fibre matrix was good and, thus, restricted the mobility of polymer chains (Razali et al., 2021). In this case, the increasing content of PMDI decreased the value of tan delta, thus producing good interface adhesion between the natural fibre matrix and PMDI resin. The decreasing value of tan delta was also directly proportional to the value of T_g, indicating the increasing value of interfacial adhesion for the composites (Nurazzi et al., 2021).

There are two explanations for the increasing T_g that need to be appointed. The first reason is due to the formation of an amorphous fraction in the composite structure in which the polymer and filler coexisted in a tightly linked form, thus lowering the free volume of the composites and increasing their T_g. Possible secondary bonds that operate as quasi-crosslinks and constrain the Brownian motion of long-chain molecules may also lead to a rise in T_g (Sahoo et al., 2011). The T_g for composites increased to 8% and then rapidly decreased for 10% of PMDI concentration. The decreasing T_g of 10% is due to the plasticisation of the materials that create free volume between interfacial adhesion of the composites, thus decreasing the T_g (Hetayothin, 2010). Another possible reason for

increasing T_g is regarding the density of composites. DSF/8PMDI have the highest value of density, followed by DSF/6PMDI, DSF/10PMDI and then DSP/0PMDI. The increasing density value indicates that interfacial adhesion also increased due to smaller pores and thus increased the T_g (Mandal & Alam, 2012).

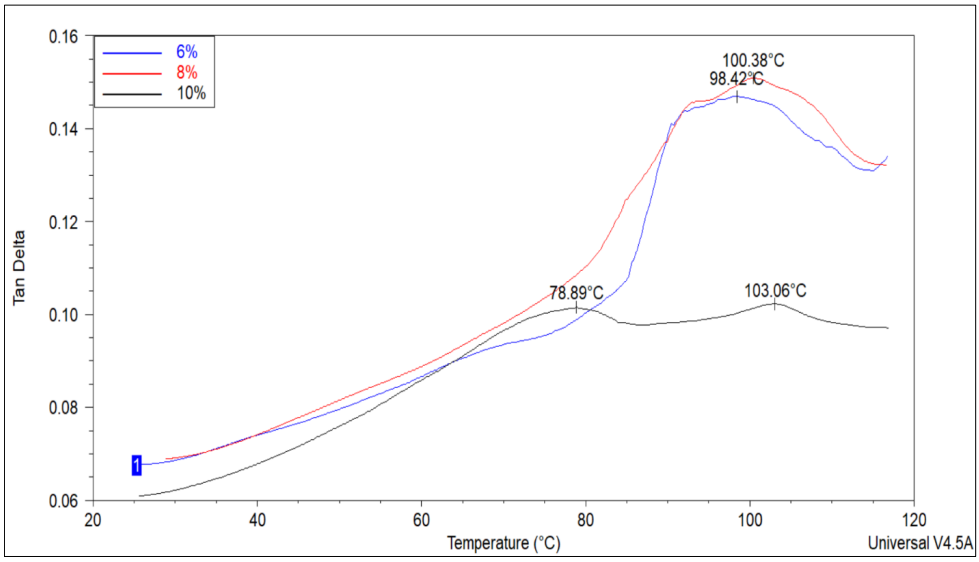

Figure 13. Tan delta curves for DSF/PMDI boards

Thermal Conductivity Measurement

Thermal conductivity measurements are highly related to heat transfer as thermal conductivity is inversely proportional to thermal resistance (Corumlu et al., 2018). Thermal conductivity value for the insulation materials is crucial as it could be the key factor in choosing the suitable composites used as an insulator in the building. In other words, the lowest thermal conductivity value will be concluded as the best composite for the insulation purpose. It also shows that the heat will flow slower when the conductivity value is minimal (Ramlee et al., 2021). Based on Figure 16, it can be said that DSF/0PMDI had the lowest value for thermal conductivity of 0.07892 W/m.k, followed by DSF/6PMDI (0.08275 W/m.K), DSF/10PMDI (0.08694 W/m.K), and then DSF/8PMDI(0.08940 W/m.K).

Based on Figure 2, DSF/0PMDI exhibited the lowest density, while DSF/8PMDI had the highest density compared to other composites. These values of thermal conductivity are directly proportional to the board density. In other words, the increasing value of density resulted in the increasing value of thermal conductivity (Khedari et al., 2003; Luamkanchanaphan et al., 2012). The structure of the boards has several voids, although it seems solid in its appearance. Void positions in the fibres are inversely related

to board density. The air inside the voids decreases the thermal conductivity value (Luamkanchanaphan et al., 2012). In addition, it is strongly suggested to utilise natural fibres such as DSF, which contain cellulose, hemicellulose, and lignin that are bound together to serve as a heat barrier (Ibraheem et al., 2011b).

Apart from that, by comparing the value of thermal conductivity from multiple types of materials, DSF/PMDI composites achieved the standard with other materials such as oil palm (0.055 W/m.K) (Manohar, 2012), coconut husk (0.046 W/m.K) (Panyakaew & Fotios, 2011), and durian combine with coconut coir (0.064 W/m.K) (Khedari et al., 2003). Furthermore, all samples' thermal conductivity values were below 0.1 W/m.K, indicating excellent thermal insulation materials (Ramlee et al., 2021). Figure 14 shows the thermal conductivity, while Figure 15 displays the thermal resistance of the boards.

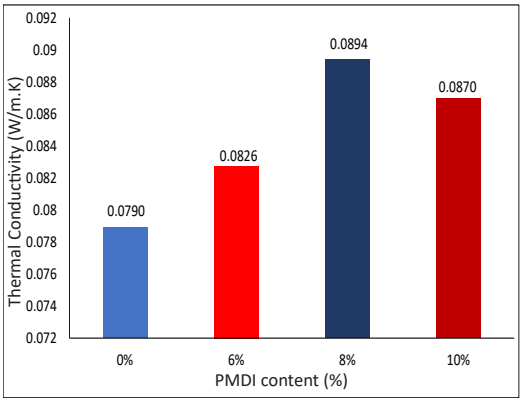

Figure 14. Thermal conductivity of the DSF/PMDI boards

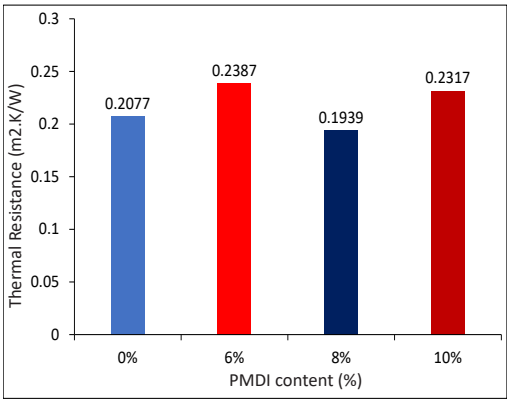

Figure 15. Thermal resistance of the DSF/PMDI boards

Furthermore, thermal resistance is one of the most important factors in choosing the best insulation materials. The higher thermal resistance value indicates that the material has excellent insulation quality. Based on the values that were achieved and presented in Figure 15, DSF/6PMDI gave the highest value of thermal resistance, which is 0.2387 m^2K/W, followed by DSF/10PMDI, DSF/0PMDI, and DSF/8PMDI.

CONCLUSION

The findings suggest that incorporating durian waste can be an alternative solution for utilising the waste management problem. The resin content affects all the board properties. The insulation board with 6% PMDI content resulted in ideal mechanical and thermal properties. Low resin content produced board with excellent all-bending properties, good bonding properties, high thermal stability, and good thermal conductivity compared to other composites. Overall, the DSF/6PMDI board has better board properties, particularly their

mechanical properties, as the MOE and MOR are the most crucial aspects in developing an insulation board and the thermal properties. It also cut the cost of producing the board as the low resin was used. Although it has average dimensional stability, the board can be covered using a waterproof coating. Nonetheless, the potential uses of these boards have enabled the use of agricultural waste composites in construction and building applications.

ACKNOWLEDGEMENTS

The authors are grateful to acknowledge Noorashikin Soh binti Zulariffin Soh and Aleif Hakimi bin Ismail of Universiti Putra Malaysia for help in collecting the data.

REFERENCES

Adunphatcharaphon, S., Petchkongkaew, A., Greco, D., D'Ascanio, V., Visessanguan, W., & Avantaggiato, G. (2020). The effectiveness of durian peel as a multi-mycotoxin adsorbent. *Toxins*, *12*(2), 108. https://doi.org/10.3390/toxins12020108

Aimi, M. N., Anuar, H., Maizirwan, M., Sapuan, S. M., Wahit, M. U., & Zakaria, S. (2015). Preparation of durian skin nanofibre (DSNF) and its effect on the properties of polylactic acid (PLA) biocomposites. *Sains Malaysiana*, *44*(11), 1551-1559.

Aimi, N. N., Anuar, H., Manshor, M. R., Nazri, W. W., & Sapuan, S. M. (2014). Optimizing the parameters in durian skin fibre reinforced polypropylene composites by response surface methodology. *Industrial Crops and Products*, *54*, 291-295. https://doi.org/10.1016/j.indcrop.2014.01.016

Aisyah, H. A., Paridah, M. T., Sapuan, S. M., Khalina, A., Berkalp, O. B., Lee, S. H., Lee, C. H., Nurazzi, N. M., Ramli, N., Wahab, M. S. & Ilyas, R. A. (2019). Thermal properties of woven kenaf/carbon fibre-reinforced epoxy hybrid composite panels. *International Journal of Polymer Science*, *2019*, 1-8. https://doi.org/10.1155/2019/5258621

Alamri, H., & Low, I. M. (2012). Mechanical properties and water absorption behaviour of recycled cellulose fibre reinforced epoxy composites. *Polymer Testing*, *31*(5), 620-628. https://doi.org/10.1016/j.polymertesting.2012.04.002

Ali, A., Shaker, K., Nawab, Y., Jabbar, M., Hussain, T., Militky, J., & Baheti, V. (2018). Hydrophobic treatment of natural fibers and their composites—A review. *Journal of Industrial Textiles*, *47*(8), 2153-2183. https://doi.org/10.1177/15280837166544

Ali, A., Shaker, K., Nawab, Y., Ashraf, M., Basit, A., Shahid, S., & Umair, M. (2015). Impact of hydrophobic treatment of jute on moisture regain and mechanical properties of composite material. *Journal of Reinforced Plastics and Composites*, *34*(24), 2059-2068. https://doi.org/10.1177/0731684415610007

Alomayri, T., Assaedi, H., Shaikh, F. U. A., & Low, I. M. (2014). Effect of water absorption on the mechanical properties of cotton fabric-reinforced geopolymer composites. *Journal of Asian Ceramic Societies*, *2*(3), 223-230. https://doi.org/10.1016/j.jascer.2014.05.005

Asyraf, M. R. M., Syamsir, A., Ishak, M. R., Sapuan, S. M., Nurazzi, N. M., Norrrahim, M. N. F., Ilyas, R. A., Khan, T., & Rashid, M. Z. A. (2023). Mechanical properties of hybrid lignocellulosic fiber-reinforced biopolymer green composites: A review. *Fibers and Polymers*, *24*(2), 337-353. https://doi.org/10.1007/s12221-023-00034-w

Asyraf, M. R. M., Nurazzi, N. M., Norrrahim, M. N. F., Hazrati, K. Z., Ghani, A., Sabaruddin, F. A., Lee, S. H., Shazleen, S. S., & Razman, M. R. (2023). Thermal properties of oil palm lignocellulosic fibre reinforced polymer composites: A comprehensive review on thermogravimetry analysis. *Cellulose*, *30*(5), 2753-2790. https://doi.org/10.1007/s10570-023-05080-4

Asyraf, M. R. M., Rafidah, M., Ebadi, S., Azrina, A., & Razman, M. R. (2022). Mechanical properties of sugar palm lignocellulosic fibre reinforced polymer composites: A review. *Cellulose*, *29*(12), 6493-6516. https://doi.org/10.1007/s10570-022-04695-3

ASTM D1895. (2003). *Standard test methods for direct moisture content measurement of wood and wood-base materials*. ASTM International. https://www.astm.org/d4442-92r03.html

ASTM E1640. (2018). *Standard test method for assignment of the glass transition temperature by dynamic mechanical analysis*. ASTM International. https://www.astm.org/e1640-18.html

ASTM D1037. (2020). *Standard test methods for evaluating properties of wood-base fibre and particle panel materials.* ASTM International. https://www.astm.org/d1037-12r20.html

ASTM E1131. (2020). *Standard test method for compositional analysis by thermogravimetry* ASTM International. https://www.astm.org/e1131-20.html

ASTM C518. (2021). *Standard test method for steady-state thermal transmission properties by means of the heat flow meter apparatus*. ASTM International. https://www.astm.org/c0518-21.html

ASTM D3418. (2021). *Standard test method for transition temperatures and enthalpies of fusion and crystallization of polymers by differential scanning calorimetry*. ASTM International. https://www.astm.org/d3418-21.html

ASTM D2395. (2022). *Standard test methods for density and specific gravity (relative density) of wood and wood-based materials*. ASTM International. https://www.astm.org/d2395-17r22.html

Azammi, A. N., Ilyas, R. A., Sapuan, S. M., Ibrahim, R., Atikah, M. S. N., Asrofi, M., & Atiqah, A. (2020). Characterization studies of biopolymeric matrix and cellulose fibres based composites related to functionalized fibre-matrix interface. In Interfaces in particle and fibre reinforced composites (pp. 29-93). Woodhead Publishing. https://doi.org/10.1016/B978-0-08-102665-6.00003-0

Azlin, M. N. M., Sapuan, S. M., Zuhri, M. Y. M., Zainudin, E. S., & Ilyas, R. A. (2022). Thermal stability, dynamic mechanical analysis and flammability properties of woven kenaf/polyester-reinforced polylactic acid hybrid laminated composites. *Polymers*, *14*(13), 2690. https://doi.org/10.3390/polym14132690

Azman, M. A., Asyraf, M. R. M., Khalina, A., Petrů, M., Ruzaidi, C. M., Sapuan, S. M., Wan Nik, W. B., Ishak, M. R., Ilyas, R. A., & Suriani, M. J. (2021). Natural fiber reinforced composite material for product design: A short review. *Polymers*, *13*(12), 1917. https://doi.org/10.3390/polym13121917

Chee, S. S., Jawaid, M., Sultan, M. T. H., Alothman, O. Y., & Abdullah, L. C. (2019). Accelerated weathering and soil burial effects on colour, biodegradability and thermal properties of bamboo/kenaf/epoxy hybrid composites. *Polymer Testing*, *79*, 106054. https://doi.org/10.1016/j.polymertesting.2019.106054

Corumlu, V., Ozsoy, A., & Ozturk, M. (2018). Fabrication and investigation of silver water nanofluids for long-term heat transfer application. In I. Dincer., C. Ozgur Colpan., & O. Kizilkan (Eds.), *Exergetic, energetic and environmental dimensions* (pp. 779-791). Academic Press. https://doi.org/10.1016/B978-0-12-813734-5.00044-5

E'zzati, M. S. N., Anuar, H., & Salimah, A. S. M. (2018). Effect of coupling agent on durian skin fibre nanocomposite reinforced polypropylene. *IOP Conference Series: Materials Science and Engineering, 290*(1), 012032. https://doi.org/ 10.1088/1757-899X/290/1/012032

El-Shekeil, Y. A., Sapuan, S. M., Abdan, K., Zainudin, E. S., & Al-Shuja'a, O. M. (2012). Effect of pMDI isocyanate additive on mechanical and thermal properties of kenaf fibre reinforced thermoplastic polyurethane composites. *Bulletin of Materials Science*, *35*(7), 1151-1155.

Hetayothin, B. (2010). Effect of structure and plasticizer on the glass transition of adsorbed polymer [Doctoral dissertation, Missouri University of Science and Technology]. Missouri University of Science and Technology. https://scholarsmine.mst.edu/doctoral_dissertations/1901/

Ho, L. H., & Bhat, R. (2015). Exploring the potential nutraceutical values of durian (*Durio zibethinus* L.)–An exotic tropical fruit. *Food Chemistry*, *168*, 80-89. https://doi.org/10.1016/j.foodchem.2014.07.020

Ibraheem, S. A., Ali, A., & Khalina, A. (2011). Development of green insulation boards from kenaf fibres and polyurethane. *Polymer-plastics Technology and Engineering*, *50*(6), 613-621. https://doi.org/10.1080/03602559.2010.551379

Jani, S. M., & Izran, K. (2013). Mechanical and physical properties of ureaformaldehyde bonded kenaf core particle boards. *Journal of Tropical Agriculture and Food Science*, *41*(2), 341-347.

Jesuarockiam, N., Jawaid, M., Zainudin, E. S., Thariq Hameed Sultan, M., & Yahaya, R. (2019). Enhanced thermal and dynamic mechanical properties of synthetic/natural hybrid composites with graphene nanoplateletes. *Polymers*, *11*(7), 1085. https://doi.org/10.3390/polym11071085

Khedari, J., Charoenvai, S., & Hirunlabh, J. (2003). New insulating particleboards from durian peel and coconut coir. *Building and Environment*, *38*(3), 435-441. https://doi.org/10.1016/S0360-1323(02)00030-6

Khedari, J., Nankongnab, N., Hirunlabh, J., & Teekasap, S. (2004). New low-cost insulation particleboards from mixture of durian peel and coconut coir. *Building and Environment*, *39*(1), 59-65. https://doi.org/10.1016/j.buildenv.2003.08.001

Koay, S. C., Subramanian, V., Chan, M. Y., Pang, M. M., Tsai, K. Y., & Cheah, K. H. (2018). Preparation and characterisation of wood plastic composite made up of durian husk fibre and recycled polystyrene foam. *MATEC Web of Conferences*, *152*, 02019. https://doi.org/10.1051/matecconf/201815202019

Kusumah, S. S., Umemura, K., Guswenrivo, I., Yoshimura, T., & Kanayama, K. (2017). Utilisation of sweet sorghum bagasse and citric acid for manufacturing of particleboard II: influences of pressing temperature and time on particleboard properties. *Journal of Wood Science*, *63*(2), 161-172.

Liu, R., Long, L., Sheng, Y., Xu, J., Qiu, H., Li, X., Wang, Y., & Wu, H. (2019). Preparation of a kind of novel sustainable mycelium/cotton stalk composites and effects of pressing temperature on the properties. *Industrial Crops and Products*, *141*, 111732. https://doi.org/10.1016/j.indcrop.2019.111732

Luamkanchanaphan, T., Chotikaprakhan, S., & Jarusombati, S. (2012). A study of physical, mechanical and thermal properties for thermal insulation from narrow-leaved cattail fibres. *APCBEE Procedia*, *1*, 46-52. https://doi.org/10.1016/j.apcbee.2012.03.009

Mandal, S., & Alam, S. (2012). Dynamic mechanical analysis and morphological studies of glass/bamboo fibre reinforced unsaturated polyester resin-based hybrid composites. *Journal of Applied Polymer Science*, *125*(S1), E382-E387. https://doi.org/10.1002/app.36304

Manohar, K. (2012). Experimental investigation of building thermal insulation from agricultural by-products. *British Journal of Applied Science & Technology*, *2*(3), 227-239.

Manshor, M. R., Anuar, H., Aimi, M. N., Fitrie, M. A., Nazri, W. W., Sapuan, S. M., El-Shekeil, Y. A., & Wahit, M. U. (2014). Mechanical, thermal and morphological properties of durian skin fibre reinforced PLA biocomposites. *Materials & Design*, *59*, 279-286. https://doi.org/10.1016/j.matdes.2014.02.062

Manshor, R. M., Anuar, H., Wan Nazri, W. B., & Fitrie, M. I. (2012). Preparation and characterisation of physical properties of durian skin fibres biocomposite. *Advanced Materials Research*, *576*, 212-215. https://doi.org/10.4028/www.scientific.net/AMR.576.212

Masrifah, A., Setyaningrum, H., Susilo, A., & Haryadi, I. (2021). Perancangan Sistem Pengelolaan Limbah Durian Layak Kompos Di Agrowisata Kampung Durian Ponorogo. *Engagement: Jurnal Pengabdian Kepada Masyarakat*, *5*(1), 268-282.

Mohammed, B. R., Leman, Z., Jawaid, M., Ghazali, M. J., & Ishak, M. R. (2017). Dynamic mechanical analysis of treated and untreated sugar palm fibre-based phenolic composites. *BioResources*, *12*(2), 3448-3462.

Mossello, A. A., Harun, J., Shamsi, S. R. F., Resalati, H., Tahir, P. M., Rushdan, I., & Mohmamed, A. Z. (2010). A review of literatures related to kenaf as a alternative for pulpwoods. *Agricultural Journal*, *5*(3), 131-138.

Nazri, W., Ezdiani, Z., Romainor, M., Erma, K. S., Jurina, J., & Fadzlina, I. N. (2014). Effect of fibre loading on mechanical properties of durian skin fibre composite. *Journal of Tropical Agricultural Food Science*, *42*(2), 169-174.

Norfarhana, A. S., Ilyas, R. A., & Ngadi, N. (2022). A review of nanocellulose adsorptive membrane as multifunctional wastewater treatment. *Carbohydrate Polymers*, Article 119563. https://doi.org/10.1016/j.carbpol.2022.119563.

Nurazzi, N. M., Norli, A., Norrrahim, M. N. F., Rafiqah, S. A., Khalina, A., Sapuan, S. M., & Ilyas, R. A. (2021). Thermal properties of sugar palm yarn reinforced unsaturated polyester composites as an alternative for automotive applications. In S. M., Sapuan., & R. A., Ilyas (Eds.) *Biocomposite and synthetic composites for automotive applications* (pp. 19-49). Woodhead Publishing.

Ostendorf, K., Ahrens, C., Beulshausen, A., Tene Tayo, J. L., & Euring, M. (2021). On the feasibility of a pMDI-reduced production of wood fibre insulation boards by means of kraft lignin and ligneous canola hulls. *Polymers*, *13*(7), 1088. https://doi.org/10.3390/polym13071088

Panyakaew, S., & Fotios, S. (2011). New thermal insulation boards made from coconut husk and bagasse. *Energy and Buildings*, *43*(7), 1732-1739. https://doi.org/10.1016/j.enbuild.2011.03.015

Payus, C. M., Refdin, M. A., Zahari, N. Z., Rimba, A. B., Geetha, M., Saroj, C., Gasparatos, A., Fukushi, K., & Oliver, P. A. (2021). Durian husk wastes as low-cost adsorbent for physical pollutants removal: Groundwater supply. *Materials Today: Proceedings*, *42*(1), 80-87. https://doi.org/10.1016/j.matpr.2020.10.006

Penjumras, P., Rahman, R. A., Talib, R. A., & Abdan, K. (2015). Mechanical properties and water absorption behaviour of durian rind cellulose reinforced poly (lactic acid) biocomposites. *International Journal on Advanced Science, Engineering and Information Technology*, *5*(5), 343-349.

Ramlee, N. A., Jawaid, M., Ismail, A. S., Zainudin, E. S., & Yamani, S. A. K. (2021). Evaluation of thermal and acoustic properties of oil palm empty fruit bunch/sugarcane bagasse fibres based hybrid composites for wall buildings thermal insulation. *Fibres and Polymers*, *22*(9), 2563-2571.

Razali, N., Sultan, M. T. H., Shah, A. U. M., & Safri, S. N. A. (2021). Low velocity impact characterisation of flax/kenaf/glass fibre reinforced epoxy hybrid composites. In M. Thariq Hameed Sultan, A. U., Md Shah., & N., Saba (Eds.) *Impact Studies of Composite Materials* (pp. 195-208). Springer.

Saad, M. J., & Kamal, I. (2012). Mechanical and physical properties of low density kenaf core particleboards bonded with different resins. *Journal of Science and Technology*, *4*(1), 17-32.

Sabaruddin, F. A., Paridah, M. T., Sapuan, S. M., Ilyas, R. A., Lee, S. H., Abdan, K., Mazlan, N., Roseley, A. S. M., & Khalil, H. P. S. (2020). The effects of unbleached and bleached nanocellulose on the thermal

and flammability of polypropylene-reinforced kenaf core hybrid polymer bionanocomposites. *Polymers*, *13*(1), 116. https://doi.org/10.3390/polym13010116.

Sahoo, S., Misra, M., & Mohanty, A. K. (2011). Enhanced properties of lignin-based biodegradable polymer composites using injection moulding process. *Composites Part A: Applied Science and Manufacturing*, *42*(11), 1710-1718. https://doi.org/10.1016/j.compositesa.2011.07.025

San Ha, N., Lu, G., Shu, D., & Yu, T. X. (2020). Mechanical properties and energy absorption characteristics of tropical fruit durian (*Durio zibethinus*). *Journal of the Mechanical Behaviour of Biomedical Materials*, *104*, 103603. https://doi.org/10.1016/j.jmbbm.2019.103603

Sargent, R. (2019). Evaluating dimensional stability in solid wood: A review of current practice. *Journal of Wood Science*, *65*(1), 1-11.

Shaker, K., Umair, M., Shahid, S., Jabbar, M., Ullah Khan, R. M. W., Zeeshan, M., & Nawab, Y. (2022). Cellulosic fillers extracted from *Argyreia speciose* waste: a potential reinforcement for composites to enhance properties. *Journal of Natural Fibers*, *19*(11), 4210-4222. https://doi.org/10.1080/15440478.2020.1856271

Shaker, K., Khan, R. M. W. U., Jabbar, M., Umair, M., Tariq, A., Kashif, M., & Nawab, Y. (2020). Extraction and characterization of novel fibers from *Vernonia elaeagnifolia* as a potential textile fiber. *Industrial Crops and Products*, *152*, 112518. https://doi.org/10.1016/j.indcrop.2020.112518

Shih, Y. F., Lee, W. C., Jeng, R. J., & Huang, C. M. (2006). Water bamboo husk-reinforced poly (butylene succinate) biodegradable composites. *Journal of Applied Polymer Science*, *99*(1), 188-199. https://doi.org/10.1002/app.22220

Wong, E. D., Zhang, M., Han, G., Kawai, S., & Wang, Q. (2000). Formation of the density profile and its effects on the properties of fibreboard. *Journal of Wood Science*, *46*(3), 202-209.

Yousefi, J., Mohamadi, R., Saeedifar, M., Ahmadi, M., & Hosseini-Toudeshky, H. (2016). Delamination characterisation in composite laminates using acoustic emission features, micro visualization and finite element modeling. *Journal of Composite Materials*, *50*(22), 3133-3145. https://doi.org/10.1177/00219983156156

Yuan, C., Chen, W., Pham, T. M., & Hao, H. (2019). Effect of aggregate size on bond behaviour between basalt fibre reinforced polymer sheets and concrete. *Composites Part B: Engineering*, *158*, 459-474. https://doi.org/10.1016/j.compositesb.2018.09.089

Zakaria, A. A. (2020). *Managing Durian Orchards in Malaysia*. Universiti Putra Malaysia Press.

Pertanika J. Sci. & Technol. 31 (S1): 87 - 110 (2023)

PERTANIKA JOURNALS

SCIENCE & TECHNOLOGY

Journal homepage: http://www.pertanika.upm.edu.my/

Review Article

A Comprehensive Review of Real-time Monitoring and Predictive Maintenance Techniques: Revolutionizing Natural Fibre Composite Materials Maintenance with IoT

Felix Sahayaraj Arockiasamy[1], Indran Suyambulingam[2], Iyyadurai Jenish[3], Divya Divakaran[2], Sanjay Mavinkere Rangappa[2]* and Suchart Siengchin[2]

[1]Department of Mechanical Engineering, KIT-Kalaignarkarunanidhi Institute of Technology, Coimbatore, Tamil Nadu 641402, India

[2]Natural Composites Research Group Lab, Department of Materials and Production Engineering, The Sirindhorn International Thai-German School of Engineering (TGGS), King Mongkut's University of Technology North Bangkok (KMUTNB), Bangkok 10800, Thailand

[3]Department of Applied Mechanics, Seenu Atoll School, Hulhu-medhoo, Addu City 19060, Maldives

ABSTRACT

Integrating the Internet of Things (IoT) and natural fiber-reinforced polymer composites (NFPCs) can revolutionize monitoring and maintaining composites. By incorporating sensors and wireless communication technology into the composites, real-time monitoring and predictive maintenance can be achieved. This review provides a comprehensive overview of the current state-of-the-art in the use of IoT for real-time monitoring and predictive maintenance of NFPCs. This paper covers the various types of sensors used, IoT networks and protocols employed, and data analysis techniques to detect potential issues and predict failures. This paper also highlights the benefits and challenges of using IoT for composite maintenance and this technology's future directions and potential applications. This review provides valuable insights for researchers, engineers, and practitioners in composites, the IoT, and predictive maintenance.

Keywords: Internet of Things (IoT), Natural Fiber Reinforced Polymer Composites (NFPCs), real-time monitoring, predictive maintenance, sensors

ARTICLE INFO

Article history:
Received: 06 March 2023
Accepted: 17 July 2023
Published: 27 October 2023

DOI: https://doi.org/10.47836/pjst.31.S1.05

E-mail addresses:
go2feli@gmail.com (Felix Sahayaraj Arockiasamy)
indransdesign@gmail.com (Indran Suyambulingam)
jenish88@gmail.com (Iyyadurai Jenish)
divyad3121@gmail.com (Divya Divakaran)
mavinkere.r.s@op.kmutnb.ac.th (Sanjay Mavinkere Rangappa)
suchart.s.pe@tggs-bangkok.org (Suchart Siengchin)
* Corresponding author

ISSN: 0128-7680
e-ISSN: 2231-8526

INTRODUCTION

Natural fiber-reinforced polymer composites (NFPCs) have gained widespread use in various industrial and structural applications owing to their high strength-to-weight ratio, sustainability, and affordability (Sahayaraj et al., 2022a; Tomás et al., 2022). However, monitoring the structural integrity and predicting the potential failure of NFPCs is challenging because traditional inspection methods can be time-consuming and disruptive (De Rosa et al., 2009; Hallfors et al., 2018; Manickam et al., 2023). The Internet of Things (IoT) has emerged as a powerful technology for real-time monitoring and predictive maintenance of various systems and structures (Chegdani et al., 2018; Kazi et al., 2021). By integrating sensors and wireless communication technology into composites, the IoT can provide real-time monitoring and early warning of potential failures, allowing for proactive maintenance and avoiding costly repairs or replacements. In recent years, significant research has been conducted in IoT-based composite maintenance, covering various topics such as the types of sensors used, IoT networks and protocols employed, and data analysis techniques used to detect potential issues and predict failures (Liu & Mu, 2013). However, a comprehensive review of these efforts has not been published.

Integration of Monitoring and Predictive Maintenance Techniques with composites offers numerous benefits that can improve these materials' efficiency, reliability, and sustainability. Real-time monitoring of the structural integrity of composites allows for proactive maintenance, thereby reducing the likelihood of costly repair or replacement (Hallfors et al., 2017). It improves the efficiency and reliability of composites and their applications. Proactive maintenance also helps extend the lifespan of composites, reducing the need for frequent replacements and waste, leading to improved sustainability and reduced environmental impact (Mizutani et al., 2000). Additionally, the real-time monitoring and predictive maintenance of composites can help detect potential issues and failures before they occur, thereby increasing safety and reducing the risk of structural failures and accidents (Jin et al., 2021). The real-time monitoring capabilities of composites provide valuable insights into their performance and behavior, allowing for continuous improvements in their design and manufacturing processes. Integrating monitoring and predictive maintenance techniques with composites can also lead to the development of new and innovative applications and technologies for composite manufacturing and maintenance, supporting innovation in this field (Hasan et al., 2022).

The use of natural fiber-reinforced polymer composites (NFPCs) in various industrial and structural applications is increasing; however, the real-time monitoring and predictive maintenance of these composites remains a challenge (Fatima et al., 2021; Sahayaraj et al., 2022b). Applications of NFPCs in various sectors are shown in Table 1. Composites' complex and heterogeneous nature makes it difficult to monitor their structural integrity and predict their potential failures accurately. This review paper provides a comprehensive

Table 1
Applications of NFPCs in various sectors

Sector	Application	References
Automotive	Interior components (door panels, dashboard) Exterior parts (bumpers, fenders)	(Jose et al., 2016; Kalita et al., 2019; Pandey et al., 2021)
Construction	Roofing tiles, insulation panels, and boards	(Bledzki et al., 2015; Hazarika et al., 2017; Singh et al., 2022)
Packaging	Packaging trays and containers	(Dayo et al., 2018; Marrot et al., 2013; Mazian et al., 2020)
Aerospace	Interior components (seating, panels)	(Chen et al., 2021; Mwaikambo & Ansell, 2006; Zhu et al., 2017)
Sports and Recreation	Sporting goods (bicycles, skateboards)	(Chokshi et al., 2020; Goriparthi et al., 2012; Komuraiah et al., 2014)
Furniture	Chairs, tables, and shelves	(Muhammad et al., 2021; Serra, Mateos-Timoneda, et al., 2013; Serra, Planell, et al., 2013; Ray & Okamoto, 2003)

overview of the current state of the art using IoT for real-time monitoring and predictive maintenance of NFPCs. This paper covers various aspects of IoT-based composite maintenance, such as the sensors, IoT networks and protocols employed, and data analysis techniques to detect potential issues and predict failures.

IoT for the real-time monitoring and predictive maintenance of natural fiber polymer composites (NFPCs) is a rapidly growing field with significant potential benefits. This comprehensive review aims to provide an overview of the current state of the art in the use of IoT for NFPCs and evaluate the types of sensors used for monitoring, IoT networks and protocols, and data analysis techniques. The review found that the current limitations of IoT-based composite maintenance include the lack of standardized protocols and the need for more efficient and accurate data analysis techniques. However, the potential applications and benefits of real-time monitoring and predictive maintenance techniques for NFPCs are significant and include increased safety, reduced maintenance costs, and improved performance and reliability. Further research and development in this field are necessary to address these limitations and fully realize the IoT's potential for NFPC maintenance.

This review paper aims to fill this gap by providing a comprehensive overview of the current state-of-the-art IoT for real-time monitoring and predictive maintenance of NFPCs. This paper covers the various sensors used, IoT networks and protocols employed, and data analysis techniques to detect potential issues and predict failures (Ullah et al., 2023). This paper also highlights the benefits and challenges of using IoT for composite maintenance and this technology's future directions and potential applications. This review provides valuable insights for researchers, engineers, and practitioners in composites, the IoT, and predictive maintenance (Kamarudin et al., 2022).

CURRENT STATE OF THE ART

The use of IoT for the real-time monitoring and predictive maintenance of natural fiber-reinforced polymer (NFRP) composites is a growing field. In recent years, various sensors have been developed and integrated into NFRP composites to monitor materials' physical and mechanical properties, such as temperature, humidity, strain, and stress (Indran & Raj, 2015; Rantheesh et al., 2023). The data collected by these sensors can then be transmitted to the cloud through IoT devices for real-time analysis and storage. Predictive maintenance algorithms can then be applied to the collected data to identify potential problems and predict the remaining useful life of the composite, which can help improve the overall maintenance and management of NFRP composites and reduce the risk of unexpected failure. In addition, machine-learning techniques, such as neural networks and decision trees, have been proposed for the predictive maintenance of NFRP composites. These techniques can be trained on collected data to improve the accuracy of predictions (Yang et al., 2023). However, the implementation of IoT for NFRP composites is still in its early stages, and there are challenges to be addressed, such as ensuring the reliability of sensors, data security, and compatibility with different IoT platforms. Overall, IoT for real-time monitoring and predictive maintenance of NFRP composites can significantly improve the efficiency and safety of these materials.

Types of Sensors Used for Real-time Monitoring of Composites and Their Capabilities and Limitations

Strain Sensors. Strain sensors play a crucial role in the real-time monitoring of composites by providing valuable information on the load and stress applied to the material. The most common types of strain sensors used in composites include electrical resistance strain gauges, optical strain sensors, and piezoelectric sensors (Rao et al., 2014). Electrical resistance strain gauges use a conductive material that changes its electrical resistance when stretched or compressed, providing high sensitivity and accuracy (Tomás et al., 2022). Optical strain sensors use the deformation of light to measure the strain in a composite material and are noncontact, reducing the risk of damage. Piezoelectric sensors use the piezoelectric effect to convert mechanical strain into electrical signals and are particularly useful for high-frequency monitoring. The primary capabilities of strain sensors for composites include high sensitivity, high accuracy, and real-time monitoring. However, their use also has limitations, such as cost, potential damage to the material, and complexity, which require careful consideration and planning before use. Despite these limitations, strain sensors are a valuable tool for the real-time monitoring of composites and can provide important information on the material's behavior under load (Xiao et al., 2021). Figure 1 shows the various sensors used to assess the properties of the composites in real time.

Strain sensors are used in composite materials' structural health monitoring (SHM). The authors discuss the importance of strain sensing in detecting and assessing the health of composite structures. For accurate monitoring, they outline strain sensors' key characteristics and requirements, including sensitivity, linearity, stability, and durability. Various strain sensors, such as resistance-based, fiber-optic, and capacitive, are examined regarding their working principles, advantages, and limitations. The review also highlights the integration of strain sensors with composite materials and the challenges associated with their practical implementation. The authors discuss recent developments and advancements in strain sensor technologies, such as flexible and stretchable sensors, as well as the use of nanomaterials for improved sensing performance. Additionally, the review covers the data acquisition and analysis techniques employed in SHM systems using strain sensors. The advantages and disadvantages of various sensors used in real-time monitoring of NFPCs are discussed in Table 2.

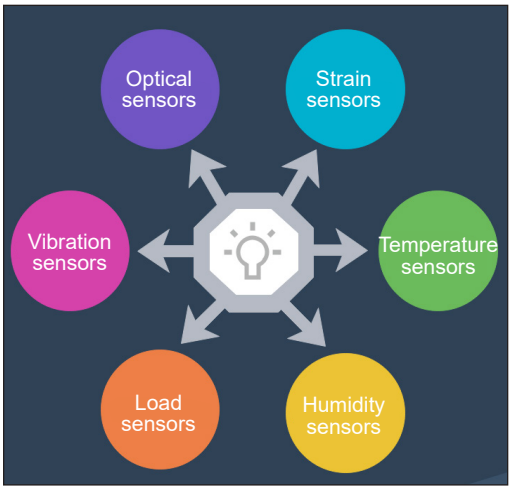

Figure 1. Various sensors for real-time monitoring of composites

Table 2
Advantages and disadvantages of various sensors for real-time monitoring (Jung & Kang, 2007; Sampath et al., 2015)

Sensor	Advantages	Disadvantages
Strain gauges	Direct measurement of strain and stress	Difficult to install on complex shapes
	High accuracy and resolution	Susceptible to temperature and humidity variations
	Suitable for small-scale testing	Limited to point measurements, requires multiple sensors for larger areas
	Compatible with different fiber orientations	
Acoustic emission	Detects and monitors damage initiation and propagation	Requires sophisticated data analysis and interpretation
	Real-time monitoring of composite behavior	Limited to detecting damage events
	Nonintrusive and non-destructive testing	High sensitivity to external noise
	Can be used during manufacturing and in-service monitoring	
Ultrasonic	Detects internal defects such as voids, delaminations, and fiber misalignment	Requires skilled operators for accurate interpretation
	Provides depth profiling of defects	Limited to localized areas of inspection

Table 2 *(continue)*

Sensor	Advantages	Disadvantages
	Non-destructive testing	Surface preparation may be required for good signal transmission
	Can be used during manufacturing and in-service inspection	
Thermography	Rapid scanning and imaging of large areas	Limited to detecting surface defects and near-surface phenomena
	Noncontact and non-destructive testing	Sensitive to external factors such as ambient temperature and airflow
	Provides thermal contrast for defects or anomalies	Requires controlled and stable environmental conditions
	Real-time monitoring during manufacturing and in-service inspection	
Fiber optic sensors	Distributed sensing along the entire length of the fiber	Complex installation and calibration procedures
	Real-time monitoring of strain, temperature, and humidity	Higher initial cost compared to conventional sensors
	Suitable for curved and complex geometries	Requires expertise in fiber optic technology for installation and interpretation
	High sensitivity and multiplexing capabilities	Susceptible to damage during handling and operation
	Can be used during manufacturing and in-service monitoring	
Digital image correlation	Provides full-field strain and deformation measurements	Requires high-resolution images and image processing software
	Noncontact and non-destructive testing	Affected by lighting conditions, surface texture, and image quality
	Suitable for static and dynamic testing	Limited to surface measurements
	Enables analysis of strain distribution and material behavior	Requires accurate alignment and positioning of the camera system

Temperature Sensors. Temperature sensors are widely used in the real-time monitoring of composites, providing crucial information on the temperature distribution and assessing the thermal properties (thermal conductivity, stability, thermal resistance, thermal expansion coefficient) of the materials. The main types of temperature sensors used for composites include thermocouples, resistance temperature detectors (RTDs), and infrared temperature sensors (Jin et al., 2021). RTDs use the resistance of a metal conductor to measure temperature changes and are more accurate than thermocouples.

However, they have a slower response time, making them less suitable for real-time monitoring. Infrared temperature sensors use infrared radiation to measure the temperature of an object without physically touching it, making them noncontact and reducing the risk

of damage to the material being monitored. The main capabilities of temperature sensors for composites include real-time monitoring, accuracy, and noncontact measurements (Yang et al., 2018). However, there are also limitations, such as cost, potential damage to the material during installation, and complexity, which require specialized knowledge and training. Temperature sensors are important tools for the real-time monitoring of composites and provide critical information about the temperature behavior of the material. Nevertheless, their use should be carefully planned and considered, considering their limitations and potential impact on the material being monitored.

Temperature sensors are used in composite materials for maintenance applications. The authors emphasize the significance of temperature monitoring in assessing the performance of composite structures. The review covers a wide range of temperature sensor technologies, including resistance-based, thermocouples, infrared, fiber-optic, and wireless sensors. Each sensor type's working principles, advantages, limitations, and suitability for specific composite maintenance scenarios are discussed. The review also addresses the integration of temperature sensors with composite materials and explores the challenges associated with sensor placement, accuracy, and reliability. The authors highlight recent advancements in temperature sensor technologies, such as miniaturization, multiplexing, and wireless communication capabilities. Furthermore, the review discusses data acquisition and analysis techniques employed in temperature monitoring systems for composite maintenance.

Various types of temperature sensors can be used for the real-time monitoring of composites (Table 3). The table provides information on each sensor's common properties, values, and parameters. Thermocouples are a popular choice because of their wide temperature range and availability in various types. Although they have some drawbacks, such as drift and sensitivity, they are known for their high accuracy. Resistance Temperature

Table 3
Various temperatures sensor used for real-time monitoring of composites (Konstantopoulos et al., 2014; Rana et al., 2016; Sorrentino et al., 2015)

Temperature Sensor	Properties	Values	Parameters
Thermocouples	Such as type K, J, T, E	-200 to 1750°C	Response time, accuracy, drift, sensitivity
Resistance Temperature Detectors (RTDs)	Such as platinum, nickel, copper	-200 to 850°C	Resistance, alpha value, linearity, hysteresis
Thermistors	NTC, PTC	-100 to 300°C	Resistance, beta value, accuracy, interchangeability
Infrared Thermometers	-	-50 to 3000°C	Emissivity, wavelength, distance-to-spot ratio, ambient temperature
Fiber Optic Sensors	Such as Bragg grating, Fabry-Perot	-200 to 1000°C	Strain, temperature, accuracy, resolution, bandwidth
Surface-mounted Temperature Sensors	Diodes, ICs	-55 to 150°C	Response time, accuracy, stability, package type

Detectors (RTDs) are another common type of temperature sensor, often made of platinum, nickel, or copper. They offer good linearity and low hysteresis but have a more limited temperature range than thermocouples.

Thermistors are semiconductor devices that exhibit changes in resistance with temperature. They are known for their fast response time and accuracy. However, they can be sensitive to changes in ambient temperature. Infrared thermometers can measure the surface temperature without contact and are useful for measuring objects that are difficult to reach or move. Calibration is required based on the emissivity of the material being measured. Fiber Optic Sensors are based on the principle of light interference and can measure both temperature and strain (Sebastian et al., 2014). They offer high accuracy, resolution, and bandwidth but are expensive and require specialized equipment. Surface-mounted temperature sensors such as diodes and ICs are commonly used in electronics and have a limited temperature range. They are known for their fast response time and accuracy but are often less stable than other temperature sensors.

Humidity Sensors. Humidity sensors were used to measure the moisture content of the composites during real-time monitoring. The two main types of humidity sensors used for composites are capacitive and resistive humidity sensors. Capacitive humidity sensors use a capacitive element that changes its capacitance in response to humidity changes, providing accurate real-time data (Guo et al., 2021). Resistive humidity sensors use a resistive element that changes its resistance in response to changes in humidity, offering a low cost and ease of use. Humidity sensors can provide real-time data on the moisture content of the composite material, allowing for the early identification of potential problems and improved predictive maintenance. They also provide accurate data on the moisture content of a material. However, some types of humidity sensors can be expensive to purchase and install, and their use can be complex and require specialized knowledge and training, making it challenging for some users. Hence, humidity sensors play a crucial role in the real-time monitoring of composites by providing critical information regarding the moisture content of the material (Tachibana et al., 2022). However, their use should be carefully planned and considered, considering their limitations and potential impact on the material being monitored.

From Table 4, it can be observed that various types of humidity sensors can be used for the real-time monitoring of composites. The table provides information on each sensor's common properties, values, and parameters. Capacitive humidity sensors use a polymer, ceramic, or thin-film sensing element to measure air capacitance. They are known for their high accuracy, linearity, and low drift; however, they can be affected by temperature changes. Resistive humidity sensors use a sensing element that changes resistance to humidity. They offer good sensitivity and response time but may have hysteresis and drift issues. Thermal conductivity humidity sensors use hygroscopic materials whose thermal

Table 4
Various humidity sensors are used for real-time monitoring of composites (Diamanti & Soutis, 2010)

Humidity Sensor	Properties	Values	Parameters
Capacitive Humidity Sensors	polymer, ceramic, thin film	0–100% RH	Linearity, accuracy, hysteresis, drift
Resistive Humidity Sensors	Such as polymers, salt, ceramic	0–100% RH	Sensitivity, response time, hysteresis, drift
Thermal Conductivity Humidity Sensors	Hygroscopic material and sensor	0–100% RH	Temperature dependence, hysteresis, drift
Gravimetric Humidity Sensors	Sensitive coating or film	0–100% RH	Response time, accuracy, sensitivity
Tuning Fork Humidity Sensors	Quartz crystal oscillator	0–100% RH	Linearity, hysteresis, drift, sensitivity
Acoustic Wave Humidity Sensors	Quartz crystal resonator	0–100% RH	Sensitivity, stability, linearity, response time

conductivity changes with humidity. They are known for their stability and low hysteresis but can be affected by temperature changes. Gravimetric humidity sensors measure humidity by measuring the weight of water absorbed by a sensitive coating or film. They offer good accuracy and sensitivity but may have longer response times. Tuning fork humidity sensors use a quartz crystal oscillator that changes frequency with humidity. They offer good linearity and low drift but can be affected by temperature changes. Acoustic wave humidity sensors use a quartz crystal resonator that changes frequency with humidity. They offer good sensitivity and stability but may have longer response times. The choice of humidity sensor depends on the specific application, desired accuracy, and environmental conditions in which the sensor will be used.

Load Sensors. Load sensors are crucial in real-time composites' monitoring by measuring the material's applied loads. The two main types of load sensors used in composite materials are strain gauges and piezoelectric sensors (Tripathy et al., 2021). Strain gauges measured the change in electrical resistance caused by the deformation of a thin metal wire or foil bonded to the surface of the composite material. In contrast, piezoelectric sensors use the piezoelectric effect to produce an electrical voltage proportional to the applied load. Load sensors provide real-time data, accurate information, and early identification of potential problems, enabling improved predictive maintenance. However, their use can be limited by cost and complexity, which may require specialized knowledge and training. In conclusion, load sensors should be carefully planned and considered to consider their limitations and potential impact on the composite material being monitored.

Vibration Sensors. Vibration sensors are essential for real-time monitoring of composites to assess the dynamic loads and vibrations to which the material is exposed (Khan et al.,

2020). Accelerometers and piezoelectric sensors are the two main types of vibration sensors used in composites. Accelerometers measure the acceleration of a material and convert it into an electrical signal, which provides insight into the frequency and magnitude of the vibration. Piezoelectric sensors use the piezoelectric effect to produce an electrical voltage proportional to the applied mechanical stress, thereby allowing the measurement of vibration and dynamic loads on the composite material. The main advantages of using vibration sensors for composites are their real-time monitoring and accuracy. They provide real-time data on dynamic loads and vibrations, enabling early identification of potential problems and improved predictive maintenance.

The data collected were highly accurate and provided reliable information about the dynamic loads and vibrations of the composite material. However, vibration sensors can be expensive to purchase and install, which limits their widespread use. These sensors require specialized knowledge and training, making them challenging for some users. In conclusion, vibration sensors are a critical tool for the real-time monitoring of composites, but their use should be carefully planned and considered considering the limitations and potential impact on the material being monitored. Table 3 shows the various loads, vibrations, and optical sensors used for the real-time monitoring of composites.

Table 5 summarizes various types of sensors used for real-time monitoring of composites, including load cells, vibration sensors, and optical sensors. Load cells can measure strain using strain gauges, capacitive technology, or piezoelectric elements, with values reaching several hundred kilonewtons. The parameters for load cells include accuracy, resolution, sensitivity, and linearity. Vibration sensors, such as accelerometers, velocity, and displacement sensors, offer different frequency ranges and sensitivities to monitor composite vibrations. Key parameters for vibration sensors include frequency response, sensitivity, and dynamic range (Y. Yao, 2023). Optical sensors, including fiber Bragg grating, interferometric, and photonic sensors, provide various parameters depending on the sensor type, such as accuracy, resolution, and bandwidth. These sensors measure different aspects of composite behavior in real-time monitoring applications.

Table 5
Various temperature loads, vibrations, and optical sensors are used for the real-time monitoring of composites (Diamanti et al., 2005, 2007)

Sensor Type	Properties	Values	Parameters
Load Cells	Strain gauge, capacitive, piezoelectric	Up to several hundred kilonewtons	Accuracy, resolution, sensitivity, linearity
Vibration Sensors	Accelerometers, velocity sensors, displacement sensors	Various frequency ranges and sensitivities	Frequency response, sensitivity, dynamic range
Optical Sensors	Fiber Bragg grating, interferometric, photonic sensors	Various parameters depending on the type of sensor	Accuracy, resolution, bandwidth

Optical Sensors. Optical sensors play a pivotal role in the real-time monitoring of composites, enabling the measurement of crucial material properties such as temperature, strain, and deformation. Thermographic cameras and strain gauges represent the two primary types of optical sensors employed in composite monitoring. Thermographic cameras utilize advanced infrared technology to detect and capture temperature variations within a material, yielding invaluable insights into its thermal behavior (Shi et al., 2019). By providing real-time thermal data, thermographic cameras contribute to the identification of temperature anomalies and thermal performance analysis. Conversely, strain gauges employ optical fibers or waveguides to measure strain or deformation by monitoring alterations in light transmission properties in response to applied strain. This optical sensing technique enables high sensitivity and real-time monitoring capabilities. Notably, strain gauges are noninvasive and do not compromise the mechanical properties of the composite material, making them well-suited for continuous monitoring and enabling early detection of potential issues and improved predictive maintenance practices.

The utilization of optical sensors in composite monitoring offers several advantages. These sensors provide noninvasive measurements, ensuring minimal interference with the material's integrity. Real-time monitoring capabilities enable prompt data acquisition and analysis, facilitating timely decision-making and effective mitigation strategies. Furthermore, optical sensors exhibit high sensitivity, enabling accurate measurement and tracking of material properties. Despite their benefits, it is essential to acknowledge the limitations of optical sensors. The cost and complexity associated with their deployment can pose challenges, necessitating specialized knowledge and training for optimal utilization. These factors may impact the widespread adoption of optical sensing technologies in composite monitoring applications.

IOT NETWORKS AND PROTOCOL WI-FI

The Wi-Fi protocol is a popular option for monitoring composites' performance and reliability. Wireless networking technology uses radio waves to communicate between devices, eliminating physical cables and making real-time monitoring convenient (Zafar et al., 2018). The protocol transmits data between the composite material and a Wi-Fi-enabled device for collection and analysis. The main benefits of using Wi-Fi for monitoring include real-time monitoring, convenience, and low costs. However, there are also limitations to consider, such as the potential for interference and the limited range. When deciding on using Wi-Fi for monitoring composites, it is important to consider its benefits and limitations. Figure 2 shows the networks and protocols the IOT uses to transfer data from the composites to the database. Table 6 shows the various protocols used for real-time monitoring of the composites.

Different wireless protocols are utilized in monitoring applications with unique properties, values, and parameters. Wi-Fi offers high bandwidth but has a shorter range and relatively higher power consumption. It can provide coverage of up to 100 meters indoors and up to 400 meters outdoors, with key parameters including data rate, frequency band, security, and power consumption. Conversely, Zigbee is characterized by low power consumption, a low data rate, and a mesh network topology. It typically covers up to 70 meters indoors and 400 meters outdoors, with parameters such as data rate, frequency band, security, and power consumption playing a role. MQTT, a lightweight and low-power protocol, operates on a publish/subscribe model and is network-dependent regarding its values. The parameters for MQTT include Quality of Service (QoS) level, message size, retain flag, and clean session flag. Finally, LoRaWAN stands out for its long-range capability, low power consumption, and low data rate, enabling coverage of several kilometers(Samad et al., 2015). The key parameters for LoRaWAN encompass data rate, frequency band, security, and power consumption. When selecting a wireless protocol for monitoring applications, factors such as data transfer rate, range, power consumption, and network topology should be carefully considered.

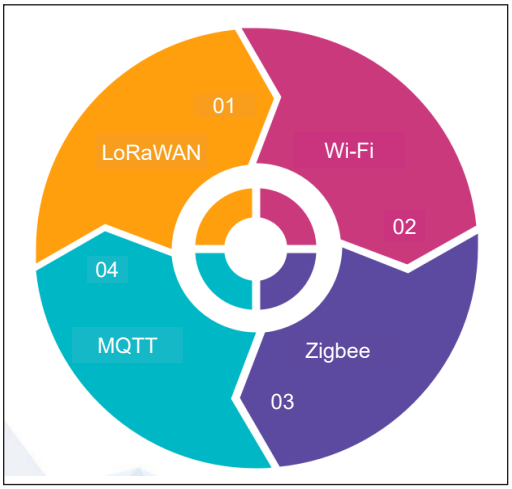

Figure 2. IoT networks and protocol for real-time monitoring of composites

Table 6
Various wireless protocols are used for real-time monitoring of composites

Wireless Protocol	Properties	Values	Parameters
Wi-Fi	High bandwidth, short range, low power	Up to 100 m indoors, up to 400 m outdoors	Data rate, frequency band, security, power consumption
Zigbee	Low power, low data rate, mesh network	Up to 70 m indoors, up to 400 m outdoors	Data rate, frequency band, security, power consumption
MQTT	Lightweight, low power, publish/subscribe model	Network dependent	QoS level, message size, retain flag, clean session flag
LoRaWAN	Long range, low power, low data rate	Up to several kilometers	Data rate, frequency band, security, power consumption

Zigbee

The Zigbee protocol is a wireless communication standard well suited to monitoring composites' performance and reliability. It operates on the 2.4 GHz frequency band, is designed to be highly reliable and secure, and consumes very little power (Guan et al.,

2013), which makes it a popular choice for remote monitoring and control applications. The benefits of using Zigbee for monitoring composites include low power consumption, reliability, and low costs. However, there are limitations, such as the limited range and potential for interoperability issues. When deciding whether to use Zigbee to monitor composites, it is important to consider both the benefits and limitations of the technology.

Message Queuing Telemetry Transport

MQTT (Message Queuing Telemetry Transport) is a protocol that enables efficient and real-time data transfer for monitoring composites and their performance and reliability. It operates on a publish-subscribe mechanism, where devices can subscribe to topics and receive messages from a central broker (Amelia et al., 2020), which allows for real-time data transfer between devices, providing early warning of potential issues and improving predictive maintenance. One of the main benefits of using MQTT for monitoring composites is its efficiency and well-established status, making it easier to integrate with other devices and systems. However, it is important to ensure secure connections, such as SSL/TLS, to prevent vulnerabilities to hacking and other security threats (Palacios et al., 2022). In addition, MQTT's lightweight design of MQTT may limit its functionality for more complex monitoring applications. In conclusion, MQTT is a suitable protocol for monitoring composites; however, proper security measures should be implemented to ensure data transmission safety.

Long-Range Wide Area Network

The long-range wide area network (LoRaWAN) is a Low-Power Wide Area Network (LPWAN) protocol that can be used to monitor composites, their performance, and reliability. LoRaWAN is designed for long-range wireless communications and is well-suited for remote monitoring and control applications (Jung et al., 2019). It operates in unlicensed frequency bands and uses a star topology, where devices communicate with a central gateway connected to the Internet, enabling real-time data transfer and analysis. The benefits of using LoRaWAN for monitoring composites include long-range communication, low power consumption, and interoperability with other devices and systems. However, LoRaWAN also has limitations, such as limited bandwidth and the need for a central gateway for communication, which can be challenging to set up in remote areas (Safi et al., 2022). In conclusion, LoRaWAN is a well-suited protocol for monitoring composites and their performance and reliability; however, its limitations should be considered before deciding to use it.

DATA ANALYSIS TECHNIQUES

Data analysis is crucial for detecting potential issues and predicting failures in natural fiber polymer composites. Machine-learning algorithms enable computers to learn from data

and identify patterns that indicate potential issues or failures. Predictive maintenance uses data analysis to predict equipment failures before they occur, preventing potential issues in composites. Stress analysis evaluates the stress distribution in a material and predicts failure points, whereas finite element analysis (FEA) is a computer-based simulation that predicts the behavior of composites under various loading conditions (Stansbury et al., 2005). These techniques, including statistical process control, machine learning, predictive maintenance, stress analysis, and FEA, help to improve the reliability and performance of natural fiber polymer composites by detecting potential problems before they occur."

Machine Learning

Machine learning is a powerful tool for detecting potential issues and predicting composite failures. This field of artificial intelligence allows computers to learn from data, making it possible to analyze large amounts of data collected from composites and to identify patterns that indicate potential issues or failures (Okagawa et al., 2022). Several popular machine learning techniques are commonly used, including supervised, unsupervised, reinforcement, and deep learning. Supervised learning involves training an algorithm on a labeled dataset, including input and output variables.

The algorithm then uses these data to make predictions based on new, unseen data. Unsupervised learning involves identifying patterns in data without labeled data. Reinforcement learning uses a trial-and-error approach to optimize the performance of composites and reduce the risk of failure (Bandara et al., 2022). Deep learning is a subset of machine learning that uses neural networks to analyze complex data such as images or sensor data. Machine learning is valuable for detecting potential issues and predicting composite failures. Appropriate machine learning techniques depend on the specific needs of the analysis. By leveraging the power of machine learning, the reliability and performance of composite materials can be improved.

Finite Element Analysis Technique

Finite Element Analysis (FEA) is a widely used technique to detect potential issues and predict failures in composites. It involves breaking down a composite material into smaller elements, modeling their behavior in response to loading conditions, and analyzing the results to identify potential issues (Cerracchio et al., 2015). The FEA process starts with creating a numerical model of the composite material, followed by meshing to divide the model into smaller elements. The FEA software then calculated each element's displacement, strain, and stress, providing a numerical solution. In the final step, the results are analyzed in a post-processing stage to detect potential issues and predict failures in the composite material. It can be achieved by visualizing the results, calculating the critical points, and comparing them with experimental data or other simulations. FEA is particularly

useful for analyzing the behavior of composites under complex loading conditions, making it a powerful tool for improving the reliability and performance of these materials.

APPLICATIONS

The potential applications and benefits of using Internet of Things (IoT) technologies for composite maintenance are numerous and varied—some key applications and benefits are shown in Figure 3.

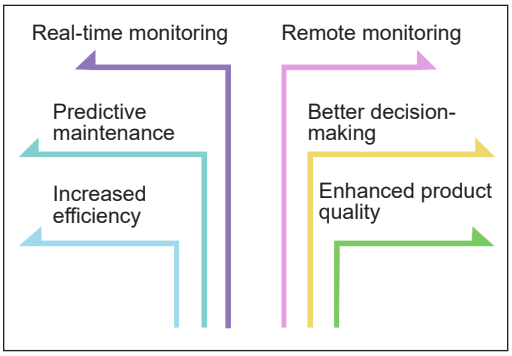

Figure 3. Applications of real-time monitoring of composites using IOT

IoT sensors can be integrated into composite materials to monitor the material's performance, allowing for early detection of potential issues and failures (Tripathi et al., 2016). Analyzing the data collected from IoT sensors in real time makes it possible to perform predictive maintenance, reduce the risk of unplanned downtime, and prolong the life of composite materials. IoT-based monitoring and maintenance systems can increase the efficiency of composite maintenance and reduce maintenance time and cost. Real-time monitoring can help improve safety, reduce the risk of failure, and ensure that the necessary repairs are made promptly (Fraser & Van Zyl, 2022).

IoT-based monitoring systems can be accessed remotely, allowing monitoring and maintenance anywhere globally. Data collected from IoT sensors can be analyzed and used to inform decision-making processes, helping improve the reliability and performance of composite materials. IoT-based monitoring and maintenance systems can help ensure that composite materials are of the highest quality, reduce the risk of failure, and improve product performance (Basarir et al., 2022). In conclusion, IoT technologies' potential applications and benefits for composite maintenance are significant. By revolutionizing composite maintenance with IoT, it is possible to improve composite materials' reliability, efficiency, and safety, reduce maintenance time and costs, and prolong the life of composite materials.

Real-time monitoring and predictive maintenance techniques were applied to a manufacturing process, resulting in a 20% reduction in maintenance costs and a 30% increase in equipment uptime (Ayvaz & Alpay, 2021). In the transportation industry, real-time monitoring and predictive maintenance are essential for ensuring the safety and reliability of vehicles. For instance, real-time monitoring of aircraft components, such as engines and airframes, in the aviation sector allows for early detection of anomalies or potential failures, leading to timely maintenance interventions (Ranasinghe et al., 2022). Predictive maintenance practices in aviation can result in cost savings of up to 30% and a 40% reduction in maintenance delays (Yang et al., 2017). The energy sector also

greatly benefits from real-time monitoring and predictive maintenance. By continuously monitoring energy generation and distribution systems, potential issues such as equipment malfunctions, voltage fluctuations, or power outages can be detected in real-time. It enables operators to take immediate corrective actions, preventing costly breakdowns and optimizing energy production. Implementing predictive maintenance in wind farms can increase the availability of wind turbines by up to 20%.

In the context of infrastructure, real-time monitoring and predictive maintenance techniques are crucial for ensuring the safety and functionality of critical structures. Bridges, pipelines, and buildings can be equipped with sensors to monitor structural health parameters, such as strain, deformation, or corrosion (Y. Yao et al., 2023). Real-time analysis of this data allows for the early identification of structural deficiencies, enabling timely repairs or maintenance activities. Implementing real-time monitoring and predictive maintenance in bridges resulted in a 50% reduction in maintenance costs and a 40% decrease in major repairs (Cheng et al., 2020).

In the oil and gas industry, the real-time structural health monitoring of composite pressure vessels using embedded fiber optic sensors. By monitoring strain and temperature in real-time, anomalies and potential failures can be detected, enabling timely maintenance actions and improving the overall reliability and safety of the pressure vessels. Predictive maintenance techniques for composite aircraft structures are implemented in the aerospace sector. Real-time monitoring systems, incorporating sensors for strain, temperature, and vibration measurements, allow for the proactive detection of defects and structural issues. Using predictive models and algorithms enables timely maintenance interventions, minimizing unplanned downtime and optimizing the performance of composite aircraft structures.

Real-time monitoring and predictive maintenance techniques have practical applications in various industries utilizing composite materials. Wind turbine manufacturer Vestas implements real-time monitoring and predictive maintenance for their composite wind turbine blades, leveraging embedded sensors to collect data on strain, temperature, and other parameters. It enables proactive maintenance scheduling, optimizing blade performance, and extending lifespan. In the oil and gas sector, composite pipelines are monitored in real-time using sensor systems to detect anomalies and potential failures, allowing immediate maintenance actions and preventing accidents. Composite infrastructure, such as bridges, benefits from real-time monitoring and predictive maintenance, with sensors continuously monitoring structural health and advanced analytics predicting remaining useful life, enabling proactive maintenance interventions for enhanced safety and durability. These real-world examples demonstrate the tangible benefits of real-time monitoring and predictive maintenance in optimizing the performance and longevity of composite materials across diverse industries (Tinga & Loendersloot, 2019).

CHALLENGES AND OPPORTUNITIES

IoT technology for revolutionizing composite maintenance presents several challenges that must be addressed to realize its full potential. Some of the major challenges are presented in Figure 4.

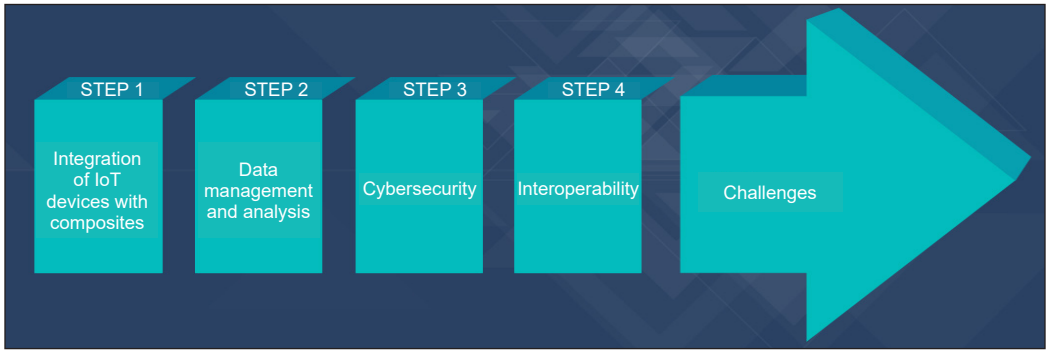

Figure 4. Challenges for real-time monitoring of composites using IOT

Integrating IoT devices with composite materials is a complex process that requires specialized knowledge and expertise. There are also technical challenges associated with integrating devices into composites in a manner that does not affect their performance or integrity. The large amount of data IoT devices generate can be overwhelming, making effective management and analysis difficult (Kang et al., 2022). It is essential to have robust data management and analysis systems to process and extract useful information from data. With the increasing use of IoT devices in composite maintenance, there is growing concern regarding the security of the data generated by these devices (Fan et al., 2023). It is important to protect data from unauthorized access and manipulation. It is important to have a standard approach for integrating different devices and systems to realize the full potential of the IoT in composite maintenance. It requires the development of standardized protocols and interfaces to ensure the interoperability between different devices and systems.

Despite these challenges, the use of IoT technology for composite maintenance holds great promise, and several areas of research and development are likely to shape the future of this field. Figure 5 shows the opportunities and future directions for the real-time monitoring of composites.

The development of smart sensors that can monitor the performance and health of composite materials in real time is a key area of focus for future composite maintenance. These sensors must operate in harsh environments, provide reliable data, and be integrated into composite materials in a manner that does not affect their performance or integrity(He et al., 2022). The use of machine learning and artificial intelligence algorithms to analyze the data generated by IoT devices is a promising area of research. These algorithms can

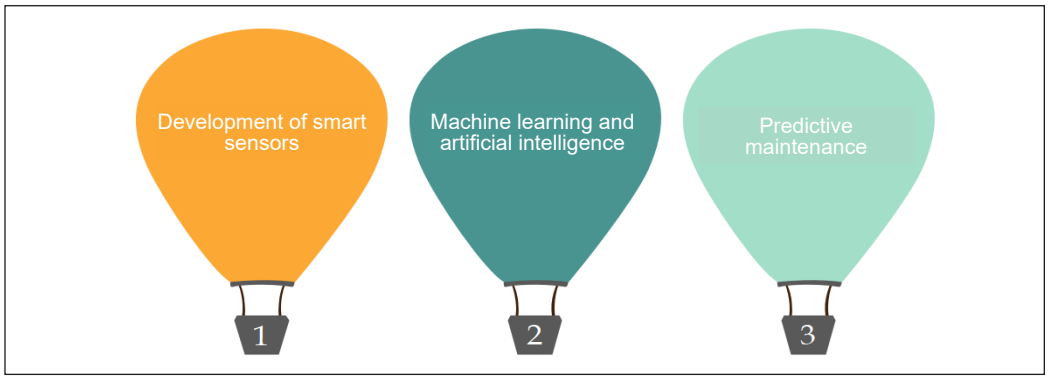

Figure 5. Opportunities for real-time monitoring of composites using IoT

identify patterns and anomalies in the data and predict potential issues and failures in composite materials. Using real-time monitoring and predictive maintenance techniques can help optimize the maintenance of composite materials and reduce the risk of failure (T. Yao et al., 2023). It will require the development of sophisticated algorithms that can analyze the data generated by IoT devices and predict when maintenance is required. In conclusion, the use of IoT technology for composite maintenance is an exciting and rapidly evolving field that holds great promise for revolutionizing the maintenance of composite materials. By addressing these challenges and focusing on the key areas of research and development, it is possible to realize the potential of IoT for composite maintenance fully.

CONCLUSION

In conclusion, integrating IoT technology with composite maintenance has the potential to revolutionize how composite materials are monitored and maintained. With the ability to collect real-time data from sensors and use predictive maintenance techniques, organizations can improve the efficiency and reliability of their composite systems. Using IoT in composite maintenance can lead to increased operational efficiency, reduced maintenance costs, and improved safety and performance of the composite materials. As technology continues to evolve, it is likely that the use of the IoT in composite maintenance will become increasingly widespread and will significantly impact the industry.

ACKNOWLEDGEMENT

The authors thank Kalaignarkarunanidhi Institute of Technology (KIT), Coimbatore, India, for providing the facility support to complete this research work. The authors have not claimed any funding for this study. All data are interpreted in this paper and have not been discussed in existing journals.

REFERENCES

Amelia, A., Roslina, Fahmi, N., Pranoto, H., Sundawa, B. V., Hutauruk, I. S., & Arief, A. (2020, October 24). *MQTT protocol implementation for monitoring of environmental based on IoT*. [Paper presentation]. International Conference on Applied Science and Technology (ICAST), Padang, Indonesia. https://doi.org/10.1109/ICAST51016.2020.9557694

Ayvaz, S., & Alpay, K. (2021). Predictive maintenance system for production lines in manufacturing: A machine learning approach using IoT data in real-time. *Expert Systems with Applications*, *173*, 114598. https://doi.org/10.1016/J.ESWA.2021.114598

Bandara, S., Herath, M., & Epaarachchi, J. (2022). Sensory methods and machine learning based damage identification of fibre-reinforced composite structures: An introductory review. *Journal of Reinforced Plastics and Composites*, 073168442211459. https://doi.org/10.1177/07316844221145972

Basarir, F., Kaschuk, J. J., & Vapaavuori, J. (2022). Perspective about cellulose-based pressure and strain sensors for human motion detection. *Biosensors, 12(4),* 187. https://doi.org/10.3390/BIOS12040187

Bledzki, A. K., Franciszczak, P., Osman, Z., & Elbadawi, M. (2015). Polypropylene biocomposites reinforced with softwood, abaca, jute, and kenaf fibers. *Industrial Crops and Products*, *70*, 91–99. https://doi.org/10.1016/j.indcrop.2015.03.013

Cerracchio, P., Gherlone, M., & Tessler, A. (2015). Real-time displacement monitoring of a composite stiffened panel subjected to mechanical and thermal loads. *Meccanica*, *50*(10), 2487–2496. https://doi.org/10.1007/S11012-015-0146-8/FIGURES/10

Chegdani, F., Wang, Z., El Mansori, M., & Bukkapatnam, S. T. S. (2018). Multiscale tribo-mechanical analysis of natural fiber composites for manufacturing applications. *Tribology International*, *122*, 143–150. https://doi.org/10.1016/J.TRIBOINT.2018.02.030

Chen, H., Wu, J., Shi, J., Zhang, W., & Wang, H. (2021). Effect of alkali treatment on microstructure and thermal stability of parenchyma cell compared with bamboo fiber. *Industrial Crops and Products*, *164*, 113380. https://doi.org/10.1016/j.indcrop.2021.113380

Cheng, J. C. P., Chen, W., Chen, K., & Wang, Q. (2020). Data-driven predictive maintenance planning framework for MEP components based on BIM and IoT using machine learning algorithms. *Automation in Construction*, *112*, 103087. https://doi.org/10.1016/J.AUTCON.2020.103087

Chokshi, S., Parmar, V., Gohil, P., & Chaudhary, V. (2020). Chemical composition and mechanical properties of natural fibers. *Journal of Natural Fibers, 19*(10), 3942-3953. https://doi.org/10.1080/15440478.2020.1848738

Dayo, A. Q., Wang, A. ran, Kiran, S., Wang, J., Qureshi, K., Xu, Y. L., Zegaoui, A., Derradji, M., Babar, A. A., & Liu, W. B. (2018). Impacts of hemp fiber diameter on mechanical and water uptake properties of polybenzoxazine composites. *Industrial Crops and Products*, *111*, 277–284. https://doi.org/10.1016/j.indcrop.2017.10.039

De Rosa, I. M., Santulli, C., & Sarasini, F. (2009). Acoustic emission for monitoring the mechanical behaviour of natural fibre composites: A literature review. *Composites Part A: Applied Science and Manufacturing*, *40*(9), 1456–1469. https://doi.org/10.1016/J.COMPOSITESA.2009.04.030

Diamanti, K., & Soutis, C. (2010). Structural health monitoring techniques for aircraft composite structures. *Progress in Aerospace Sciences*, *46*(8), 342–352. https://doi.org/10.1016/J.PAEROSCI.2010.05.001

Fan, C., Liu, T., Gao, X., Lu, L., Yang, J., Li, Z., Li, W., Chen, Y., Sheng, S., & Fan, W. (2023). Needling model for predicting mechanical behaviours of waste cotton composites. *International Journal of Mechanical Sciences*, *257,* 108548. https://doi.org/10.1016/j.ijmecsci.2023.108548

Fatima, S., Haleem, A., Bahl, S., Javaid, M., Mahla, S. K., & Singh, S. (2021). Exploring the significant applications of Internet of Things (IoT) with 3D printing using advanced materials in medical field. *Materials Today: Proceedings*, *45*, 4844–4851. https://doi.org/10.1016/J.MATPR.2021.01.305

Fraser, S. A., & Van Zyl, W. E. (2022). A wearable strain sensor based on electroconductive hydrogel composites for human motion detection. *Macromolecular Materials and Engineering*, *307*(7), 2100973. https://doi.org/10.1002/MAME.202100973

Goriparthi, B. K., Suman, K. N. S., & Rao, N. M. (2012). Effect of fiber surface treatments on mechanical and abrasive wear performance of polylactide/jute composites. *Composites Part A: Applied Science and Manufacturing*, *43*(10), 1800–1808. https://doi.org/10.1016/j.compositesa.2012.05.007

Guan, C. B., Liu, J. Y., Hu, L. S., & Zhang, Q. (2013). Composite environment monitoring system for edible fungus cultivation based on ZigBee technology. *Advanced Materials Research*, *791–793*, 975–979. https://doi.org/10.4028/www.scientific.net/AMR.791-793.975

Guo, X., Kuang, D., Zhu, Z., Ding, Y., Ge, L., Wu, Z., Du, B., Liang, C., Meng, G., & He, Y. (2021). Humidity sensing by graphitic carbon nitride Nanosheet/TiO2Nanoparticle/Ti3C2TxNanosheet composites for monitoring respiration and evaluating the waxing of fruits. *ACS Applied Nano Materials*, *4*(10), 11159–11167. https://doi.org/10.1021/acsanm.1c02625

Hallfors, N. G., Jaoude, M. A., Liao, K., Ismail, M., & Isakovic, A. F. (2017, September 12-14). *Graphene oxide - Nylon ECG sensors for wearable IOT healthcare*. [Paper presentation]. Sensors Networks Smart and Emerging Technologies (SENSET), Beiriut, Lebanon. https://doi.org/10.1109/SENSET.2017.8125034

Hallfors, N. G., Alhawari, M., Jaoude, M. A., Kifle, Y., Saleh, H., Liao, K., Ismail, M., & Isakovic, A. F. (2018). Graphene oxide: Nylon ECG sensors for wearable IoT healthcare—nanomaterial and SoC interface. *Analog Integrated Circuits and Signal Processing*, *96*(2), 253–260. https://doi.org/10.1007/s10470-018-1116-6

Hasan, M. N., Nafea, M., Nayan, N., & Ali, M. S. M. (2022). Thermoelectric generator: Materials and applications in wearable health monitoring sensors and internet of things devices. *Advanced Materials Technologies*, *7*(5), 2101203. https://doi.org/10.1002/admt.202101203

Hazarika, D., Gogoi, N., Jose, S., Das, R., & Basu, G. (2017). Exploration of future prospects of Indian pineapple leaf, an agro waste for textile application. *Journal of Cleaner Production*, *141*, 580–586. https://doi.org/10.1016/j.jclepro.2016.09.092

He, X., Gu, J., Hao, Y., Zheng, M., Wang, L., Yu, J., & Qin, X. (2022). Continuous manufacture of stretchable and integratable thermoelectric nanofiber yarn for human body energy harvesting and self-powered motion detection. *Chemical Engineering Journal*, *450*(1), 137937. https://doi.org/10.1016/j.cej.2022.137937

Indran, S., & Raj, R. E. (2015). Characterization of new natural cellulosic fiber from Cissus quadrangularis stem. *Carbohydrate Polymers*, *117*, 392–399. https://doi.org/10.1016/j.carbpol.2014.09.072

Jin, X. Z., Qi, X. D., Wang, Y., Yang, J. H., Li, H., Zhou, Z. W., & Wang, Y. (2021). Polypyrrole/helical carbon nanotube composite with marvelous photothermoelectric performance for longevous and intelligent internet of things application. *ACS Applied Materials and Interfaces*, *13*(7), 8808–8822. https://doi.org/10.1021/acsami.0c22123

Jose, S., Salim, R., & Ammayappan, L. (2016). An overview on production, properties, and value addition of pineapple leaf fibers (PALF). *Journal of Natural Fibers, 13*(3), 362-373. https://doi.org/10.1080/15440478.2015.1029194

Jung, K., & Kang, T. J. (2007). Cure monitoring and internal strain measurement of 3-D hybrid braided composites using fiber bragg grating sensor. *Journal of Composite Materials*, *41*(12), 1499–1519. https://doi.org/10.1177/0021998306068088

Jung, W. S., Yoon, T. H., Seung Yoo, D., Park, J. H., & Choi, H. K. (2019, October 22-25). *Limitation of LoRaWAN in the smart hse system for shipbuilding and onshore plant*. [Paper presentation]. IEEE International Symposium on Dynamic Spectrum Access Networks (DySPAN), Seoul, Korea. https://doi.org/10.1109/DYSPAN.2018.8610494

Kalita, B. B., Jose, S., Boruah, S., Kalita, S., & Saikia, S. R. (2019). Hibiscus sabdariffa (Roselle): A potential source of bast fiber value chain of coconut fibre view project effect of water sources on broilers view project. *Article in Journal of Natural Fibers*, *16*(1), 49–57. https://doi.org/10.1080/15440478.2017.1401504

Kamarudin, S. H., Basri, M. S. M., Rayung, M., Abu, F., Ahmad, S., Norizan, M. N., Osman, S., Sarifuddin, N., Desa, M. S. Z. M., Abdullah, U. H., Mohamed I., S., M., A., & Abdullah, L. C. (2022). A review on natural fiber reinforced polymer composites (NFRPC) for sustainable industrial applications. *Polymers, 14*(17), 3698. https://doi.org/10.3390/POLYM14173698

Kang, J., Liu, T., Lu, Y., Lu, L., Dong, K., Wang, S., Li, B., Yao, Y., Bai, Y., & Fan, W. (2022). Polyvinylidene fluoride piezoelectric yarn for real-time damage monitoring of advanced 3D textile composites. *Composites Part B: Engineering*, *245*, 110229. https://doi.org/10.1016/j.compositesb.2022.110229

Kazi, M. K., Eljack, F., & Mahdi, E. (2021). Data-driven modeling to predict the load vs. displacement curves of targeted composite materials for industry 4.0 and smart manufacturing. *Composite Structures*, *258*, 113207. https://doi.org/10.1016/j.compstruct.2020.113207

Khan, A. A., Rana, M. M., Huang, G., Mei, N., Saritas, R., Wen, B., Zhang, S., Voss, P., Rahman, E. A., Leonenko, Z., Islam, S., & Ban, D. (2020). Maximizing piezoelectricity by self-assembled highly porous perovskite–polymer composite films to enable the internet of things. *Journal of Materials Chemistry A*, *8*(27), 13619–13629. https://doi.org/10.1039/D0TA03416A

Komuraiah, A., Kumar, N. S., & Prasad, B. D. (2014). Chemical composition of natural fibers and its influence on their mechanical properties. *Mechanics of Composite Materials*, *50*(3), 359–376. https://doi.org/10.1007/s11029-014-9422-2

Liu, F., & Mu, J. C. (2013). The building of composite materials information system based on internet of things technology. *Applied Mechanics and Materials*, *281*, 155–158. https://doi.org/10.4028/www.scientific.net/AMM.281.155

Manickam, T., Iyyadurai, J., Jaganathan, M., Babuchellam, A., Mayakrishnan, M., & Arockiasamy, F. S. (2023). Effect of stacking sequence on mechanical, water absorption, and biodegradable properties of

novel hybrid composites for structural applications. *International Polymer Processing*, *38*(1), 88-96. https://doi.org/10.1515/ipp-2022-4274

Marrot, L., Lefeuvre, A., Pontoire, B., Bourmaud, A., & Baley, C. (2013). Analysis of the hemp fiber mechanical properties and their scattering (Fedora 17). *Industrial Crops and Products*, *51*, 317–327. https://doi.org/10.1016/j.indcrop.2013.09.026

Mazian, B., Bergeret, A., Benezet, J. C., & Malhautier, L. (2020). Impact of field retting and accelerated retting performed in a lab-scale pilot unit on the properties of hemp fibres/polypropylene biocomposites. *Industrial Crops and Products*, *143,* 111912. https://doi.org/10.1016/j.indcrop.2019.111912

Mizutani, Y., Nagashima, K., Takemoto, M., & Ono, K. (2000). Fracture mechanism characterization of cross-ply carbon-fiber composites using acoustic emission analysis. *NDT and E International*, *33*(2), 101–110. https://doi.org/10.1016/S0963-8695(99)00030-4

Muhammad, A., Rahman, Md. R., Baini, R., & Bin Bakri, M. K. (2021). Applications of sustainable polymer composites in automobile and aerospace industry. In M. R. Rahman (Ed.) *Advances in sustainable polymer composites* (pp. 185–207). Woodhead Publishing. https://doi.org/10.1016/b978-0-12-820338-5.00008-4

Mwaikambo, L. Y., & Ansell, M. P. (2006). Mechanical properties of alkali treated plant fibres and their potential as reinforcement materials. I. hemp fibres. *Journal of Materials Science*, *41*(8), 2483–2496. https://doi.org/10.1007/s10853-006-5098-x

Okagawa, S., Bernus, P., & Noran, O. (2022). Realtime health monitoring of composite structures using FBG sensors. *IFAC-PapersOnLine*, *55*(19), 157–162. https://doi.org/10.1016/J.IFACOL.2022.09.200

Palacios, I., Placencia, J., Muñoz, M., Samaniego, V., González, S., & Jiménez, J. (2022). MQTT based event detection system for structural health monitoring of buildings. In M. Botto-Tobar, H. Cruz, A. D. Cadena & B. Durakovic (Eds.) *Emerging research in intelligent systems* (pp.56-70). Springer. https://doi.org/10.1007/978-3-030-96043-8_5

Pandey, R., Jose, S., Basu, G., & Sinha, M. K. (2021). Novel methods of degumming and bleaching of Indian flax variety tiara. *Journal of Natural Fibers, 18*(8), 1140-1150. https://doi.org/10.1080/15440478.2019.1687067

Ranasinghe, K., Sabatini, R., Gardi, A., Bijjahalli, S., Kapoor, R., Fahey, T., & Thangavel, K. (2022). Advances in integrated system health management for mission-essential and safety-critical aerospace applications. *Progress in Aerospace Sciences*, *128*, 100758. https://doi.org/10.1016/j.paerosci.2021.100758

Rantheesh, J., Indran, S., Raja, S., & Siengchin, S. (2023). Isolation and characterization of novel micro cellulose from Azadirachta indica A. Juss agro-industrial residual waste oil cake for futuristic applications. *Biomass Conversion and Biorefinery, 13*(5), 4393-4411. https://doi.org/10.1007/s13399-022-03467-0

Rao, P., Bukkapatnam, S., Beyca, O., Kong, Z., & Komanduri, R. (2014). Real-time identification of incipient surface morphology variations in ultraprecision machining process. *Journal of Manufacturing Science and Engineering*, *136*(2), 021008. https://doi.org/10.1115/1.4026210

Ray, S. S., & Okamoto, M. (2003). Biodegradable polylactide and its nanocomposites: Opening a new dimension for plastics and composites. *Macromolecular Rapid Communications*, *24*(14), 815–840. https://doi.org/10.1002/marc.200300008

Safi, A., Ahmad, Z., Jehangiri, A. I., Latip, R., Zaman, S. K. uz, Khan, M. A., & Ghoniem, R. M. (2022). A fault tolerant surveillance system for fire detection and prevention using LoRaWAN in smart buildings. *Sensors, 22*(21), 8411. https://doi.org/10.3390/S22218411

Sahayaraj, A. F., Muthukrishnan, M., & Ramesh, M. (2022a). Experimental investigation on physical, mechanical, and thermal properties of jute and hemp fibers reinforced hybrid polylactic acid composites. *Polymer Composites*, *43*(5), 2854–2863. https://doi.org/10.1002/pc.26581

Sahayaraj, A. F., Muthukrishnan, M., & Ramesh, M. (2022b). Influence of Tamarindus indica seed nano-powder on properties of Luffa cylindrica (L.) fruit waste fiber reinforced polymer composites. *Polymer Composites*, *43*(9), 6442–6452. https://doi.org/10.1002/pc.26957

Samad, Y. A., Li, Y., Schiffer, A., Alhassan, S. M., & Liao, K. (2015). Graphene foam developed with a novel two-step technique for low and high strains and pressure-sensing applications. *Small*, *11*(20), 2380–2385. https://doi.org/10.1002/smll.201403532

Sampath, U., Kim, H., Kim, D. G., Kim, Y. C., & Song, M. (2015). In-situ cure monitoring of wind turbine blades by using fiber bragg grating sensors and fresnel reflection measurement. *Sensors*, *15*(8), 18229–18238. https://doi.org/10.3390/S150818229

Sebastian, J., Schehl, N., Bouchard, M., Boehle, M., Li, L., Lagounov, A., & Lafdi, K. (2014). Health monitoring of structural composites with embedded carbon nanotube coated glass fiber sensors. *Carbon*, *66*, 191–200. https://doi.org/10.1016/j.carbon.2013.08.058

Serra, T., Mateos-Timoneda, M. A., Planell, J. A., & Navarro, M. (2013). 3D printed PLA-based scaffolds. *Organogenesis*, *9*(4), 239–244. https://doi.org/10.4161/org.26048

Serra, T., Planell, J. A., & Navarro, M. (2013). High-resolution PLA-based composite scaffolds via 3-D printing technology. *Acta Biomaterialia*, *9*(3), 5521–5530. https://doi.org/10.1016/j.actbio.2012.10.041

Singh, G., Jose, S., Kaur, D., & Soun, B. (2022). Extraction and characterization of corn leaf fiber. *Journal of Natural Fibers, 19*(5), 1581-1591. https://doi.org/10.1080/15440478.2020.1787914

Stansbury, J. W., Trujillo-Lemon, M., Lu, H., Ding, X., Lin, Y., & Ge, J. (2005). Conversion-dependent shrinkage stress and strain in dental resins and composites. *Dental Materials*, *21*(1), 56–67. https://doi.org/10.1016/j.dental.2004.10.006

Tachibana, S., Wang, Y. F., Sekine, T., Takeda, Y., Hong, J., Yoshida, A., Abe, M., Miura, R., Watanabe, Y., Kumaki, D., & Tokito, S. (2022). A printed flexible humidity sensor with high sensitivity and fast response using a cellulose nanofiber/carbon black composite. *ACS Applied Materials and Interfaces*, *14*(4), 5721–5728. https://doi.org/10.1021/acsami.1c20918

Tinga, T., & Loendersloot, R. (2019). Physical model-based prognostics and health monitoring to enable predictive maintenance. In E. Lughofer & M. Sayed-Mouchaweh (Eds.) *Predictive maintenance in dynamic systems: Advanced methods, decision support tools and real-world applications* (pp.313–353). Springer. https://doi.org/10.1007/978-3-030-05645-2_11

Tomás, M., Jalali, S., & Silva de Vargas, A. (2022). Creep evaluation and temperature dependence in self-sensing micro carbon polymer-based composites for further development as an internet of things sensor device. *Journal of Composite Materials*, *56*(6), 961-973. https://doi.org/10.1177/002199832110588

Tripathi, K. M., Vincent, F., Castro, M., & Feller, J. F. (2016). Flax fibers – epoxy with embedded nanocomposite sensors to design lightweight smart bio-composites. *Nanocomposites, 2*(3), 125-134. https://doi.org/10.1080/20550324.2016.1227546

Tripathy, A. R., Choudhury, A., Dash, A., Panigrahi, P., Kumar, S. S., Pancham, P. P., Sahu, S. K., & Mallik, S. (2021). Polymer matrix composite engineering for PDMS based capacitive sensors to achieve high-performance and broad-range pressure sensing. *Applied Surface Science Advances*, *3*, 100062. https://doi.org/10.1016/j.apsadv.2021.100062

Ullah, M., Gopalraj, S. K., Gutierrez-Rojas, D., Nardelli, P., & Kärki, T. (2023). IoT framework and requirement for intelligent industrial pyrolysis process to recycle cfrp composite wastes: Application study. In C. Y. Huang, S. F., Chiu & L. Quezada (Eds.) *Intelligent and transformative production in pandaemic time* (pp.275–282). https://doi.org/10.1007/978-3-031-18641-7_26

Xiao, T., Qian, C., Yin, R., Wang, K., Gao, Y., & Xuan, F. (2021). 3D printing of flexible strain sensor array based on uv-curable multiwalled carbon nanotube/elastomer composite. *Advanced Materials Technologies*, *6*(1), 2000745. https://doi.org/10.1002/admt.202000745

Yang, L., Ma, X., Peng, R., Zhai, Q., & Zhao, Y. (2017). A preventive maintenance policy based on dependent two-stage deterioration and external shocks. *Reliability Engineering & System Safety*, *160*, 201–211. https://doi.org/https://doi.org/10.1016/j.ress.2016.12.008

Yang, Y., Chiesura, G., Plovie, B., Vervust, T., Luyckx, G., Degrieck, J., Sekitani, T., & Vanfleteren, J. (2018). Design and integration of flexible sensor matrix for in situ monitoring of polymer composites. *ACS Sensors*, *3*(9), 1698–1705. https://doi.org/10.1021/acssensors.8b00425

Yang, Y., Guo, X., Zhu, M., Sun, Z., Zhang, Z., He, T., & Lee, C. (2023). Triboelectric nanogenerator enabled wearable sensors and electronics for sustainable internet of things integrated green earth. *Advanced Energy Materials*, *13*(1), 2203040. https://doi.org/10.1002/aenm.202203040

Yao, T., Chen, X., Li, J., Wu, K., & Su, X. (2023). Experimental study of tensile and flexural performances and failure mechanism of none-felt needled composites. *Thin-Walled Structures*, *188*, 110805. https://doi.org/10.1016/j.tws.2023.110805

Yao, Y., Dou, H., Liu, T., Wang, S., Gao, Y., Kang, J., Gao, X., Xia, C., Lu, Y., & Fan, W. (2023). Micro- and nano-scale mechanisms of enzymatic treatment on the interfacial behaviors of sisal fiber reinforced bio-based epoxy resin. *Industrial Crops and Products*, *194*, 116319. https://doi.org/10.1016/j.indcrop.2023.116319

Zafar, S., Miraj, G., Baloch, R., Murtaza, D., & Arshad, K. (2018). An IoT based real-time environmental monitoring system using arduino and cloud service. *Technology & Applied Science Research*, *8*(4), 3238–3242.

Zhu, Z., Wu, H., Ye, C., & Fu, W. (2017). Enhancement on mechanical and thermal properties of PLA biocomposites due to the addition of hybrid sisal fibers. *Journal of Natural Fibers*, *14*(6), 875–886. https://doi.org/10.1080/15440478.2017.1302382

Pertanika J. Sci. & Technol. 31 (S1): 111 - 124 (2023)

PERTANIKA JOURNALS

SCIENCE & TECHNOLOGY

Journal homepage: http://www.pertanika.upm.edu.my/

Flammability and Soil Burial Performance of Sugar Palm (*Arenga pinnata (wurmb) merr*) Fiber Reinforced Epoxy Composites

Tarique Jamal[1,2] and Salit Mohd Sapuan[1]*

[1]Advanced Engineering Materials and Composites Research Centre (AEMC), Department of Mechanical and Manufacturing Engineering, Universiti Putra Malaysia, UPM 43400 Serdang, Selangor, Malaysia
[2]Institute of Energy Infrastructure, College of Engineering, Universiti Tenaga Nasional Putrajaya Campus, Jalan IKRAM-UNITEN, 43000 Kajang, Selangor, Malaysia

ABSTRACT

This study investigates the effects of soil burial and flammability on sugar palm fibre (SPF) (*Arenga pinnata (wurmb) merr*)-reinforced epoxy composites. In order to determine the flammability and biodegradability properties, experiments are conducted in accordance with ASTM standards. The hand lay-up method was used to fabricate composite samples with two different weight ratios between epoxy and SPF, which were 70:30 and 50:50. Biodegradability and flammability properties were investigated using horizontal burning tests, limiting oxygen index (LOI), cone calorimetry, and soil burial. It was found that the Epoxy/SPF-50 was the composite that exhibited the fastest degradability at 0.81%/week. The result of the horizontal burning test showed that the addition of SPF reduced the burning rate but slightly increased it at 50 wt% because the ratio between epoxy and SPF exceeds the optimum fibre loading. The Epoxy/SPF-50 exhibited a better LOI value at 23.3 than pure epoxy (control), which was 19.8. From the cone calorimetry test, it was observed that the time to ignition (TTI) and total heat release (THR) values were decreased when the amount of SPF increased. Char production increases the flame-retardant protection of SPF-reinforced epoxy composites. To the best of the authors' knowledge, no published study has been conducted on the flammability and biodegradability characteristics of SPF-reinforced epoxy composites.

Keywords: Biocomposites, cone calorimetry, flammability, soil burial, sugar palm fibre

ARTICLE INFO

Article history:
Received: 06 March 2023
Accepted: 24 July 2023
Published: 27 October 2023

DOI: https://doi.org/10.47836/pjst.31.S1.06

E-mail addresses:
tarique5496@gmail.com (Tarique Jamal)
sapuan@upm.edu.my (Salit Mohd Sapaun)
* Corresponding author

ISSN: 0128-7680
e-ISSN: 2231-8526

INTRODUCTION

Over the last decade, the increasing use of natural fibres in polymer composites has significantly reduced environmental impacts. Owing to their biodegradability, availability, simplicity of processing, low cost, considerable features, and lightweight, lignocellulose fibre-reinforced polymer composites are recommended for use in construction, automotive and furniture industries (Song et al., 2023; Alaseel et al., 2022; Ibrahim et al., 2012; Jawaid & Abdul Khalil, 2011; Sanjay et al., 2018; Tarique et al., 2021). Sugar palm trees could produce various products, including palm sugar, fruits, and fibres (Aworinde et al., 2021; Ilyas et al., 2018; Khan et al., 2021). The SP tree is a forest plant that was previously classified as a Palmae family member but now belongs to the subfamily *Arecoideae* as well as the tribe *Caryoteae* (Alaaeddin et al., 2019; Atiqah et al., 2018; Ilyas et al., 2020; Tarique et al., 2021). The SP is likewise a fast-growing palm that can reach maturity in as little as ten years (Mogea et al., 1991). Indo-Malay region, South Asia, and Southeast Asia are covered by the geographical distribution of SPs (Atiqah et al., 2019; Tarique et al. et al., 2021). Furthermore, by utilizing SPF, plant waste can be recycled. Furthermore, SPF is widely available at a low cost and is easily accessible. Bachtiar et al. (2009) evaluated the mechanical behaviour of SPF and found it to have Young's modulus of 3.69 GPa, a tensile strength of 190.29 MPa, a strain to failure of 19.6%, and a density of 1.26 kg/m^3.

Owing to their outstanding mechanical, thermal, and electrical characteristics, modified epoxy resins are now utilized to fabricate natural fibre-reinforced composite (NFRCs) and create various industrial products. Natural fibre integration is also the most intriguing approach to altering epoxy resin. Natural fibres as reinforcement in polymers have seen a rise in attention and use in recent years in engineering as well as research technology (Mohammed et al., 2023; Alamri & Low, 2012; Farhana Mat Nasir et al., 2020; Low et al., 2007; Shih, 2007; Tarique et al., 2022). Das and Biswas (2016) investigated the impact of fibre length on the mechanical behaviour of coir fibre-reinforced epoxy composites, finding that tensile strength attained its maximum value at 12 mm fibre length. Venkateshwaran et al. (2011) examined the estimate of optimal fibre length for banana epoxy composite, finding that increasing fibre length and weight ratio enhanced tensile strength and modulus, likely a 15 mm fibre length. Aji et al. (2011) investigated the effect of fibre length on tensile characteristics of epoxy resin composite reinforced with kenaf/PALF fibres, finding that a fibre length of 0.25 mm provided the best maximum tensile strength, although a fibre length of 2 mm reduced tensile modulus property owing to weak interface bonding between the matrix and reinforcement.

In addition, the mechanical properties of epoxy composites based on a stacking sequence of *Cyperus pangorei* and jute fibres were studied by Vijay and Singaravelu (2016) when compared to the other three composites, the mechanical strength of one

produced with *C. pangorei* as the core and jute fibres as the skin layer was shown to be better. Edhirej et al. (2017) demonstrate that the observation of sugar palm fibres' usage as rope and traditional construction material inspired them to investigate the possibility of employing them as a composite material. The fibres are twisted to the proper diameter before being woven into rope. The fibres must endure wind loads and give protection from rain and tropical sun to be used as traditional roofing in rural tropical conditions because sugar palm fibres have adequate endurance. Previous research on tensile as well as flexural properties of sugar palm epoxy composites has focused on the use of woven roving, long random, and chopped random fibre composites, with the results showing that the woven roving sugar palm epoxy composites gave better properties than the long random and chopped random fibre composites (Sharba et al., 2016). However, all the samples performed poorly compared to glass fibre epoxy composites, meaning fibre treatment was essential for improving the materials.

Several studies have demonstrated that natural fibre can increase biocomposites' resistance to ignition. By reinforcing twill woven hemp fabric with epoxy composites, Kozłowski and Władyka-Przybylak (2008) found that the flammability of the base matrix composites was lowered, as measured by higher limiting oxygen index (LOI) values and a reduced heat release rate of 25%. Additionally, composites' static and dynamic mechanical properties from the modified fabric were enhanced. Bharath et al. (2014) report that treated composites performed better in fire and flame resistance tests (UL 94 V and UL 94 HB) and had lower rates of flame propagation and mass loss. Treated sisal fibre (SF)-reinforced recycled polypropylene (RPP) composites' flammability was evaluated using a horizontal burning test with UL-94 (Gupta et al., 2012). In light of issues about safety, waste disposal, and the decline of nonrenewable resources, researchers and scientists are also concentrating on using renewable resources (Alaseel et al., 2022; Hisham et al., 2011; Liu et al., 2006). Numerous research activities have been done on reinforcing natural fibres that could replace synthetic fibres (glass and carbon fibres) in composite applications, such as coir, date palm, bamboo, oil palm empty fruit bunch (OPEFB), hemp, sisal, flax, jute, and others (de Vasconcellos et al., 2014; Deo & Acharya, 2010; Mahjoub et al., 2014; Mishra & Biswas, 2013; Scida et al., 2013; Yousif et al., 2012).

Because the current scenario concerns using naturally abundant material to substitute synthetic material, this research deals with NFRCs and using innovative plant fibres to reinforce polymer composite. However, to our knowledge, studies dealing with SPF/Epoxy composites have not been performed. As a result, the primary purpose of this research was to investigate the biodegradability and flammability characteristics of epoxy-based composites reinforced with SPF.

MATERIALS AND METHODS

Materials

The SPF was collected from sugar palm trees at Kampung Kuala Jempol, Negeri Sembilan, Malaysia, as shown in Figure 1. The epoxy resin and hardener, namely Zeepoxy HL002 TA/B, are supplied by ZKK Sdn. Bhd, Cheras, Kuala Lumpur, Malaysia, were used in the fabrication process of the composites.

Figure 1. Sugar palm tree and sugar palm fibre

Fabrication of SPF/Epoxy Composites Testing Sample

The SPF-reinforced epoxy composites were produced at room temperature using a hand lay-up technique. SPF was mixed into the matrix with a stirrer with 500 RPM to create a matrix and filler mixture; as a result, a homogeneous mixture of matrix and filler was created. The resin is a colourless, viscous liquid with a viscosity of 5500–1000Cps at 30°C, while the hardener has a viscosity of 30–20Cps at 30°C. The ratio of epoxy resin to hardener was 2:1. Table 1 lists the compositions of the SPF-reinforced epoxy composites. A thin plastic sheet is put to the bottom and top of the mould to achieve a smooth surface for the composites. The epoxy was combined with the SPF before being placed into the 300 mm × 300 mm × 3 mm mould. The mould was cured at room temperature for 24 hrs, after which composite samples were removed.

Table 1
The formulations of the SPF-reinforced epoxy composites

Name of composites	Epoxy Resin (wt. %)	SPF (wt. %)
Pure Epoxy	100	0
Epoxy/SPF-30	70	30
Epoxy/SPF-50	50	50

Characterization of Composite Sample

Soil Burial Test. A soil burial test was accomplished to evaluate composites' biodegradability. Specimens were prepared with four replicates of each sample and cut to the following dimensions: 10 cm (L) × 4 cm (W) × 0.3 cm (H). 4, 8, 12, and 16 weeks were used for the biodegradability test. Specimens were buried 10 beneath the surface in moist soil in a polybag. Throughout the test period, the polybags were outdoors. After a specified time the specimens were taken out of the soil and cleaned with distilled water. Using Equation 1, the weight loss, W_{loss} (%), was calculated.

$$W_{loss} = \frac{W_{initial} - W_{final}}{W_{initial}} \times 100\% \qquad (1)$$

Horizontal Burning Test. The flammability test was carried out in a horizontal position. The specimens had dimensions of 125 mm × 13 mm × 3 mm when ready, according to ASTM D635-18 (2018). Two reference lines were drawn as starting and finishing points at 25 mm and 100 mm intervals. The sample was clamped horizontally at the end, making both reference lines visible using a retort stand. The specimen was lit from the other end, and the timer was started as soon as the flame was 25 mm away from the sample. The test was run in triplicate, and it was noted how long the flame took to advance 100 mm. Equation 2 was used to determine the sample's burning rate.

$$V = L\ t \qquad (2)$$

Where V, L, and t represent linear burning rate (mm/min), burnt length (mm), and time (min), respectively.

Limiting Oxygen Index (LOI)

The ASTM D2863-09 (2010) is used to evaluate the LOI. This experiment aimed to identify the lowest oxygen content of the sample combustion. The specimens had the following measurements: 100 mm × 6.5 mm × 3 mm. The specimen was placed vertically in the middle of a glass chamber and lit for 10 seconds until ignition. Ten replicate specimens were used in the test until the last five specimens, which were tested, had an oxygen concentration deviation of 0.2 vol%. Equation 3 calculated LOI based on the last five test specimens that burned.

$$LOI\ (vol\%) = C_f + kd \qquad (3)$$

Where C_f is the final oxygen value concentrations, in volume % to one decimal place for the previous five measurements, d is the interval difference between oxygen concentration levels in per cent volume, and k is a factor derived from experimental values.

Cone Calorimetry

The cone calorimetry testing was conducted following ISO 5660-1 (2002). The specimens had dimensions of 100 mm × 10 mm × 3 mm. The specimen was wrapped in aluminium foil on the sides and bottom before being placed horizontally on the specimen holder. The specimens' surfaces were spark-ignited and irradiated with a 35 kW/m^2 heat flux.

RESULTS AND DISCUSSION

Soil Burial

Soil burial testing for SPF-reinforced epoxy composite was done for 16 weeks. It was observed that the weight loss of an epoxy resin was raised in the natural soil environment after the reinforcement of SPF. As expected, loss of weight loss of composite was more significant with an increase in burial time in soil. The weight of pure epoxy had lost 3.55% of its original weight by the end of week 16, while the weights of Epoxy/SPF-30 and Epoxy/SPF-50 had lost 9.74% and 12.88%, respectively. The average degradation rates for pure epoxy and Epoxy/SPF-30 are 0.22%/week and 0.61%/week, respectively. Epoxy/SPF-50 had the highest average degradation rate of 0.81%/week. Figure 2 illustrates the trend of weight loss (%) of SPF-reinforced epoxy composites as a function of biodegradation time after soil burial analysis.

Pure epoxy recorded a minimal weight loss because the polymer matrix is not easy to degrade. It was noticed that increasing the amount of SPF increased the degradability rate. Epoxy/SPF-50 recorded the highest rate of degradability. The existence of cellulose in SPF allows water molecules to easily absorb. Due to its hygroscopic nature, cellulose in SPFs can absorb water from the environment and swell. The increasing hygroscopic properties of composites enhanced microbial activity, resulting in weight loss (Ilyas et al., 2020; Minh et al., 2019). The mechanism of biological degradation comprises water

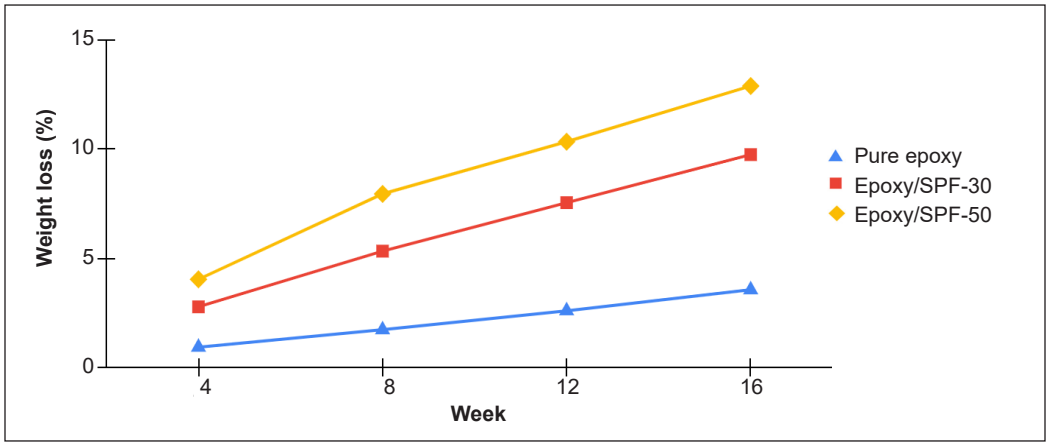

Figure 2. The trend of the sample's weight loss (%)

molecules penetrating the material, strong covalent bonds breaking, and microorganisms degrading the hemicellulose and cellulose.

Horizontal Burning Test

The SPF-reinforced epoxy composites' horizontal burning test was tested following ASTM D635 (2018). The fire was stopped when it reached the 100 mm mark of the specimens. Figure 3 shows the average burning rate of the samples.

According to the findings, incorporating SPF reduces the rate of burning. Epoxy/SPF-30 burned at a lower rate of 15.4 mm min^{-1} than pure epoxy, which burned at 26 mm min^{-1}. The flame took time to propagate alongside the Epoxy/SPF-30 sample and produced char simultaneously. The SPF frequently flows into char during burning, providing additional flame-retardant protection (Suriani et al., 2021). This finding indicates that reinforcing the SPF reduced the epoxy composite's burning rate. However, the burning rate increased slightly in Epoxy/SPF-50 due to the SPF/EP ratio being more than optimum fibre loadings. As a result, the composite's ability to produce char is reduced during the burning process (Xiao et al., 2018; Tarique et al., 2022). Compatibility of fibre and matrix is critical for providing the best flame-retardant characteristics to composite. The matrix polymer determines a composite's flammability, the variety of fibre used, and the interfacial bonding between the two. The compatibility of fibre and matrix is affected by their interfacial connection.

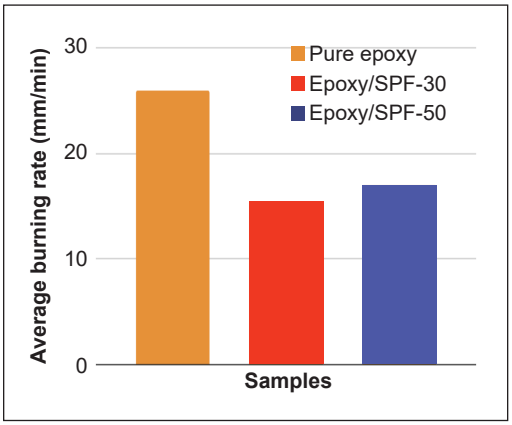

Figure 3. The average rate of burning of composite samples

Limiting Oxygen Index (LOI)

The LOI is a widely used fire index for characterizing the flammability of polymer material. It describes the lowest oxygen concentrations required to help a material's flammable combustion. The LOI values of specimens are shown in Table 2.

The limit Oxygen value of pure epoxy is 19.8% and is classified as combustible as its LOI value is lower compared to the oxygen contents of air, which is 21%. Material with less than 21% LOI value is classified as flammable under the standard LOI criteria. Conversely, materials are considered to be

Table 2
The limiting oxygen index (LOI) of the samples

Samples	LOI
Pure Epoxy	19.8
Epoxy/SPF-30	22.5
Epoxy/SPF-50	23.3

self-extinguishing if their LOI value is greater compared to 21% because, according to the standard air composition, oxygen content in the air is 21%, as materials with a value higher compared to this cannot support burning at room temperature without an external fire source (Karunakaran et al., 2016). Pure epoxy possessed a low LOI value due to the poor flammability properties of the polymer matrix. According to Prabhakar et al. (2015), polymer matrices are weak against flame propagation and thermal load. Polymer matrices themselves depend upon reinforcement and filler. The Epoxy/SPF-50 recorded a better LOI value of 23.3 compared to the Epoxy/SPF-50, which is 22.5. Composites' flammability is influenced by interactions between and among its constituent parts. However, the burning rate of the epoxy/SPF-50 was lower because higher LOI values indicate lower flammability, a lower burning rate, and better flame retardance. Combining them can make the composite less flammable (Gurunathan et al., 2015). However, the LOI value was not significantly increased between the 30 wt.% and 50 wt.% of SPF, which may be related to the non-polar behaviour of SPF that affects low fibre dispersion.

Cone Calorimetry

Cone calorimetry gathers data like TTI, HRR, and THR. Table 3 shows selected data obtained from the cone calorimetry test.

TTI describes the time needed for ignition when materials are exposed to a constant heat flux (35 kW/m^2) and in an oxygen-controlled environment. Thus, the higher TTI is preferable as well as considered to be less flammable. From Table 4, Epoxy/SPF-50 has the lower TTI at 62 seconds, while Epoxy/SPF-30 has the higher TTI at 97 seconds. The fast ignition of Epoxy/SPF-50 could be due to the high lignin content of SPF. Lignin breakdown contributes more to char generation than cellulose and hemicellulose. However, lignin decomposition begins at a lower temperature, between 160 and 400°C (Ali et al., 2021; Fu et al., 2017). Therefore, the increase in lignin content will increase flammability.

The heat release rate is a crucial and additional factor in determining a material's flammability (HRR). When a material is exposed to fire, HRR is the heat released per unit area. In addition to being a crucial parameter for describing fire behaviour, it also plays a role in defining concepts like a fire hazard. HRR curve for specimens is shown in Figure 4.

According to observation, the HRR curve for SPF-reinforced epoxy composites has two peaks. By forming carbonic char structures, the first peak reflects the charring process. The

Table 3
The selected data obtained from the cone calorimetry test

Samples	TTI (S)	pHRR (kW/m^2)	THR (MJ/m^2)
Pure Epoxy	82	706.3	99
Epoxy/SPF-30	97	468.5	79
Epoxy/SPF-50	62	355.1	71

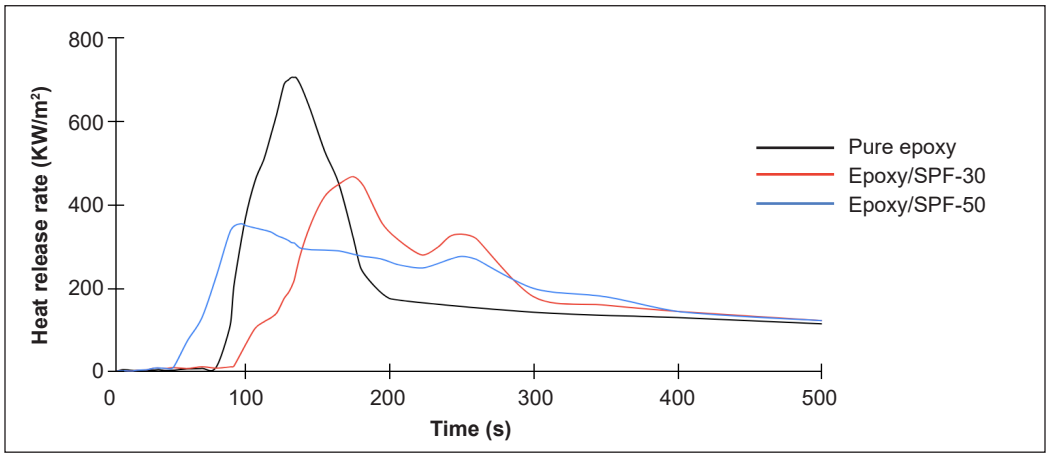

Figure 4. The HRR curves for the samples

char layer protects and prevents the movement of mass and volatiles from the condensed to the gas phase. Therefore, after the first peak, the combustion rate decreased, and a drop in the HRR curve was seen. As the burning process goes on, a surplus of trapped volatiles causes high internal pressures during the escape, which accelerates the formation of voids and causes the char residue to crack and degrade, which further encourages combustion and results in another peak HRR (Chee et al., 2020).

The maximum amount of heat released during combustion is referred to as the peak HRR (pHRR), and the total amount of heat released is shown by the area under the HRR curve (THR). From Figure 4, the pure epoxy exhibited the highest pHRR at 706.3 kW/m^2. When the amount of SPF increased, the TTI and THR values from the cone calorimetry test decreased. The Epoxy/SPF-30 showed better thermal stability than Epoxy/SPF-50. Additionally, char production supports the flame-retardant resistance of SPF-reinforced epoxy composites. A significant reduction of pHRR between 33% and 50% was seen on the SPF-reinforced epoxy composites than pure epoxy. The greatest reduction was observed on Epoxy/SPF-50, with a pHRR of 355.1 kW/m^2 and a THR of 75 MJ/m^2. The reduction of pHRR and THR of the sugar palm composite could represent the increase in char production (Hatanaka et al., 2016).

CONCLUSION

This research aims to develop an epoxy composite reinforced with SPF. The Epoxy/SPF-30 composite recorded the lowest burning rate for horizontal burning at 15.4 mm/min due to char production from SPF, which increased flame-retardant protection. The LOI value increases when the amount of SPF is increased. Epoxy/SPF-30 is better than Epoxy/SPF-50 due to the low dispersion of fibre when the amount of SPF is increased. From the cone calorimetry test, TTI and THR values decreased when SPF increased. In

addition, the char production helps to increase flame-retardant protection of SPF-reinforced epoxy composites. The degradability rate of sugar palm-reinforced epoxy composites was increased as the amount of SPF increased. After 16 weeks of soil burial testing, pure epoxy recorded the lowest weight loss, 3.55%, and Epoxy/SPF-50 recorded the highest weight loss, 12.88%. Nonetheless, the progress in this field has enabled the use of natural-fibre-based composites in a wide range of industries, including construction, automotive, and aerospace.

ACKNOWLEDGEMENTS

The author acknowledges Universiti Putra Malaysia for funding this research through Geran Putra Inisiatif (GPI/2022/9720100). Special thanks to Muhammad Haziqh bin Mohd Rizalludin who had helped in data collection.

REFERENCES

Aji, I. S., Zainudin, E. S., Khalina, A., Sapuan, S. M., & Khairul, M. D. (2011). Studying the effect of fiber size and fiber loading on the mechanical properties of hybridized kenaf/PALF-reinforced HDPE composite. *Journal of Reinforced Plastics and Composites*, *30*(6), 546–553. https://doi.org/10.1177/0731684411399141

Alaaeddin, M. H., Sapuan, S. M., Zuhri, M. Y. M., Zainudin, E. S., & Al- Oqla, F. M. (2019). Physical and mechanical properties of polyvinylidene fluoride - Short sugar palm fiber nanocomposites. *Journal of Cleaner Production*, *235*, 473–482. https://doi.org/10.1016/j.jclepro.2019.06.341

Alamri, H., & Low, I. M. (2012). Microstructural, mechanical, and thermal characteristics of recycled cellulose fiber-halloysite-epoxy hybrid nanocomposites. *Polymer Composites*, *33*(4), 589–600. https://doi.org/10.1002/pc.22163

Alaseel, B. H., Nainar, M. A. M., Nordin, N. A., Yahya, Z., & Rahim, M. N. A. (2022). Effect of water absorption on flexural properties of Kenaf/Glass fibres reinforced unsaturated polyester hybrid composites rod. *Pertanika Journal of Science and Technology*, *30*(1), 397–412. https://doi.org/10.47836/pjst.30.1.22

Ali, I. M., Hussain, T. H., & Naje, A. S. (2021). Surface treatment of cement based composites: Nano coating technique. *Pertanika Journal of Science & Technology*, *29*(1), 349-362. https://doi.org/10.47836/pjst.29.1.20

ASTM D635-18. (2018). *Standard test method for rate ofburning and/or extent and time of burning of plastics in a horizontal position*. ASTM International. https://www.astm.org/d0635-18.html

ASTM D2863-09. (2010). *Standard Test Method for Measuring the Minimum Oxygen Concentration to Support Candle-like Combustion of Plastics (Oxygen Index).* ASTM International. https://www.astm.org/d2863-09.html

Atiqah, A., Jawaid, M., Sapuan, S. M., Ishak, M. R., & Alothman, O. Y. (2018). Thermal properties of sugar palm/glass fiber reinforced thermoplastic polyurethane hybrid composites. *Composite Structures*, *202*, 954–958. https://doi.org/10.1016/j.compstruct.2018.05.009

Atiqah, A., Jawaid, M., Sapuan, S. M., Ishak, M. R., Ansari, M. N. M., & Ilyas, R. A. (2019). Physical and thermal properties of treated sugar palm/glass fibre reinforced thermoplastic polyurethane hybrid

composites. *Journal of Materials Research and Technology*, *8*(5), 3726–3732. https://doi.org/10.1016/j.jmrt.2019.06.032

Aworinde, A. K., Emagbetere, E., Adeosun, S. O., & Akinlabi, E. T. (2021). Polylactide and its Composites on Various Scales of Hardness. *Pertanika Journal of Science and Technology*, *29*(2), 1213-1322. https://doi.org/10.47836/pjst.29.2.34

Bachtiar, D., Sapuan, S. M., & Hamdan, M. M. (2009). The influence of alkaline surface fibre treatment on the impact properties of sugar palm fibre-reinforced epoxy composites. *Polymer-Plastics Technology and Engineering*, *48*(4), 379–383. https://doi.org/10.1080/03602550902725373

Bharath, K. N., & Basavarajappa, S. (2014). Flammability characteristics of chemical treated woven natural fabric reinforced phenol formaldehyde composites. *Procedia Materials Science*, *5*, 1880–1886. https://doi.org/10.1016/j.mspro.2014.07.507

Chee, S. S., Jawaid, M., Alothman, O. Y., & Yahaya, R. (2020). Thermo-oxidative stability and flammability properties of bamboo/kenaf/nanoclay/epoxy hybrid nanocomposites. *RSC Advances*, *10*(37), 21686–21697. https://doi.org/10.1039/D0RA02126A

Das, G., & Biswas, S. (2016). Effect of fiber parameters on physical, mechanical and water absorption behaviour of coir fiber-epoxy composites. *Journal of Reinforced Plastics and Composites*, *35*(8), 628–637. https://doi.org/10.1177/0731684415626594

de Vasconcellos, D. S., Touchard, F., & Chocinski-Arnault, L. (2014). Tension–tension fatigue behaviour of woven hemp fibre reinforced epoxy composite: A multi-instrumented damage analysis. *International Journal of Fatigue*, *59*, 159–169. https://doi.org/10.1016/j.ijfatigue.2013.08.029

Deo, C., & Acharya, S. K. (2010). Effect of moisture absorption on mechanical properties of chopped natural fiber reinforced epoxy composite. *Journal of Reinforced Plastics and Composites*, *29*(16), 2513–2521. https://doi.org/10.1177/0731684409353352

Edhirej, A., Sapuan, S. M., Jawaid, M., & Zahari, N. I. (2017). Cassava/sugar palm fiber reinforced cassava starch hybrid composites: Physical, thermal and structural properties. *International Journal of Biological Macromolecules*, *101*, 75–83. https://doi.org/10.1016/j.ijbiomac.2017.03.045

Fu, S., Song, P., & Liu, X. (2017). Thermal and flame retardancy properties of thermoplastics/natural fiber biocomposites. In F. Mizi & F. Feng (Eds.) *Advanced high strength natural fibre composites in construction* (pp. 479–508). Elsevier. https://doi.org/10.1016/B978-0-08-100411-1.00019-4

Gupta, A. K., Biswal, M., Mohanty, S., & Nayak, S. K. (2012). Mechanical, thermal degradation, and flammability studies on surface modified sisal fiber reinforced recycled polypropylene composites. *Advances in Mechanical Engineering*, *4,* 418031. https://doi.org/10.1155/2012/418031

Gurunathan, T., Mohanty, S., & Nayak, S. K. (2015). A review of the recent developments in biocomposites based on natural fibres and their application perspectives. *Composites Part A: Applied Science and Manufacturing*, *77*, 1–25. https://doi.org/10.1016/j.compositesa.2015.06.007

Hatanaka, L. C., Ahmed, L., Sachdeva, S., Wang, Q., Cheng, Z., & Mannan, M. S. (2016). Thermal degradation and flammability of nanocomposites composed of silica cross-linked to poly(methyl methacrylate). *Plastics, Rubber and Composites*, *45*(9), 375–381. https://doi.org/10.1080/14658011.2016.1204773

Hisham, S., Faieza, A. A., Ismail, N., Sapuan, S. M., & Ibrahim, M. S. (2011). Flexural mechanical characteristic of sawdust and chipwood filled epoxy composites. *Key Engineering Materials*, *471–472*, 1064–1069. https://doi.org/10.4028/www.scientific.net/KEM.471-472.1064

Ibrahim, M. S., Sapuan, S. M., & Faieza, A. A. (2012). Mechanical and thermal properties of composites from unsaturated polyester filled with oil palm ash. *Journal of Mechanical Engineering and Sciences, 2,* 133-147. https://doi.org/10.15282/jmes.2.2012.1.0012

Ilyas, R. A., Sapuan, S. M., Atikah, M. S. N., Ibrahim, R., Hazrol, M. D., Sherwani, S. F. K., Jamal, T., Nazrin, A., & Syafiq, R. (2020, November 16). *Natural fibre: A promising source for the production of nanocellulose*. [Paper presentation]. 7th Postgraduate Seminar on Natural Fibre reinforced Polymer Composites, Selangor, Malaysia.

Ilyas, R. A., Sapuan, S. M., & Ishak, M. R. (2018). Isolation and characterization of nanocrystalline cellulose from sugar palm fibres (Arenga Pinnata). *Carbohydrate Polymers*, *181*(June 2017), 1038–1051. https://doi.org/10.1016/j.carbpol.2017.11.045

ISO 5660-1. (2002). *Reaction-to-fire tests-Heat release, smoke production and mass loss rate-Part 1: heat release rate (cone calorimeter method)*. International Organization for Standardization Geneva. https://www.iso.org/standard/35351.html

Jawaid, M., & Abdul Khalil, H. P. S. (2011). Cellulosic/synthetic fibre reinforced polymer hybrid composites: A review. *Carbohydrate Polymers*, *86*(1), 1–18. https://doi.org/10.1016/j.carbpol.2011.04.043

Karunakaran, S., Majid, D. L., & Tawil, M. L. M. (2016). Flammability of self-extinguishing kenaf/ABS nanoclays composite for aircraft secondary structure. *IOP Conference Series: Materials Science and Engineering*, *152*(1), 012068. https://doi.org/10.1088/1757-899X/152/1/012068

Khan, Z. I., Mohamad, Z., Rahmat, A. R., & Habib, U. (2021). Synthesis and characterization of composite materials with enhanced thermo-mechanical properties for unmanned aerial vehicles (Uavs) and aerospace technologies. *Pertanika Journal of Science & Technology*, *29*(3), 2003-2015. https://doi.org/10.47836/pjst.29.3.15

Kozłowski, R., & Władyka-Przybylak, M. (2008). Flammability and fire resistance of composites reinforced by natural fibers. *Polymers for Advanced Technologies*, *19*(6), 446–453. https://doi.org/10.1002/pat.1135

Liu, Z., Erhan, S. Z., Akin, D. E., & Barton, F. E. (2006). "Green" composites from renewable resources: Preparation of epoxidized soybean oil and flax fiber composites. *Journal of Agricultural and Food Chemistry*, *54*(6), 2134–2137. https://doi.org/10.1021/jf0526745

Low, I. M., McGrath, M., Lawrence, D., Schmidt, P., Lane, J., Latella, B. A., & Sim, K. S. (2007). Mechanical and fracture properties of cellulose-fibre-reinforced epoxy laminates. *Composites Part A: Applied Science and Manufacturing*, *38*(3), 963–974. https://doi.org/10.1016/j.compositesa.2006.06.019

Mahjoub, R., Yatim, J. M., Mohd Sam, A. R., & Hashemi, S. H. (2014). Tensile properties of kenaf fiber due to various conditions of chemical fiber surface modifications. *Construction and Building Materials, 55,* 103-113. https://doi.org/10.1016/j.conbuildmat.2014.01.036

Minh, N. P., Nhi, T. T. Y., Nguyen, T. N., Bich, S. N., & True, D. T. T. (2019). Some factors influencing the properties of dried watermelon powder during spray drying. *Journal of Pharmaceutical Sciences and Research*, *11*(4), 1416–1421.

Mishra, V., & Biswas, S. (2013). Physical and mechanical properties of bi-directional jute fiber epoxy composites. *Procedia Engineering*, *51*, 561–566. https://doi.org/10.1016/j.proeng.2013.01.079

Mogea, J., Seibert, B., & Smits, W. (1991). Multipurpose palms: the sugar palm (Arenga pinnata (Wurmb) Merr.). *Agroforestry Systems*, *13*(2), 111–129. https://doi.org/10.1007/BF00140236

Mohammed, A. A. B. A., Hasan, Z., Omran, A. A. B., Elfaghi, A. M., Khattak, M. A., Ilyas, R. A., & Sapuan, S. M. (2023). Effect of various plasticizers in different concentrations on physical, thermal, mechanical, and structural properties of wheat starch-based films. *Polymers, 15*(1), 63. https://doi.org/10.3390/polym15010063

Nasir, N. A. F. M., Jamaluddin, J., Zainudin, Z., Busheri, M. M., Adrus, N., Azim, F. S. S., & Hasham, R. (2020). The effect of alkaline treatment onto physical, thermal, mechanical and chemical properties of lemba leaves fibres as new resources of biomass. *Pertanika Journal of Science and Technology*, *28*(4). https://doi.org/10.47836/pjst.28.4.21

Prabhakar, M. N., Shah, A. U. R., & Song, J. I. (2015). A Review on the flammability and flame retardant properties of natural fibers and polymer matrix based composites. *Composites Research*, *28*(2), 29–39. https://doi.org/10.7234/composres.2015.28.2.029

Sanjay, M. R., Madhu, P., Jawaid, M., Senthamaraikannan, P., Senthil, S., & Pradeep, S. (2018). Characterization and properties of natural fiber polymer composites: A comprehensive review. *Journal of Cleaner Production 172*, 566-581. https://doi.org/10.1016/j.jclepro.2017.10.101

Scida, D., Assarar, M., Poilâne, C., & Ayad, R. (2013). Influence of hygrothermal ageing on the damage mechanisms of flax-fibre reinforced epoxy composite. *Composites Part B: Engineering*, *48*, 51–58. https://doi.org/10.1016/j.compositesb.2012.12.010

Sharba, M. J., Leman, Z., Sultan, M. T. H., Ishak, M. R., & Hanim, M. A. A. (2016). Tensile and compressive properties of woven kenaf/glass sandwich hybrid composites. *International Journal of Polymer Science*, *2016,* 1235048. https://doi.org/10.1155/2016/1235048

Shih, Y. F. (2007). Mechanical and thermal properties of waste water bamboo husk fiber reinforced epoxy composites. *Materials Science and Engineering: A*, *445–446*, 289–295. https://doi.org/10.1016/j.msea.2006.09.032

Song, L., Wang, D., Liu, X., Yin, A., & Long, Z. (2023). Prediction of mechanical properties of composite materials using multimodal fusion learning. *Sensors and Actuators A: Physica*l, *358*, 114433. https://doi.org/10.1016/j.sna.2023.114433

Suriani, M. J., Radzi, F. S. M., Ilyas, R. A., Petrů, M., Sapuan, S. M., & Ruzaidi, C. M. (2021). Flammability, tensile, and morphological properties of oil palm empty fruit bunches fiber/pet yarn-reinforced epoxy fire retardant hybrid polymer composites. *Polymers*, *13*(8), 1282. https://doi.org/10.3390/polym13081282

Tarique, J., Sapuan, S. M., Khalina, A., Sherwani, S. F. K., Yusuf, J., & Ilyas, R. A. (2021). Recent developments in sustainable arrowroot (Maranta arundinacea Linn) starch biopolymers, fibres, biopolymer composites and their potential industrial applications: A review. *Journal of Materials Research and Technology*, *13*, 1191–1219. https://doi.org/10.1016/j.jmrt.2021.05.047

Tarique, J, Sapuan, S. M., & Khalina, A. (2021). Effect of glycerol plasticizer loading on the physical, mechanical, thermal, and barrier properties of arrowroot (Maranta arundinacea) starch biopolymers. *Scientific Reports*, *11*(1), 13900. https://doi.org/10.1038/s41598-021-93094-y

Tarique, J, Sapuan, S. M., Khalina, A., Ilyas, R. A., & Zainudin, E. S. (2022). Thermal, flammability, and antimicrobial properties of arrowroot (Maranta arundinacea) fiber reinforced arrowroot starch biopolymer composites for food packaging applications. *International Journal of Biological Macromolecules*, *213*(January), 1–10. https://doi.org/10.1016/j.ijbiomac.2022.05.104

Tarique, J., Sapuan, S. M., & Khalina, A. (2022). Extraction and characterization of a novel natural lignocellulosic (Bagasse and Husk) fibers from arrowroot (Maranta Arundinacea). *Journal of Natural Fibers*, *19*(15), 9914–9930. https://doi.org/10.1080/15440478.2021.1993418

Venkateshwaran, N., Elayaperumal, A., & Jagatheeshwaran, M. S. (2011). Effect of fiber length and fiber content on mechanical properties of banana fiber/epoxy composite. *Journal of Reinforced Plastics and Composites*, *30*(19), 1621–1627. https://doi.org/10.1177/0731684411426810

Vijay, R., & Singaravelu, D. L. (2016). Experimental investigation on the mechanical properties of *Cyperus pangorei* fibers and jute fiber-based natural fiber composites. *International Journal of Polymer Analysis and Characterization*, *21*(7), 617–627. https://doi.org/10.1080/1023666X.2016.1192354

Xiao, F., Bedane, A. H., Zhao, J. X., Mann, M. D., & Pignatello, J. J. (2018). Thermal air oxidation changes surface and adsorptive properties of black carbon (char/biochar). *Science of The Total Environment*, *618*, 276–283. https://doi.org/10.1016/j.scitotenv.2017.11.008

Yousif, B. F., Shalwan, A., Chin, C. W., & Ming, K. C. (2012). Flexural properties of treated and untreated kenaf/epoxy composites. *Materials & Design*, *40*, 378–385. https://doi.org/10.1016/j.matdes.2012.04.017

Pertanika J. Sci. & Technol. 31 (S1): 125 - 138 (2023)

PERTANIKA JOURNALS

SCIENCE & TECHNOLOGY

Journal homepage: http://www.pertanika.upm.edu.my/

Extraction and Characterization of Novel Ligno-cellulosic Fiber from *Wrightia tinctoria* and *Cebia pentandra* Plant for Textile and Polymer Composite Applications

Divya Sundarraj[1], Grace Annapoorani Soundarajan[2], Indran Suyambulingam[3], Divya Divakaran[3], Sanjay Mavinkere Rangappa[3]* and Suchart Siengchin[3]

[1]Department of Costume Design and Fashion, Kongunadu Arts And Science College, Coimbatore, Tamil Nadu - 641029, India

[2]Department of Textiles and Apparel Design, Bharathiar University, Coimbatore, Tamil Nadu - 641046, India

[3]Natural Composites Research Group Lab, Department of Materials and Production Engineering, The Sirindhorn International Thai-German School of Engineering (TGGS), King Mongkut's University of Technology North Bangkok (KMUTNB), Bangkok - 10800, Thailand

ABSTRACT

Natural fibers derived from cellulose and ligno-celluloses materials have many advantages, such as being renewable, low density, inexhaustible, and cheap rather than synthetic fibers. Researchers and scientists are searching for a new fiber source that can be processed environmentally sustainable. The aim is to produce an organic and Eco-friendly product. The present investigation aims to extract and characterize ligno-cellulosic fiber from the seedpod of *Wrightia tinctoria* (WT) and *Cebia pentandra* (CP) plants. The extraction of WT fibers (WTFs) and CP fibers (CPFs) was carried out using the hand-stripping method. The structural and functional Characterization of WTFs and CPFs were determined using Scanning Electron Microscope (SEM), Fourier Transform Infrared (FT-IR) spectroscopy, Chemical analysis, X-ray diffraction studies (XRD), and the thermal behavior of fibers determined by using Thermo Gravimetric Analysis (TGA). The results indicated that WTFs composed of 75% cellulose, 14% lignin, and 0.55% wax content were, as the CPFs were composed of 38% cellulose, 15% lignin, and wax content of 2.34%. The SEM micrograph confirms that both fibers were hollow structures with thin cell walls and luminous because of the wax content presence on the surface of the fiber. The crystallinity percentage of WTFs and CPFs was calculated from XRD studies and is

ARTICLE INFO

Article history:
Received: 06 March 2023
Accepted: 24 July 2023
Published: 27 October 2023

DOI: https://doi.org/10.47836/pjst.31.S1.07

E-mail addresses:
divya16091988@gmail.com (Divya Sundarraj)
gracetad@buc.edu.in (Grace Annapoorani Soundarajan)
indransdesign@gmail.com (Indran Suyambulingam)
divyad3121@gmail.com (Divya Divakaran)
mcemrs@gmail.com (Sanjay Mavinkere Rangappa)
suchart.s.pe@tggs-bangkok.org (Suchart Siengchin)
*Corresponding author

ISSN: 0128-7680
e-ISSN: 2231-8526

valued at 62% and 52%. Thermo gravimetric analysis revealed that WTFs and CPFs were thermally stable up to 460°C and 350°C. The above characterization results confirm that WTFs and CPFs have a wide scope in textile and polymer composite applications.

Keywords: *Cebia pentandra*, lignocelluloses, SEM, TGA, *wrightia tinctoria*, XRD

INTRODUCTION

India has many natural fibers with approaching use in various industrialized products based on existing technology (Ramasamy et al., 2022). Natural fibers derived from plant materials are more eco-friendly, low-cost, renewable, and bio-compatible than petroleum-based synthetic fibers. Cellulose fiber has ample applications in the textile industry (Durai et al., 2022). During past decades, the usage of natural products has gained more attraction globally. The cellulose fiber materials show interest among the researchers to search for the best materials for each application (Mohan et al., 2022). The natural, conventional lignocellulosic fibers derived from jute, hemp, sisal, and ramie have been widely studied and reported. On the other hand, a few nonconversational lignocellulose fibers remain unutilized and are going as natural disposal (Divya, Jenish, et al., 2022). Two different natural fibers were collected from *Wrightia tinctoria* R.Br. and *Ceiba pentandra* only because of local seed pod-based fibers. It is available in large quantities to analyze and select a suitable product for futuristic applications.

Wrightia tinctoria R.Br. is a small deciduous tree that grows in a wide range of soil types. All parts of the plant have numerous meditational properties. In the Tamil Nadu state of India, the tree is called a "Jaundice curative tree" (Desore & Narula, 2018). The blackish-green fruits with white dots resembling two or more fruits were united at the tip (Ramalakshmi et al., 2012). The fibers were collected from matured dried fruit-like white hairs attached to the seed at the chalaza end. Numerous investigations have been developed to find a new product to replace the existing one (Subramanian et al., 2005).

Ceiba pentandra (CPFs) is one of the less given consideration agricultural products (Macedo et al., 2020). The fibers are grown in arid environments and distributed throughout warmer parts of India. The CPFs is a hollow lumen fiber with a hydrophobic character due to its waxy cutin; it can be used as a sorbent in oil. Fiber characteristics will vary depending on the soil and climatic conditions. Much research was carried out on CPFs in foreign countries, but in Indian fiber, only limited works were documented (Rangappa et al., 2022). Concerning the above, this recent report deals with the extraction of two lignocellulose natural fibers, *Wrightia tinctoria* (WT) and *Cebia pentandra* (CP) fiber, from the seedpod of plant and analyzes important properties like morphology, crystallinity, chemical composition, FT-IR spectroscopy and thermal properties concerning plantation environment.

MATERIALS AND METHODS

Extraction of Fibers

WTFs and CPF are collected from healthy and matured seedpods were obtained from the plants located at Therampalayam village, Mettupalayam Taluk (Latitude and longitude coordinates are: 11.289087, 76.940971), Coimbatore district of Tamil Nadu, India. The fibers were removed from the pods, seed, and cover. The entangled fibers were separated by hand and dried at room temperature at (28 ± 2°C) to remove moisture (Figure 1) (Raja et al., 2021). The collected fiber was authenticated from the Botanical Survey of India and the Institute of Forest Genetics and Tree Breeding, Coimbatore, Tamil Nadu, India.

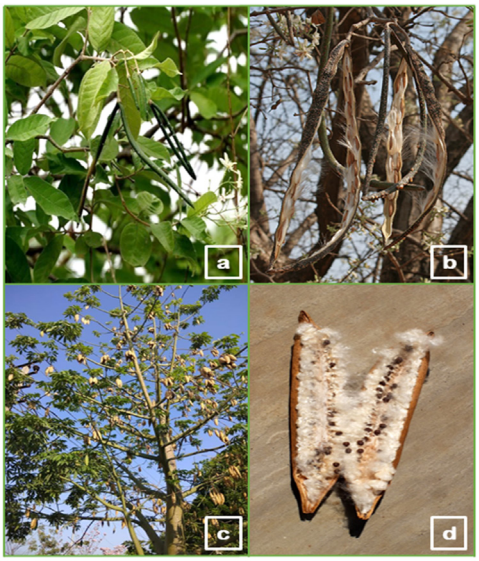

Figure 1. (a & b) *Wrightia tinctoria* tree and its seed pod fiber (b & C) *Cebia pentandra* tree and its seed pod fiber

Chemical Analysis

A typical testing procedure studied the chemical composition of cellulose, lignin, wax, ash, and moisture contents of CPFs and WTFs. The density of the fibers was assessed using the Mettler Toledo XSZ05 balance method. The wax content of CPFs and WTFs was estimated using the Conrad procedure, and the ash content was calculated by the ASTM E1755-01 method. The moisture content of fibers was assessed by the conversion weight loss method (Conrad, 1944; Divya, Suyambulingam, et al., 2022; Selvan et al., 2022).

Fourier Transform Infrared Analysis (FT-IR)

FT-IR spectrometer analysis was carried out to determine the presence of organic and inorganic components in the fibers using the SHIMADZU spectrometer. The infra-red passed on the surface of the sample, which may be solid, liquid, or gaseous form; the material absorbs the light, and the absorbency of the energy was measured at various wavelengths, which produces the output of an Infrared spectrum(Sanjay et al., 2019; Senthamaraikannan et al., 2019). The WTFs and CPFs were powdered, approximately 2 mg of powder mixed with 200mg potassium bromide (KBr), and compressed to 1 mm thick disks. The spectrum recorded in the frequency range from 4000-500cm^{-1} with a resolution of 2 cm^{-1}.

X-ray Diffraction Analysis (XRD)

The Super molecular structure of the WTFs and CPFs was investigated by X-ray diffraction analysis (XRD) using BRUKER ECO d8 Advance analyzer and PANALYTICAL system Netharland (Powder XRD) using Cukα radiation (λ = 1.5406 Å), operating 40 kV and 30 mA. Both fiber crystallinity index was calculated using the peak height method and Segal empirical equation (1) (Segal et al., 1959):

$$\mathrm{Crl} = \frac{I_{max} - I_{min}}{I_{max}} X\ 100 \quad (1)$$

Where I_{max} is a Crystalline Fraction, and I_{min} is a Diffracted intensity. Scherer's relation was admirable in establishing the crystallite size of the optimally surface-modified fiber, which is given in Equation 2. In this relation, 'K' represents the constant (0.89), 'λ' indicates the intensity of radiation, 'β' symbolizes the full width at half-maximum (FWHM), and 'θ' signifies the Bragg's angle (Saravanakumar et al., 2013; Pillai et al., 2022).

$$CS = \frac{K\lambda}{\beta \cos\theta} \quad (2)$$

Thermo Gravimetric Analysis (TGA)

Thermal gravimetric analysis is used to determine the thermal stability of the materials. Usually, cellulosic fibers decompose easily at low temperatures depending upon the fiber characteristic's morphology, crystallinity, and molecular weight (Khan et al., 2021a; Vinod et al., 2021). The thermograph of both fibers was recorded using the NETZSCH STA 449F3 A-1100M instrument. TG-DSC experiment was examined with an Alumina crucible with a lid in a programmed temperature range of 30 to 1000°C under a nitrogen gas atmosphere at 10°C/min.

Scanning Electron Microscopy Analysis (SEM)

The Surface morphology of WTFs and CPFs are examined using a Scanning Electron Microscope (SEM) Carl Zeiss tester. The SEM analysis is a powerful magnification tool to characterize the sample shape, size, and surface structure. A focused electron beam with low energy is radiated on the sample's surface, producing the sample's images by scanning (Bharath et al., 2016; Witayakran et al., 2017). The dried fibers were sputtered with gold before analysis to make the fiber conductivity, and then observed the image at an accelerating voltage of 30 kV.

RESULTS AND DISCUSSION

Chemical Analysis

The main components of the natural fibers are cellulose, lignin, wax, and Ash content. The chemical component in the plant fiber will differ from place to place due to the plant's maturity, relative humidity, temperature, and soil conditions (Karthik & Murugan, 2013). The evaluated WTFs and CPFs had WTFs composed of (75 wt%) cellulose, (14 wt%) lignin, (0.55 wt%) of wax content and (2.40%) of ash content were as the CPFs Cellulose (38 wt%), lignin (15 wt%), wax content (2.34 wt%) and Ash (2%) (Rantheesh et al., 2023; Sundaram et al., 2021). The Density of the CPFs and WTFs was 1.5 g/cc and 1.2 g/cc, slightly higher than other natural fibers. The analyzed Chemical composition of WTFs and CPFs are compared and are listed in Table 1. *Wrightia tinctoria* (WT) and *Cebia pentandra* (CP).

Table 1

Chemical composition of Wrightia tinctoria *(WT) and* Cebia pentandra *(CP) fibers*

S. No	Chemical Composition	WT (Wt.%)	CP (Wt.%)
1	Cellulose	75	42
2	Lignin content	15	20
3	Wax	2	23
4	Moisture	8	10
5	Ash content	2	1

Fourier Transform Infrared analysis (FT-IR)

FT-IR measure the main functional group present in the WTFs and CPFs by absorbance of infrared light at various wavelength. The IR spectrum of both samples is illustrated in Figures 2a and b. There were a total of eight well-defined peaks absorbed, and some similar absorption bands were observed for both fibers. WTFs broad absorption band is at 3335,2918,1732, 1506, 1421,1370,1231, and 896 cm^{-1}. CPFs show peaks at 3350,2887,1739, 1506,1375,1246,1055 and 896 cm^{-1}. The elongated absorption peaks at 3350 and 3335cm^{-1} represent cellulose's stretching vibration mode (–OH) bond in both fibers (Gandhi et al., 2022). The WTFs band peak of 2918 cm^{-1} in the spectrum indicates the asymmetric and symmetric stretching of methylene (–CH2–) groups in long alkyl chains (Ilangovan et al., 2018; Jagadeesan et al., 2023). The stretching vibrations (NH_3) of free amino acids were found at a wavelength of 2887cm^{-1} in CPFs. The carbonyl group (C=O) peak in 1739 and 1732 cm^{-1} shows the presence of acetyl groups C=O, degree of acetylation (Babu et al., 2020; Indran et al., 2018; Rajeshkumar et al., 2021). The medium absorption peak of CPFs

and WTFs at 1375 and 1370 cm^{-1} indicates bond stretching CH bending. The bands in the region 1506 cm^{-1} are for C=C aromatic symmetrical stretching(Vijay et al., 2019). The CPFs' broad absorption peak at 1055 cm^{-1} is associated with the carbohydrate structure's stretching vibrations (C-C) (Babu et al., 2020). These peaks prove the presence of waxes. The Absorption at 1421.51cm^{-1} represents the symmetrical CH_2 bending vibration of crystalline cellulose (Indran et al., 2016; Jagadeesan et al., 2022). The peak 1231 cm^{-1} provides the presence of COH bending at C_6. The peak at 896 indicates the anomeric region of carbohydrates in both fibers(Sunesh et al., 2022).

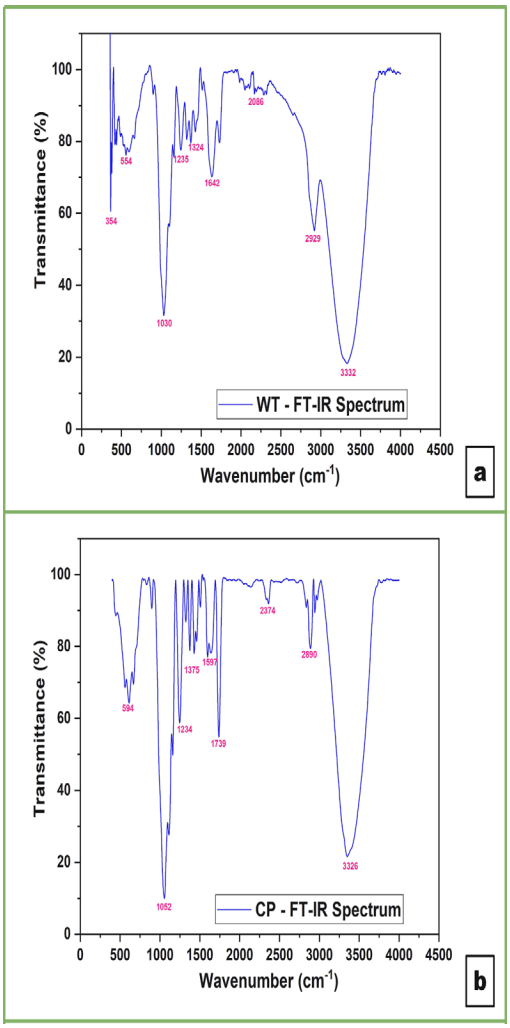

Figure 2. FT-IR analysis of (a) *Wrightia tinctoria* (WT) and (b) *Cebia pentandra* (CP) fibers

X-ray Diffraction Analysis (XRD)

The X-ray diffractogram of WTFs and CPFs has been recorded and shown in Figure 3. From the graph by XRD analysis of both fibers, crystalline size and the percentage of the crystallinity index were calculated. The crystalline size of the fiber reflects the diffusion of particles into the complex structure of the fiber (Gandhi et al., 2022). The particle size and crystallinity index will coincide, reflecting the fiber's moisture absorbency capacity and chemical reactivity (Divya, Jenish, et al., 2022). CPFs and WTFs major intensity peak at 2θ = 23° and 2θ = 21.9° and corresponds to the crystallographic part of cellulose, where the second peak at 2θ = 18° and 2θ = 15.9° corresponding to the amorphous part of cellulose (Moshi, Ravindran, Bharathi, Indran et al., 2020; Moshi, Ravindran, Bharathi, Padma, et al., 2020; Rajan et al., 2022; Surendran et al., 2022). The crystallinity Index CrI of both the fibers calculated using equation (1) is 57% for CPFs and 62.22% for WTFs, and the crystalline size of CPFs was 2.12 nm and WTFs fiber was 2.55 nm. The crystalline size of both fibers was lower than other lignocellulosic fibers: Luffa cylindrical fiber 4.52 nm, cotton 4.7 nm, and curaua fiber 3.4 nm, respectively (Azwa et al., 2013).

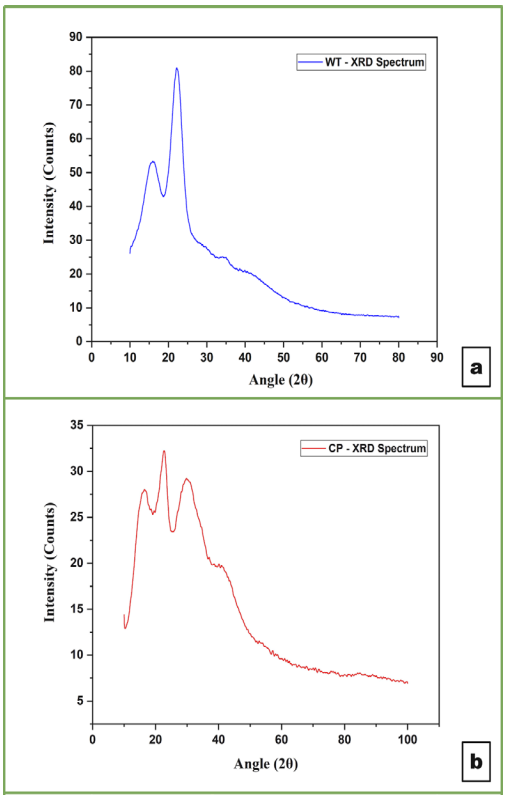

Figure 3. X-ray diffraction spectroscopy of (a) *Wrightia tinctoria* (WT) and (b) *Cebia pentandra* CP fibers

Thermogravimetric Analysis (TGA)

The thermal analysis was carried out on WTFs and CPFs to analyze the thermal stability and evaluate the sample's mass loss at respective times and temperatures. The thermal stability of the materials depends upon the characteristics, crystallinity, and molecular weight; most of the natural fibers are low in thermal stability (Ilangovan et al., 2020). The thermal decomposition and weight loss are observed in three main stages: first-stage water evaporation, second-stage devolatilization of organic matters like cellulose, hemicelluloses, and lignin content and final-stage decomposition and charcoal formation (Khan et al., 2021b).

From the TGA result (Figures 4a and 5b), WTFs and CPFs indicate a similar fiber degradation process. In the first stage, minor mass loss is below 100°C for both fibers due to moisture evaporation (Divya et al., 2021; Divya, Jenish, et al., 2022; Iyyadurai et al., 2023; Raja et al., 2022). The second mass loss starts at below 230–325°C for CPFs and 275–330°C for WTFs` which can be attributed to the degradation of lignin and cellulose. The third stage CPFs show pyrolysis between 360–900°C

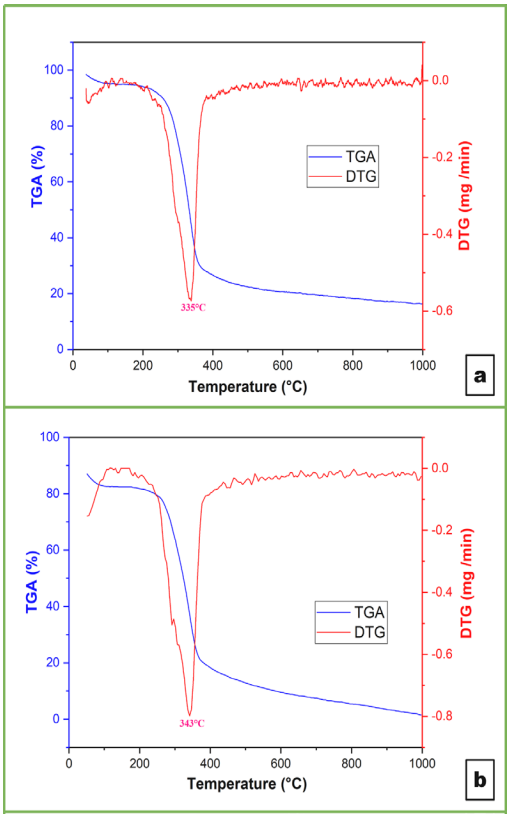

Figure 4. Thermal analysis images of (a) *Wrightia tinctoria* (WT) and (b) *Cebia pentandra* (CP) fibers

corresponding to the charcoal formation residual mass 16.34% at 998.3°C. Above 400°C of WTFs shows a slow decomposition of lignin, cellulose, and charcoal formation, and the charcoal yield at 997.8°C and the residual is 1.42% (Loganathan et al., 2020; Madhu et al., 2019).

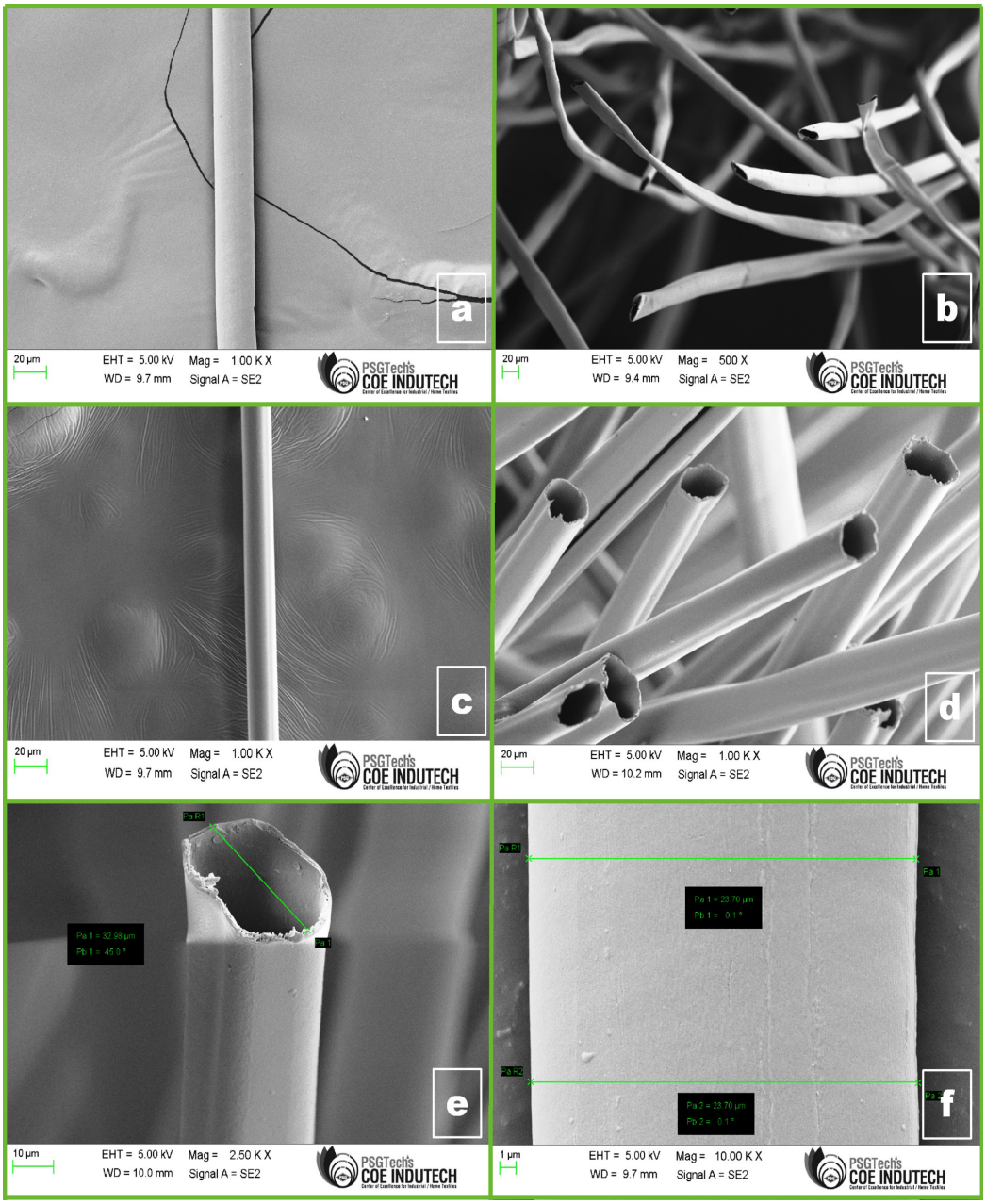

Figure 5. SEM images of (a, c) Longitudinal morphology of *Wrightia tinctoria* (WT) and *Cebia pentandra* (CP), (b, d) Cross-sectional morphology of WT and CP, and (e, f) Diameter of WT and CP

Scanning Electron Microscopy Analysis (SEM)

The Surface morphology of the WTFs and CPFs was examined in a cross-sectional and long-sectional direction using a Scanning Electron Microscope (SEM) at different magnifications (Figure 5a–d). Figure 4a and b, cross-section and long sectional view of CPFs at the magnification of 500x (20 µm), shows a thin fiber wall covered with a large layer of wax, making the fiber hydrophobic. The oval and hollow structure shows that the fiber retains warmth and is lightweight. The fiber contains large luminous which leads to a lower density of fiber (Fatma & Jahan, 2018; Manimekalai et al., 2021; Moshi, Ravindran, Bharathi, Indran, et al., 2020; Moshi, Ravindran, Bharathi, Padma, et al., 2020; Sumesh et al., 2021). The average diameter of fiber was measured and computed as 27.30 µm from Figures 5b, 4c, and 4d, which show the cross-section and long-sectional view of WTFs at the magnification of 1 kx (20 µm) and 250 kx (10 µm), showing thin cell wall, cylindrical structure with a thin line and small microfibers on the entire surface on the fiber which means the higher porosity and good air permeability in nature—the diameter of the fibers calculated as 22.54 µm which clearly shows the WTFs lighter then CPFs. The staple length of both fibers was manually calculated; the mean average value of the CPFs was 37.42 mm, and the WTFs were 35 mm. Both fibers have analogous characteristics because of their similar morphology (Sari et al., 2021).

CONCLUSION

This investigation analyzes the complete characterization of WTFs and CPFs to select futuristic applications using surface morphology, FT-IR, Chemical analysis, crystallinity, and thermal analysis techniques. SEM micrograph of both the fibers shows a smooth surface and hollow structure with a large lumen, which leads to a hydrophobic nature. The diameter and length of the fibers were calculated as 27.30 µm and 37.42 mm for CPF and 22.54 µm and 35 mm. which indicates that both fibers have less staple length when compared with other natural fibers, which means it is quite difficult to construct 100% fabric. The cellulose content of CPFs and WTFs is 38 and 75%, with WTFs showing high cellulose content with low density, contributing largely to the end product's feature. FT-IR studies indicate the presence of functional groups in the fibers. CPFs and WTFs showed similar absorption bands and confirmed the fiber's hydrophobicity. The crystallinity index (CrI) of CPFs and WTFs was found to be 57% and 62.2%, and crystalline size was 2.12 nm and 2.15 nm, which confirms the presence of crystalline cellulose, affecting the fiber's moisture absorbency. The thermal analysis indicates that fibers were thermally stable up to 330°C for CPFs and 360°C for WTFs. Since considering the deserved properties of CPFs and WTFs, like good thermal resistance and lightweight, they can be utilized for technical textile products. Future recommends giving mild alkali treatment to the fiber, which can also be utilized in the apparel industry.

ACKNOWLEDGEMENTS

The first author acknowledges the Natural Composites Research Group Lab, Department of Materials and Production Engineering, The Sirindhorn International Thai-German Graduate School of Engineering, King Mongkut's University of Technology North Bangkok, Bangkok-10800, Thailand, for supporting the completion of this research work.

This research was funded by the National Science, Research and Innovation Fund (NSRF) and King Mongkut's University of Technology North Bangkok, Thailand with Contract no. KMUTNB-FF-66-01.

REFERENCES

Azwa, Z. N., Yousif, B. F., Manalo, A. C., & Karunasena, W. (2013). A review on the degradability of polymeric composites based on natural fibres. *Materials and Design*, *47*, 424–442. https://doi.org/10.1016/j.matdes.2012.11.025

Babu, B. G. G., Princewinston, D., Saravanakumar, S. S. S., Khan, A., Aravind Bhaskar, P. V. V., Indran, S., & Divya, D. (2020). Investigation on the physicochemical and mechanical properties of novel alkali-treated *phaseolus vulgaris* fibers. *Journal of Natural Fibers*, *19*(2), 770-781. https://doi.org/10.1080/15440478.2020.1761930

Bharath, K. N., Pasha, M., & Nizamuddin, B. A. (2016). Characterization of natural fiber (sheep wool)-reinforced polymer-matrix composites at different operating conditions. *Journal of Industrial Textiles*, *45*(5), 730–751. https://doi.org/10.1177/1528083714540698

Conrad, C. M. (1944). Determination of wax in cotton fiber: A new alcohol extraction method. *Industrial and Engineering Chemistry*, *16*(8), 745–748. https://doi.org/10.1021/i560136a007

Desore, A., & Narula, S. A. (2018). An overview on corporate response towards sustainability issues in textile industry. *Environment, Development and Sustainability*, *20*(4), 1439-1459. https://doi.org/10.1007/s10668-017-9949-1

Divya, D., Indran, S., Sanjay, M. R., & Siengchin, S. (2021). Forecasts of natural fiber reinforced polymeric composites and its degradability concerns – A review. In A. Khan, M. Sanjay, Rangappa, S. Siengchin., & A. M. Asiri (Eds.), *Biobased composites: Processing, characterization, properties, and applications* (pp. 175–1960). Wiley. https://doi.org/10.1002/9781119641803.CH13

Divya, D., Jenish, I., & Raja, S. (2022). Comprehensive characterization of *Furcraea selloa* K. *Koch* peduncle fiber-reinforced polyester composites—Effect of fiber length and weight ratio. *Advances in Materials Science and Engineering*, *2022*, Article 8099500. https://doi.org/10.1155/2022/8099500

Divya, D., Suyambulingam, I., Sanjay, M. R., & Siengchin, S. (2022). Suitability examination of novel cellulosic plant fiber from *Furcraea selloa* K. *Koch* peduncle for a potential polymeric composite reinforcement. *Polymer Composites*, *43*(7), 4223-4243. https://doi.org/10.1002/pc.26683

Durai, P. N., Viswalingam, K., Divya, D., & Senthilkumar, B. (2022). Mechanical, thermal, and surface morphological properties of *Musa acuminate* peduncle fiber-reinforced polymeric composite: Effect of alkalization and fiber loading. *Polymer Composites*, *43*(8), 5107–5118. https://doi.org/10.1002/pc.26800

Fatma, T., & Jahan, S. (2018). Extraction of unconventional bast fibers from *Kydia calycina* plant and their characterisation. *Journal of Natural Fibers*, *15*(5), 697–706. https://doi.org/10.1080/15440478.2017.1354745

Gandhi, V. C. S., Jenish, I., Indran, S., & Rajan, D. Y. (2022). Mechanical and thermal analysis of *Cissus quadrangularis* stem fiber/epoxy composite with micro-red mud filler composite for structural application. *Transactions of the Indian Institute of Metals*, *75*(3), 737–747. https://doi.org/10.1007/s12666-021-02478-1

Ilangovan, M., Guna, V., Hu, C., Nagananda, G. S., & Reddy, N. (2018). *Curcuma longa* L. plant residue as a source for natural cellulose fibers with antimicrobial activity. *Industrial Crops and Products*, *112*, 556–560. https://doi.org/10.1016/j.indcrop.2017.12.042

Ilangovan, M., Guna, V., Prajwal, B., Jiang, Q., & Reddy, N. (2020). Extraction and characterisation of natural cellulose fibers from *Kigelia africana*. *Carbohydrate Polymers*, *236*, 115996. https://doi.org/10.1016/j.carbpol.2020.115996

Indran, S., Raj, R. D. E., Daniel, B. S. S., & Binoj, J. S. (2018). Comprehensive characterization of natural *Cissus quadrangularis* stem fiber composites as an alternate for conventional FRP composites. *Journal of Bionic Engineering*, *15*(5), 914–923. https://doi.org/10.1007/s42235-018-0078-9

Indran, S., Raj, R. D. E., Daniel, B. S. S., & Saravanakumar, S. S. (2016). Cellulose powder treatment on *Cissus quadrangularis* stem fiber-reinforcement in unsaturated polyester matrix composites. *Journal of Reinforced Plastics and Composites*, *35*(3), 212–227. https://doi.org/10.1177/0731684415611756

Iyyadurai, J., Arockiasamy, F. S., Manickam, T., Rajaram, S., Suyambulingam, I., & Siengchin, S. (2023). Experimental investigation on mechanical, thermal, viscoelastic, water absorption, and biodegradability behavior of *Sansevieria ehrenbergii* fiber reinforced novel polymeric composite with the addition of coconut shell ash powder. *Journal of Inorganic and Organometallic Polymers and Materials*, *33*(3), 796-809. https://doi.org/10.1007/S10904-023-02537-8

Jagadeesan, R., Suyambulingam, I., Divakaran, D., & Siengchin, S. (2022). Novel sesame oil cake biomass waste derived cellulose micro-fillers reinforced with basalt/banana fibre-based hybrid polymeric composite for lightweight applications. *Biomass Conversion and Biorefinery*, *13*(5), 4443-4458. https://link.springer.com/article/10.1007/s13399-022-03570-2

Jagadeesan, R., Suyambulingam, I., Somasundaram, R., Divakaran, D., & Siengchin, S. (2023). Isolation and characterization of novel microcellulose from *Sesamum indicum* agro-industrial residual waste oil cake: conversion of biowaste to wealth approach. *Biomass Conversion and Biorefinery*, *13*(5), 4427-4441. https://doi.org/10.1007/S13399-022-03690-9

Karthik, T., & Murugan, R. (2013). Characterization and analysis of ligno-cellulosic seed fiber from *Pergularia daemia* plant for textile applications. *Fibers and Polymers*, *14*(3), 465–472. https://doi.org/10.1007/s12221-013-0465-0

Khan, A., Vijay, R., Singaravelu, D. L., Sanjay, M. R., Siengchin, S., Verpoort, F., Alamry, K. A., & Asiri, A. M. (2021a). Characterization of natural fibers from *Cortaderia selloana* grass (Pampas) as reinforcement material for the production of the composites. *Journal of Natural Fibers*, *18*(11), 1893–1901. https://doi.org/10.1080/15440478.2019.1709110

Khan, A., Vijay, R., Singaravelu, D. L., Sanjay, M. R., Siengchin, S., Verpoort, F., Alamry, K. A., & Asiri, A. M. (2021b). Extraction and characterization of natural fiber from *Eleusine indica* grass as reinforcement of sustainable fiber reinforced polymer composites. *Journal of Natural Fibers*, *18*(11), 1742–1750. https://doi.org/10.1080/15440478.2019.1697993

Loganathan, T. M., Sultan, M. T. H., Ahsan, Q., Jawaid, M., Naveen, J., Md Shah, A. U., & Hua, L. S. (2020). Characterization of alkali treated new cellulosic fibre from *Cyrtostachys renda*. *Journal of Materials Research and Technology*, *9*(3), 3537–3546. https://doi.org/10.1016/j.jmrt.2020.01.091

Macedo, M. J. P., Silva, G. S., Feitor, M. C., Costa, T. H. C., Ito, E. N., & Melo, J. D. D. (2020). Surface modification of kapok fibers by cold plasma surface treatment. *Journal of Materials Research and Technology*, *9*(2), 2467–2476. https://doi.org/10.1016/j.jmrt.2019.12.077

Madhu, P., Sanjay, M. R., Pradeep, S., Subrahmanya Bhat, K., Yogesha, B., & Siengchin, S. (2019). Characterization of cellulosic fibre from *Phoenix pusilla* leaves as potential reinforcement for polymeric composites. *Journal of Materials Research and Technology*, *8*(3), 2597–2604. https://doi.org/10.1016/j.jmrt.2019.03.006

Manimekalai, G., Kavitha, S., Divya, D., Indran, S., & Binoj, J. S. (2021). Characterization of enzyme treated cellulosic stem fiber from *Cissus quadrangularis* plant: An exploratory investigation. *Current Research in Green and Sustainable Chemistry*, *4*, Article 100162. https://doi.org/10.1016/j.crgsc.2021.100162

Mohan, S. J., Devasahayam, P. S. S., Suyambulingam, I., & Siengchin, S. (2022). Suitability characterization of novel cellulosic plant fiber from *Ficus benjamina* L. aerial root for a potential polymeric composite reinforcement. *Polymer Composites*, *43*(12), 9012-9026. https://doi.org/10.1002/pc.27080

Moshi, A. A. M., Ravindran, D., Bharathi, S. R. S., Indran, S., & Priyadharshini, G. S. (2020). Characterization of surface-modified natural cellulosic fiber extracted from the root of *Ficus religiosa* tree. *International Journal of Biological Macromolecules*, *156*, 997–1006. https://doi.org/10.1016/j.ijbiomac.2020.04.117

Moshi, A. A. M., Ravindran, D., Bharathi, S. R. S., Padma, S. R., Indran, S., & Divya, D. (2020). Characterization of natural cellulosic fiber extracted from *Grewia damine* flowering plant's stem. *International Journal of Biological Macromolecules*, *164*, 1246–1255. https://doi.org/10.1016/j.ijbiomac.2020.07.225

Moshi, A. A. M., Ravindran, D., Bharathi, S. S., Indran, S., Saravanakumar, S. S., & Liu, Y. (2020). Characterization of a new cellulosic natural fiber extracted from the root of *Ficus religiosa* tree. *International Journal of Biological Macromolecules*, *142*, 212–221. https://doi.org/10.1016/j.ijbiomac.2019.09.094

Pillai, R. S. S., Rajamoni, R., Suyambulingam, I., Goldy, I. R. S., & Divakaran, D. (2022). Synthesis and characterization of cost-effective industrial discarded natural ceramic particulates from *Cymbopogon flexuosus* plant shoot for potential polymer/metal matrix reinforcement. *Polymer Bulletin*, *79*(10), 8765-8806. https://doi.org/10.1007/s00289-021-03913-5

Raja, S., Rajesh, R., Indran, S., Divya, D., & Priyadharshini, G. S. (2022). Characterization of industrial discarded novel *Cymbopogon flexuosus* stem fiber: A potential replacement for synthetic fiber. *Journal of Industrial Textiles*, *51*(1), 1207S-1234S. https://doi.org/10.1177/15280837211007507

Rajan N. M. C., Indran, S., Divya, D., Narayanasamy, P., Khan, A., Asiri, A. M., & Nagarajan, S. (2022). Mechanical and thermal properties of *Chloris barbata* flower fiber/epoxy composites: Effect of alkali treatment and fiber weight fraction. *Journal of Natural Fibers*, *19*(9), 3453-3466. https://doi.org/10.1080/15440478.2020.1848703

Rajeshkumar, G., Hariharan, V., Indran, S., Sanjay, M. R., Siengchin, S., Maran, J. P., Al-Dhabi, N. A., & Karuppiah, P. (2021). Influence of sodium hydroxide (NaOH) treatment on mechanical properties and morphological behaviour of phoenix sp. fiber/epoxy composites. *Journal of Polymers and the Environment*, *29*(3), 765–774. https://doi.org/10.1007/s10924-020-01921-6

Ramalakshmi, S., Edaydulla, N., Ramesh, P., & Muthuchelian, K. (2012). Investigation on cytotoxic, antioxidant, antimicrobial and volatile profile of *Wrightia tinctoria* (Roxb.) R. Br. flower used in Indian medicine. *Asian Pacific Journal of Tropical Disease*, *2*(SUPPL.1), S68-S75. https://doi.org/10.1016/S2222-1808(12)60126-1

Ramasamy, S., Karuppuchamy, A., Jayaraj, J. J., Suyambulingam, I., Siengchin, S., & Fischer, S. (2022). Comprehensive characterization of novel Robusta (AAA) banana bracts fibers reinforced polylactic acid based biocomposites for lightweight applications. *Polymer Composites*, *43*(11), 8569-8580. https://doi.org/10.1002/pc.27025

Rangappa, S. M., Parameswaranpillai, J., Siengchin, S., Jawaid, M., & Ozbakkaloglu, T. (2022). Bioepoxy based hybrid composites from nano-fillers of chicken feather and lignocellulose *Ceiba pentandra*. *Scientific Reports*, *12*(1), 397. https://doi.org/10.1038/s41598-021-04386-2

Rantheesh, J., Indran, S., Raja, S., & Siengchin, S. (2023). Isolation and characterization of novel micro cellulose from *Azadirachta indica* A. Juss agro-industrial residual waste oil cake for futuristic applications. *Biomass Conversion and Biorefinery*, *13*(5), 4393-4411. https://doi.org/10.1007/s13399-022-03467-0

Sanjay, M. R., Siengchin, S., Parameswaranpillai, J., Jawaid, M., Pruncu, C. I., & Khan, A. (2019). A comprehensive review of techniques for natural fibers as reinforcement in composites: Preparation, processing and characterization. *Carbohydrate Polymers*, *207*, 108–121. https://doi.org/10.1016/j.carbpol.2018.11.083

Saravanakumar, S. S., Kumaravel, A., Nagarajan, T., Sudhakar, P., & Baskaran, R. (2013). Characterization of a novel natural cellulosic fiber from *Prosopis juliflora* bark. *Carbohydrate Polymers*, *92*(2), 1928–1933. https://doi.org/10.1016/j.carbpol.2012.11.064

Sari, N. H., Suteja, Ilyas, R. A., Syafri, E., & Indran, S. (2021). Characterization of the density and mechanical properties of corn husk fiber reinforced polyester composites after exposure to ultraviolet light. *Functional Composites and Structures*, *3*(3), 034001. https://doi.org/10.1088/2631-6331/ac0ed3

Segal, L. G. J. M. A., Creely, J. J., Martin Jr, A. E., & Conrad, C. M. (1959). Empirical method for estimating the degree of crystallinity of native cellulose using the X-ray diffractometer. *Textile Research Journal*, *29*(10), 786–794. https://doi.org/10.1177/004051755902901003

Selvan, M. T. G. A., Binoj, J. S., Moses, J. T. E. J., Sai, N. P., Siengchin, S., Sanjay, M. R., & Liu, Y. (2022). Extraction and characterization of natural cellulosic fiber from fragrant screw pine prop roots as potential reinforcement for polymer composites. *Polymer Composites*, *43*(1), 320–329. https://doi.org/10.1002/pc.26376

Senthamaraikannan, P., Saravanakumar, S. S., Sanjay, M. R., Jawaid, M., & Siengchin, S. (2019). Physico-chemical and thermal properties of untreated and treated *Acacia planifrons* bark fibers for composite reinforcement. *Materials Letters*, *240*, 221–224. https://doi.org/10.1016/j.matlet.2019.01.024

Subramanian, K., Senthil Kumar, P., Jeyapal, P., & Venkatesh, N. (2005). Characterization of ligno-cellulosic seed fibre from *Wrightia tinctoria* plant for textile applications-an exploratory investigation. *European Polymer Journal*, *41*(4), 853–861. https://doi.org/10.1016/j.eurpolymj.2004.10.037

Sumesh, K. R., Kavimani, V., Rajeshkumar, G., Indran, S., & Saikrishnan, G. (2021). Effect of banana, pineapple and coir fly ash filled with hybrid fiber epoxy based composites for mechanical and morphological study. *Journal of Material Cycles and Waste Management*, *23*(4), 1277–1288. https://doi.org/10.1007/s10163-021-01196-6

Sundaram, R. S., Rajamoni, R., Suyambulingam, I., & Isaac, R. (2021). Comprehensive characterization of industrially discarded *Cymbopogon flexuosus* stem fiber reinforced unsaturated polyester composites: Effect of fiber length and weight fraction. *Journal of Natural Fibers*, *19*(13), 7241-7256. https://doi.org /10.1080/15440478.2021.1944435

Sunesh, N. P., Indran, S., Divya, D., & Suchart, S. (2022). Isolation and characterization of novel agrowaste-based cellulosic micro fillers from *Borassus flabellifer* flower for polymer composite reinforcement. *Polymer Composites*, *43*(9), 6476–6488. https://doi.org/10.1002/pc.26960

Surendran, A. N., Ajjarapu, K. P. K., Arumugham, A. A., Kate, K., & Satyavolu, J. (2022). Characterization of industry grade soybean wax for potential applications in natural fiber reinforced composite (NFRC) filaments. *Industrial Crops and Products*, *186*, Article 115163. https://doi.org/10.1016/J.INDCROP.2022.115163

Vijay, R., Singaravelu, D. L., Vinod, A., Sanjay, M. R., Siengchin, S., Jawaid, M., Khan, A., & Parameswaranpillai, J. (2019). Characterization of raw and alkali treated new natural cellulosic fibers from *Tridax procumbens*. *International Journal of Biological Macromolecules*, *125*, 99–108. https://doi.org/10.1016/j.ijbiomac.2018.12.056

Vinod, A., Yashas Gowda, T. G., Vijay, R., Sanjay, M. R., Gupta, M. K., Jamil, M., Kushvaha, V., & Siengchin, S. (2021). Novel *Muntingia calabura* bark fiber reinforced green-epoxy composite: A sustainable and green material for cleaner production. *Journal of Cleaner Production*, *294*, Article 126337. https://doi.org/10.1016/j.jclepro.2021.126337

Witayakran, S., Smitthipong, W., Wangpradid, R., Chollakup, R., & Clouston, P. L. (2017). Natural fiber composites: Review of recent automotive trends. In *Encyclopedia of Renewable and Sustainable Materials*, *2*, 166-174. https://doi.org/10.1016/b978-0-12-803581-8.04180-1

Pertanika J. Sci. & Technol. 31 (S1): 139 - 155 (2023)

PERTANIKA JOURNALS

SCIENCE & TECHNOLOGY

Journal homepage: http://www.pertanika.upm.edu.my/

Mechanical, Morphological, and Fire Behaviors of Sugar Palm/ Glass Fiber Reinforced Epoxy Hybrid Composites

Vasi Uddin Siddiqui[1], Salit Mohd Sapuan[1]* and Tarique Jamal[1,2]

[1]Advanced Engineering Materials and Composites Research Centre (AEMC), Department of Mechanical and Manufacturing Engineering, Universiti Putra Malaysia, UPM 43400 Serdang, Selangor, Malaysia
[2]Institute of Energy Infrastructure, College of Engineering, Universiti Tenaga Nasional Putrajaya Campus, Jalan IKRAM-UNITEN, 43000 Kajang, Selangor, Malaysia

ABSTRACT

This research aims to investigate using sugar palm fiber (SPF) and glass fiber (GF) in an epoxy matrix to develop composite materials with improved mechanical, morphological, and flammability properties. The mechanical and flammability properties are examined per ASTM standards, while the morphological study examines the fractured surfaces of the samples. Using the hand lay-up technique, the hybrid composite comprises 15% SPF, 15% GF, and 70% epoxy resin. Three treatments are applied to the SPF: untreated, alkaline treated, and benzoyl chloride treated, which enables research into the effect of fiber treatment on mechanical properties and flammability. The morphological investigation reveals that both treated SPF/GF/EP composites exhibit lower tensile strength than the untreated SPF/GF/EP composite due to inadequate mechanical interlocking at the fiber-matrix interface. However, the alkaline-treated SPF/GF/EP composite demonstrates a 24.8% improvement in flexural strength, a 1.52% increase in impact strength, and a 9.76% enhancement in flammability. Similarly, the benzoyl chloride-treated SPF/GF/EP composite improves flexural strength, impact strength, and flammability by 24.6%, 0.51%, and 5.66%, respectively. These results highlight the potential of fiber treatment to improve composite materials' mechanical and flammability properties.

ARTICLE INFO

Article history:
Received: 06 March 2023
Accepted: 29 August 2023
Published: 27 October 2023

DOI: https://doi.org/10.47836/pjst.31.S1.08

E-mail addresses:
vasi.siddiqui@gmail.com (Vasi Uddin Siddiqui)
sapuan@upm.edu.my (Salit Mohd Sapuan)
tarique5496@gmail.com (Tarique Jamal)
* Corresponding author

ISSN: 0128-7680
e-ISSN: 2231-8526

Keywords: flammability, hybrid composites, mechanical properties, morphology, sugar palm fiber

INTRODUCTION

Researchers are now paying attention to natural fiber-reinforced composites, and materials have shown significant demand

from numerous sectors to be employed in diverse goods such as furniture, packaging, automotive components, and construction (Ilyas, Sapuan, Atikah, et al., 2020; Tarique et al., 2022). Natural fiber sources such as rice straw, roselle, sugar palm, jute, bamboo, kenaf, and others are easily accessible, and natural fiber is utilized as an alternative filler or reinforcement for synthetic fibers and fillers (Ilyas et al., 2021). Furthermore, the usage of petroleum-based polymers in human everyday activities is expanding. Plastic disposal is one of the environmental contamination concerns (Sapuan et al., 2018). As a result, increasing awareness activities in society is one strategy for minimizing the environmental effect (Azammi et al., 2019). As a result, one solution to this issue is to utilize natural fibers. These natural sources are affordable in cost, low in density, simple to recycle, biodegradable, environmentally friendly, and long-lasting (Harussani et al., 2021). Advanced composites are frequently employed in engineering applications because of their superior strength-to-weight and particular stiffness-to-weight ratios (Ibrahim et al., 2012; Lau et al., 2018). These composites are suitable for various industries since they provide higher mechanical performance while lightweight. Researchers are investigating natural fibers as potential reinforcements in composite materials due to the need for environmentally acceptable and sustainable products.

Sugar palm fiber (SPF, Arenga pinnata Wurmb. Merr) is one of these natural fibers and offers much promise as Malaysia's most abundant natural resource. SPF has numerous benefits, including low cost, biodegradability, non-toxicity, low density, and high mechanical strength (Huzaifah et al., 2016). Sugar palm fibers are utilized in various industries (Sapuan et al., 2018). These fibers are also used to make brushes, brooms, roofing materials, thatching materials, fishing equipment, traditional prayer headgear, and other small commodities (Bachtiar et al., 2008; Tarique et al., 2021). The SPF is safe for humans and the environment as it is a natural source of *Arenga Pinnata*, which is degradable and will not harm the environment as synthetic fibers do. Thus, this is one of the factors that researchers have been eager to use natural fibers as reinforcement to the fiber composite. Glass fiber (GF) is a synthetic fiber, which has been commonly used as reinforcement in composites to enhance mechanical properties. Unfortunately, touching the glass fiber with bare hands will irritate the skin. Tsunoda et al. (2014) state that skin irritation is called "*Dermatitis,*" in which the glass stimulates the skin mechanically but not chemically. However, it can be safely touched once it has been bound with resin, as it will not be exposed. Epoxy resin is a thermosetting plastic that exhibits huge smoke once ignited and burnt. These smokes are harmful to the environment as well as air pollution. Saba et al. (2016) claim that petroleum-based resin is highly flammable and produces huge amounts of smoke when burned. Despite its environmental issues, epoxy is a good thermosetting plastic that can be a matrix of composite that gives good mechanical properties.

Recent research on SPF/GF/EP composites has shown promising property improvement, fabrication, and characterization results. Researchers have made significant progress in improving the mechanical, thermal, and physical properties of SPF/GF/EP composites. Adding glass fibers to sugar palm fiber composites has increased tensile strength by up to 55.7% (Saba et al., 2016). In addition, the addition of nanofillers in the phenolic resin has shown outstanding multifunctional properties compared to traditional polymeric composites (Kamaruddin et al., 2022). Hybrid composites of SPF/GF have been shown to enhance the characteristics of SPF composites, overcoming the weakness of SPF (Huzaifah et al., 2019). However, there are still challenges and limitations to using these composites, such as their higher cost and limited availability of raw materials. Further research is needed to fully understand the potential benefits and limitations of SPF/GF/EP composites compared to traditional materials. The research on SPF/GF/EP composites is still in its early stages, and more work is needed to understand these materials' potential benefits and limitations fully.

This research has developed a composite material with natural sugar palm fiber and synthetic glass fiber as reinforcement. Sugar palm fiber's main constituents are cellulose (43.88 wt.%), hemicelluloses (7.24 wt.%), lignin (33.24 wt.%), and ash (1.01 wt.%) (Ilyas, Sapuan, Kadier, et al., 2020). E-glass fiber has been widely used as a reinforcement in polymer composites due to its excellent mechanical properties and low cost. The matrix for the hybrid composite is taken to be epoxy. Table 1 lists the mechanical characteristics of the hybrid material inputs. The developed hybrid composite's combination of good strength and fire retardancy will widen the opportunity for industries to produce various potential products.

In this study, glass fiber (GF) and sugar palm (SPF) fiber (*Arenga pinnata (wurmb) merr*) fiber were combined in an epoxy matrix to produce composite materials. Unlike earlier research, this novel hybrid technique intends to capitalize on the synergistic effects

Table 1
Mechanical properties of used materials and others

Material	Density (g/cm^3)	Strength (MPa)	Modulus (GPa)	Elongation at break (%)	Reference
Sugar Palm Fiber	1.2-1.3	15.5	4.189	-	Sherwani et al., 2021
Sugar palm frond fiber	-	421.4	10.4	9.8	Sahari et al., 2012
Sugar palm bunch fiber	-	365.1	8.6	12.5	Sahari et al., 2012
Sugar palm trunk fiber	-	198.3	3.1	29.7	Sahari et al., 2012
ijuk	-	276.6	5.9	22.3	Sahari et al., 2012
Glass	2.5	1.	70	2.5	Davoodi et al., 2010
Epoxy	1.1-1.4	35-100	3-6	1-6	Davoodi et al., 2010
Carbon	1.8	4900	230	-	Dong & Davies, 2015
S-glass	2.5	4700 (@25°C)	85	-	Jones & Huff, 2018
A-glass	2.46	3100(@25°C)	72	-	Jones & Huff, 2018

of SPF and GF, potentially resulting in improved mechanical and flammability features. Investigating several SPF treatments (alkaline and benzoyl chloride) adds to the originality, providing insights into maximizing composite performance. The research focuses on sustainability, employing SPF as Malaysia's renewable and abundant resource. This study addresses crucial factors generally missed in similar studies by analyzing mechanical, flammability, and morphological qualities, paving the path for creative applications in various industries.

MATERIALS AND METHODS

Materials

The SPF was collected from a sugar palm tree at Kampung Kuala Jempol, Negeri Sembilan, Malaysia. Sodium hydroxide (NaOH), Benzoyl Chloride with reagent 99.9%, and ethanol for the fiber treatments were supplied by Evergreen Engineering and Services, Taman Semenyih Sentral, Selangor, Malaysia. Lastly, chopped E-glass fiber, epoxy resin, and hardener were Zeegen brand with a ratio of 3:1, were supplied by Mecha Solve Engineering, Petaling Jaya, Selangor, Malaysia, and used for the SPF/GF/EP composites.

Fiber Treatments

Alkaline Treatment of SPF. SPF was alkaline treated to remove impurities of surface and hemicelluloses within fibers. Thus, in this study, SPF proceeded with an alkaline treatment where the fibers were immersed in 6% NaOH for 1000 mL for 1 hour at room temperature (RT). After that, the soaked SPF was then moved to an acetic acid solution until it hit a neutral pH value and rinsed with distilled water. Lastly, SPF was dried in the oven for 24 hours at 60°C.

Benzoyl Chloride Treatment of SPF. 50g of SPF was first soaked in an 18% concentration of NaOH solutions and then rinsed with water to rinse off the NaOH. The next step was immersing the fibers in a mixed solution of 50 ml benzoyl chloride and 10% NaOH solution for 15 minutes. For the period of immersing the fibers, it was found that 15 minutes of soaked fiber showed the best performance in Izwan et al. (2022). Lastly, the fibers were removed and soaked in ethanol for 60 minutes before being cleaned and dried in the oven at 60 for 24 hours.

Fabrication of SPF/GF/Epoxy Hybrid Composites Testing Samples

According to Syaqira et al. (2020), the best performance of the composite was achieved at 20% SPF with short-cut fibers (0.1 to 0.5 cm). For epoxy mixing, by following Ahmed (2013), the ratio of epoxy and hardener in the study was 4:1, and treated and untreated

SPF will be mixed with epoxy for 5 minutes at RT. However, Zeegen brand epoxy resin and its hardener require a ratio of 3:1 to cure properly; thus, a ratio of 3:1 was used for the curing process. Table 2 describes the hybrid composite formulation to ensure the sugar palm and chopped E-glass fibers and epoxy were mixed properly to develop a high-quality and durable composite plate. After that, the mold-releasing agent was applied to the open mold, and the mixture of resin and fibers was poured and spread evenly using the hand-layout technique. The mold was left to be fully hardened for 24 hours and removed after being cured. The composites were developed into sheets, which were then cut into test samples as per the ASTM standard for tensile, flexural, impact, and flammability tests, namely, ASTM D638-10, ASTM D790, ASTM D256-10, and ASTM D635, respectively.

Table 2
Formulations of treated and untreated hybrid composites

Composite	Matrix as	Reinforcement		
	Epoxy (wt.%)	Sugar Palm Fiber		Glass Fiber
		Treatment	wt.%	
USPF/GF/EP	70	-	30	-
ASPF/GF/EP	70	6% NaOH	15	15
BSPF/GF/EP	70	Benzoyl chloride	15	15

Note. USPF: Untreated SPF; ASPF: Alkaline treated SPF; BSPF: Benzoyl chloride

Characterization

Tensile Test. The tensile test was performed using an Instron 3366 universal testing machine (Instron, Norwood, MA, USA) following ASTM D638-10 (ASTM D638-10, 2015). With a 5kN load cell, the gauge length for hybrid composites follows the ASTM standard D638-10, where the gauge length was 33 mm, and the crosshead velocity was set to 2 mm/min. Five samples were prepared for the tensile testing with dimensions of 115 mm × 19 mm × 3 mm. The average value was taken from among the results taken from five specimens.

Flexural Test. The flexural properties of treated and untreated composites were evaluated using an Instron 3365 columns tabletop Universal Testing Machine with a span length of 50 mm as well as a crosshead speed of 12 mm/min, as specified by the ASTM D790 (3-point bending) standard (ASTM D790, 2017). Composite plates produced five composite samples measuring 127 mm × 12.7 mm × 3 mm. The results were calculated using the average of five specimens.

Impact Test. The five specimens, kept separate from the composite plate for the Izod impact test, were 65 mm × 15 mm × 3 mm in size and adhered to ASTM D256-10 (ASTM D256-10, 2015). Five identical specimens of each composite type were positioned tightly

vertically and hit with a pendulum at a force of 10 J in the instrument's center. The averages of the five specimens were used to measure the impact's energy and velocity, which were 2.75 J and 3.46 m/s, respectively.

Scanning Electron Microscopy (SEM). Adhesion of fibers with polymer matrix of treated and untreated fiber composite was observed under the scanning electron microscope, SEM (Coxem-EM-30AX +), at 5 kV of an acceleration voltage. Specimens were mounted on the aluminum stubs using double-sided adhesive tape. In order to stop charging, specimens were covered in a thin layer of gold (0.01-0.1 m).

Flammability Test. The flammability test determines the fire resistance of composites when burnt by taking the total time taken for the specimen to be fully burnt and calculating the burning rate. A UL-94 horizontal burning test conducted the flammability test of untreated and treated biocomposite samples according to the ASTM D635 (2022) standard. For specimens with dimensions of 125 mm × 13 mm × 3 mm, were 2 marks made on the specimen where 25 mm was measured from each side. The purpose of the one end was to burn first to test whether the specimen was flammable, and once the fire passed through the first mark, the time was recorded for it to burn until the fire reached the second mark. Therefore, the length between the 2 marks was 75 mm, divided by the total minutes taken for the specimen to be burnt to calculate the burning rate. Finally, the burning rate of biocomposite samples was calculated as follows:

$$V = 60L/t$$

Where V, L, and t represent the burning rates (mm/min), burned length (mm), and burning time (s), respectively.

Statistical Analysis. SPSS software analyzed variance (ANOVA) on the experimentally collected data. Duncan's test compared means at a 5% significance level ($p \leq 0.05$).

RESULTS AND DISCUSSION

Tensile Test

Figure 1 shows the average value of the tensile strength tested in agreement with the ASTM standards of D638-04. The USPF/GF/Epoxy exhibited the highest tensile strength value compared to the ones with fiber treatment, which showed 47.17 MPa. Meanwhile, the ASPF/GF/Epoxy showed 42.43 MPa in its tensile strength, which is slightly higher than the BSPF/GF/Epoxy with a value of 40.67 MPa. It has clearly shown that the untreated fiber hybrid composite has the best performance as it was 10.05% higher than ASPF/GF/Epoxy and 13.8% better than the BSPF/GF/Epoxy.

However, as stated by Izwan et al. (2022), the higher treated Kenaf Fiber ratio exhibited the best mechanical properties, with the highest tensile (19.4 MPa), impact (1.2 J/m^2), and flexural values (18.4 MPa). Furthermore, the benzoyl chloride-treated fiber composite was ranked the lowest for its tensile performance. Sherwani et al. (2021) report a similar case in which the benzoyl-treated SPF with glass fiber-reinforced PLA was the weakest, with the lowest slope among the alkaline-treated and untreated fiber composites. Furthermore, according to Table 3, the treated specimens were heavier than the untreated specimens, whereas results showed that untreated specimens had the highest tensile strength. Thus, the adhesion of fibers and polymer will be the major concern in this case.

Even though alkaline-treated fiber composites have degraded tensile properties, several studies found that alkaline-treated fibers showed improved and enhanced mechanical properties. In a study conducted by Bachtiar et al. (2011), the application of alkali treatment to sugar palm fibers increased the composites' strength, surpassing the tensile strength of neat, high-impact polystyrene. In another study conducted by Ibrahim et al. (2010) on kenaf fiber, it was found that the alkaline treatment enhanced its composite tensile

Table 3
The mass for each tensile test specimen

Sample	Specimen	Mass (g)
USPF/GF/EP	1	8.34
	2	8.21
	3	8.45
	4	8.41
	5	8.36
ASPF/GF/EP	1	8.48
	2	8.43
	3	8.51
	4	8.78
	5	8.82
BSPF/GF/EP	1	8.41
	2	8.39
	3	8.46
	4	8.76
	5	8.79

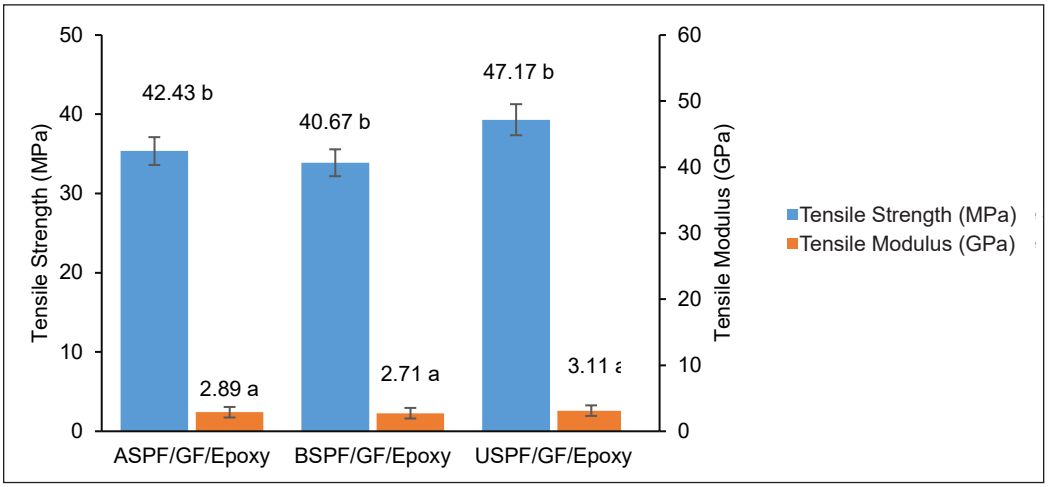

Figure 1. Tensile strength of hybrid composite samples. Values with different letters in the figures are significantly different ($p < 0.05$)

strength. However, at a higher concentration, the tensile strength later dropped due to the degradation of lignocellulose on the fiber surface. The study further explained that the alkaline treatment facilitates the removal of impurities and the protective waxy layer from the outer surface of fibers, leaving a rough surface after treatment, which enhances adhesion between fibers and the matrix. The experiment improved the mechanical properties of flax fiber-reinforced epoxy composites with the alkaline treatment, especially with an increment of the solution concentration up to 3%. On the other hand, a similar case to the degraded tensile strength result was found in the study of Orue et al. (2016). The tensile strengths of alkaline-treated sisal fibers dropped and were lower than untreated sisal fibers, which was explained by the removal of non-cellulosic compounds, which created voids in the fibers and led to weaker mechanical properties.

Flexural Test

The flexural stress of the composites with different treatments has been evaluated by taking an average value out of five specimens tested. Figure 2 clearly shows that the treated fiber composites have much higher flexural stress in their capability to resist deflection while against the force applied. The highest flexural stress found is 131.69 MPa ($p < 0.05$) on ASPF/GF/Epoxy, while the second highest is 122.42 MPa on BSPF/GF/Epoxy. The alkaline-treated fiber composite (ASPF/GF/Epoxy) improved its performance by at least 24.8% higher than the untreated fiber composite. Meanwhile, the BSPF/GF/Epoxy is 24% higher than untreated and was, however, 7% lower than the ASPF/GF/Epoxy.

As shown by the results, it has been proven that the fiber treatment has significantly improved the mechanical properties of the composites by bringing them better adhesion with polymers. According to Siakeng et al. (2019), natural fiber itself has a significant disadvantage when it comes to the choice of synthetic fiber or natural fiber, which is the hydrophilic nature that causes poor adhesion between the fibers and the polymer in composites. Therefore, with the treatment, the natural fibers will overcome the problem by improving their adhesion with the matrix by removing substances like lignin, waxes, and oil-based layers. Moreover, in both work done by Kabir et al. (2012) and Safri et al. (2018), the results have proven that benzoyl treatment brought improvement to the fibers in terms of the mechanical

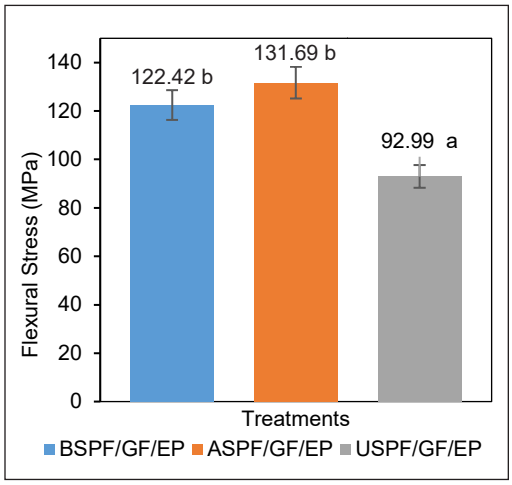

Figure 2. Flexural stress of the hybrid composites with different treatments. Values with different letters in the figures are significantly different ($p < 0.05$)

strength, adhesion with the matrix, and reduction in water absorption by reducing hydrophilic nature of natural fiber itself.

According to Figure 3, the graph shown was in compressive load (N) against the compressive extension (mm). It was, however, to be used for flexural testing on compression software due to the breakdown of the flexural testing machine. Apart from that, by referring to the behavior of the graphs based on these composites with various treatments, it was found that the ASPF/GF/EP exhibited the highest slope in the curves, while the BSPF/GF/EP had second highest among the curves, and yet the USPF/GF/EP has the lowest slope as compared to the other two. Moreover, the result was obvious that three of these composites showed similar extensions. The results highlight the importance of fiber treatment in influencing the mechanical performance of the composites. The distinct slopes and responses of the curves suggest that the treatments impact the interfacial adhesion between the fibers and the epoxy matrix, influencing the overall composite strength and stiffness. Notably, despite the differences in slope and stiffness, all three composites exhibited similar extensions, indicating a consistent level of ductility. This finding indicates that the chosen treatments did not compromise the ability of the composites to withstand deformation before failure.

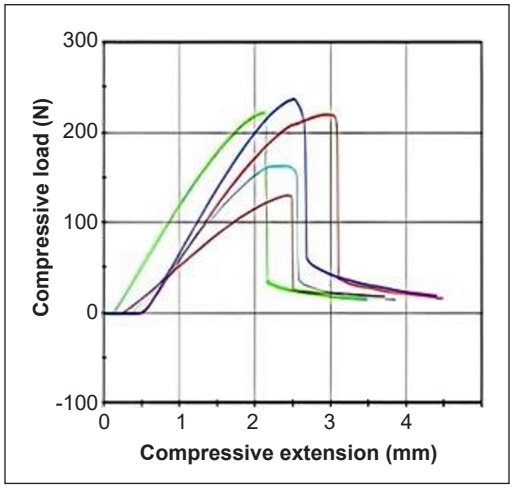

(a)

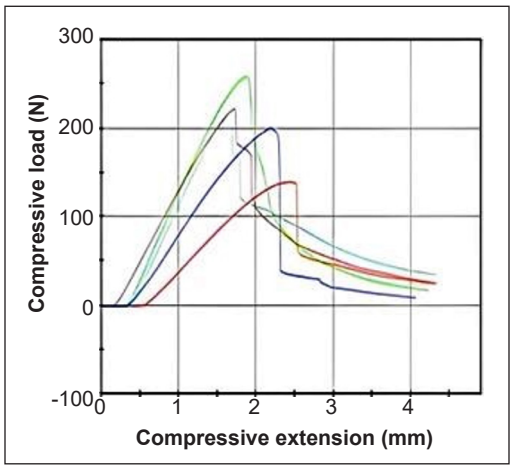

(b)

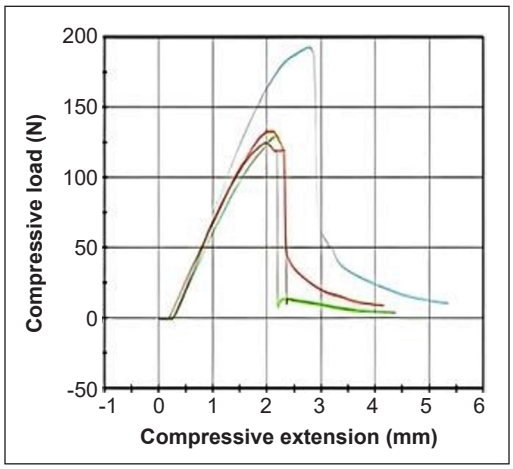

(c)

Figure 3. The compressive load (N) versus compressive extension (mm) of the composites: (a) BSPF/GF/EP; (b) ASPF/GF/EP; and (c) USPF/GF/EP

Overall, these results provide valuable insights into the significance of fiber treatments in enhancing the mechanical properties of the composites. The findings offer new possibilities for tailoring the mechanical behavior of natural fiber-reinforced composites through appropriate treatment approaches by providing a more detailed result, in which each composite's strain has been calculated, as shown in Table 4. The highest strain was shown in ASPF/GF/EP with a value of 0.033, whereas the other two composites showed similar results to the ASPF/GF/EP with values of 0.031 and 0.032 for BSPF/GF/EP and USPF/GF/EP, respectively. Based on the behavior of the composites that reacted towards the flexural testing, one major factor may be due to the brittleness of the epoxy itself, as thermoset matrices are known for their extreme brittleness as compared to thermoplastic materials (Turk et al., 2017).

Table 4
The average values of mechanical properties out of five specimens

Sample	Tensile (MPa)	Tensile Modulus (GPa)	Flexural (MPa)	Strain (mm/mm)	Impact (kJ/m²)
USPF/GF/EP	47.17 ± 0.7 [b]	3.112± 0.09 [a]	92.99 ± 0.3 [a]	0.032	19.4 ± 0.4 [a]
ASPF/GF/EP	42.43± 0.8 [b]	2.886 ± 0.08 [a]	131.69 ± 0.9 [b]	0.033	19.7± 0.3 [a]
BSPF/GF/EP	40.67± 0.6 [b]	2.707 ± 0.04 [a]	122.41± 0.7 [b]	0.031	19.5± 0.5 [a]

Note. Data are expressed as the mean value of replication (n) ± SD; for the same column, the different letter indicates a significant difference ($p < 0.05$)

Impact Test

The impact test of this study has been summarized in Figure 4. As it can be seen from the graph shown in Figure 4, ASPF/GF/EP has the highest impact strength at 19.7 kJ/m² and yet the BSPF/GF/EP is ranked as second in the impact test at 19.5 kJ/m² while USPF/GF/EP has the lowest with a slightly lower value at 19.4 kJ/m² as compared with the two samples. There are no significant changes. During the impact test, all the specimens, after being hit by the heavy blow, appeared to be hinge broken.

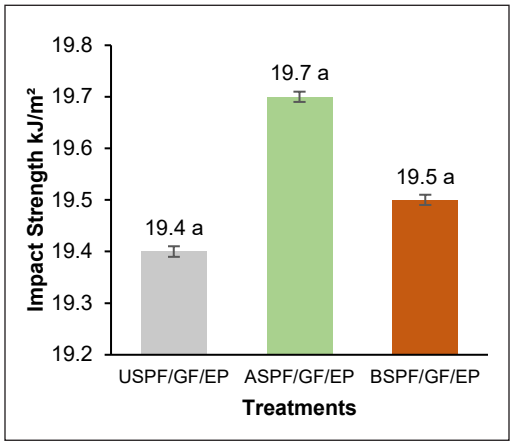

Figure 4. Impact strength of composite samples with various treatments

With the results given, it has been proven that the benefits gained by having fiber treatment that removes the outer layers of fibers, such as lignin, hemicelluloses, and pectin, have significantly improved adhesion between fibers and the polymer and thus an improvement in mechanical properties as an output. For the contribution of such improved

results, it has been shown that the engagement of fibers with the epoxy as the matrix of composites was in good condition, and yet it allowed for the optimal absorption of the energy that was crushed towards the specimen. Furthermore, Swain and Biswas (2017) find that benzoyl chloride-treated jute fiber-reinforced epoxy significantly improves its impact strength compared to untreated.

According to Cartie and Irving (2002), the resin toughness is still the most important factor in influencing impact strength, rather than the strength of the fibers as well as their stiffness. Epoxy was the matrix of the tested composites, which is well known for its excellent mechanical strength despite its brittleness. In comparing the thermoset plastic with thermoplastics such as PLA, in the study of Sherwani et al. (2021), the same composition of the reinforcement with 15 wt.% of SPF, GF, and PLA as the matrix, the highest impact strength that was exhibited was 3.10 kJ/m². As a result, there is a large gap between the thermoset plastic and the thermoplastic.

Scanning Electron Microscopy (SEM)

Throughout the mechanical tests, it was found that all the treated SPF/GF/EP composite have improved properties except for the tensile test, where the untreated SPF/GF/EP has the best outcome. By referring to the studies done by Bachtiar et al. (2008), Ibrahim et al. (2010), Swain and Biswas (2017), and Sherwani et al. (2021), all alkaline-treated fibers showed a significant improvement in improving mechanical properties of the composite, especially in tensile strength and flexural strength. However, the ASPF/GF/EP was somehow gotten with a lower tensile strength than the USPF/GF/EP. Therefore, the morphological observation will be focused on the ASPF/GF/EP and USPF/GF/EP.

According to Table 5, both SEM analyses of USPF/GF/EP and ASPF/GF/EP have been shown. For USPF/GF/EP, the breakage of the SPF can be seen, which indicates a good interlocking of fibers with the matrix, as it shows that more energy was absorbed when the specimen was being pulled during the tensile test. In contrast, the ASPF/GF/EP fiber was shown in a pulled-out condition instead of broken due to the tension applied. Ishak et al. (2009) found a similar result: the SPF was also pulled out with holes remaining, but this time with untreated SPF. That being said, this indicates poor interfacial bonding owing to poor adhesion between fibers and matrix. Moreover, based on SEM analysis of ASPF/GF/EP, many voids can be seen, and these voids have guaranteed poor mechanical performances due to poor adhesion. However, one explanation from Swain and Biswas (2017) states that the presence of the holes can be either air entrapments or voids. Air entrapments are mostly known to be a common problem for epoxy resins. The gassy issue happens when the temperature rises during the curing process and gets trapped.

Suppose the alkaline treated SPF would have a better adhesion with the matrix due to its rougher fibers' outer surface. Benyahia and Merrouche (2014) reported that the removal of

the lignins, pectin, hemicelluloses, and others of Alfa fibers after alkaline treatment caused the outer surface of the fiber itself to be rougher than untreated, and thus, the rough surface helps in the adhesion between fibers as well as polymer due to exposure of hydroxyl groups to the matrix. Therefore, by considering the factor for the result that untreated has higher tensile strength, the factor could be either the chemical treatment that leads to degradation in the fiber structure or the air entrapments during the curing process.

Table 5
The morphological investigation of fractured tensile samples for untreated and alkaline-treated

Sample	Tensile Test
USPF/GF/EP	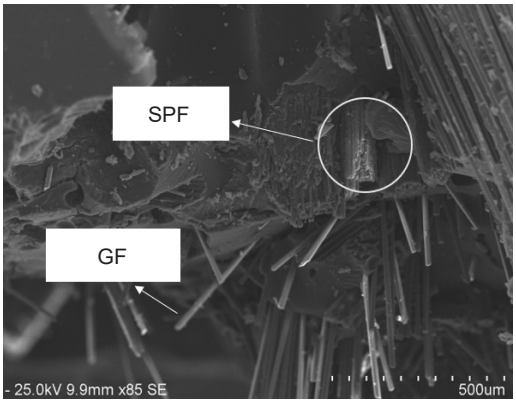
ASPF/GF/EP	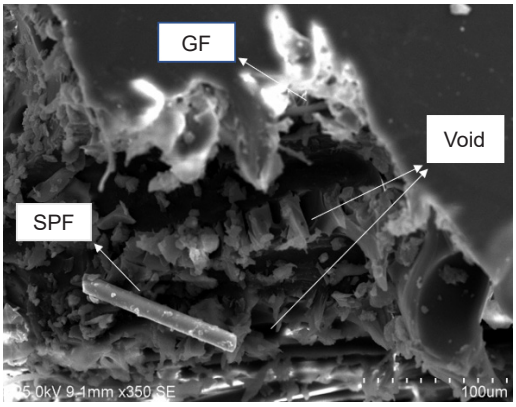

Flammability Test

The flammability test determines the fire resistance of composites when burnt by taking the total time for the specimen to be fully burnt and calculating the burning rate (Sherwani et al., 2021; Suriani et al., 2021).

The five specimens of each sample were tested with the burning test in accordance with the standard of the UL-94 horizontal burning test. Based on Table 6, the average time

taken for the specimens to finish burning the marked parts has been calculated based on the time recorded for five specimens of each. It was found that the treated fiber composites took a longer time to burn than the untreated fiber composites. Based on Figure 5, it is noticeable that ASPF/GF/EP has the lowest burning rate at 17.01 mm/min as compared to the other two samples. However, BSPF/GF/EP has a lower burning rate at 18.03 mm/min compared with the USPF/GF/EP, where the burning rate is the highest among the tested samples at 18.85 mm/min. Such a result may be attributed to the main factor, which belongs to the treatments done on the fibers for benzoyl chloride and alkaline. As Izwan et al. (2022) stated, benzoylation-treated fibers improved fire retardancy. Moreover, Shukor et al. (2014) claim that the alkaline-treated kenaf fiber showed a 5% improvement in its fire retardancy after removing lignin after being alkali-treated.

By observing the burning behaviors of all samples, it was observed that the flames on all samples were high flame, and high smoke was produced. For such a phenomenon, the high flame and high smoke produced are due to the matrix of the composites, as the composite itself has 70 wt.% of the epoxy resin as a petroleum-based polymer. Saba et al. (2016) state that petroleum-based polymers are mostly known to be extremely flammable as epoxies dissipate heat and produce smoke when they are burnt. Apart from that, after being burnt, all the samples showed the same results where char was formed, and no dripping happened throughout the burning process. Char formation could be caused by the high content of fibers, which account for up to 30 wt.% of composites. Comparable observations have been reported by Chee et al. (2020). The fibers were up to 40%, and the cohesive char formed after the burning test.

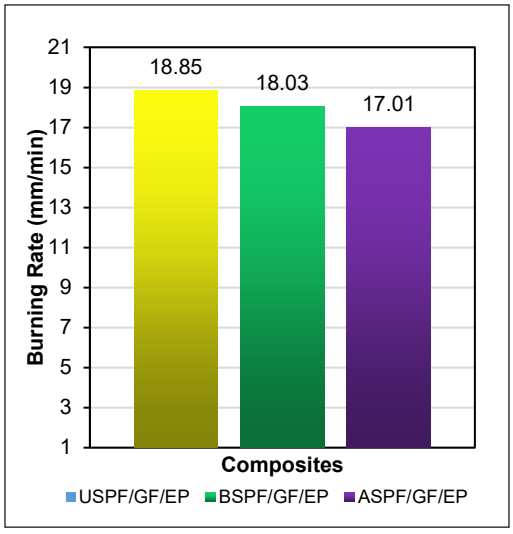

Figure 5. The burning rate of the composite samples

Table 6
The time recorded for the samples to be burnt and the burning behavior of various samples

Sample	Time taken to burn (minute)	Burning Behaviour
USPF/GF/EP	4.09	Fully burnt, high flame, high smoke production, no dripping, and char formed.
BSPF/GF/EP	4.27	Fully burnt, high flame, high smoke production, no dripping, and char formed.
ASPF/GF/EP	4.53	Fully burnt, high flame, produces high smoke, no dripping, and char formed.

CONCLUSION

This novel composite material was successfully fabricated and tested for mechanical, morphological, and flammability properties. The flexural and impact strength of SPF hybrid composites treated with alkaline and benzoyl chloride improved by 24.8%, 1.52%, 24%, and 0.51%, respectively. However, both treated SPF hybrid composites exhibited weaker tensile strength compared to the untreated SPF hybrid composite due to poor mechanical interlocking at the fiber-matrix interface. For flammability, alkaline-treated, as well as benzoyl chloride-treated SPF hybrid composites showed improvements of 9.76% and 5.66%, respectively, in lowering the burning rate, owing to the reduction of lignin content in SPF after treatment. Based on the findings, it can be concluded that the fabrication of SPF/GF/EP hybrid composites offers promise for various industrial applications, including automotive components, aerospace structures, marine applications, and lightweight construction materials for vehicles, aircraft, and ships. These composites provide superior mechanical performance and lightweight construction. In addition, SPF, a readily available, renewable, biodegradable material with excellent tensile properties, can substantially impact and contribute to environmental sustainability. Further research, including thermal loading studies, should be conducted on such hybrid composites to explore their full potential.

ACKNOWLEDGEMENTS

The authors wish to thank Andy Wong Hoe Kiu of Universiti Putra Malaysia, for his contribution.

REFERENCES

Ahmed, Q. I. (2013). Fracture toughness of sugar palm fiber reinforced epoxy composites. *International Journal of Science and Research*, *2*(12), 273–279.

ASTM D635. (2022). *Standard test method for rate of burning and/or extent and time of burning of plastics in a horizontal position*. ASTM International. https://www.astm.org/d0635-18.html

ASTM D790. (2017). *Standard test method for flexural properties ofunreinforced and reinforced plastics and electrical insulation materials*. ASTM International. https://www.astm.org/d0790-03.html

ASTM D256-10. (2015). *Determining the izod pendulum impact resistance of plastic*. ASTM International. https://www.astm.org/d0256-23e01.html

ASTM D638-10. (2015). *Standard test method for tensile properties of plastics*. ASTM International. https://www.astm.org/d0638-10.html

Azammi, A. M. N., Ilyas, R. A., Sapuan, S. M., Ibrahim, R., Atikah, M. S. N., Asrofi, M., & Atiqah, A. (2019). Characterization studies of biopolymeric matrix and cellulose fibres based composites related to functionalized fibre-matrix interface. In K. L. Goh, M. K. Aswathi, R. T. De Silva & S. Thomas (Eds.)

Interfaces in particle and fibre reinforced composites- From macro to nano scales (pp.1–68). Woodhead Publishing. https://doi.org/10.1016/B978-0-08-102665-6.00003-0

Bachtiar, D., Salit, M. S., Zainuddin, E., Abdan, K., & Dahlan, K. Z. H. M. (2011). Effects of alkaline treatment and a compatibilizing agent on tensile properties of sugar palm fibre-reinforced high impact polystyrene composites. *BioResources*,*6*(4), 4815-4823.

Bachtiar, D., Sapuan, S. M., & Hamdan, M. M. (2008). The effect of alkaline treatment on tensile properties of sugar palm fibre reinforced epoxy composites. *Materials & Design*, *29*(7), 1285–1290. https://doi.org/10.1016/j.matdes.2007.09.006

Benyahia, A., & Merrouche, A. (2014). Effect of chemical surface modifications on the properties of alfa fiber-polyester composites. *Polymer-Plastics Technology and Engineering*, *53*(4), 403–410. https://doi.org/10.1080/03602559.2013.844828

Cartié, D. D. R., & Irving, P. E. (2002). Effect of resin and fibre properties on impact and compression after impact performance of CFRP. *Composites Part A: Applied Science and Manufacturing*, *33*(4), 483–493. https://doi.org/10.1016/S1359-835X(01)00141-5

Chee, S. S., Jawaid, M., Alothman, O. Y., & Yahaya, R. (2020). Thermo-oxidative stability and flammability properties of bamboo/kenaf/nanoclay/epoxy hybrid nanocomposites. *RSC Advances*, *10*(37), 21686–21697. https://doi.org/10.1039/D0RA02126A

Davoodi, M. M., Sapuan, S. M., Ahmad, D., Ali, A., Khalina, A., & Jonoobi, M. (2010). Mechanical properties of hybrid kenaf/glass reinforced epoxy composite for passenger car bumper beam. *Materials and Design*, *31*(10), 4927–4932. https://doi.org/10.1016/j.matdes.2010.05.021

Dong, C., & Davies, I. J. (2015). Flexural strength of bidirectional hybrid epoxy composites reinforced by E glass and T700S carbon fibres. *Composites Part B: Engineering*, *72*, 65–71. https://doi.org/10.1016/j.compositesb.2014.11.031

Harussani, M. M., Sapuan, S. M., Khalina, A., Rashid, U., & Tarique, J. (2021, April 7-9). *Slow pyrolysis of disinfected COVID-19 non-woven polypropylene (PP) waste*. [Paper presentation]. International Symposium on Applied Sciences and Engineering (ISASE), Erzurum, Turkey.

Huzaifah, M. R. M., Sapuan, S. M., Leman, Z., & Ishak, M. R. (2019). Effect of soil burial on physical, mechanical and thermal properties of sugar palm fibre reinforced vinyl ester composites. *Fibers and Polymers*, *20*(9), 1893–1899. https://doi.org/10.1007/s12221-019-9159-6

Huzaifah, M. R. M., Sapuan, S. M., Leman, Z., & Ishak, M. R. (2016, Month date PLEASE PROVIDE THE INFORMATION). *A review on sugar palm (Arenga Pinnata): Characterization of sugar palm fibre*. [Paper presentation]. Proceedings of the 5th Postgraduate Seminar on Natural Fiber Composites, Selangor, Malaysia.

Ibrahim, M. S., Sapuan, S. M., & Faieza, A. A. (2012). Mechanical and thermal properties of composites from unsaturated polyester filled with oil palm ash. *Journal of Mechanical Engineering and Sciences*, *2*, 133-147. https://doi.org/10.15282/jmes.2.2012.1.0012

Ibrahim, N. A., Hadithon, K. A., & Abdan, K. (2010). Effect of Fiber Treatment on Mechanical Properties of Kenaf Fiber-Ecoflex Composites. *Journal of Reinforced Plastics and Composites*, *29*(14), 2192–2198. https://doi.org/10.1177/0731684409347592

Ilyas, R. A, Sapuan, S. M., Kirubaanand, W., Zahfiq, Z. M., Atikah, M. S. N., Ibrahim, R., Radzi, A. M., Nadlene, R., Asyraf, M. R. M., Hazrol, M. D., Sherwani, S. F. K., Harussani, M. M., Tarique, J., Nazrin, A., & Syafiq, R. (2021). Roselle: Production, product development, and composites. In S. M. Sapuan & A. M. Radzi (Eds.) *Roselle* (pp.1–23). Academic Press. https://doi.org/10.1016/B978-0-323-85213-5.00009-3

Ilyas, R. A., Sapuan, S. M., Atikah, M. S. N., Ibrahim, R., Hazrol, M. D., Sherwani, S. F. K., Jamal, T., Nazrin, A., & Syafiq, R. (2020, November Date PLEASE PROVIDE THE INFORMATION). *Natural fibre : A promising source for the production of nanocellulose*. [Paper presentation]. 7th Postgraduate Seminar On Natural Fibre Reinforced Polymer Composites, Selangor, Malaysia.

Ilyas, R. A., Sapuan, S. M., Kadier, A., Krishnan, S., Atikah, M. S. N., Ibrahim, R., Nazrin, A., Syafiq, R., Misri, S., Huzaifah, M. R. M., & Hazrol, M. D. (2020). Mechanical testing of sugar palm fiber reinforced sugar palm biopolymer composites. *Advanced Processing, Properties, and Applications of Starch and Other Bio-Based Polymers, 2020,* 89-110. https://doi.org/10.1016/b978-0-12-819661-8.00007-x

Ishak, M. R., Leman, Z., Sapuan, S. M., Salleh, M. Y., & Misri, S. (2009). The effect of sea water treatment on the impact and flexural strength of sugar palm fibre reinforced epoxy composites. *International Journal of Mechanical and Materials Engineering*, *4*(3), 316–320.

Jones, F. R., & Huff, N. T. (2018). The structure and properties of glass fibers. In A. R. Bunsell (Ed.) *Handbook of properties of textile and technical fibres* (pp.757–803). Woodhead Publishing. https://doi.org/10.1016/B978-0-08-101272-7.00019-5

Kabir, M. M., Wang, H., Lau, K. T., & Cardona, F. (2012). Composites : Part B Chemical treatments on plant-based natural fibre reinforced polymer composites : An overview. *Composites Part B*, *43*(7), 2883–2892. https://doi.org/10.1016/j.compositesb.2012.04.053

Kamaruddin, Z. H., Jumaidin, R., Ilyas, R. A., Selamat, M. Z., Alamjuri, R. H., & Yusof, F. A. M. (2022). Influence of alkali treatment on the mechanical, thermal, water absorption, and biodegradation properties of cymbopogan citratus fiber-reinforced, thermoplastic cassava starch–palm wax composites. *Polymers*, *14*(14), 2769. https://doi.org/10.3390/polym14142769

Lau, K., Hung, P., Zhu, M. H., & Hui, D. (2018). Properties of natural fibre composites for structural engineering applications. *Composites Part B: Engineering*, *136*, 222–233. https://doi.org/10.1016/j.compositesb.2017.10.038

Izwan, S. M., Sapuan, S. M., Zuhri, M. Y. M., & Muhamed, A. R. (2022). Effect of benzoyl treatment on the performance of sugar palm/kenaf fiber-reinforced polypropylene hybrid composites. *Textile Research Journal*, *92*(5–6), 706–716. https://doi.org/10.1177/00405175211043248

Orue, A., Jauregi, A., Unsuain, U., Labidi, J., Eceiza, A., & Arbelaiz, A. (2016). The effect of alkaline and silane treatments on mechanical properties and breakage of sisal fibers and poly(lactic acid)/sisal fiber composites. *Composites Part A: Applied Science and Manufacturing*, *84*, 186–195. https://doi.org/10.1016/j.compositesa.2016.01.021

Saba, N., Jawaid, M., Alothman, O. Y., Paridah, M. T., & Hassan, A. (2016). Recent advances in epoxy resin, natural fiber-reinforced epoxy composites and their applications. *Journal of Reinforced Plastics and Composites*, *35*(6), 447–470. https://doi.org/10.1177/0731684415618459

Safri, S. N. A., Sultan, M. T. H., Saba, N., & Jawaid, M. (2018). Effect of benzoyl treatment on flexural and compressive properties of sugar palm/glass fibres/epoxy hybrid composites. *Polymer Testing*, *71*, 362–369. https://doi.org/10.1016/j.polymertesting.2018.09.017

Sahari, J., Sapuan, S. M., Ismarrubie, Z. N., & Rahman, M. Z. (2012). Physical and chemical properties of different morphological parts of sugar palm fibres. *Fibres and Textiles in Eastern Europe*, *91*(2), 21–24.

Sapuan, S. M., Ilyas, R. A., Ishak, M. R., Leman, Z., Huzaifah, M. R. M., Ammar, I. M., & Atikah, M. S. N. (2018). Development of sugar palm–based products: A community project. In S. M. Sapuan, J. Sahari, M. R. & Ishak, M. L. Sanyang. *Sugar palm biofibers, biopolymers, and biocomposites* (pp. 245–266). CRC Press. https://doi.org/10.1201/9780429443923-12

Sherwani, S. F. K., Zainudin, E. S., Sapuan, S. M., Leman, Z., & Abdan, K. (2021). Mechanical properties of sugar palm (Arenga pinnata Wurmb. Merr)/glass fiber-reinforced poly(lactic acid) hybrid composites for potential use in motorcycle components. *Polymers*, *13*(18), 3061. https://doi.org/10.3390/polym13183061

Shukor, F., Hassan, A., Saiful Islam, M., Mokhtar, M., & Hasan, M. (2014). Effect of ammonium polyphosphate on flame retardancy, thermal stability and mechanical properties of alkali treated kenaf fiber filled PLA biocomposites. *Materials & Design (1980-2015)*, *54*, 425–429. https://doi.org/10.1016/j.matdes.2013.07.095

Siakeng, R., Jawaid, M., Ariffin, H., & Sapuan, S. M. (2019). Mechanical, dynamic, and thermomechanical properties of coir/pineapple leaf fiber reinforced polylactic acid hybrid biocomposites. *Polymer Composites*, *40*(5), 2000–2011. https://doi.org/10.1002/pc.24978

Suriani, M. J., Radzi, F. S. M., Ilyas, R. A., Petrů, M., Sapuan, S. M., & Ruzaidi, C. M. (2021). Flammability, tensile, and morphological properties of oil palm empty fruit bunches fiber/pet yarn-reinforced epoxy fire retardant hybrid polymer composites. *Polymers*, *13*(8), 1282. https://doi.org/10.3390/polym13081282

Swain, P. T. R., & Biswas, S. (2017). Influence of fiber surface treatments on physico-mechanical behaviour of jute/epoxy composites impregnated with aluminium oxide filler. *Journal of Composite Materials*, *51*(28), 3909–3922. https://doi.org/10.1177/0021998317695420

Syaqira S, S. N., Leman, Z., Sapuan, S. M., Dele-Afolabi, T. T., Azmah Hanim, M. A., & Budati, S. (2020). Tensile strength and moisture absorption of sugar palm-polyvinyl butyral laminated composites. *Polymers*, *12*(9). https://doi.org/10.3390/POLYM12091923

Tarique, J., Sapuan, S. M., Khalina, A., Sherwani, S. F. K., Yusuf, J., & Ilyas, R. A. (2021). Recent developments in sustainable arrowroot (Maranta arundinacea Linn) starch biopolymers, fibres, biopolymer composites and their potential industrial applications: A review. *Journal of Materials Research and Technology*, *13*, 1191–1219. https://doi.org/10.1016/j.jmrt.2021.05.047

Tarique, J., Zainudin, E. S., Sapuan, S. M., Ilyas, R. A., & Khalina, A. (2022). Physical, mechanical, and morphological performances of arrowroot (Maranta arundinacea) Fiber reinforced arrowroot starch biopolymer composites. *Polymers*, *14*(3), 388. https://doi.org/10.3390/polym14030388

Tsunoda, M., Kido, T., Mogi, S., Sugiura, Y., Miyajima, E., Kudo, Y., Kumazawa, T., & Aizawa, Y. (2014). Skin irritation to glass wool or continuous glass filaments as observed by a patch test among human Japanese volunteers. *Industrial Health*, *52*(5), 439–444. https://doi.org/10.2486/indhealth.2012-0222

Turk, M., Hamerton, I., & Ivanov, D. S. (2017). Ductility potential of brittle epoxies: Thermomechanical behaviour of plastically-deformed fully-cured composite resins. *Polymer*, *120*, 43–51. https://doi.org/10.1016/j.polymer.2017.05.052

Pertanika J. Sci. & Technol. 31 (S1): 157 - 173 (2023)

PERTANIKA JOURNALS

SCIENCE & TECHNOLOGY

Journal homepage: http://www.pertanika.upm.edu.my/

Effect of Coconut Fiber Loading on the Morphological, Thermal, and Mechanical Properties of Coconut Fiber Reinforced Thermoplastic Starch/Beeswax Composites

Ridhwan Jumaidin[1]*, Syahmah Shafie[1], Rushdan Ahmad Ilyas[2,3,4,5] and Muchlis[6]

[1]Fakulti Teknologi dan Kejuruteraan Industri dan Pembuatan, Universiti Teknikal Malaysia Melaka, Hang Tuah Jaya, 76100 Durian Tunggal, Melaka, Malaysia
[2]Faculty of Chemical and Energy Engineering, Universiti Teknologi Malaysia, 81310 UTM, Johor, Malaysia
[3]Centre for Advanced Composite Materials, Universiti Teknologi Malaysia (UTM), Johor Bahru 81310, Malaysia
[4]Institute of Tropical Forest and Forest Products (INTROP), Universiti Putra Malaysia, 43400 UPM Serdang, Selangor, Malaysia
[5]Centre of Excellence for Biomass Utilization, Universiti Malaysia Perlis, 02600, Arau, Perlis, Malaysia
[6]Environmental Engineering Department, Institut Sains & Teknologi AKPRIND Yogyakarta, Yogyakarta 55222, Indonesia

ABSTRACT

The increasing concern about global warming and the accumulation of non-biodegradable plastic has caused serious environmental issues. Hence, the need to create a more environmentally friendly material such as thermoplastic starch (TPS) has grown. However, the poor properties of TPS, such as high moisture sensitivity and low mechanical properties, have limited the potential application of this biopolymer. This study aims to modify TPS's thermal and mechanical properties by incorporating coconut fiber. The composites were prepared by incorporating various coconut fiber loading (0, 10, 20, 30, 40, and 50 wt.%) into the TPS matrix. The mixture was fabricated using a hot press at 145°C for 1 hour. The sample is then characterized using thermogravimetric analysis and tensile and flexural tests. The results show that the composite with 50 wt.% coconut fiber had higher thermal stability than samples with lower fiber content. A significant increment in tensile strength and modulus of up to 20.7 MPa and 2890 MPa were recorded for samples with 50 wt.% fiber content—the sample with 50wt.% fiber also demonstrated the highest flexural strength and modulus of up to 30.3 MPa and 3266.3 MPa, respectively. These changes are consistent with the FTIR

ARTICLE INFO

Article history:
Received: 06 March 2023
Accepted: 28 August 2023
Published: 27 October 2023

DOI: https://doi.org/10.47836/pjst.31.S1.09

E-mail addresses:
ridhwan@utem.edu.my (Ridhwan Jumaidin)
b071710172@student.utem.edu.my (Syahmah Shafie)
ahmadilyas@utm.my (Rushdan Ahmad Ilyas)
muchlis@akprind.ac.id (Muchlis)
* Corresponding author

ISSN: 0128-7680
e-ISSN: 2231-8526

and SEM findings, which show good compatibility of TPCS and coconut fiber with a homogeneous structure. Overall, coconut fiber shows good potential as reinforcement for biodegradable-based polymer composites.

Keywords: Coconut fiber, cellulose, mechanical, natural fiber, thermal, thermoplastic starch

INTRODUCTION

Increased awareness of environmental protection has led to vast amounts of studies conducted on biodegradable polymers. Biodegradable polymers are made of sub-components of plants, such as cellulose, protein, and starch. Among the biopolymers, thermoplastic starch (TPS) is one of the most promising materials due to the abundance of resources, low cost, and the fact that the raw material is renewable (Asyraf et al., 2022). However, TPS is often associated with several limitations, such as poor mechanical properties, which limits the widespread application of the end product (Thakur et al., 2019). Hence, several modifications on TPS have been conducted previously to improve the properties of TPS, such as blending with biopolymer or reinforcement with natural fiber (Saepoo et al., 2023; S. Wang et al., 2023).

Moreover, researchers have explored various techniques to overcome the inherent limitations of TPS and enhance its mechanical properties for broader industrial utilization. These efforts have led to significant advancements in the field of bioplastics. Blending TPS with biopolymers, such as starch or cellulose derivatives (Sanyang et al., 2016), has shown promising results in improved tensile strength, impact resistance, and thermal stability. This synergy between TPS and other biopolymers enhances the overall mechanical performance and contributes to the final product's biodegradability.

Another avenue of improvement involves reinforcing TPS with natural fibers or lignocellulosic fiber, such as sugar palm, kenaf, water hyacinth, jute, flax, or hemp. Table 1 shows the lignocellulosic fiber-reinforced starch biocomposites. Incorporating these fibers into the TPS matrix enhances its structural integrity and provides excellent strength-to-weight ratios (Bahloul et al., 2023; Khalili et al., 2023). It addresses the mechanical limitations and offers an environmentally friendly alternative to traditional petroleum-based plastics. The resulting composite materials exhibit enhanced properties, making them suitable for a wider range of applications, from packaging materials to automotive components.

Coconut fiber is a sustainable, renewable, biodegradable, and recyclable material, which makes it a suitable candidate for various applications. Adding coconut fiber to the polymer matrix has been reported to improve the mechanical properties of the composites, such as tensile strength and modulus of elasticity (Meráz-Rivera et al., 2020). Surface treatments, such as pretreating the surfaces of coconut fiber or removing wax, lignin, and hemicellulose from the fiber surface, can enhance the interaction between the fiber and the starch matrix,

Table 1
Lignocellulosic fiber-reinforced starch biocomposites

Starch source (plasticizer)	Polymer/reinforcement (natural fiber dimension)	Fabrication technique	References
Corn (glycerol and natural rubber latex)	Sisal, hemp (10–15 mm)	Melt blending	Gironès et al., 2012
Corn starch (glycerol)	Poly(vinyl alcohol) fiber	Compression molding	Zhou et al., 2020
Maize starch (glycerin)	Flax fiber	Extrusion	Borowski et al., 2020
Rice (glycerol)	Cotton fiber (2.11 and 5.27 mm)	Compression molding	Prachayawarakorn et al., 2011
Arrowroot starch (glycerol)	Arrowroot fiber	Solution casting	Tarique et al., 2022
Cassava (sorbitol and glycerol)	Cellulose nanocrystal from kenaf fiber (70–190 nm)	Solution casting	Zainuddin et al., 2013
Sugar palm starch (sorbitol and glycerol)	Nanocrystalline cellulose from sugar palm	Solution casting	Ilyas et al., 2018
Potato starch (glycerol)	Kaolin clay	Casting method	Kwaśniewska et al., 2020
Cassava starch	Cogon grass fiber	Compression molding	Jumaidin et al., 2020
Corn starch	Kenaf fiber	Casting method	Hazrol et al., 2022
Sugar palm starch	Tin oxide/ Oil Palm Empty Fruit Bunches (OPEFB) nanofibril cellulose	Casting method	Azra et al., 2023
Sugar palm starch (sorbitol and glycerol)	PLA/sugar palm nanocellulose	Compression molding	Nazrin et al., 2020; 2021
Cassava	Durian peel	Compression molding	Jumaidin et al., 2023
Sugar palm starch (sorbitol and glycerol)	Nanofibrillated cellulose from sugar palm	Solution casting	Ilyas et al., 2019, 2020
Pea starch (glycerol and water)	PCL/flax fiber	Compression molding	Fabunmi et al., 2011
Cassava starch (glycerol)	PLA/PBAT/jute fiber	Extrusion	Yokesahachart et al., 2021

leading to better mechanical properties (Gomes et al., 2019; Norfarhana et al., 2022; Norrrahim et al., 2021). Crosslinking agents, such as boric acid, can also affect the density, tensile strength, hardness, water absorption, and biodegradation of the composite (Nansu et al., 2019). Overall, coconut fiber shows promising properties as environmentally friendly reinforcement and biodegradable materials for various applications, including packaging and shockproof materials. Meanwhile, beeswax is a natural hydrophobic agent that can reduce natural materials' moisture sensitivity. Our previous work reported beeswax's effectiveness in reducing TPS's moisture sensitivity (Diyana et al., 2021).

Despite the effectiveness of beeswax and the potential of coconut fiber as reinforcement, to the best of our knowledge, no study was reported on coconut fiber as reinforcement for thermoplastic starch/beeswax composite. Hence, this study aims to develop a thermoplastic

cassava starch/beeswax blend reinforced with coconut fiber to investigate this bio-based material's thermal and mechanical properties.

MATERIALS AND METHODS

Materials

The colorless, odorless, viscous white powder cassava starch for TPS sample preparation obtained for this study was from Antik Sempurna Sdn. Bhd, Shah Alam, Malaysia. Glycerol was purchased from QReC (Asia) Sdn. Bhd., Rawang, Malaysia, with an AR grade of 99.5%. The Aldrich Chemistry Sdn. Bhd., Petaling Jaya, Malaysia, supplied beeswax, and the coconut fiber (CF) was collected from Sungai Petani, Kedah, Malaysia. The retting process was then carried out by soaking the husks for about 2 to 3 weeks. The materials of the husk, which bind together fiber, were degraded, and fibers were loosened during retting. The dried CF was ground to smaller sizes of about 2 to 3 mm.

Sample Preparation

TPS/Beeswax reinforced with coconut fiber was modified by merging different amounts of coconut fiber (0, 10, 20, 30, 40, and 50 wt.%), as shown in Table 2. After the compaction of the composites into the mold was completed, the composite underwent a heating process inside the hot press at 145°C for approximately 1 hour and a cooling process at 30°C for about 15 minutes. Figure 1 shows the sample preparation process, and Figure 2 shows the TPCS/beeswax reinforced with coconut fiber.

Figure 1. TPS/beeswax reinforced with coconut fiber

Figure 2. TPS/beeswax reinforced with coconut fiber

Table 2
Composite formulation

Composite	Modified TPS mixture (%)	Fiber Loading (wt.%)
0%	100	-
10%	90	10
20%	80	20
30%	70	30
40%	60	40
50%	50	50

Thermal Testing

Thermo-Gravimetric Analysis (TGA). TGA was performed using a Mettler-Toledo AG, Analytical (Schwerzenbach, Switzerland) at the Faculty of Mechanical and Manufacturing Engineering Universiti Teknikal Malaysia Melaka, UTeM. The specimen weight amounted to around 10 ± 2 mg. The study was performed in aluminum panels at 25 to 800°C at a fixed heating rate of 10°C min^{-1} in a complex nitrogen atmosphere.

Mechanical Testing

Tensile Testing. The tensile test samples were cut following the ASTM D638 standard. The tests were conducted on three replications using universal testing equipment (INSTRON556) with a 5kN and a crosshead speed of 5 mm/min. The air temperature of 23 ±1°C and relative humidity of 50 ± 5% were used in this study.

Flexural Testing. The flexural test for this study was performed at 23 ± 1°C and a relative humidity of 50 ± 5% according to ASTM D790. The dimension of 130 mm (L) × 13 mm (W) × 3 mm (T) was set for all samples. Crosshead speeds were fixed at 2 mm/min, and the tests were performed on three replications in Universal Test Machines (INSTRON 5556) with a 5kN load cell.

Fourier Transform Infrared Spectroscopy (FTIR)

FTIR was used to detect functional groups in coconut fiber and starch composite. Material spectra were obtained with an IR (Jasco FT/IR 6100) spectrometer. Dimensions of the samples were set to 10 mm (L) × 10 mm (W) × 3 mm (T). The sample FTIR spectrum was collected in a range of 4000 to 400 cm^{-1}.

Scanning Electron Microscope (SEM)

A scanning electron microscope (SEM), Zeiss Evo 18 model, and a 10 kV acceleration voltage were used to analyze the morphology of tensile fractured surfaces. The samples were coated with gold using an argon plasma metallizer (sputter coater K575X) (Edwards Limited, Crawley, United Kingdom) to avoid unwanted charging.

RESULTS AND DISCUSSION

Thermal Analysis

Figure 3 presents the Thermogravimetric Analysis (TGA) curve of thermoplastic cassava starch/beeswax reinforced with coconut fiber from 0 to 50 wt.% fiber, while Figure 4 shows the DTG curve of these materials. The starch began to degrade at approximately 250°C. According to Lomelí-Ramírez et al. (2011), although relatively similar and overlaid, the

TGA curves and composites of the TPS matrix exhibit some differences with the inset (fiber and starch) curves. Besides, there was a small and incremental mass loss of 25–200 °C in the cassava starch matrix and its components related to water losses and possibly glycerol (glycerol boiling point of 198°C). Before the TGA analysis, the composites, as well as the matrix, were dried up at 60°C, indicating a reduction in mass losses of matrix and composites due to most humidity already eliminated. Further dehydration of 25–200°C in this range was minimal. The DTG curve also confirmed no observed inflection point (peak) within this temperature range.

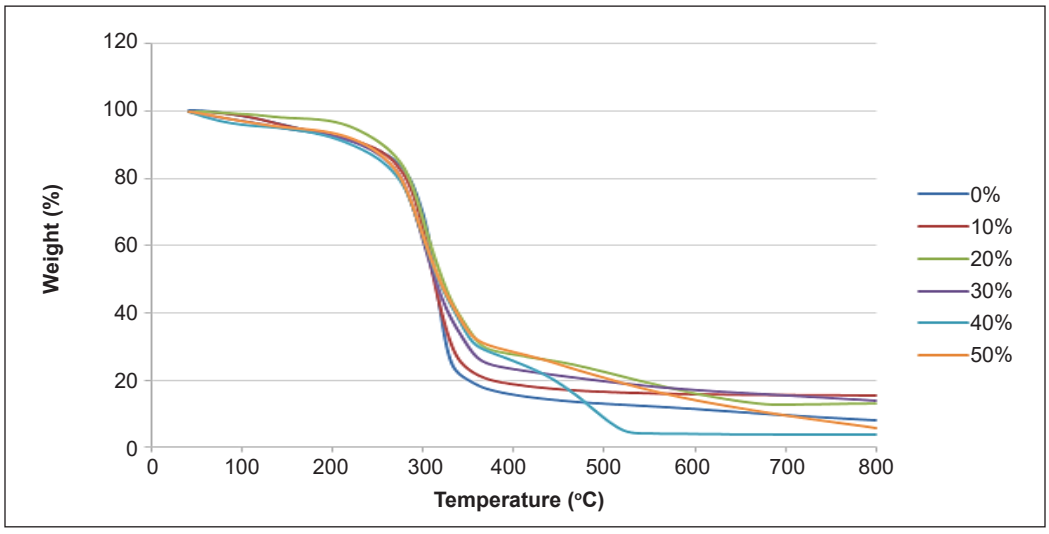

Figure 3. TGA curve of TPS/Beeswax + coconut fiber composite

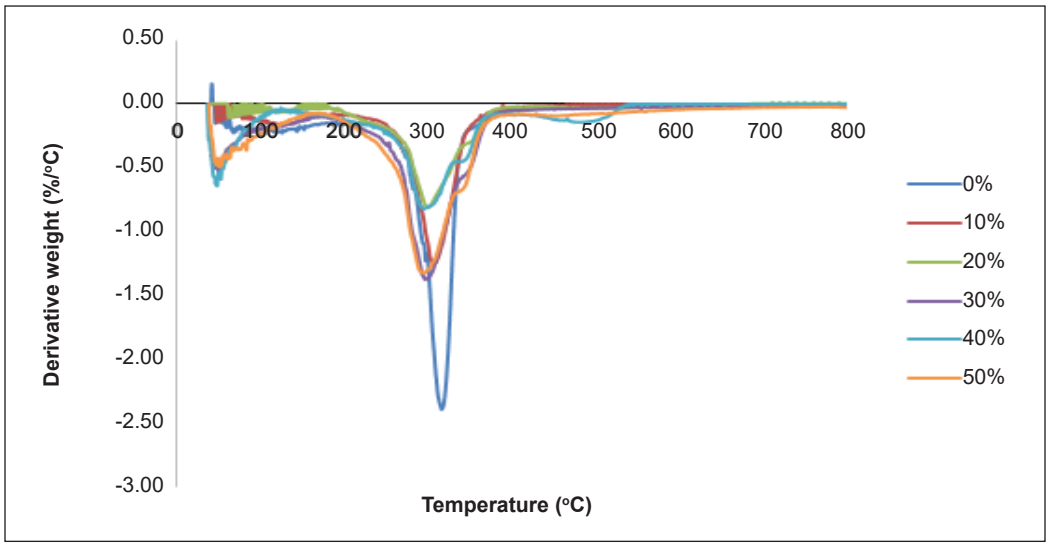

Figure 4. DTG curve of TPS/Beeswax reinforced with coconut fiber composite

This study parallels Gómez et al. (2006), who noted no mass loss associated with humidity and ascribed to the processing conditions. The dehydration mass losses observed for coir fibers and native starch in the 20 to 200℃ range were still greater. The fiber additions to the starch matrix have been reported to increase their thermal stability if the fiber and the matrix are well adhered to and thus reduce the mass loss in the sample (Ilyas et al., 2018; Ma et al., 2009). Figure 3 demonstrates that cassava starch degradation commenced after 300℃, while coconut fiber thermal degradation starts with hemicellulose degradation (200–260℃), lignin (280–500℃), and cellulose (240–350℃) (Ilyas, Sapuan, & Ishak, 2017; Ilyas, Sapuan, Ishak, & Zainudin, 2017; Lomelí-Ramírez et al., 2014).

Alemdar and Sain (2008) conducted a prior investigation wherein they examined the thermal stability of biocomposites derived from wheat straw nanofibres through TGA analysis—the TGA thermo grams with 5 wt.% nanofibers demonstrated starch degradation began at around 275℃ with thermoplastic starch (TPS) and nanocomposite. The temperature of degradation was about 296℃ for the nanofibers. Evaporation of glycerol contributed to the lesser weight losses of TPS and nanocomposites. Additionally, the results indicated that the temperature at which the polymer matrix and nanocomposites degrade was comparable to and less than that of each component.

In terms of fiber loading, adding coconut fiber improved the material's thermal stability. It can be seen through the higher residue content upon degradation for samples with coconut fiber as compared to the TPS matrix. The residue content was increased from 5.9% to 14.1% as the coconut fiber content increased from 0 to 30 wt.%. This finding can be attributed to higher carbonate content in the fiber than the TPS matrix (Kamaruddin et al., 2022).

Mechanical Testing

Tensile Properties. Table 3 presents the findings of analysis of variance (ANOVA) of the tensile testing. Since the P-value was less than 0.05, the average tensile strength and modulus varying from one level of polymer mixture to another is statistically important. Figure 5 displays the tensile and tensile modulus of starch composite and coconut fiber with 0 to 50 wt.% of coconut fiber obtained in the present study. From the data, we can observe a clear trend of increasing tensile strength as the loading percentage of coconut fiber increases. At 0% coconut fiber loading, the composite material exhibits a tensile strength of 5.42 MPa. As the percentage of coconut fiber loading increases to 10%, a notable improvement in tensile strength can be observed, which rises to 8.12 MPa. The trend continues with further increases

Table 3
Summary of the analysis of variance (ANOVA) of TPS/ Beeswax reinforced with coconut fiber

Variable	df	Strength	Modulus
Mixture	5	.000	.000

Note. *Significantly different at $p \leq 0.05$

in tensile strength as the coconut fiber loading increases to 20%, 30%, and 40%, resulting in a value of 9.26 MPa, 13.57 MPa, and 14.95 MPa, respectively.

Finally, at 50% coconut fiber loading, the composite material exhibits its highest tensile strength of 20.47 MPa. The phenomenon behind this trend lies in the reinforcing nature of the coconut fibers. Coconut fibers are known for their high strength and stiffness, which can enhance the mechanical properties of composite materials when incorporated as a reinforcement. The interfacial bonding between the coconut fibers and the TPS/Beeswax matrix also contributes to the improved tensile properties. Good bonding at the fiber-matrix interface allows efficient load transfer and minimizes stress concentration, enhancing tensile strength. These values demonstrated that the tensile strength and modulus were greater. Incorporating coconut fiber into the starch composite increased the tensile properties of the composite material.

According to Lomeli et al. (2014), these increments in Young's Modulus and Ultimate Tensile Strength may be associated with the strong fiber-matrix bonding, which resulted in increased adhesion between the fibers, thereby leading to a higher matrix-fiber stress transmission. Besides, an optimum fraction of the fiber volume is necessary to achieve better mechanical performance. In this study, the highest fiber content of 50 wt.% resulted in the highest strength. The increment in coconut fiber loading would increase the composite's tensile modulus. Figure 6 shows the tensile modulus increasing rapidly from 10 to 20 wt.% with increased fiber content and the tensile modulus values.

Since natural fiber is very hydrophilic, it helps to absorb moisture for a longer period using natural fiber composites (Dhakal et al., 2007). The increase in percentage length for both composites was lessened by increasing fiber content (treated and untreated) (Lai et al., 2005). The effect of matrix/composite treatment on the findings can be demonstrated

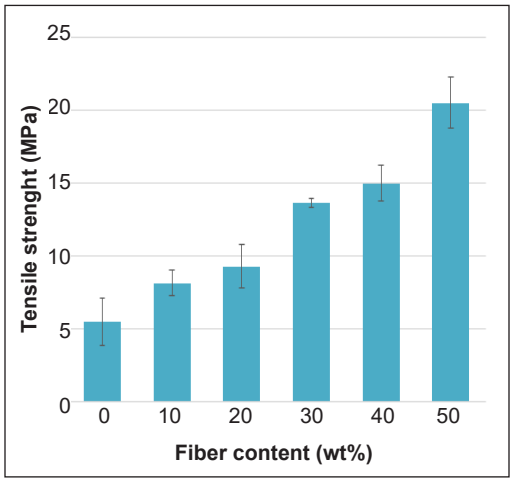

Figure 5. Tensile strength of TPS/Beeswax + coconut fiber

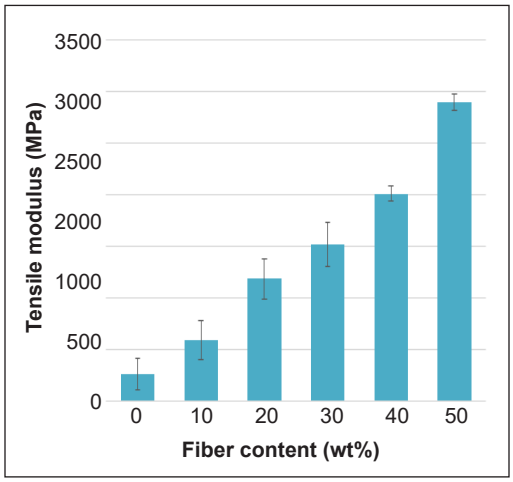

Figure 6. Tensile modulus of TPS/Beeswax + coconut fiber

based on a discrete molecular organization, which created a more ordered structure with less free energy (Lomelí-Ramírez et al., 2011).

According to Lai et al. (2005), with the incorporation of natural lignocellulose fibers into the polymer matrix, the strength of the composite may increase or decrease. Typically, lignocellulose fibers like coconut fiber can withstand the stress of polymer transfer as they are able to improve strength. However, the strength of the composites is impacted by some fibers that are inconsistent or irregularly created. The strength decreased as a result of the fiber's inability to withstand stress transferred from the polymer matrix.

Flexural Properties. Table 4 presents the summarized findings of the analysis of variance (ANOVA) of flexural testing. The finding shows that the statistically significant difference ($p<0.05$) between the mean flexural strength and modulus from one composite-to-one stage is statistically important. In general, with tensile testing, the effects of flexural testing meet a similar pattern. The flexural properties of a composite incorporated with coconut fiber were demonstrated by significant improvements ($p<0.05$). The obtained flexural strength data showed a consistent and significant improvement with increasing coconut fiber loading. At 0% coconut fiber loading, the composite exhibited a flexural strength of 2.49 MPa.

However, as the percentage of coconut fiber loading increased to 10%, the flexural strength improved significantly to 9.66 MPa. This initial increase in flexural strength can be attributed to the inherent mechanical properties of the coconut fibers, such as their high strength and stiffness (Khalil et al., 2010; Martinelli et al., 2023; Surnam & Imrith, 2023). As the loading percentage increased to 20%, a further enhancement in flexural strength to 11.65 MPa was observed. This improvement can be explained by the increased distribution and alignment of the coconut fibers within the matrix, resulting in improved load transfer and resistance to bending forces.

Furthermore, the interfacial bonding between the coconut fibers and the TPS/Beeswax matrix played a crucial role in enhancing the flexural strength. At 30% coconut fiber loading, a substantial jump in flexural strength to 18.16 MPa was observed. This increase can be attributed to the effective stress distribution and load-bearing capacity of the coconut fibers, along with the improved interfacial bonding. The progressive increase in flexural strength continued with 40% and 50% coconut fiber loading, resulting in values of 28.15 MPa and 30.25 MPa, respectively. The trend indicates that the higher the loading percentage of coconut fiber, the stronger the composite becomes in terms of flexural properties.

Figure 7 demonstrates that the introduction of fiber loading had an equivalent influence on the enhancement of flexural strength as it did on the improvement

Table 4
Summary of the analysis of variance (ANOVA) of TPS/ Beeswax reinforced with coconut fiber

Variable	df	Strength	Modulus
Mixture	5	.001	.000

Note. *Significantly different at $p\leq0.05$

of tensile strength, thereby augmenting the overall flexural strength property. Figure 8 shows the flexural modulus of TPS/Beeswax + coconut fiber. It was observed that the flexural strength and modulus were increasing gradually from 10 to 50 wt.%. The finding might be due to the polymer chain having a strong interaction with the fiber, which overcame the weak adhesive of the fiber matrix with increased fiber content. According to Lai et al. (2005), the higher aspect ratio might be why higher bending strength resulted from greater fibers. Other factors that influenced the mechanical strength of the composites include the fiber aspect ratio.

The previous study of mechanical properties of the TPS, TPS/jute fiber, and TPS/kapok fiber composites noted that adding jute or kapok fibers increased the flexural strength and Young's TPS modulus. The flexural strength and Young's TPS modulus were found to be significantly increasing by adding jute or kapok fibers. Besides, the increased content of the two cellulosic fibers significantly improved the flexural strength at full load and the TPS Young's modulus (Prachayawarakorn et al., 2013).

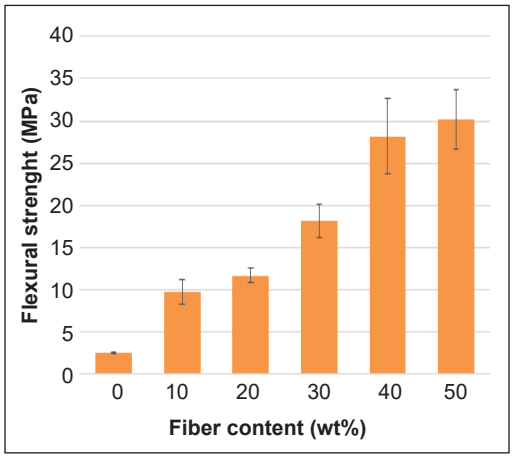

Figure 7. Flexural strength of TPS/Beeswax + coconut fiber

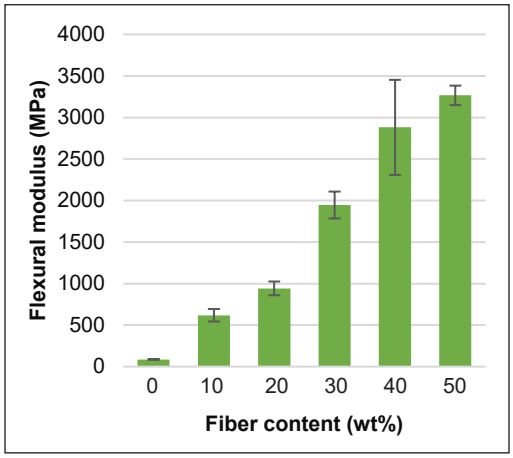

Figure 8. Flexural modulus of TPS/Beeswax + coconut fiber

Fourier Transform Infrared Spectroscopy (FTIR)

Figure 9 shows that the IR spectrums were identical for both the TPS and the composites, provided the main starch composite and coconut fiber were based on the structure of cellulose. In general, both the TPS and the composite spectrums showed the same band pattern. The chemical composition of starch remained unaltered during the plasticization process, regardless of the presence of glycerol or the quantity of fiber added. The observed relationship between these factors can be attributed solely to molecular interactions.

The peak in the 3400–3200 cm^{-1} range was attributed to the hydroxyl hydrogen-bonded group as a result of the free, inter, and intra-molecular bounded hydroxyl groups—axial

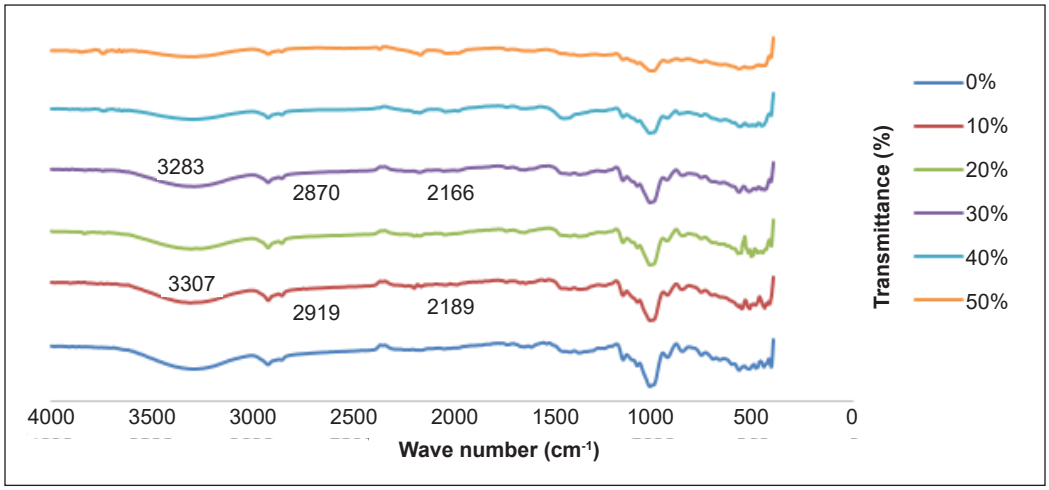

Figure 9. FT-IR spectra of the TPS/Beeswax reinforced with coconut fiber composites

deformations of the O–H group attributed to the large band. From 10 to 30% of coconut fiber, the wavenumber started to drop slowly from 3307 to 3283 cm^{-1}, respectively. The finding from Prachayawarakom et al. (2013) is strong evidence that new hydrogen relations were formed between the cellulosic fibers and the TPS matrix. The change in the IR peak position of O–H detention was also recorded and believed to occur between two compatibility polymers because of the hydrogen bonding. It was also reported that the plasticizing process may have been attributed to this improvement (Ma et al., 2005). It means that glycerol is affected by intra- and intermolecular hydrogen bonding networks between starch molecules.

The band of approximately 2936–2916 cm^{-1} is related to C–H aliphatic group vibrations of hydrocarbon starch, glycerol-starch (matrix), and TPS composites observed in all the spectra. Inversely, the effect of raising fiber content in composites is represented by this band (less defined band) (Lomelí-Ramírez et al., 2014). Tongdeesoontorn et al. (2011) reported that the TPS matrix sample and its biocomposites decreased this band. Besides, the band's intensity gradually changed (decreased) when the amount of fibers was added in certain thermoplastic samples. This finding indicates that starch is primarily responsible for this water belt, and thus, because of its low moisture content, coconut fibers have no detectable contribution.

The other band is N–H stretching vibration at 2800–2000 cm^{-1}. According to F. C. Wang et al. (1994), for the results that attributed to N–H bonding and strength or variation on the integrated absorption coefficient with the change from the linked N–H band limit, there was a significant decrease in the integrated absorbing of the N–H band with increasing temperatures. These results were comparable to the N–H region. The decline in integrated absorption with increased temperature indicated the association of certain aromatic rings.

Scanning Electron Microscope (SEM)

Figure 10 shows the SEM micrograph of a fracture surface of TPS/beeswax reinforced with coconut fiber composites. The microstructures of the specimens were different due to the amount of fiber in the samples. Based on the results obtained, for coconut fiber content increasing from 10 to 50 wt.%, a cleavage structure was found on the surface of the fracture, which may be due to the polymer-polymer-bonding, which resisted loading deformations before being fractured (Jumaidin, 2016).

Additionally, Figure 10(b) shows that the cracks propagating through the brittle TPS matrix were avoided by the coconut fibers sticking out of the matrix. It facilitated premature failure and decreased the strength and rigidity of the composite of up to 20% of coconut fibers. The amount of coconut fibers was a strong barrier to crack propagation, and both tensile performances of the composites were improved for 50 wt.% composites.

According to Santafé Júnior et al. (2010), the amount of coconut fibers in composites of 40 wt.% is, by itself, was sufficient to withstand tensile loads and, thus, in contrast to the pure polyester matrix, increased both composite resistance and rigidity. Also, a similar finding was reported by Ma et al. (Ma et al., 2005) for thermoplastic processing of TPS by showing that the fiber in the granular starch fusion was affected by the increased fiber content. The fiber content was decreased during processing by high viscosity or inadequate dispersion.

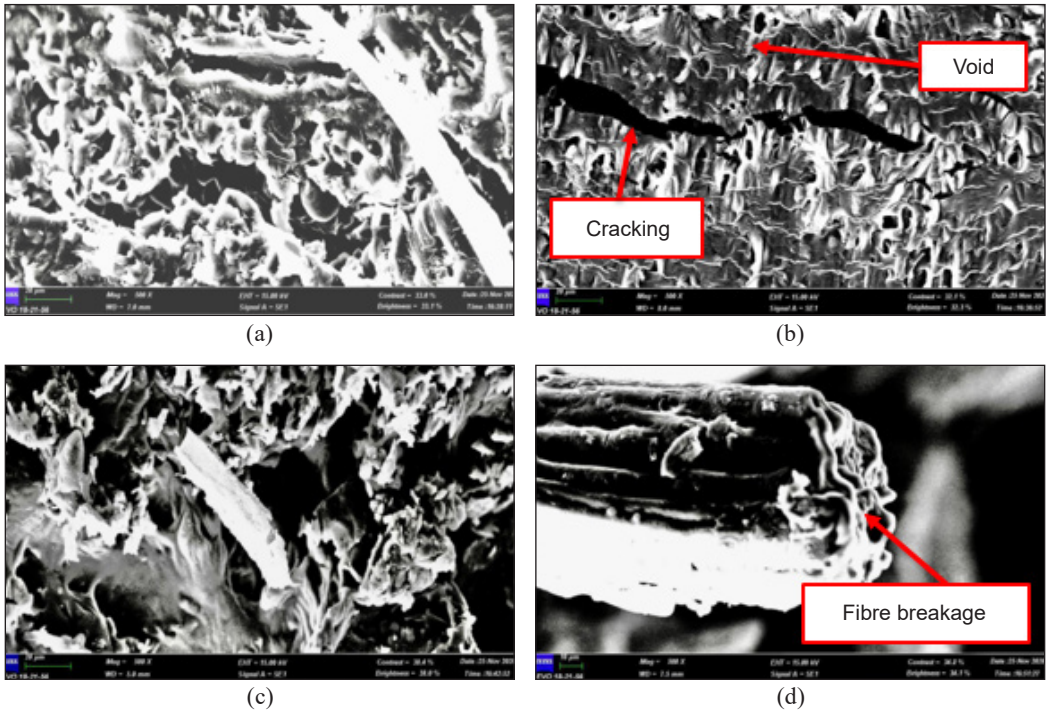

(a) (b)

(c) (d)

Figure 10. SEM micrograph of a fracture surface of TPCS/Beeswax + coconut fiber composites: (a) 10% fiber; (b) 20% fiber; (c) 30% fiber; and (d) 50% fiber

CONCLUSION

Thermoplastic cassava starch/beeswax reinforced with coconut fiber has been developed using the hot press method. The thermal and mechanical properties of the composites were evaluated using TGA, tensile, and flexural tests, as well as FT-IR and SEM. TGA results demonstrated a major improvement in the composite's thermal stability by incorporating coconut fiber. The residue content was increased from 5.9% to 14.1% as the coconut fiber content increased from 0 to 30 wt.%. A significant increment in tensile strength and modulus of up to 20.7 MPa and 2890 MPa were recorded for samples with 50 wt.% fiber content. The sample with 50 wt.% fiber also demonstrated the highest flexural strength and modulus of up to 30.3 MPa and 3266.3 MPa, respectively. These changes were consistent with the findings of FTIR and SEM, proving the compatibility of TPS and coconut fiber with a homogeneous structure. Overall, coconut fiber has shown promising characteristics as a natural reinforcement material, which could benefit the composites manufacturing sector.

ACKNOWLEDGMENTS

The authors thank Universiti Teknikal Malaysia Melaka for providing financial assistance for the research works through research grant PJP/2021/FTKMP/S01815. The publication incentive grant JURNAL/2018/FTKMP/Q00062 supported the proofreading fee.

REFERENCES

Alemdar, A., & Sain, M. (2008). Biocomposites from wheat straw nanofibers: Morphology, thermal and mechanical properties. *Composites Science and Technology*, *68*(2), 557–565. https://doi.org/10.1016/j.compscitech.2007.05.044

Asyraf, M. R. M., Syamsir, A., Supian, A. B. M., Usman, F., Ilyas, R. A., Nurazzi, N. M., Norrrahim, M. N. F., Razman, M. R., Zakaria, S. Z. S., Sharma, S., Itam, Z., & Rashid, M. Z. A. (2022). Sugar palm fibre-reinforced polymer composites: Influence of chemical treatments on its mechanical properties. *Materials*, *15*(11). https://doi.org/10.3390/ma15113852

Azra, N. A., Atiqah, A., Jalar, A., Manar, G., Supian, A. B. M., & Ilyas, R. A. (2023). Sustainable substrate tin oxide/nanofibril cellulose/thermoplastic starch: Dimensional stability and tensile properties. *Journal of Materials Research and Technology*, *26*, 99–108. https://doi.org/10.1016/j.jmrt.2023.07.088

Bahloul, A., Semlali, F. Z., Oumam, M., Hannache, H., Kassab, Z., & El Achaby, M. (2023). Starch bio-nanocomposites based on phosphorylated and sulphated cellulose nanocrystals extracted from pepper plant residue: Effect of surface functionality on property improvements. *Cellulose*, *30*(8), 5051–5070. https://doi.org/10.1007/s10570-023-05199-4

Borowski, G., Klepka, T., Pawłowska, M., Lavagnolo, M. C., Oniszczuk, T., Wójtowicz, A., & Combrzyński, M. (2020). Effect of flax fibers addition on the mechanical properties and biodegradability of biocomposites based on thermoplastic starch. *Archives of Environmental Protection*, *46*(2), 74–82. https://doi.org/10.24425/aep.2020.133477

Dhakal, H. N., Zhang, Z. Y., & Richardson, M. O. W. (2007). Effect of water absorption on the mechanical properties of hemp fibre reinforced unsaturated polyester composites. *Composites Science and Technology*, *67*(7–8), 1674–1683. https://doi.org/10.1016/j.compscitech.2006.06.019

Diyana, Z. N., Jumaidin, R., Selamat, M. Z., & Suan, M. S. M. (2021). Thermoplastic starch / beeswax blend : Characterization on thermal mechanical and moisture absorption properties. *International Journal of Biological Macromolecules*, *190*, 224–232. https://doi.org/10.1016/j.ijbiomac.2021.08.201

Fabunmi, O. O., Tabil, L. G., Panigrahi, S., & Chang, P. R. (2011). Effects of incorporating polycaprolactone and flax fiber into glycerol-plasticized pea starch. *Journal of Polymers and the Environment*, *19*(4), 841–848. https://doi.org/10.1007/s10924-011-0374-5

Gironès, J., López, J. P., Mutjé, P., Carvalho, A. J. F., Curvelo, A. A. S., & Vilaseca, F. (2012). Natural fiber-reinforced thermoplastic starch composites obtained by melt processing. *Composites Science and Technology*, *72*(7), 858–863. https://doi.org/10.1016/j.compscitech.2012.02.019

Gomes, Á. V. R., Gonçalves, F. C. P., da Silva, M. Q. J., da, Leite, R. H. L., dos Santos, F. K. G., & Aroucha, E. M. M. (2019). Effect of carnauba wax and coconut fiber contents on tensile properties of corn starch-based biocomposites. *Materials Research*, *22*(suppl 1). https://doi.org/10.1590/1980-5373-mr-2019-0053

Gómez, C., Torres, F. G., Nakamatsu, J., & Arroyo, O. H. (2006). Thermal and structural analysis of natural fiber reinforced starch-based biocomposites. *International Journal of Polymeric Materials and Polymeric Biomaterials*, *55*(11), 893–907. https://doi.org/10.1080/00914030500522547

Hazrol, M. D., Sapuan, S. M., Zainudin, E. S., Wahab, N. I. A., & Ilyas, R. A. (2022). Effect of kenaf fibre as reinforcing fillers in corn starch-based biocomposite film. *Polymers*, *14*(8), 1590. https://doi.org/10.3390/polym14081590

Ilyas, R. A., Sapuan, S. M., Atiqah, A., Ibrahim, R., Abral, H., Ishak, M. R., Zainudin, E. S., Nurazzi, N. M., Atikah, M. S. N., Ansari, M. N. M., Asyraf, M. R. M., Supian, A. B. M., & Ya, H. (2020). Sugar palm (Arenga pinnata [Wurmb.] Merr) starch films containing sugar palm nanofibrillated cellulose as reinforcement: Water barrier properties. *Polymer Composites*, *41*(2), 459-467. https://doi.org/10.1002/pc.25379

Ilyas, R. A., Sapuan, S. M., Ibrahim, R., Abral, H., Ishak, M. R., Zainudin, E. S., Asrofi, M., Atikah, M. S. N., Huzaifah, M. R. M., Radzi, A. M., Azammi, A. M. N., Shaharuzaman, M. A., Nurazzi, N. M., Syafri, E., Sari, N. H., Norrrahim, M. N. F., & Jumaidin, R. (2019). Sugar palm (Arenga pinnata (Wurmb.) Merr) cellulosic fibre hierarchy: A comprehensive approach from macro to nano scale. *Journal of Materials Research and Technology*, *8*(3), 2753-2766. https://doi.org/10.1016/j.jmrt.2019.04.011

Ilyas, R. A., Sapuan, S. M., & Ishak, M. R. (2017). Isolation and characterization of nanocrystalline cellulose from sugar palm fibres (Arenga Pinnata). *Carbohydrate Polymers*, *181*, 1038-1051. https://doi.org/10.1016/j.carbpol.2017.11.045

Ilyas, R. A., Sapuan, S. M., Ishak, M. R., & Zainudin, E. S. (2017). Effect of delignification on the physical, thermal, chemical, and structural properties of sugar palm fibre. *BioResources*, *12*(4), 8734–8754. https://doi.org/10.15376/biores.12.4.8734-8754

Ilyas, R. A., Sapuan, S. M., Ishak, M. R., & Zainudin, E. S. (2018). Development and characterization of sugar palm nanocrystalline cellulose reinforced sugar palm starch bionanocomposites. *Carbohydrate Polymers*, *202*, 186–202. https://doi.org/10.1016/j.carbpol.2018.09.002

Jumaidin, R., Whang, L. Y., Ilyas, R. A., Hazrati, K. Z., Hafila, K. Z., Jamal, T., & Alia, R. A. (2023). Effect of durian peel fiber on thermal, mechanical, and biodegradation characteristics of thermoplastic cassava starch composites. *International Journal of Biological Macromolecules*, *250*, 126295. https://doi.org/10.1016/j.ijbiomac.2023.126295

Jumaidin, R., Sapuan, S. M., Jawaid, M., Ishak, M. R., & Sahari, J. (2016). Characteristics of thermoplastic sugar palm Starch/Agar blend: Thermal, tensile, and physical properties. *International Journal of Biological Macromolecules, 89*, 575-581. https://doi.org/10.1016/j.ijbiomac.2016.05.028

Jumaidin, R., Khiruddin, M. A. A., Saidi, Z. A. S., Salit, M. S., & Ilyas, R. A. (2020). Effect of cogon grass fibre on the thermal, mechanical and biodegradation properties of thermoplastic cassava starch biocomposite. *International Journal of Biological Macromolecules*, *146*, 746–755. https://doi.org/10.1016/j.ijbiomac.2019.11.011

Kamaruddin, Z. H., Jumaidin, R., Ilyas, R. A., Selamat, M. Z., Alamjuri, R. H., & Yusof, F. A. M. (2022). Biocomposite of cassava starch-cymbopogan citratus fibre : Mechanical , thermal , and biodegradation properties. *Polymers*, *14*(3), 514. https://doi.org/10.3390/polym14030514

Khalil, H. P. S. A., Firoozian, P., Bakare, I. O., Akil, H. M., & Noor, A. M. (2010). Exploring biomass based carbon black as filler in epoxy composites: Flexural and thermal properties. *Materials and Design*, *31*(7), 3419–3425. https://doi.org/10.1016/j.matdes.2010.01.044

Khalili, H., Bahloul, A., Ablouh, E. H., Sehaqui, H., Kassab, Z., Hassani, F. Z. S. A., & El Achaby, M. (2023). Starch biocomposites based on cellulose microfibers and nanocrystals extracted from alfa fibers (Stipa tenacissima). *International Journal of Biological Macromolecules*, *226*, 345–356. https://doi.org/10.1016/j.ijbiomac.2022.11.313

Kwaśniewska, A., Chocyk, D., Gładyszewski, G., Borc, J., Świetlicki, M., & Gładyszewska, B. (2020). The influence of kaolin clay on the mechanical properties and structure of thermoplastic starch films. *Polymers*, *12*(1), 73. https://doi.org/10.3390/polym12010073

Lai, C. Y., Sapuan, S. M., Ahmad, M., Yahya, N., & Dahlan, K. Z. H. M. (2005). Mechanical and electrical properties of coconut coir fiber-reinforced polypropylene composites. *Polymer-Plastic Technology and Engineering*, *44*(4), 619–632. https://doi.org/10.1081/PTE-200057787

Lomelí-Ramírez, M. G., Kestur, S. G., Manríquez-González, R., Iwakiri, S., De Muniz, G. B., & Flores-Sahagun, T. S. (2014). Bio-composites of cassava starch-green coconut fiber: Part II - Structure and properties. *Carbohydrate Polymers*, *102*(1), 576–583. https://doi.org/10.1016/j.carbpol.2013.11.020

Lomelí-Ramírez, M. G., Satyanarayana, K. G., Iwakiri, S., De Muniz, G. B., Tanobe, V., & Flores-Sahagun, T. S. (2011). Study of the properties of biocomposites. Part I. Cassava starch-green coir fibers from Brazil. *Carbohydrate Polymers*, *86*(4), 1712–1722. https://doi.org/10.1016/j.carbpol.2011.07.002

Ma, X., Chang, P. R., Yu, J., & Stumborg, M. (2009). Properties of biodegradable citric acid-modified granular starch/thermoplastic pea starch composites. *Carbohydrate Polymers*, *75*(1), 1–8. https://doi.org/10.1016/j.carbpol.2008.05.020

Ma, X., Yu, J., & Kennedy, J. F. (2005). Studies on the properties of natural fibers-reinforced thermoplastic starch composites. *Carbohydrate Polymers*, *62*(1), 19–24. https://doi.org/10.1016/j.carbpol.2005.07.015

Martinelli, F. R. B., Ribeiro, F. R. C., Marvila, M. T., Monteiro, S. N., Filho, F. D. C. G., & Azevedo, A. R. G. D. (2023). A review of the use of coconut fiber in cement composites. *Polymers*, *15*(5), 1309. https://doi.org/10.3390/polym15051309

Meráz-Rivera, J., Cruz-Rivero, L., Méndez-Hernández, M. L., Rivera-Armenta, J. L., Angeles-Herrera, D., & Ramírez-López, C. (2020). Development of a composite from TPS–EVOH–SBR reinforced with coconut fiber. *Sustainability*, *12*(19), 7838. https://doi.org/10.3390/su12197838

Nansu, W., Ross, S., Ross, G., & Mahasaranon, S. (2019). Effect of crosslinking agent on the physical and mechanical properties of a composite foam based on cassava starch and coconut residue fiber. *Materials Today: Proceedings*, *17*(4), 2010-2019. https://doi.org/10.1016/j.matpr.2019.06.249

Nazrin, A., Sapuan, S. M., & Zuhri, M. Y. M. (2020). Mechanical, physical and thermal properties of sugar palm nanocellulose reinforced thermoplastic Starch (TPS)/poly (lactic acid)(PLA) blend bionanocomposites. *Polymers*, *12*(10), 2216. https://doi.org/10.3390/polym12102216

Nazrin, A., Sapuan, S. M., Zuhri, M. Y. M., Tawakkal, I. S. M. A., & Ilyas, R. A. (2021). Water barrier and mechanical properties of sugar palm crystalline nanocellulose reinforced thermoplastic sugar palm starch (TPS)/poly(lactic acid) (PLA) blend bionanocomposites. *Nanotechnology Reviews*, *10*(1), 431–442. https://doi.org/10.1515/ntrev-2021-0033

Norfarhana, A. S., Ilyas, R. A., & Ngadi, N. (2022). A review of nanocellulose adsorptive membrane as multifunctional wastewater treatment. *Carbohydrate Polymers*, *291*, 119563. https://doi.org/10.1016/j.carbpol.2022.119563

Norrrahim, M. N. F., Norizan, M. N., Jenol, M. A., Farid, M. A. A., Janudin, N., Ujang, F. A., Yasim-Anuar, T. A. T., Najmuddin, S. U. F. S., & Ilyas, R. A. (2021). Emerging development on nanocellulose as antimicrobial material: An overview. *Materials Advances, 2*(11), 3538-3551. https://doi.org/10.1039/d1ma00116g

Prachayawarakorn, J., Chaiwatyothin, S., Mueangta, S., & Hanchana, A. (2013). Effect of jute and kapok fibers on properties of thermoplastic cassava starch composites. *Materials and Design*, *47*, 309–315. https://doi.org/10.1016/j.matdes.2012.12.012

Prachayawarakorn, J., Ruttanabus, P., & Boonsom, P. (2011). Effect of cotton fiber contents and lengths on properties of thermoplastic starch composites prepared from rice and waxy rice starches. *Journal of Polymers and the Environment*, *19*, 274–282. https://doi.org/10.1007/s10924-010-0273-1

Saepoo, T., Sarak, S., Mayakun, J., Eksomtramage, T., & Kaewtatip, K. (2023). Thermoplastic starch composite with oil palm mesocarp fiber waste and its application as biodegradable seeding pot. *Carbohydrate Polymers*, *299*, 120221. https://doi.org/10.1016/j.carbpol.2022.120221

Sanyang, M. L., Sapuan, S. M., Jawaid, M., Ishak, M. R., & Sahari, J. (2016). Palm fiber reinforced starch. *BioResources*, *11*(2), 4134–4145. https://doi.org/10.15376/biores.11.2.4134-4145

Santafé Júnior, H. P., Lopes, F. P. D., Costa, L. L., & Monteiro, S. N. (2010). Mechanical properties of tensile tested coir fiber reinforced polyester composites. *Revista Materia, 15*(2), 113-118.

Surnam, B. Y. R., & Imrith, G. (2023). Investigation on the mechanical properties of coconut leaf stalk fibres reinforced composites. *Journal of Natural Fibers*, *20*(2), 2198276. https://doi.org/10.1080/15440478.2023.2198276

Tarique, J., Zainudin, E. S., Sapuan, S. M., Ilyas, R. A., & Khalina, A. (2022). Physical, mechanical, and morphological performances of arrowroot (Maranta arundinacea) fiber reinforced arrowroot starch biopolymer composites. *Polymers*, *14*(3), 388. https://doi.org/10.3390/polym14030388

Thakur, R., Pristijono, P., Scarlett, C. J., Bowyer, M., Singh, S. P., & Vuong, Q. V. (2019). Starch-based films: Major factors affecting their properties. *International Journal of Biological Macromolecules, 132,* 1079-1089. https://doi.org/10.1016/j.ijbiomac.2019.03.190

Tongdeesoontorn, W., Mauer, L. J., Wongruong, S., Sriburi, P., & Rachtanapun, P. (2011). Effect of carboxymethyl cellulose concentration on physical properties of biodegradable cassava starch-based films. *Chemistry Central Journal*, *5*(1), 1–8. https://doi.org/10.1186/1752-153X-5-6

Wang, F. C., Feve, M., Lam, T. M., & Pascault, J. P. (1994). FTIR analysis of hydrogen bonding in amorphous linear aromatic polyurethanes. II. Influence of styrene solvent. *Journal of Polymer Science Part B: Polymer Physics*, *32*(8), 1315–1320. https://doi.org/10.1002/polb.1994.090320802

Wang, S., Zhang, P., Li, Y., Li, J., Li, X., Yang, J., Ji, M., Li, F., & Zhang, C. (2023). Recent advances and future challenges of the starch-based bio-composites for engineering applications. *Carbohydrate Polymers*, *307*, 120627. https://doi.org/10.1016/j.carbpol.2023.120627

Yokesahachart, C., Yoksan, R., Khanoonkon, N., Mohanty, A. K., & Misra, M. (2021). Effect of jute fibers on morphological characteristics and properties of thermoplastic starch/biodegradable polyester blend. *Cellulose*, *28*(9), 5513–5530. https://doi.org/10.1007/s10570-021-03921-8

Zainuddin, S. Y. Z., Ahmad, I., Kargarzadeh, H., Abdullah, I., & Dufresne, A. (2013). Potential of using multiscale kenaf fibers as reinforcing filler in cassava starch-kenaf biocomposites. *Carbohydrate Polymers*, *92*(2), 2299–2305. https://doi.org/10.1016/j.carbpol.2012.11.106

Zhou, W., Zha, D., Zhang, X., Xu, J., Guo, B., & Huang, Y. (2020). Ordered long polyvinyl alcohol fiber-reinforced thermoplastic starch composite having comparable mechanical properties with polyethylene and polypropylene. *Carbohydrate Polymers*, *250*, 116913. https://doi.org/10.1016/j.carbpol.2020.116913

REFEREES FOR THE PERTANIKA
JOURNAL OF SCIENCE AND TECHNOLOGY

VOL. 31 (S1) 2023

The Editorial Board of the Pertanika Journal of Science and Technology wishes to thank the following:

Atiqah Mohd Afdzaluddin
(UKM, Malaysia)

Azmah Hanim Mohamed Ariff
(UPM, Malaysia)

Chow Wen Shyang
(USM, Malaysia)

Edi Syafri
(PPNP, Indonesia)

Khubab Shaker
(NTU, Pakistan)

Mastura Mohamad Taha
(UTeM, Malaysia)

Md Mainul Islam
(UniSQ, Australia)

Mohd Nor Faiz Nurrrahim
(UPNM, Malaysia)

Mohd Zuhri Mohamad Yusuf
(UPM, Malaysia)

Muhammad Asyraf Muhammad Rizal
(UTM, Malaysia)

Muhammad Harussani Moklis
(Tokyo Tec, Japan)

Muhd Ridzuan Mansor
(UTEM, Malaysia)

Nabilah Afiqah Mohd Radzuan
(UKM, Malaysia)

Sani Amril Samsudin
(UTM, Malaysia)

Teuku Rihayat
(PNL, Indonesia)

Yasir Nawab
(NTU, Pakistan)

NTU - National Textile University
PNL - Politeknik Negeri Lhokseumawe
PPNP - Politeknik Pertanian Negeri Payakumbuh
UKM - Universiti Kebangsaan Malaysia
UPM - Universiti Putra Malaysia
UPNM - Universiti Pertahanan Nasional Malaysia
USM - Universiti Sains Malaysia
UTeM - Universiti Teknikal Malaysia Melaka
UTM - Universiti Teknologi Malaysia
Tokyo Tech - Tokyo Institute of Technology Tokyo
UniSQ - University of Southern Queensland

While every effort has been made to include a complete list of referees for the period stated above, however if any name(s) have been omitted unintentionally or spelt incorrectly, please notify the Chief Executive Editor, *Pertanika* Journals at executive_editor.pertanika@upm.edu.my

Any inclusion or exclusion of name(s) on this page does not commit the *Pertanika* Editorial Office, nor the UPM Press or the University to provide any liability for whatsoever reason.

Pertanika Journal of Science & Technology
Vol. 31 (S1) 2023

Toward Successful Implementation of Circular Economy

Pertanika Editorial Office, Journal Division
Putra Science Park,
1st Floor, IDEA Tower II,
UPM-MTDC Technology Centre
Universiti Putra Malaysia
43400 UPM Serdang
Selangor Darul Ehsan
Malaysia

http://www.pertanika.upm.edu.my/
E-mail: executive_editor.pertanika@upm.edu.my
Tel: +603 9769 1622

PENERBIT UPM
UNIVERSITI PUTRA MALAYSIA
BERILMU BERBAKTI
PRESS

http://penerbit.upm.edu.my
E-mail : penerbit@upm.edu.my
Tel : +603 9769 8855

ISSN 0128-7680
S1 >
9 770128 768083